



HAL
open science

Différenciation du trophoblaste humain - Implication des macrocomplexes PKA/AKAP lors de la fusion cellule-cellule

Guillaume Pidoux

► **To cite this version:**

Guillaume Pidoux. Différenciation du trophoblaste humain - Implication des macrocomplexes PKA/AKAP lors de la fusion cellule-cellule. Sciences du Vivant [q-bio]. Paris Descartes, 2013. tel-02556193

HAL Id: tel-02556193

<https://inserm.hal.science/tel-02556193>

Submitted on 27 Apr 2020

HAL is a multi-disciplinary open access archive for the deposit and dissemination of scientific research documents, whether they are published or not. The documents may come from teaching and research institutions in France or abroad, or from public or private research centers.

L'archive ouverte pluridisciplinaire **HAL**, est destinée au dépôt et à la diffusion de documents scientifiques de niveau recherche, publiés ou non, émanant des établissements d'enseignement et de recherche français ou étrangers, des laboratoires publics ou privés.

UNIVERSITE PARIS DESCARTES

HABILITATION A DIRIGER DES RECHERCHES

FACULTE DES SCIENCES PHARMACEUTIQUES ET BIOLOGIQUES

Travaux présentés par **GUILLAUME PIDOUX**

UMR-S-767

Grossesse Normale et Pathologique

Université Paris Descartes, Faculté de pharmacie

4, Avenue de l'Observatoire

75006 Paris, France

Directrice: Dr. D. Evain-Brion

SOMMAIRE

CURRICULUM VITAE	4
I. INFORMATIONS PERSONNELLES	4
II. FONCTION ACTUELLE	4
III. EXPERIENCES PROFESSIONNELLES	4
IV. CURSUS UNIVERSITAIRE	5
V. ACTIVITE D'ENCADREMENT	6
VI. SUPPORTS FINANCIERS	7
VII. RESEAU ET GROUPE DE TRAVAIL	7
VIII. PRIX	7
IX. COLLABORATIONS SCIENTIFIQUES	7
PUBLICATIONS	9
I. PUBLICATIONS INTERNATIONALES	9
II. PUBLICATION NATIONALE	10
III. COMMUNICATIONS ORALES INTERNATIONALES	10
IV. COMMUNICATIONS ORALES NATIONALES	11
V. COMMUNICATIONS INTERNATIONALES ET NATIONALES	11
VI. BREVET	12
SYNTHESE DES TRAVAUX DE RECHERCHE	15
I. TRAVAUX EFFECTUES EN THESE	15
1.1 - CARACTERISATION DU RECEPTEUR hCG AU COURS DE LA DIFFERENCIATION DU TROPHOBLASTE HUMAIN	15
1.2 - IMPLICATION D'UNE FORME D'hCG ANORMALE ET DE SON RECEPTEUR (R-LH/CG) DANS LE DEFAUT DE FORMATION DU SYNCYTIOTROPHOBLASTE OBSERVE LORS D'UNE GROSSESSE ASSOCIEE A UNE TRISOMIE 21 FETALE	16
1.3 - ROLE DE LA CONNEXINE 43 ET DE ZO-1 (ZONA OCCLUDENS 1) DANS LE PROCESSUS DE FUSION CELLULAIRE	18
II. TRAVAUX EFFECTUES EN POSTDOC	18
2.1 - L'ACTIVIN-A REVERSE LE DEFAUT DE FUSION DES TROPHOBLASTES HUMAINS ISSUS DE GROSSESSE ASSOCIEE A UNE TRISOMIE 21	18
2.2 - OPA1 EST UNE AKAP LOCALISEE AU NIVEAU DES GOUTTELETTES LIPIDIQUES CONTROLANT LA LIPOLYSE SOUS ADRENO-STIMULATION	19
CAPACITE A DIRIGER DES RECHERCHES	22
I. AU COURS DE MA THESE	22
1.1 - PROJET hCG/LHR (O. MARPEAU, MASTER 2)	22
1.2 - PROJET ZO-1 (M. GRYNBERG, MASTER 2)	22
II. AU COURS DE MON POSTDOC (L. MYRVOLD, MASTER 2)	23
III. DEPUIS MON RETOUR EN FRANCE	24
3.1 - LES ETUDIANTS EN MASTER, IUT ET BTS	24
3.1.1 <i>Emilie Branger (IUT)</i>	24
3.1.2 <i>Maxime Bourgeois (BTS)</i>	25
3.1.3 <i>Audrey Laurent (IUT)</i>	25
3.1.4 <i>Mélody Monthéard (Master 1)</i>	25
3.1.5 <i>Audrey Menault (Master 2)</i>	26
3.2 - LA POSITION DE POSTDOC	27
3.3 - L'EQUIPE SCIENTIFIQUE: 'CELL FUSION'	27
3.3.1 - <i>TCN Inserm (Mme F. Ferreira)</i>	28
3.3.2 - <i>IE-HC Inserm (Dr. P. Gerbaud)</i>	28

PROJETS ET PROSPECTIVE	30
I. ETAT DE L'ART:	30
1.1 - DIFFERENCIATION DES CYTOTROPHOBLASTES VILLEUX EN SYNCYTIOTROPHOBLASTE	31
1.2 - LA VOIE DE SIGNALISATION DE LA PROTEINE KINASE A (PKA)	33
II. BUT, ORIGINALITE ET INNOVATION DU PROJET DE RECHERCHE	35
III. ASPECTS TECHNIQUE ET SCIENTIFIQUE DU PROJET	37
3.1 - INTRODUCTION ET ACQUIS SCIENTIFIQUE	37
3.2 - DETERMINATION DE L'IMPLICATION DE L'EZRIN DANS LA FUSION CELLULE-CELLULE	38
3.2.1 <i>Résultats acquis</i>	38
3.2.2 <i>Rôle des PDEs</i>	39
3.2.3 <i>Détermination du message fusogène</i>	40
3.3 - DETERMINATION DE L'IMPLICATION DE L'AKAP18 DANS LA FUSION CELLULE-CELLULE	42
3.3.1 <i>Résultats acquis</i>	42
3.3.2 <i>Perspectives</i>	42
3.4 - DETERMINATION DE L'IMPLICATION DE L'AKAP450 DANS LA FUSION CELLULE-CELLULE	43
IV. ENVIRONNEMENT SCIENTIFIQUE	43
V. FAISABILITE	45
REFERENCES	48

CURRICULUM VITAE

I. Informations personnelles

Guillaume Pidoux

Né le 17 Juillet 1978 (Paris, France)

Nationalité: Française

Situation de famille: deux enfants

Adresse personnelle: 5, Rue Magellan
91300 Massy, France
Tél: +33 (0)6 80 06 97 66
Email: guillaume.pidoux@me.com

Adresse professionnelle: INSERM U767
Faculté de Pharmacie, Université Paris Descartes
4, avenue de l'observatoire
75006 Paris
Tél: +33 (0)1 53 73 96 02
Email: guillaume.pidoux@parisdescartes.fr

II. Fonction actuelle

Chercheur Inserm CR2.

Laboratoire de la grossesse normale et pathologique. (Directeur: Dr. D. Evain-Brion, MD, PhD), UMR-S-767; faculté des sciences pharmaceutiques et biologiques. Université Paris Descartes.

Sujet de recherche: Différenciation du trophoblaste humain. Implication des macrocomplexes PKA/AKAP au cours la fusion cellule-cellule.

III. Expériences professionnelles

2011-2012 ***Chercheur post-doctorant.***

Laboratoire de la grossesse normale et pathologique. (Directeur: Dr. D. Evain-Brion, MD, PhD), UMR-S-767; faculté des sciences pharmaceutiques et biologiques. Université Paris Descartes.

Sujet de recherche: Différenciation du trophoblaste humain. Implication des macrocomplexes PKA/AKAP au cours la fusion cellule-cellule.

Financement: Fondation PremUP *via* ANR: PlacentA5 (2012).

2010-2011 ***Chercheur post-doctorant.***

Laboratoire de la grossesse normale et pathologique. (Directeur: Dr. D. Evain-Brion, MD, PhD), UMR-S-767; faculté des sciences pharmaceutiques et biologiques. Université Paris Descartes.

Sujet de recherche: Impact de l'exposition des xénobiotiques sur le développement du placenta humain.

Financement: Région Ile-de-France.

2007-2010 ***Chercheur post-doctorant.***

The Biotechnology Centre of Oslo, Nordic EMBL. (Directeur: Pr. K. Tasken, MD, PhD), Universitet i Oslo, Oslo, Norvège.

Sujet de recherche: La D-AKAP OPA1 organise un complexe de signalisation sur les gouttelettes lipidiques des adipocytes pour le contrôle de la lipolyse induite par une stimulation adrénérergique.

Financement: European project on metabolic disease.

2002-2006 ***Doctorant.***

Laboratoire du développement humain: croissance et différenciation. (Directeur: Dr. D. Evain-Brion, MD, PhD), Inserm U427; faculté des sciences pharmaceutiques et biologiques. Université Paris Descartes.

Sujet de recherche: Implication d'une forme d'hCG anormale et de son récepteur (R-LH/CG) dans le développement placentaire lors d'une grossesse associée à une trisomie 21 (Dr. JL. Frendo).

Financement: Région Ile-de-France *via* projet Avenir

2001-2002 ***Master 2.***

Physiologie du développement et de la différenciation fonctionnelle (GC2ID). Inserm U427; faculté des sciences pharmaceutiques et biologiques. Université Paris Descartes.

IV. Coursus universitaire

2006 ***Thèse de doctorat*** "Physiologie du développement et de la différenciation fonctionnelle". Université Denis Diderot, Paris VII.

Titre de la thèse: “Implication d’une forme d’hCG anormale et de son récepteur (R-LH/CG) dans le développement placentaire lors d’une grossesse associée à une trisomie 21”.

Composition du jury: Président Pr. D. Luton
Rapporteur Pr. P. Bischof
Rapporteur Pr. Y. Combarous
Examineur Dr. AL. Delozoidé
Examineur Dr. D. Evain-Brion
Examineur Dr. JL. Frenco

- 2002 **Diplôme de Master 2** “Physiologie du développement et de la différenciation fonctionnelle”.
Université Denis Diderot, Paris VII.
- 2001 **Diplôme de Master 1**: Biologie cellulaire et physiologie
Université Orsay, Paris-Sud, Paris XI.
- 2000 **Diplôme de Licence**: Biologie cellulaire et physiologie
Université Orsay, Paris-Sud, Paris XI.

V. Activité d’encadrement

J’ai été responsable de la formation et de l’encadrement de plusieurs étudiants au cours de mes années de recherche :

- 2011-2012 Audrey Menault étudiante en Master 2 (BCPP, reproduction et développement).

Melody Montheard étudiante en Master 1 (BCPP, reproduction et développement).

Audrey Laurent étudiante en première année d’IUT génie biologie.
- 2011-2011 Maxime Bourgeois étudiant en BTS biotechnologie 2^{ème} année.
- 2010-2010 Emilie Branger étudiante en dernière année d’IUT génie biologie.
- 2008-2009 Linda Myrvold étudiante en Master 2 (Høgskolen i Oslo).
- 2005-2006 Michaël Grymberg étudiant en Master 2 (BCPP, reproduction et développement).
- 2004-2005 Olivier Marpeau étudiant en Master 2 (BCPP, reproduction et développement).

VI. Supports financiers

- 2011 Projet Yggdrasil de collaboration franco-Norvégienne (18 k€).
- 2010 SFBBM bourse pour le 35^{ème} congrès FEBS.
- 2010 FEBS bourse pour le workshop “spatiotemporal dynamics of cell signalling”.

VII. Réseau et groupe de travail

- 2011 Initiateur et co-manager du “réseau français sur l’AMPc” (avec Dr. P. Vincent).
- 2011 Elu par l’European Placenta Group Business Meeting comme faisant parti du “EPG Planning Committee”.
- 2011 Membre du GDR2588: Microscopie fonctionnelle du vivant (www.gdr2588.cnrs.fr/).
- 2006 Membre de la SFBBM.

VIII. Prix

- 2012 Prix de la meilleure ‘short communication’ à la Gordon Research Conference – Cyclic Nucleotide Phosphodiesterases – Lucca – Mai.
- 2012 Prix SFBBM de l’article du mois de mars 2012 (Optic Atrophy 1 is an A-kinase anchoring protein that mediates adrenergic control of lipolysis. *EMBO J.* 2011).

IX. Collaborations scientifiques

Internationales

Kjetil Tasken, MD, PhD
NCMM group Disease Mechanisms
Gaustadalléen 21
Forskningsparken
0349 Oslo, Norway

Annetine Staff, MD, PhD
Department of Obstetrics and Gynaecology
Sognsvannsveien 20
Rikshospitalet
0450 Oslo, Norway

Elke Winterhager, PhD
Institut für Molekularbiologie
Universitätsklinikum Essen
Hufelandstr. 55
45122 Essen, Germany

George Baillie, PhD
Institute of Cardiovascular and Medical Sciences
University of Glasgow
College of Medical, Veterinary & Life Sciences
Glasgow, G12 8QQ, Scotland

Nationales

Alain Brisson, PhD
Chimie et biologie des membranes et des nanoobjets
Imagerie moléculaire et nanobiotechnologie
UMR5248
Université de Bordeaux
33600 Pessac, France

Olivier Laprévotte, PhD
EA4463
Université Paris descartes
Faculté de pharmacie
75006 Paris, France

Pierre Vincent, PhD
Intégration Cellulaire des Signaux Neuromodulateurs
UMR7102
Université PMC
75005 Paris, France

Violaine Simon, PhD
Physiologie de l'axe gonadotrope
BFA EAC4413
Université Paris Diderot
75013 Paris, France

PUBLICATIONS

I. Publications internationales

Pidoux G., Witzak O., Jarnæss E., Myrvold L., Urlaub H., Stokka A.J., & Taskén K. Optic Atrophy 1 is an A-kinase anchoring protein that mediates adrenergic control of lipolysis. *EMBO J.* 2011, 30: 4371-86. doi: 10.1038/emboj.2011.365.

Pidoux G., Gerbaud P., Guibourdenche J., Pathirage N., Costa JM., Badet J., Frenedo JL., Murthi P., & Evain-Brion D. Mesenchymal Activin-A Overcomes Defective Human Trisomy 21 Trophoblast Fusion. *Endocrinology.* 2011, 152 :5017-28.

Pidoux G., Gerbaud P., Cocquebert M., Segond N., Badet J., Fournier T., Guibourdenche J & Evain-Brion D. Human trophoblast fusion and differentiation: Lessons from trisomy 21 placenta. *Placenta.* 2011. [Epub ahead of print].

Malassiné A., Pidoux G., Gerbaud P., Frenedo JL & Evain-Brion D. Human trophoblast in trisomy 21: a model for cell-cell fusion dynamic investigation. *Adv Exp Med Biol.* 2011, 714: 103-12.

Pidoux G., & Taskén K. AKAP specificity and spatial dynamics of PKA signalling. *J Mol Endocrinol.* 2010, 44: 271-84.

Pidoux G., Gerbaud P., Gnidehou S., Grynberg M., Cronier L., Guibourdenche J., Ferreira F., Badet J., Malassiné A., Evain-Brion D., & Frenedo JL. ZO-1 is required for trophoblastic cell-cell fusion in human placenta. *Am J Physiol Cell Ph.* 2010, 298: 1517-26.

Pidoux G., Gerbaud P., Marpeau O., Guibourdenche J., Ferreira F., Badet J., Evain-Brion D., & Frenedo JL. Human placental development is impaired by an abnormal hCG signaling in trisomy 21 pregnancies. *Endocrinology.* 2007, 148: 5403-13.

Pidoux G., Gerbaud P., Tsatsaris V., Marpeau O., Ferreira F., Meduri G., Guibourdenche J., Badet J., Evain-Brion D., & Frenedo JL. Biochemical characterization and modulation of LH/CG-receptor during human trophoblast differentiation. *J Cell Physiol.* 2007, 212: 26-35.

Pidoux G., Gerbaud P., Laurendeau I., Guibourdenche J., Bertin G., Vidaud M., Evain-Brion D., & Frenedo JL. Large variability of trophoblast genes expression within and between human normal term placentas. *Placenta.* 2004, 25: 469-73.

Pidoux G., Guibourdenche J., Frenedo JL., Gerbaud P., Conti M., Luton D., Muller., Evain-Brion D. Impact of trisomie 21 on human trophoblast behaviour and hormonal functions. *Placenta.* 2004, 25 Suppl: S79-84.

Frendo JL., Guibourdenche J., Pidoux G., Vidaud M., Luton D., Giovagrandi Y., Porquet D., Muller F., & Evain-Brion D. Trophoblast production of a weakly bioactive hCG in trisomy 21-affected pregnancy. *J Clin Endocrinol Metab.* 2004, 89: 727-732.

Cronier L, Frendo JL, Defamie N, Pidoux G, Bertin G, Guibourdenche J, Pointis G, et Malassiné A. Requirement of transient gap junctional intercellular communication for villous trophoblast differentiation of the human placenta. *Biol Reprod.* 2003, 69: 1472-1480.

Guibourdenche J, Frendo JL, Pidoux G, Bertin G, Luton D, Muller F, Porquet D, et Evain-Brion D. Expression of pregnancy-associated plasma protein-A (PAPPA) during human villous trophoblast differentiation in vitro. *Placenta.* 2003, 24: 532-539.

Lacroix MC, Guibourdenche J, Frendo JL, Pidoux G, et Evain-Brion D. Placental growth hormones. *Endocrine.* 2002, 19: 73-79.

II. Publication nationale

Pidoux G., Guibourdenche J., Gerbaud P., Marpeau O., Ferreira F., Vidaud M., Luton D., Giovagrandi Y., Muller F., Evain-Brion D., Frendo JL. Reasons of increased level of hCG in serum of mothers bearing a trisomic foetus. *IBS.* 2006, 21 (article en français): 91-98.

III. Communications orales internationales

2012 FEBS workshop – Dynamics of Cell Signal Systems – Oslo, Norvège – Septembre 2012. Ezrin organizes a supramolecular complex controlling communication gap junctions during trophoblastic cell fusion.

2012 Gordon Research Conference – Cyclic Nucleotide Phosphodiesterases – Lucca, Italie – Mai 2012. Ezrin organizes a supramolecular complex controlling communication gap junctions during trophoblastic cell fusion.

2011 14^{ème} EPG Meeting – Geilo, Norvège – Septembre 2011. Ezrin organizes a supramolecular complex controlling communication gap junctions during trophoblastic cell fusion.

2011 Lecture: “Ezrin organizes a supramolecular complex controlling communication through gap junctions during trophoblastic cell fusion”. 13 Septembre 2011. The Biotechnology Centre of Oslo, Nordic EMBL, Oslo, Norvège.

2010 3^{ème} International meeting on anchored cAMP signalling pathways– Oslo, Norvège – Septembre 2010. Ezrin organizes a supramolecular complex controlling communication gap junctions during trophoblastic cell fusion.

- 2010 35^{ème} FEBS Congress – Gothenburg, Suède – Juin 2010. The A Kinase Anchoring Protein OPA1 coordinates a signal complex on lipid droplets that mediates adrenergic control of lipolysis.
- 2008 Lecture: “OPA1: a new AKAP involved in lipolysis of adipocytes”. 8 Mai 2008 (Oslo, Norvège).
- 2006 Lecture: “Impaired human development in trisomy 21-associated pregnancy is related to an abnormal hCG signalling”. 16 Novembre 2006 (Oslo, Norvège).

IV. Communications orales nationales

- 2011 Lecture: “Ezrin organizes a supramolecular complex controlling communication through gap junctions during trophoblastic cell fusion”. 15 Décembre 2011. Institut Curie, Paris, France.
- 2010 Lecture: “OPA1 : a new AKAP involved in lipolysis of adypocytes”. 18 Juin 2010. UMR-S-769, Châtenay-Malabry, France.
- 2004 2eme symposium sur la Trisomie 21: “de la fonction des gènes du chromosome 21 à la physiopathologie”. 1^{er} Juin 2004 (Paris, France).

V. Communications internationales et nationales

- 2012 Gordon Research Conference – Cyclic Nucleotide Phosphodiesterases – Lucca, Italie – May 2012. Poster. Pidoux G., Gerbaud P., Dompierre J., Solstad T., Evain-Brion D., Tasken K. Ezrin organizes a supramolecular complex controlling communication through gap junctions during trophoblastic cell fusion.
- 2011 14th EPG Meeting – Geilo, Norvège – Septembre 2011. Poster. Pidoux G., Gerbaud P., Dompierre J., Solstad T., Evain-Brion D., Tasken K. Ezrin organizes a supramolecular complex controlling communication through gap junctions during trophoblastic cell fusion.
- 2011 Gordon Research Conference – Cell-cell Fusion – Biddeford, USA – Août 2011. Poster. Pidoux G., Gerbaud P., Dompierre J., Solstad T., Evain-Brion D., Tasken K. Ezrin organizes a supramolecular complex controlling communication through gap junctions during trophoblastic cell fusion.
- 2010 3rd International meeting on anchored cAMP signalling pathways and Workshop on spatiotemporal dynamics of cell signalling – Oslo, Norvège – September, Octobre 2010. Poster. Pidoux G., Gerbaud P., Dompierre J., Solstad T., Evain-Brion D., Tasken K. Ezrin organizes a supramolecular complex controlling communication through gap junctions during trophoblastic cell fusion.

- 2010 3rd International meeting on anchored cAMP signalling pathways and Workshop on spatiotemporal dynamics of cell signalling – Oslo, Norvège – September, Octobre 2010. Poster. Pidoux G., Witczak O., Jarnæss E., Myrvold L., Stokka A.J., Tasken K. The A Kinase Anchoring Protein OPA1 coordinates a signal complex on lipid droplets that mediates adrenergic control of lipolysis.
- 2010 35th FEBS Congress – Gothenburg, Suède – Juin 2010. Poster. Pidoux G., Witczak O., Jarnæss E., Myrvold L., Stokka A.J., Tasken K. The A Kinase Anchoring Protein OPA1 coordinates a signal complex on lipid droplets that mediates adrenergic control of lipolysis.
- 2008 16th Protein Kinase Meeting – Oslo, Norvège – Septembre 2008. Poster. Pidoux G., Witczak O., Jarnæss E., Myrvold L., Stokka A.J., Tasken K. The A Kinase Anchoring Protein OPA1 coordinates a signal complex on lipid droplets that mediates adrenergic control of lipolysis.
- 2007 2nd International Conference on Anchored cAMP Signaling Mechanisms – Portland, USA – Octobre 2007. Poster. Pidoux G., Oberprieler N., Gerbaud P., Evain-Brion D., and Tasken K. Compartmentalized cAMP signaling events during syncytial formation and differentiation in the human placenta.
- 2005 12th EPG Meeting – Glasgow, UK – Septembre 2005. Poster. Pidoux G., Gerbaud P., Frendo J-L., Luton D., Muller F., Evain-Brion D., Porquet D., Guibourdenche J. Investigation of hCG glycoforms secreted by trisomy 21 villous trophoblastic cells in-vitro.
- 2005 European Placenta Group Meeting – Glasgow – Septembre 2005. Poster. Pidoux G., Marpeau O., Gerbaud P., Ferreira F., Meduri G., Evain-Brion D and Frendo JL. Expression of LH/CG receptor during differentiation of the human villous trophoblast.
- 2003 1^{er} symposia sur la Trisomie 21 – Paris, France – Juin 2003. Poster. Frendo J-L., Pidoux P., Gerbaud P., Théron P., Guibourdenche J., Luton D., Muller F. & Evain-Brion D. Trisomie 21 et différenciation du trophoblaste humain.
- 2003 9th IFPA meeting and 10th EPG meeting – Mainz, Allemagne – Septembre 2003. Poster. Malassiné A., Frendo J-L., Olivier D., Pidoux G., Guibourdenche J., Mallet F. & Evain-brion D. Direct role for Herv-w env glycoprotein and for connexin 43 in trophoblastic cell fusion demonstrated by antisense strategy.
- 2003 9th IFPA meeting and 10th EPG meeting – Mainz, Allemagne – Septembre 2003. Poster. Frendo J-L., Pidoux G., Guibourdenche J., Conti M., Evain-brion D and the french working group on normal and T21 placenta. Impact of trisomy 21 on trophoblast behavior.

VI. Brevet

- 2012 Pidoux G., Evain-brion D., Lygren B. & Tasken K. DOFI no. 12043: Method to regulate the opening of connexin-43 junctions

Ministère de la jeunesse, de l'éducation nationale et de la recherche

UNIVERSITÉ PARIS VII

DIPLÔME D'ÉTUDES APPROFONDIES

GRADE DE MASTER

Vu la loi n° 84-52 du 26 janvier 1984 modifiée sur l'enseignement supérieur, notamment ses articles 5, 16, 17 et 43
Vu le décret n° 84-573 du 5 juillet 1984 modifié relatif aux diplômes nationaux de l'enseignement supérieur
Vu le décret n° 2002-604 du 25 avril 2002 modifiant le décret n° 99-747 du 30 août 1999 relatif à la création du grade de master
Vu l'arrêté ministériel du 12 juillet 2000 relatif aux habilitations de l'Université Paris VII, de l'Université Paris V à délivrer des diplômes d'études approfondies
Vu les pièces justificatives produites par M. GUILLAUME PIDOUX, né le 17 juillet 1978 à PARIS 14 (075), en vue de son inscription au Diplôme d'Études Approfondies de Physiologie du Développement et de la Différenciation Fonctionnelle
Vu les procès-verbaux du jury attestant que l'intéressé a satisfait au contrôle des connaissances et des aptitudes prévu par les textes réglementaires
le **DIPLÔME D'ÉTUDES APPROFONDIES DE PHYSIOLOGIE DU DÉVELOPPEMENT ET DE LA DIFFÉRENCIATION FONCTIONNELLE, mention assez bien**
est décerné à **M. GUILLAUME PIDOUX**
à qui est conféré le grade de master
au titre de l'année universitaire 2001-2002.

Fait à Paris, le 14 octobre 2002

Le titulaire



N° PARVII 3606892

L:062200101350

René BLANCHET

DOCTORAT

GRADE DE DOCTEUR

Vu le code de l'éducation, notamment son article L.612-7

Vu le code de la recherche, notamment son article L.412-1

Vu le décret n°2002-481 du 8 avril 2002 relatif aux grades et titres universitaires et aux diplômés nationaux

Vu l'arrêté du 3 septembre 1998 relatif à la charte des thèses

Vu l'arrêté du 7 août 2006 relatif à la formation doctorale

Vu le procès-verbal du jury attestant que l'intéressé a soutenu, le 24 octobre 2006 une thèse portant sur le sujet suivant : Implication d'une forme d'hCG anormale et de son récepteur (R-LH/CG) dans le développement placentaire lors d'une grossesse associée à une trisomie 21 devant un jury présidé par DOMINIQUE LUTON, PROFESSEUR DES UNIVERSITÉS et composé de PAUL BISCHOF, PROFESSEUR, YVES COMBARNOUS, DIRECTEUR DE RECHERCHE, ANNE-LISE DELEZOIDE, MAITRE DE CONFÉRENCES, DANIELE EVAIN-BRION, DIRECTEUR DE RECHERCHE, JEAN-LOUIS FRENDO, CHARGE DE RECHERCHE

Vu la décision dudit jury prononçant l'admission de l'intéressé avec la mention très honorable avec félicitations

le Doctorat en PHYSIOLOGIE DU DEVELOPPEMENT est décerné à **M. GUILLAUME PIDOUX** né le 17 juillet 1978 à PARIS 14 (075) pour en jouir avec les droits et prérogatives qui y sont attachés et confère le grade de docteur.

Le titulaire

Le Président

Le Recteur d'Académie,
Chargé des affaires universitaires

N° **PARVI 6295870**

/2007200600087

Fait à Paris, le 30 janvier 2007

Maurice QUENET

SYNTHESE DES TRAVAUX DE RECHERCHE

I. Travaux effectués en thèse

1.1 - Caractérisation du récepteur hCG au cours de la différenciation du trophoblaste humain

Le placenta humain est caractérisé par une invasion des cellules trophoblastiques dans l'utérus maternel, créant un contact direct entre les trophoblastes et le sang maternel (Midgley et al., 1963). Dans les premières étapes de la grossesse, les cytotrophoblastes vont se différencier, fusionner ensemble et ainsi former le syncytiotrophoblaste (Midgley et al., 1963). Le syncytiotrophoblaste joue un rôle essentiel dans le maintien de la grossesse en assurant le

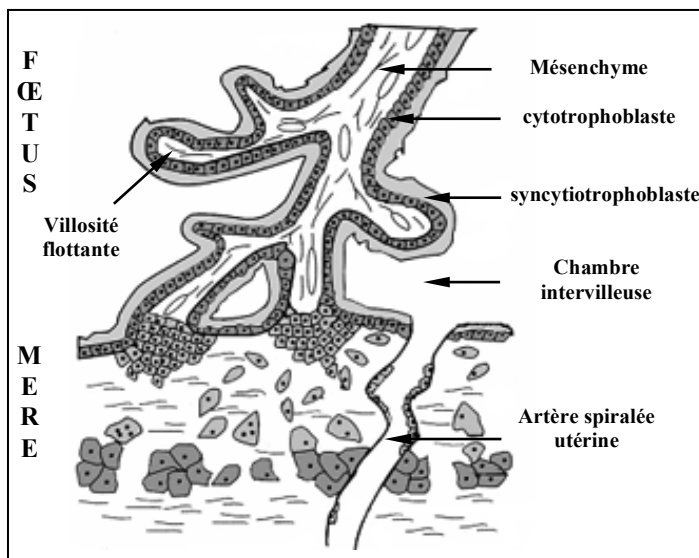


Fig.1: Représentation schématique de l'interface materno-placentaire.

transport des nutriments indispensables au développement fœtal et en sécrétant dans le sang maternel les hormones de la grossesse comme l'hCG (ou hormone chorionique gonadotrope humaine) (Eaton and Contractor, 1993; Ogren and Talamantes, 1994) (Fig.1). Plusieurs facteurs modulent la différenciation des trophoblastes, notamment l'hCG de manière auto-paracrine (Shi et al., 1993).

En raison du rôle clef de l'hCG dans le développement du placenta

humain, j'ai voulu caractériser le récepteur de cette hormone (R-LH/CG) dans le trophoblaste humain et étudier son expression au cours de la différenciation des cytotrophoblastes en syncytiotrophoblaste. J'ai déterminé par des études d'immunochimie *in situ* et *in vitro*, que le R-LH/CG est exprimé aussi bien dans les cytotrophoblastes que dans le syncytiotrophoblaste. Une diminution de l'ARNm du R-LH/CG a été observée par RT-PCR semi-quantitative au

cours de la différenciation. De plus, j'ai démontré par western-blot et immuno-précipitation que l'expression du R-LH/CG décroît au fur et à mesure de la fusion trophoblastique. Nous avons confirmé ces résultats par une analyse de Scatchard en démontrant que la forme mature du récepteur, exprimée à la surface des cellules trophoblastiques et fixant l'hCG-1²⁵, est fortement moins exprimée par le syncytiotrophoblaste que par les cytotrophoblastes. Enfin, sous stimulation par une hCG recombinante, le syncytiotrophoblaste produit moins d'AMPc que le cytotrophoblaste. L'ensemble de mes résultats indique que l'expression du R-LH/CG est régulée de manière négative au cours de la différenciation trophoblastique. Ce travail a donné lieu à une publication (Pidoux G. et al, J Cell Physiol, 2007, 212: 26-35).

1.2 - Implication d'une forme d'hCG anormale et de son récepteur (R-LH/CG) dans le défaut de formation du syncytiotrophoblaste observé lors d'une grossesse associée à une trisomie 21 fœtale

Le développement du placenta humain en cas de trisomie 21 fœtale (T21) est caractérisé par différentes anomalies, conduisant notamment à un défaut de formation et de fonctionnalité du syncytiotrophoblaste (Wright et al., 2004). Les cytotrophoblastes issus de placentas trisomiques fusionnent peu ou avec un certain retard et le syncytiotrophoblaste résultant est à l'origine d'une synthèse et d'une sécrétion d'hCG diminuée par le syncytiotrophoblaste, anormalement glycosylée et biologiquement moins active par rapport à celles issues de placenta normal (Frendo et al., 2004; Frendo et al., 2000). Cependant, lors d'une grossesse associée à une T21, l'hCG est retrouvée augmentée dans le sang maternel. Nous sommes donc confrontés à un paradoxe: d'un côté une synthèse d'hCG diminuée et de l'autre, un taux sérique maternel augmenté. J'ai montré que ce paradoxe ne s'explique pas par une anomalie de clairance de l'hCG anormalement glycosylée, ni par une augmentation de sa

demi-vie plasmatique après

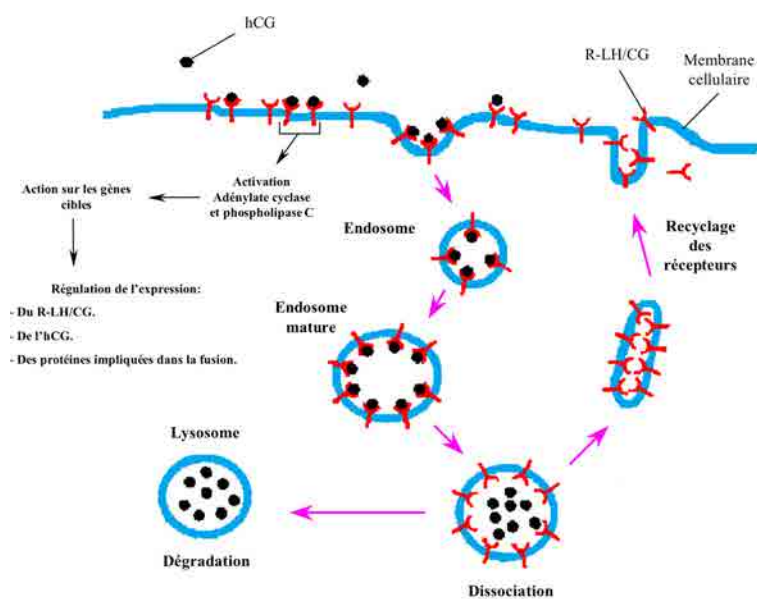


Fig.2: Représentation schématique du modèle proposé pour le 'recycling' de l'hCG et de son récepteur (R-LH-CG) dans les cellules trophoblastiques normales.

expulsion du placenta. Il s'agit d'une élimination anormale de l'hCG par le placenta dans les grossesses associées à une T21. Afin d'expliquer ce paradoxe observé, j'ai étudié la fonctionnalité et l'interaction de l'hCG anormale avec son récepteur (R-LH/CG) et j'ai caractérisé d'un point de vue biochimique et moléculaire le R-LH/CG dans les cytotrophoblastes trisomiques, montrant une diminution significative de l'expression de la forme mature du R-LH/CG dans les cellules trophoblastiques trisomiques. L'utilisation de RNAi inhibant spécifiquement l'expression du R-LH/CG dans les cytotrophoblastes normaux, m'a permis de mimer le défaut de fusion observé dans les cellules trophoblastiques trisomiques. Enfin, j'ai montré que le défaut de différenciation observé dans les cellules trisomiques est réversible par l'action d'une hCG recombinante fonctionnelle, entraînant la fusion et la différenciation des cytotrophoblastes issues de grossesses associées à une trisomie 21. L'ensemble de ces travaux montrent que la diminution de l'expression du R-LH/CG associée à une hCG anormalement glycosylée et biologiquement moins active est impliquée dans le défaut de formation syncytiale et dans le 'recaptage' de l'hormone par le placenta, permettant alors d'expliquer le paradoxe de l'hCG sérique maternelle élevée dans la trisomie

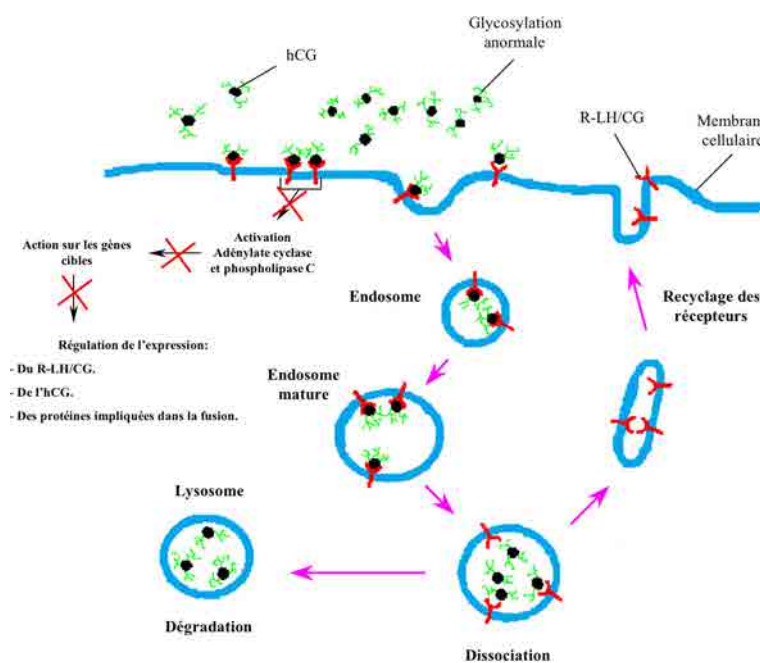


Fig.3: Représentation schématique du modèle proposé pour le 'recycling' de l'hCG et de son récepteur (R-LH-CG) dans les cellules trophoblastiques trisomiques.

21 (Fig.2 et 3). Ce travail a donné lieu à un article publié. (Pidoux G. et al, Endocrinology, 2007, 148: 5403-13). Ces résultats m'ont permis de révéler que l'étape de fusion est l'étape limitante de la différenciation du trophoblaste humain (2 articles de revues ont été publiés Pidoux G. et al, Placenta, 2011, Dec 2. [Epub ahead of print] et Malassiné A. et al, Adv Exp Med Biol. 2011;714:103-12).

1.3 - Rôle de la connexine 43 et de ZO-1 (zona occludens 1) dans le processus de fusion cellulaire

Le phénomène de fusion cellule-cellule joue un rôle important dans un grand nombre de processus biologiques comme la fertilisation, le développement et la formation des muscles, des os et du placenta (Midgley et al., 1963; Wakelam, 1985; Zamboni Zallone et al., 1984). La caractéristique du développement placentaire humain est la fusion et la différenciation des cytotrophoblastes pour former le syncytiotrophoblaste (Midgley et al., 1963). Certaines protéines sont directement impliquées dans ce processus telles que la connexin 43 (Cx43), la syncytin-1 et la cadherin 11 (Coutifaris et al., 1991; Frendo et al., 2003a; Frendo et al., 2003b). Zona occludens 1 (ZO1) est une protéine d'échafaudage qui intervient dans différents complexes de signalisation, mais aussi dans les complexes d'interaction cellule-cellule (Fanning et al., 1998). Je me suis intéressé au rôle de ZO1 dans le processus de fusion cellulaire observé dans le placenta humain. En utilisant la stratégie des RNA interférences (RNAi), j'ai démontré l'importance de ZO1 dans la fusion trophoblastique. J'ai montré par immuno-marquage et immuno-précipitation que ZO1 et la Cx43 sont co-localisées dans un macrocomplexe cellulaire. J'ai de plus démontré que l'expression de ZO1 est indispensable à la formation et la mise en place de la Cx43 à la membrane. Cette étape est essentielle pour induire la fusion cellulaire dans le trophoblaste humain. Ce travail a été réalisé au cours de ma thèse sous la direction du Dr. JL Frendo et a donné lieu à un article publié. (Pidoux G. et al, Am J Physiol Cell Ph. 2010, 298: 1517-26)

II. Travaux effectués en postdoc

2.1 - L'activin-A reverse le défaut de fusion des trophoblastes humains issus de grossesse associée à une trisomie 21

Le développement placentaire est anormal en cas de grossesses associées à une trisomie 21 (T21) (Wright et al., 2004). Dans une étude, le laboratoire a montré que les cellules du mésenchyme de la villosité chorale stimulent de manière paracrine la fusion des cytotrophoblastes et la formation du syncytiotrophoblaste. J'ai posé l'hypothèse que le

développement placentaire anormal associée à une trisomie 21 pourrait être dû à un défaut de communication entre le mésenchyme de la villosité chorale et le trophoblaste, ayant pour conséquence un défaut dans la formation du syncytiotrophoblaste (Fig.1). J'ai montré que du milieu conditionné de fibroblastes normaux purifiés à partir du mésenchyme permet de restaurer la fusion des cytotrophoblastes trisomiques. L'utilisation d'antagonistes spécifiques de la voie de signalisation du TGF β a démontré que cette voie est à l'origine de la restauration de la fusion cellulaire des cellules de T21. J'ai analysé par cytokine-array les cytokines présentes dans le milieu conditionné de fibroblastes normaux et trisomiques. L'activin-A, un membre de la famille des TGF β a été identifiée comme très fortement sécrétée par les deux types de cellules mais significativement moins dans les fibroblastes trisomiques. De plus, l'ajout d'activin-A recombinante est capable de restaurer la fusion des trophoblastes trisomiques. Enfin l'ajout d'anticorps bloquant de l'activin-A ou de follistatine (antagoniste naturel) inhibent l'activité fusogène du milieu conditionné de fibroblastes. J'ai montré que la follistatine est très fortement sécrétée par les cellules du mésenchyme de T21. Ces résultats montrent que le défaut de fusion et de différenciation associé à la T21 peut être inversé in vitro et que l'axe mésenchymateux de la villosité chorale du placenta humain joue un rôle essentiel dans ce processus, par un effet paracrine. Ce travail a été réalisé à mon retour de postdoc dans le laboratoire dirigé par le Dr. Danièle Evain-Brion et il a donné lieu à un article publié. (Pidoux G. et al, Endocrinology. 2011, 152 :5017-28).

2.2 - OPA1 est une AKAP localisée au niveau des gouttelettes lipidiques contrôlant la lipolyse sous adrénostimulation

La réponse physiologique du tissu adipeux blanc à l'insuline implique la synthèse de triglycérides (TG) à partir d'acides gras libres et de glycérol. Le stockage des TG néo synthétisés est réalisé au niveau de gouttelettes lipidiques intracellulaires des adipocytes. Les gouttelettes lipidiques sont constituées d'un cœur hydrophobe de TG entourées d'une monocouche de phospholipides et de cholestérol sur laquelle sont fixées un grand nombre de protéines. En période de jeûne, une stimulation des récepteurs β -adrénergiques des adipocytes est responsable de l'induction du processus de lipolyse qui permet la libération d'acides gras libres et de glycérol qui serviront de substrat énergétique par différents tissus.

La synthèse d'AMPc est responsable de l'activation de la PKA (protéine kinase A) et de la lipolyse. La PKA va phosphoryler la perilipin (protéine de la famille des PAT (Kimmel et al.,

2009), une protéine localisée à la surface des gouttelettes lipidiques contenant les stocks de TG. La perilipin joue le rôle de gardien et par un jeu de phosphorylation/déphosphorylation permet le contrôle de l'accès des lipases aux gouttelettes lipidiques (Blanchette-Mackie et al., 1995; Fain and Garcija-Sainz, 1983; Greenberg et al., 1991; Greenberg et al., 1993). En l'absence de stimulation, la perilipin non phosphorylée bloquent l'accès des lipases aux TG stockés dans les gouttelettes lipidiques. Une fois phosphorylée, la perilipin change de conformation donnant accès aux lipases pour la dégradation des TG et à l'induction de la lipolyse (Blanchette-Mackie et al., 1995; Brasaemle et al., 2000b; Souza et al., 2002; Tansey et al., 2003). En période de stress, d'exercices ou de jeûne, l'induction hormonale de la lipolyse entraîne l'accessibilité des gouttelettes lipidiques aux lipases qui libèrent des acides gras qui serviront de source d'énergie pour les tissus périphériques (comme le cœur et les muscles squelettiques) (Brasaemle et al., 2000a; Londos et al., 1999). De plus la PKA phosphoryle l'hormone sensitive lipase (HSL), qui a été montré comme le premier substrat de la PKA régulant la lipolyse. L'HSL a longtemps été admise comme le seul enzyme responsable de l'hydrolyse des TG stockés mais aussi du contrôle de la lipolyse (Fain and Garcija-Sainz, 1983). L'obésité est l'une des maladies métaboliques, responsable de différentes pathologies incluant celles du diabète de type 2, de l'hypertension, des troubles cardiaques, des troubles neurologiques et de certains cancers. L'obésité est le résultat du déséquilibre entre la prise et la dépense d'énergie entraînant une accumulation pathologique de lipides dans les adipocytes mais aussi une augmentation de ces derniers. Dans les adipocytes l'adréno-stimulation entraîne l'activation de la PKA (Duncan et al., 2007), la phosphorylation de la perilipin ainsi que l'activation de la lipolyse (Blanchette-Mackie et al., 1995; Fain and Garcija-Sainz, 1983; Greenberg et al., 1991). J'ai révélé que OPA1 (Optic Atrophy 1), une protéine connue pour réguler la dynamique mitochondriale (Cipolat et al., 2004; Frezza et al., 2006), agit également comme une dual-AKAP (A-kinase anchoring protein) associée aux gouttelettes lipidiques. Par différentes approches d'études d'interactions protéiques, de co-immunoprécipitations et d'analyses par immunolocalisation, j'ai montré que OPA1 organise un macro-complexe protéique associant la PKA (dans le domaine AKB) et la perilipin. De plus, par des approches de siRNA et de reconstitution en utilisant OPA1 ayant ou non la capacité de fixer la PKA, ou par l'utilisation de protéines chimères comprenant le domaine AKB d'OPA1 fusionné avec la séquence d'adressage aux gouttelettes lipidiques, ou avec l'utilisation de peptides spécifiques capables de délocaliser la PKA, j'ai démontré que OPA1 cible la PKA, dans les adipocytes au niveau des gouttelettes lipidiques pour contrôler la phosphorylation de la perilipin et l'induction de la lipolyse sous adréno-stimulation (Fig.4).

J'ai aussi démontré qu'OPA1 était une dual-AKAP capable de fixer la PKA de type I ou de type II, et de la nécessité de déplacer les deux types de PKA (avec les peptides RIAD et SuperAKAP-1S ou HT31) pour inhiber l'induction de la lipolyse. Ce travail a été réalisé au cours de mon stage postdoctoral en Norvège dans le laboratoire du Pr. Kjetil Taskén et a donné lieu à un article publié. (Pidoux G. et al, EMBO J. 2011, 30: 4371-86). Cet article a été mis en valeur par un article de revue dans les "highlighted" d'EMBO J: Greenberg AS. et al, EMBO J. 2011, 30: 4337-9 et à été sélectionné comme article du mois de mars par la SFBBM.

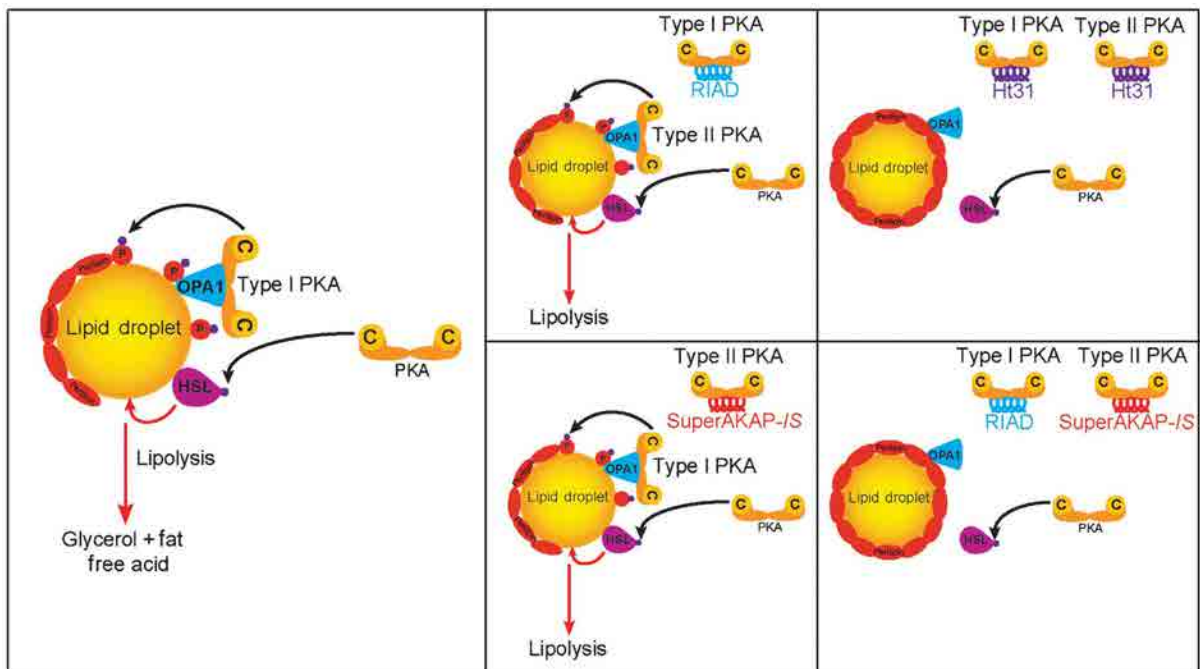


Fig.4: Représentation schématique du modèle proposé pour le contrôle de la lipolyse dans les adipocytes.

CAPACITE A DIRIGER DES RECHERCHES

I. Au cours de ma thèse

Au cours de ma thèse, réalisée dans le laboratoire Inserm U767 (Paris, France), j'ai été amené à encadrer des étudiants de Master 2^{ème} année dans leur cursus d'étude médicale (O. Marpeau et M. Grynberg).

1.1 - Projet hCG/LHR (O. Marpeau, Master 2)

Au cours de l'année universitaire 2004/2005, j'ai été invité à diriger les recherches d'Olivier Marpeau au cours de sa deuxième année de Master pour une durée de 6 mois (DEA de 'physiologie du développement et de la différenciation fonctionnelle' dirigé par le Pr. A. Ktorza de l'école doctorale GC2ID). Olivier Marpeau a été rattaché directement à mon sujet de thèse (voir partie Résumé des travaux de thèse, section 1.1 et 1.2). Il a étudié la localisation du récepteur de l'hCG (LHR) dans des trophoblastes humains ainsi que sur des coupes de placenta total issu de grossesses normales et de trisomie 21. Au cours de son année de Master 2, J'ai formé O. Marpeau à la culture primaire de trophoblastes humains, ainsi qu'aux différentes techniques d'immunofluorescence (sur cellules et sur coupes de placenta total). Le suivi des expérimentations, l'analyse des résultats ainsi que la planification des nouvelles expériences étaient réalisées deux fois par semaine. J'ai supervisé la rédaction et corrigé son mémoire de Master 2. Son travail a été validé et intégré dans deux articles scientifiques dont O. Marpeau est co-auteur (*Pidoux et al. 2007, J Cell Physiol* et *Pidoux et al. 2007, Endocrinology*). L'obtention de son Master 2 avec mention ainsi que deux articles scientifiques publiés dans des journaux à comité de lecture ont contribué à l'obtention d'un poste de chef de clinique à l'hôpital Robert Debré (Paris, France) pour O. Marpeau.

1.2 - Projet ZO-1 (M. Grynberg, Master 2)

Au cours de l'année universitaire 2005/2006, j'ai dirigé les recherches de Michaël Grynberg au cours de sa deuxième année de Master pour une durée de 6 mois (DEA de 'physiologie du développement et de la différenciation fonctionnelle' dirigé par le Pr. A. Ktorza de l'école

doctorale GC2ID). Michaël Grynberg a été rattaché à un deuxième projet de recherche que je menais en synergie avec mon projet de thèse (voir partie Résumé des travaux de thèse, section 1.3). Son projet avait pour but d'identifier les complexes protéiques associés à la connexin 43 ou la syncytin-1 au cours du processus de fusion des trophoblastes humain. J'ai formé M. Grynberg à la culture primaire de trophoblastes humains, ainsi qu'aux différentes techniques de biochimie nécessaires à la réalisation de son projet (western-blot, co-immunoprecipitation et co-immunocytofluorescence). Le suivi des expérimentations, l'analyse des résultats ainsi que la planification des nouvelles expériences étaient vérifiés deux fois par semaine. Son travail a été validé et intégré dans un article scientifique dont M. Grynberg est co-auteur (*Pidoux et al. 2010, Am J Physiol Cell Physiol*). L'obtention de son Master 2 avec mention ainsi qu'une publication en co-auteur d'un article scientifique à comité de lecture a permis à M. Grynberg d'établir des bases scientifiques solides pour la réalisation d'une thèse de science, qu'il a validée avec succès.

II. Au cours de mon postdoc (L. Myrvold, Master 2)

Au cours de mon stage postdoctoral en Norvège, dans le laboratoire du Pr. K. Tasken (Oslo, Norvège), j'ai été amené à encadrer une étudiante en Master 2 (L. Myrvold) au cours de son cursus universitaire scientifique (Høgskolen i Oslo) et sur une durée de 12 mois (2008/2009). L. Myrvold a été associée à l'un de mes projets de recherche de postdoc: 'étude du contrôle de la lipolyse par les AKAPs'. Rapidement, L. Myrvold a démontré des facilités dans les différentes techniques et démarches scientifiques proposées et enseignées (transfections, silencing, mutations, western-blot). Par conséquent, elle a souhaité obtenir un projet autonome relié à mon projet et réalisable sur la durée de son stage. Le suivi des expérimentations, l'analyse des résultats ainsi que la planification des nouvelles expériences étaient réalisés trois fois par semaine. Au cours de son Master 2, L. Myrvold a appris et maîtrisé la différenciation des cellules 3T3-L1 en adipocytes. Elle a développé une approche afin de quantifier le relargage de glycérol (lipolyse assay) par des adipocytes dans le milieu de culture après traitement par de l'isoproterenol et des peptides délocalisant l'ancrage de la PKA aux AKAPs (RIAD, SuperAKAP-1S et Ht31). Au cours de son Master 2, L. Myrvold a pu démontrer le contrôle de la lipolyse par l'utilisation de peptides délocalisant la PKA des AKAPs. Les résultats obtenus ont été intégrés dans un article scientifique à comité de lecture

dont L. Myrvold est co-auteur (*Pidoux et al. 2011, EMBO J*). Ce travail a abouti à un financement de thèse d'une durée de 3 ans, position que L. Myrvold a refusée après qu'elle ait obtenu un poste d'ingénieur dans un laboratoire scientifique du Radium Hospital d'Oslo.

III. Depuis mon retour en France

3.1 - Les étudiants en Master, IUT et BTS

Depuis mon retour de stage postdoctoral, j'ai encadré de nombreux stagiaires provenant de divers horizons (Master, IUT et BTS).

3.1.1 Emilie Branger (IUT)

M^{me} E. Branger a réalisé son stage (8 semaines) de dernière année d'IUT de génie biologie (IUT de Clermont-Ferrand, Clermont-Ferrand, France) en 2010. Au cours de son stage E. Branger a étudié le rôle de l'annexin 5 dans la fusion des trophoblastes humain. Avec une gestion au quotidien des travaux à réaliser en suivant le plan préétabli en début de stage, j'ai pu former E. Branger à la culture primaire de trophoblastes issus de placenta humain ainsi qu'à certains aspects de la biologie moléculaire et de la biochimie (siRNA annexin 5, annexin 5 recombinante immunocytofluorescence, tests de fusion, PCR et clonage). Les résultats obtenus par E. Branger, nous ont permis d'intensifier une collaboration nationale avec le laboratoire du Pr. A. Brisson (UMR-CBMN, Bordeaux, France) qui s'intéresse aux fonctions physico-chimiques de l'annexin 5. De plus le travail et les résultats obtenus par E. Branger nous ont permis de rédiger et d'obtenir avec le groupe du Pr. A. Brisson un projet ANR financé sur une période de 3 ans (PlacentA5, 2012-2015). Ce projet prévoit d'étudier le rôle de l'annexin 5 dans le placenta humain. Bien qu'après avoir obtenu d'excellents résultats universitaires lui permettant de continuer en Licence à l'université, E. Branger a décidé de se réorienter.

3.1.2 Maxime Bourgeois (BTS)

M^f M. Bourgeois a réalisé son stage (8 semaines) de dernière année de BTS de biotechnologie (Lycée Vallée de Chevreuse, Gif-sur-Yvette, France) en 2011. Au cours de son stage M. Bourgeois a étudié l'impact de l'exposition du formaldéhyde sur la fusion des trophoblastes humains. Avec une gestion au quotidien des travaux à réaliser en suivant le plan préétabli en début de stage, j'ai formé M. Bourgeois à la culture primaire de trophoblastes issus de placenta humain ainsi qu'à certains aspects de la biologie moléculaire (RT-qPCR) et de la biochimie (immunocytofluorescence et tests de fusion). M. Bourgeois a montré que le formaldéhyde induit la fusion cellulaire en modifiant le statut oxydatif de la cellule trophoblastique. Les résultats obtenus par M. Bourgeois vont être intégrés dans un article scientifique à comité de lecture en cours de rédaction (*Pidoux et al. 2012, en préparation*). Les excellents résultats obtenus au rapport de stage par M. Bourgeois lui ont permis de réaliser une Licence-professionnelle et de poursuivre sa formation en Master à l'Université Paris 7.

3.1.3 Audrey Laurent (IUT)

M^{me} A. Laurent a réalisé son stage (6 semaines) de première année d'IUT de génie biologique (IUT de Brest, Brest, France) en 2012. Au cours de son stage j'ai demandé à A. Laurent de réaliser le clonage de l'annexin 5 humaine à partir de trophoblastes humains. Avec une gestion au quotidien des travaux à réaliser en suivant le plan préétabli en début de stage, j'ai formé A. Laurent à la culture primaire de trophoblastes issus de placenta humain ainsi qu'à certaines approches de biologie moléculaire (extractions d'ARN, RT-PCR, transformations bactériennes, mini et midi-preps, digestion enzymatiques et séquençage) et biochimique (immunocytofluorescence et tests de fusion). Les résultats obtenus par A. Laurent ont été concluants car ils ont permis en 6 semaines de cloner l'annexin 5 humaine à partir de primocultures de trophoblastes humains. M^{me} A. Laurent va poursuivre en 2013 son cursus en deuxième année d'IUT.

3.1.4 Mélody Monthéard (Master 1)

Depuis Septembre 2011, le laboratoire Inserm U767 a obtenu le financement d'un projet ANR: 'Placentox' en collaboration avec le laboratoire du Pr. O. Laprévote (EA4463, Paris,

France). Ce projet prévoit jusqu'en 2014 d'étudier l'impact de l'exposition du benzo(a)pyrene (BaP) sur les fonctions du placenta humain. M^{me} M. Monthéard a réalisé son stage (8 semaines) de Master 1 (Master Reprodev, Paris, France) en 2012. Au cours de son stage j'ai demandé à M. Monthéard d'étudier l'impact de l'exposition du benzo(a)pyrene (BaP) sur la fusion des trophoblastes humains. Avec une gestion au quotidien des travaux à réaliser en suivant le plan préétabli en début de stage, j'ai formé M. Monthéard à la culture primaire de trophoblastes issus de placenta humain ainsi qu'à différents protocoles biochimiques (immunocytofluorescence, tests de fusion, western-blot et protéine-arrays). M. Monthéard a identifié les protéines intracellulaires présentant des modifications de leur statut de phosphorylation induit par l'exposition des trophoblastes humains au BaP. Les résultats obtenus par M. Monthéard vont être intégrés dans un article scientifique en cours de rédaction (*Pidoux et al. 2012, en préparation*). La validation du stage a permis de confirmer à M. Monthéard son intérêt pour la recherche publique et de poursuivre son cursus universitaire grâce à l'obtention d'un stage de Master 2 dans le but de réaliser une thèse de science à l'Université Paris 7.

3.1.5 Audrey Menault (Master 2)

Dans le cadre du projet ANR 'Placentox', j'ai demandé à A. Menault, d'étudier l'impact de l'exposition du benzo(a)pyrene (BaP) sur la fusion des trophoblastes humains au cours de son stage de Master 2 (10 mois). Afin de respecter le 'workplan' établi dans le projet ANR nous avons convenu ensemble d'une gestion bi-hebdomadaire des travaux à réaliser, du suivi des expérimentations et de l'analyse des données. J'ai formé A. Menault à la culture primaire de trophoblastes issus de placenta humain ainsi qu'à différents protocoles de biologie moléculaires (extraction d'ARN et transcriptome) et de biochimie (immunocytofluorescence, tests de fusion, western-blot, ELISA). A. Menault a démontré la dose cytotoxique maximale de l'exposition trophoblastique au BaP ainsi que son effet néfaste sur la fusion des trophoblastes humains et la formation du syncytiotrophoblaste. Cet effet est véhiculé par certaines voies de signalisation (PKB et PKC). Ces résultats vont être intégrés dans un article scientifique en cours de rédaction (*Pidoux et al. 2012, en préparation*). Les résultats obtenus par A. Menault ainsi que le sujet et le lieu (U767) de son stage de Master 2 lui ont permis d'intégrer dans un contexte compétitif sur dossier l'école de sages-femmes (hôpital Saint-Antoine, Paris, France) comme elle le souhaitait au préalable.

3.2 - La position de postdoc

Depuis Janvier 2012, le laboratoire Inserm U767 a obtenu le financement d'un projet ANR: 'PlacentA5' en collaboration avec le laboratoire du Pr. A. Brisson (UMR-CBMN, Bordeaux, France). Ce projet prévoit jusqu'en 2015 d'étudier le rôle de l'annexin 5 dans la fusion des trophoblastes humains. Dans ce projet, je suis responsable de l'aspect scientifique de la partie à réaliser sur les primo-cultures de trophoblastes (respect du 'workplan', élaboration des expérimentations et orientations scientifiques). Dans le cadre de l'ANR un budget a été prévu pour la rémunération d'une position postdoctorale (18 mois). Cette position a été obtenue par le Dr. S. Degrelle qui possède une excellente connaissance dans le domaine de la reproduction ainsi que dans l'étude de la différenciation des trophoblastes. Ce poste débutera sous ma direction à partir du 1^{er} Janvier 2013. Je prévois avec le postdoc des discussions scientifiques associées d'un suivi hebdomadaire sur l'avancée des recherches, les verrous, le respect du 'workplan' établi dans le projet et sur la mise en place de nouvelles expérimentations. Avec l'équipe 'Cell Fusion' nous avons démontré par l'utilisation de siRNA et d'annexin 5 recombinante l'implication de cette dernière dans le processus de fusion cellule-cellule observé dans le placenta humain. Dr. S. Degrelle va être chargée de la génération de différents mutants et protéines de fusion dans le but de suivre l'expression et la localisation de l'annexin 5 ainsi que les protéines associées dans la cellule trophoblastique au cours de la fusion cellulaire. Le but étant d'obtenir un grand nombre de résultats originaux afin de comprendre le rôle de l'annexin 5 dans le contrôle de la fusion, et de les publier à la fin du contrat de postdoc dans un ou plusieurs articles scientifiques dans des journaux à comité de lecture et ainsi permettre au Dr S. Degrelle de constituer un dossier pour une présentation à un recrutement de statutaire (MCF, CR).

3.3 - L'équipe scientifique: 'Cell Fusion'

Depuis mon retour en France, j'anime le groupe 'Cell Fusion' constitué de statutaires Inserm, notamment d'une technicienne (TCN) en culture cellulaire (Mme F. Ferreira) ainsi qu'une ingénieure d'étude (IE-HC, Dr. P. Gerbaud). Chaque membre de l'équipe permet à son niveau la réalisation de l'ensemble de nos projets scientifiques. Ensemble nous étudions les

événements moléculaires intervenant dans le processus de fusion cellule-cellule des trophoblastes humain.

3.3.1 - TCN Inserm (Mme F. Ferreira)

Mme F. Ferreira a rejoint l'unité Inserm U767 en 2005 en tant que vacataire Inserm. Au cours de ma thèse, je l'ai formée à la culture primaire de trophoblastes issus de placenta humain ainsi qu'aux différentes techniques de culture de lignée cellulaire (MA-10, BeWo et JEG3). En 2006, elle a obtenu un poste de statutaire AJT Inserm dédié à la culture cellulaire aux concours externes. Depuis mon retour en France, l'équipe 'Cell Fusion' a entraîné Mme F. Ferreira pour se présenter aux concours internes de techniciens de l'Inserm (rédaction du dossier et préparation de l'oral). En 2011 et pour sa première présentation, Mme F. Ferreira a obtenu un poste de TCN Inserm dédié à la culture primaire de trophoblastes humains. Depuis 2006 et son entrée à l'Inserm, le travail de Mme F. Ferreira a été valorisé en étant cité comme co-auteur ou cité dans les remerciements de plusieurs articles scientifiques à comité de lecture (*Pidoux et al. 2007, J Cell Physiol* et *Pidoux et al. 2007, Endocrinology*, *Gerbaud et al. 2011, Endocrinology*). Mme F. Ferreira est le référent auprès des maternités parisiennes pour l'organisation de l'obtention des placentas humains (signature des consentements, planning). Toutes les semaines nous organisons ensemble le planning hebdomadaire des cultures cellulaires à réaliser en fonction des priorités des différentes expérimentations en tenant compte du planning du recueil des prélèvements. Nous suivons ensemble la qualité de chaque mise en culture de trophoblaste humain, l'ensemencement nécessaire pour les différentes expérimentations, mais aussi le suivi qualité de la culture primaire (index de fusion et sécrétion d'hCG). Le travail de F. Ferreira est primordial et indispensable pour l'équipe 'cell fusion', car il est le point de départ de l'ensemble de nos projets scientifiques avec la mise en culture des trophoblastes nécessaires pour les différentes expérimentations.

3.3.2 - IE-HC Inserm (Dr. P. Gerbaud)

Dr. P. Gerbaud a été recrutée à l'Inserm en 1980, elle accède au poste d'IE2 Inserm en 1994 dans le laboratoire dirigé par le Dr. Evain-Brion. Elle soutient et obtient sa thèse de science en 1996. En 2006, alors rattachée au groupe dirigé par le Dr. J-L Frendo, elle accède au poste d'IE1 Inserm. Depuis mon retour de postdoc et grâce à un dossier scientifique remarquable

elle accède au poste d'IE-Hors Classe (IE-HC) en 2012. Le Dr. P. Gerbaud joue un rôle essentiel dans l'équipe 'Cell Fusion'. En effet, sa connaissance et son expertise de la biochimie et de biologie cellulaire permettent d'élaborer des protocoles originaux ainsi que trouver des solutions afin de faire sauter les verrous des différents projets scientifiques. Dans l'équipe, a et a été responsable de différents projets scientifiques qui ont été publiés ou sont en cours de rédaction (rôle du mésenchyme dans la fusion et LHR soluble). Depuis mon retour en France, le Dr. P. Gerbaud a souhaité être responsable des approches techniques et méthodologiques de différents projets scientifiques (*voir projets et prospective: Détermination du message fusogène ainsi que rôle de l'AKAP18 dans la fusion cellule-cellule*). Des réunions hebdomadaires sont réalisées avec le Dr. P. Gerbaud afin d'analyser ensemble les résultats, de planifier les expérimentations suivantes ainsi que les orientations scientifiques à suivre suite aux analyses des résultats et/ou bibliographiques. Depuis de nombreuses années les résultats du Dr. P. Gerbaud ont été validés et intégrés dans différents articles scientifiques à comité de lecture, que nous avons en commun soit en tant que co-premier auteur soit en tant que co-auteur (*Pidoux et al. 2007, J Cell Physiol; Pidoux et al. 2007, Endocrinology; Gerbaud et al. 2010, Am J Physiol Cell Ph; Gerbaud et al. 2011, Endocrinology*). Le travail, l'autonomie ainsi que le profil du Dr. P. Gerbaud sont essentiels au groupe 'Cell Fusion'. Son expérience et son expertise dans les domaines des sciences biologiques ainsi que les qualités techniques font du Dr. P. Gerbaud un élément indispensable de l'équipe pour la progression et la validation des projets scientifiques.

PROJETS ET PROSPECTIVE

Différenciation du trophoblaste humain - Implication des macrocomplexes PKA/AKAP lors de la fusion cellule-cellule

I. Etat de l'art:

Les processus de fusion en biologie sont des phénomènes complexes et essentiellement basés sur l'étude de la fusion d'une vésicule lipidique avec la membrane plasmique. En revanche les processus de fusion cellule-cellule sont plus rares et moins étudiés. Dans le placenta humain, la fusion cellulaire joue un rôle primordial. Elle est l'étape limitante de la différenciation du trophoblaste et ce processus est déclenché par l'activation de la voie de signalisation AMPc-PKA.

Il existe avant et durant le phénomène de fusion une importante réorganisation du cytosquelette et de la membrane plasmique. Ces changements sont dus à l'activation de voies de signalisation spécifique, préparant la cellule pour la fusion cellule-cellule.

Les messages intracellulaires induits doivent être étroitement régulés à différents niveaux afin de garantir la spécificité de la réponse cellulaire et ceci au milieu de la multitude des signaux présents dans la cellule. La spécificité de la réponse est due à l'implication de protéines spécifiques et adaptées. Toute signalisation est régulée au niveau spatial (concept de localisation cellulaire des protéines impliquées) et temporel.

Le but de ce projet est d'étudier et de déterminer les protéines impliquées dans le processus de fusion cellulaire en utilisant le modèle privilégié de différenciation des trophoblastes humains.

1.1 - Différenciation des cytotrophoblastes villex en syncytiotrophoblaste

Peu de cellules humaines sont capables de fusionner pour donner naissance à un syncytium multinucléé. Ce processus est présent dans la formation de myotubes (Wakelam, 1985), d'ostéoclastes (Zamboni Zallone et al., 1984) et du syncytiotrophoblaste placentaire (Midgley et al., 1963).

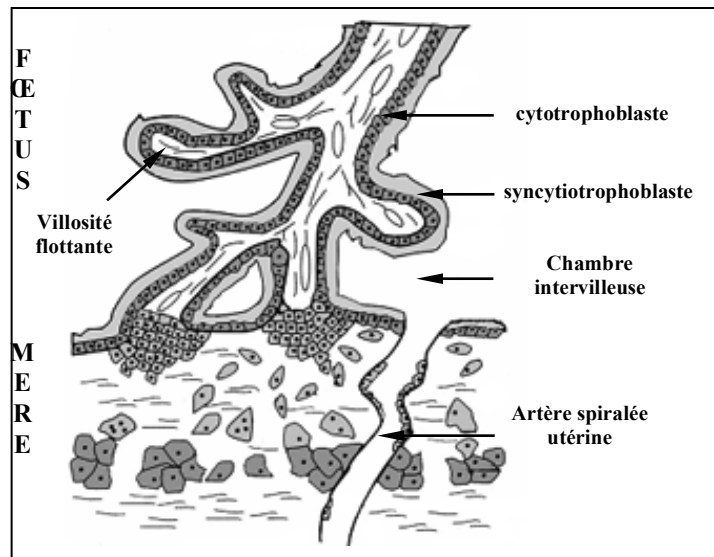


Fig.5: Représentation schématique de l'interface materno-placentaire.

Dans le placenta humain, le trophoblaste villex est la couche épithéliale qui couvre l'arborisation des villosités placentaires et qui est en contact direct avec le sang maternel à la fin du premier trimestre de la grossesse. Il est formé d'une couche de cellules mononucléées cytotrophoblastiques couverte du syncytiotrophoblaste. Ce syncytiotrophoblaste est en contact avec le sang maternel dans la chambre intervillieuse à la fin du premier trimestre de la grossesse (Midgley et al., 1963). **Le syncytiotrophoblaste joue un rôle majeur au cours de la grossesse. C'est le site de toutes les fonctions placentaires:** échange d'ions et de nutriments entre le fœtus et la mère, synthèse de stéroïdes et des hormones peptidiques indispensables pour le déroulement de la grossesse et la croissance fœtale (Eaton and Contractor, 1993; Ogren and Talamantes, 1994) (Fig.5). Certaines des hormones syncytiotrophoblastiques, telles que l'hCG (hormone chorionique gonadotrope humaine) et l'hPL (hormone placentaire lactogène humaine) sont spécifiques de la grossesse et sont utilisées comme marqueurs de la formation syncytiale ((Alsat et al., 1997; Handwerger, 1991; Jameson and Hollenberg, 1993).

Le trophoblaste villex se forme et se régénère tout au long de la grossesse. La régénération des trophoblastes villex incluent 1: la prolifération et la différenciation des cytotrophoblastes mononucléés, 2: la fusion de ces derniers avec la couche constituée du syncytiotrophoblaste, 3: l'extrusion de matériel apoptotique dans la circulation maternelle. Une balance altérée entre prolifération et apoptose du trophoblaste villex entraînent une dérégulation des fonctions du syncytiotrophoblaste. Les extrusions apoptotiques normales (reflet du "turnover" syncytial)

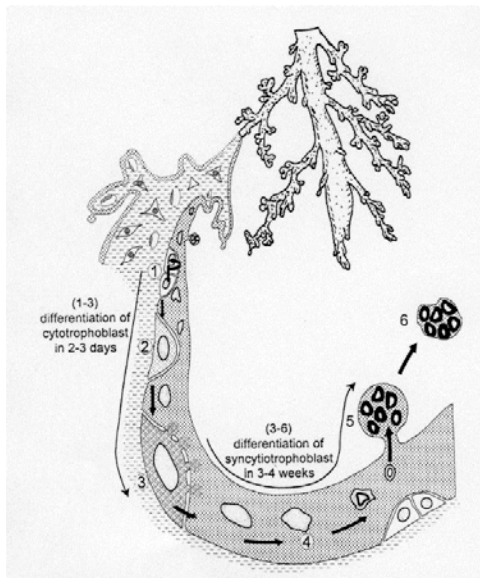


Fig.6: Représentation schématique de la régénération syncytiale dans le placenta humain. (de Huppertz 2004).

sont remplacées par des extrusions nécrotiques (reflet de la souffrance placentaire). **Toute altération du processus de régénération du syncytiotrophoblaste est responsable d'un défaut de fonctionnement placentaire** associée à un défaut de synthèse et de sécrétion des hormones placentaires, une diminution dans l'apport des nutriments et de l'oxygène au fœtus, entraînant la souffrance fœtale (Fig.6). C'est ce qui est observé et établi de longue date dans les pathologies de la grossesse d'origine placentaire telle la prééclampsie ou le retard de croissance intra utérin (RCIU) (Huppertz and Kingdom, 2004).

L'étape limitante de la régénération trophoblastique est le processus de fusion des cellules trophoblastiques, qui est un phénomène peu compris et peu étudié. La mise au point de cultures primaires de trophoblastes humains a révélé qu'*in vitro*, les cytotrophoblastes mononucléés isolés à partir de placenta humain s'agrègent et fusionnent pour former un syncytiotrophoblaste multinucléé non prolifératif. Cette différenciation morphologique s'accompagne d'une différenciation fonctionnelle, avec l'expression de gènes spécifiques du syncytiotrophoblaste. La fusion s'accompagne notamment d'une augmentation de la synthèse et de la sécrétion dans le milieu de culture des hormones de la grossesse normalement sécrétées dans le sang maternel, tel que l'hCG et l'hPL (Alsat et al., 1991; Kliman et al., 1986).

Différents facteurs sont connus pour moduler *in vitro* la différenciation du trophoblaste

villeux humain, incluant l'EGF et l'expression de son récepteur (Alsat et al., 1993; Morrish et al., 1987), l'AMPC et la protéine kinase A (PKA) (Keryer et

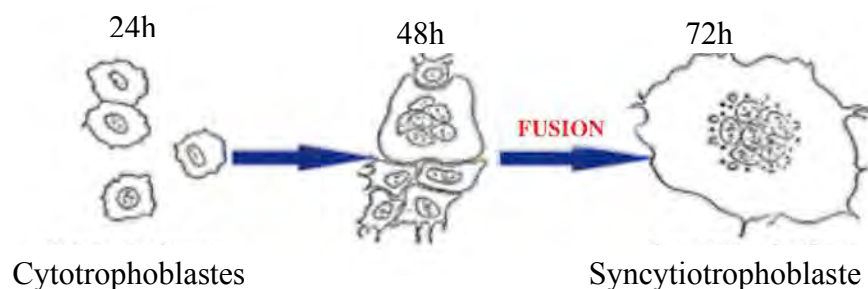


Fig.7: Représentation schématique de la fusion trophoblastique (d'après Kliman 1986).

al., 1998), l'hCG et son récepteur (Pidoux et al., 2007), le TGFβ (Morrish et al., 1991) et l'hypoxie (Alsat et al., 1996). Cependant les protéines membranaires directement impliquées

dans le processus de fusion cellule-cellule sont trop peu connues et les études sur leur implication dans la fusion doivent être approfondies (Malassine et al., 2010).

La fusion cellule-cellule est un processus dynamique complexe qui peut être résumé ainsi: 1/ les cellules doivent quitter leur état prolifératif et exprimer des gènes et des protéines impliqués dans la fusion cellulaire. 2/ les cellules doivent reconnaître et interagir avec leurs partenaires de fusion, permettant une communication entre les deux cellules et l'échange de signaux fusogènes spécifiques. Cette étape entraîne une réorganisation du cytosquelette indispensable à l'agrégation cellulaire ; la protéine zona occludens 1 (ZO-1) joue un rôle dans cette étape (Pidoux et al., 2010). L'étape de communication entre cellules, pré-requis à la fusion cellulaire (Frendo et al., 2003a) implique la connexin 43 (Cx43), protéine des jonctions communicantes. 3/ la fusion cellule-cellule prend place avec la fusion des couches lipidiques des deux membranes cellulaires. En utilisant un modèle physiologique, le laboratoire Inserm U767 a précédemment montré le rôle direct de la syncytin-1 (protéine d'enveloppe rétrovirale endogène) lors de cette dernière étape (Frendo et al., 2003b). Les cadherins (Getsios and MacCalman, 2003) et les protéines de la famille des ADAMs (Morrish et al., 2007) ont aussi été montrées comme jouant un rôle dans le processus de fusion.

Ce processus dynamique doit être étroitement régulé dans l'espace et le temps afin de coordonner chaque étape pour que la fusion cellulaire s'opère (Fig.7). De manière intéressante, l'activation de la PKA est responsable de l'induction de l'expression des syncytins, des cadherins, de la Cx43, de certaines ADAM et de l'hCG (Chen et al., 2008; Coutifaris et al., 1991; Darrow et al., 1996; Feinman et al., 1986; Gao et al., 2007; Knerr et al., 2005).

1.2 - La voie de signalisation de la protéine kinase A (PKA)

La voie de signalisation orchestrée par la PKA est caractérisée en détail dans un grand nombre de types cellulaires et d'organes. L'activation de cette dernière implique la fixation d'un ligand extracellulaire à un récepteur à sept domaines transmembranaires couplé aux protéines G (RCPG) (Sutherland and Rall, 1958), une isoforme de l'adénylate cyclase *via* les protéines G va synthétiser de l'AMPc (3',5' monophosphate cyclique) (Levitzki, 1988; Pierce et al., 2002) (Fig.8). Bien que d'autres effecteurs de l'AMPc aient été identifiés (Epac, canaux ioniques AMPc dépendant), l'effecteur le plus commun est la PKA. La voie de signalisation de l'AMPc-PKA est notamment impliquée dans la régulation du cycle cellulaire, la prolifération et la différenciation mais aussi dans la régulation des mécanismes de transport

intracellulaire, des flux d'ions et bien d'autres processus cellulaires. La génération et la dégradation de l'AMPc sont régulées par l'adénylyl cyclase d'une part et les phosphodiesterase (PDEs) d'autre part (Soderling and Beavo, 2000; Sunahara et al., 1996). La PKA est généralement reconnue comme étant l'effecteur principal de la voie de signalisation lié à l'AMPc.

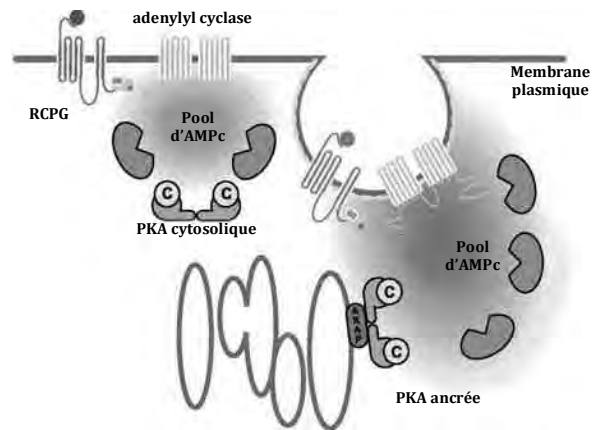


Fig.8: Représentation schématique de l'activation de la voie de signalisation AMPc-PKA (d'après Tasken 2004).

La PKA est une holoenzyme

trétramérique composée de deux sous-unités catalytiques (C) qui sont maintenues dans une conformation inactive par un dimère de sous-unité régulatrices (R) (Corbin et al., 1973).

La sous-unité R existe sous deux formes RI et RII, alors qu'une seule forme de la sous-unité C est présente dans les cellules eucaryotes. Les deux sous-unités R (RI et RII) et la sous-unité C existent sous plusieurs isoformes (RI α , RI β , RII α , RII β , C α , C β , C γ). Bien qu'il existe une différence majeure de distribution tissulaire, il existe aussi des différences dans les propriétés biochimiques et physicochimiques des isoformes de la sous-unité R. L'holoenzyme possède deux sous-unités C associées à un homo- ou hétérodimère de RI ou RII (Scott, 1991) (Tasken et al., 1993). Les sous-unités C ne sont jamais associées ensemble directement. L'activation des sous-unités C est obtenue après la fixation de deux molécules d'AMPc sur chaque sous-unité R responsable de la dissociation et activation de la sous-unité C. La sous-unité C est une sérine/thréonine kinase qui peut phosphoryler un grand nombre de protéines. Le processus est réversible par l'action de protéines phosphatases (PPs). Les séquences consensus de phosphorylation par la sous-unité C de la PKA sont K/R-R-R-X-S/T et R-X-X-S/T. La PKA de type I est majoritairement localisée dans le cytosol, alors que la PKA de type II est associée à des structures cellulaires et organelles. Pour contrôler la spécificité d'une réponse et des phosphorylations induites par la sous-unité C, la PKA va être compartimentalisée dans la cellule (Scott et al., 1990). Les PKA (de type I et II) peuvent être ancrées à des protéines particulières appelées AKAP (A Kinase Anchoring Protein) qui vont donner une localisation spécifique de la PKA dans la cellule (noyau, membrane plasmique, mitochondries).

Les AKAPs permettent de localiser la PKA dans la cellule et de limiter le nombre de cibles phosphorylées. Bien que les AKAPs contribuent à la spécificité du signal elles contrôlent également la versatilité de la voie de signalisation AMPc-PKA en formant des complexes

macroprotéiques composés de phosphatases (PPs) ou bien de protéines permettant un "cross-talk" avec d'autres voies de signalisations localisées à proximité des substrats protéiques (Diviani and Scott, 2001). L'intégration de phosphodiesterases (PDEs) dans ces complexes assure une régulation temporelle qui s'ajoute à la régulation spatiale orchestrée par les AKAPs dans le contrôle de la voie de l'AMPC (Michel and Scott, 2002; Smith and Scott, 2002). Toutes les AKAPs possèdent un domaine de fixation pour la PKA et un unique domaine localisant le complexe PKA-AKAP spécifiquement à des structures subcellulaires, membranaires ou sur des organelles. Les AKAPs modulent l'activité de multiples protéines cellulaires dans différents systèmes cellulaires.

De par leur rôle central dans l'intégration spatiale et temporelle d'effecteurs et de substrats, les AKAPs fournissent un haut niveau de spécificité et de régulation de la voie de signalisation AMPc-PKA.

II. But, originalité et innovation du projet de recherche

La voie de signalisation AMPc-PKA est impliquée dans la fusion et la différenciation des cellules trophoblastiques. Il a été montré récemment que l'hCG et son récepteur agissent de manière auto/paracrine pour l'induction de la formation syncytiale (Pidoux et al., 2007) par une très forte augmentation d'AMPc intracellulaire. Les événements moléculaires impliqués dans le processus de fusion trophoblastique cellule-cellule ne sont pas encore identifiés. Avant et pendant le processus de fusion, il y a une réorganisation importante des différents compartiments cellulaires (cytosol, membranes et cytosquelette). Cette réorganisation peut être structurale, impliquant des modifications de phosphorylation de protéines ou bien la migration de protéines. Le point commun de tous ces changements observés et intervenant au cours du processus de fusion cellulaire est l'activation de la voie de signalisation AMPc-PKA via l'hCG et son récepteur. La spécificité de la signalisation AMPc-PKA est maintenue par sa régulation dans l'espace et le temps *via* les AKAPs, qui ciblent la PKA dans des compartiments subcellulaires distincts et pour des substrats spécifiques.

Le but de ce projet est:

- D'étudier et caractériser l'ensemble des AKAPs exprimées dans les cellules trophoblastiques.
- D'étudier et comprendre le rôle et l'implication de chaque AKAPs dans le processus de fusion cellule-cellule.

Ces objectifs mèneront à:

1/ La compréhension des mécanismes intracellulaires impliqués dans le processus de fusion et de différenciation de la cellule trophoblastique.

2/ La réalisation de la cartographie des événements à partir de la synthèse de l'AMPc (de la fixation de l'hCG sur son récepteur) au processus de fusion cellule-cellule.

3/ L'identification des protéines ou complexes protéiques impliqués dans le processus de fusion, mais aussi leur régulation spatiale et temporelle.

4/ L'approfondissement des connaissances sur le phénomène de régénération du syncytiotrophoblaste, tissu essentiel du développement foetal.

Ce projet est basé sur l'utilisation *in vitro* d'un modèle innovant de culture primaire des cytotrophoblastes qui a été précédemment développé et caractérisé au sein de l'unité Inserm U767. Les cytotrophoblastes humains isolés, purifiés et mis en culture fusionnent pour former le syncytiotrophoblaste *in vitro*. Le syncytiotrophoblaste synthétise et sécrète dans le milieu de culture les hormones spécifiques de la grossesse (hCG et hPL). Les cellules trophoblastiques sont obtenues à partir de placenta à terme et ensuite stimulées avec de l'hCG recombinante pour induire la fusion cellulaire.

III. Aspects technique et scientifique du projet

3.1 - Introduction et acquis scientifique

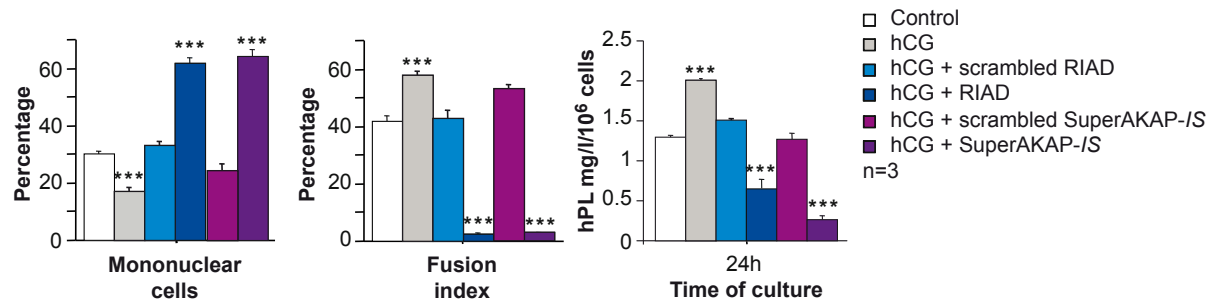


Fig.9: Rôle des peptides 'disruptants' l'ancrage de la PKA dans la fusion des trophoblastes humains. Les cellules sont traitées en présence d'hCG et avec les peptides spécifiques de la PKA de type I (RIAD) ou de type II (SuperAKAP-IS) ou leur témoins respectifs (scrambled). Les histogrammes représentent le nombre de cellules mononucléées (gauche), l'index de fusion (milieu) et la sécrétion d'hPL (droite). (mean \pm SEM de n=3; *** p < 0,001).

J'ai confirmé dans les cellules trophoblastiques la présence de la PKA RI α et RII α ainsi que différentes sous-unités de la sous unité C (α , β et γ) (Keryer et al., 1998). De plus pour établir le rôle fonctionnel de différentes AKAPs impliquées dans le contrôle et la régulation de la fusion trophoblastique, j'ai utilisé différents peptides (RIAD et SuperAKAP-IS), ces peptides permettent de délocaliser la PKA (RI et RII) de leurs ancrages aux AKAPs. En utilisant ces peptides dans les cultures de trophoblastes, j'ai inhibé la fusion cellulaire malgré la présence d'un inducteur (hCG). Ces résultats confirment le rôle indispensable des AKAPs au cours du processus de fusion (Fig.9). De plus ces résultats indiquent que plusieurs AKAPs (spécifiques pour RI ou RII) ou dual-AKAP (spécifiques pour RI et RII) sont impliquées dans la syncytialisation. Par une approche d'AMPc pull down ou RI/RII-flag pull down associée à une analyse par spectrométrie de masse (MS), j'ai déterminé un ensemble d'AKAPs exprimées dans le cytotrophoblaste et le syncytiotrophoblaste (ezrin, D-AKAP1, D-AKAP2, AKAP-KL, AKAP95, AKAP450, myomegalin et AKAP18). Dans un premier temps, l'ezrin a été identifié comme un bon candidat car elle est exprimée en très grande quantité dans la cellule trophoblastique humaine, elle est associée à la membrane plasmique (lieu de la fusion cellulaire). De plus elle a été décrite comme jouant un rôle important dans la structure de la surface cellulaire, l'adhésion, la migration et l'organisation cellulaire. Le 'screening' des AKAPs par siRNA spécifiques m'a permis de démontrer que l'ezrin, l'AKAP18, l'AKAP450,

la myomegalin et dans une moindre mesure la D-AKAP1 ont un rôle dans le contrôle de la fusion cellulaire (Fig.10).

3.2 - Détermination de l'implication de l'ezrin dans la fusion cellule-cellule

3.2.1 Résultats acquis

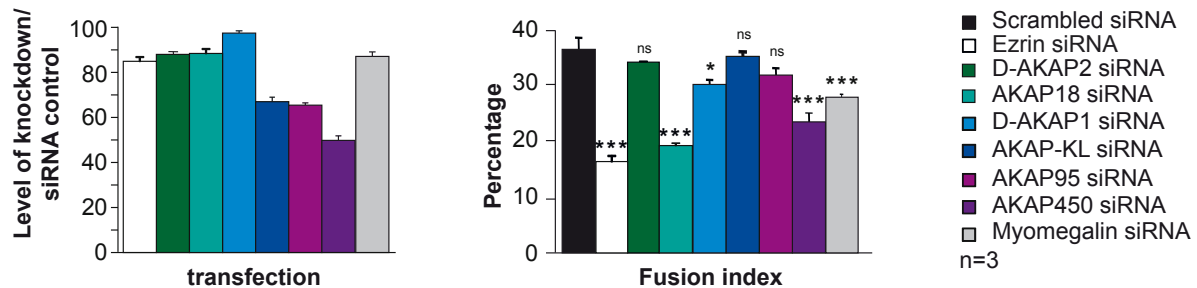


Fig.6: Rôle des différentes AKAPs dans la fusion cellulaire. Les trophoblastes ont été transfectés avec des siRNAs spécifiques des AKAPs identifiées par spectrométrie de masse ou avec un scrambled contrôle. Les histogrammes de gauche représentent le niveau de 'silencing' par rapport au témoin scrambled. Effet des siRNA AKAPs sur la fusion des trophoblastes (droite). (mean \pm SEM de n=3; *** p < 0,001; * p < 0,05; ns pour non spécifique).

Au cours de la formation du placenta humain, les cytotrophoblastes mononucléés fusionnent pour former des syncytia multinucléés sous l'action de l'hCG. Cette fusion est indispensable pour former le tissu responsable des échanges de nutriments et gazeux entre les circulations fœtale et maternelle. L'utilisation de peptides permettant de délocaliser les PKA (type I et type II) de l'ancrage des A-Kinase Anchoring Proteins (AKAPs), m'ont permis de montrer le rôle indispensables des AKAPs au cours de la fusion des trophoblastes (Fig.9). De plus l'utilisation de siRNA spécifique contre l'ezrin a permis de démontrer que cette dernière est une AKAP indispensable pour la régulation du processus de la fusion cellulaire par l'AMPC et la PKA (Fig.10). Des approches d'immunoprécipitations et d'immunolocalisations ont permis de montrer que l'ezrin ancre la PKA dans un complexe moléculaire comprenant la Cx43 et zona occudens 1 (ZO-1) dont le rôle a été précédemment démontré dans la formation des jonctions communicantes impliquées dans la fusion cellulaire (voir chapitre III, section I.1.3). De plus, en associant des expériences alliant le 'silencing' de l'ezrin par la stratégie de siRNA et de reconstitution avec la co-transfection de plasmides insensibles aux siRNAs pour l'ezrin et la Cx43 avec ou sans mutations dans leur domaine de liaison respectifs ou dans le domaine de liaison de la PKA à l'ezrin, ces expérimentations ont permis de montrer que l'ezrin d'une

part fixe la PKA et d'autre part s'associe à la Cx43 pour permettre à la PKA de phosphoryler localement la Cx43 et ainsi contrôler la communication intercellulaire comme prérequis à la fusion des trophoblastes sous induction d'hCG (Fig.11). Ce travail a donné lieu à un article soumis pour publication dans une revue internationale à comité de lecture. (Pidoux G. et al, 2012, *soumis pour publication*) ainsi qu'au dépôt d'un brevet international (DOFI no. 12043 : 'Method to regulate the opening of connexin-43 junctions') dont je suis co-inventeur avec le Pr. K. Tasken.

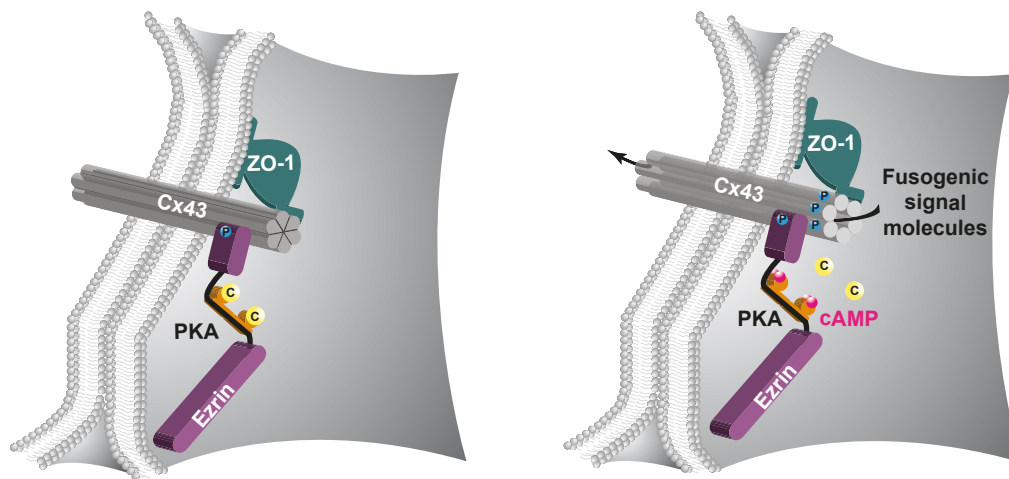


Fig.11: Représentation schématique d'une jonction communicante avec un 'pool' compartimentalisé de PKA ancré à l'eZRin associé à la Cx43 (à gauche). Sous stimulation d'hCG, l'augmentation intracellulaire d'AMPC active la PKA qui induit la phosphorylation locale de la Cx43 et ainsi la communication par les jonctions communicantes. D'après Pidoux et al., 2012.

3.2.2 Rôle des PDEs

L'ancrage de la PKA à l'eZRin permet de phosphoryler la Cx43 et ainsi contrôler l'ouverture de la jonction communicante constitué de la Cx43. Hors l'Inserm U767 a démontré précédemment que la communication intercellulaire est un prérequis à la fusion des trophoblastes (Frendo et al., 2003a). Mes résultats montrent l'importance de ce complexe ainsi que la régulation spatiale de la PKA par son ancrage à l'eZRin et dans le contrôle de la fusion trophoblastique. La régulation temporelle et plus particulièrement le rôle des PDEs n'ont pas été étudiés jusqu'à présent. En effet les PDEs sont des enzymes responsables de la dégradation de l'AMPC en AMP. Cette dégradation permet de contrôler la quantité d'AMPC intracellulaire préalablement synthétisée par les cyclases et par conséquent réguler l'activité de la PKA. Nous allons nous intéresser dans un premier temps au rôle des PDEs dans la

régulation de la fusion des trophoblastes et dans un deuxième temps à l'identification d'une ou de plusieurs PDE(s) associée(s) au complexe PKA/ezrin/Cx43.

Il existe dans la littérature très peu de données sur l'expression des PDEs dans les cellules trophoblastiques, une approche de 'screening' par RT-qPCR sera réalisée (Invitrogen, TaqMan Array Human Phosphodiesterase). Cette approche va nous permettre de déterminer l'expression des ARNm des différentes isoformes de PDEs exprimées dans les cytotrophoblastes mononucléés ainsi que dans les syncytia multinucléés. Les résultats obtenus seront confirmés par western-blot et immunocytofluorescence suite à une collaboration avec Dr. G. Baillie (University of Glasgow, UK). Nous testerons en présence d'hCG (inducteur de la fusion des trophoblastes) l'effet de certains inhibiteurs de PDEs (IBMX, Rolipram, milrinone et cilostamide) sur le processus de fusion cellulaire. L'effet des inhibiteurs de PDEs sur la fusion cellulaire sera quantifié par des tests de fusion (Frendo et al., 2003b).

Dans le but de déterminer si une PDE est associée au complexe PKA/ezrin/Cx43, nous allons réaliser des immunoprecipitations ainsi que des co-immunolocalisations par Duolink (proximity ligation assay) entre la ou les PDE(s) suspectée(s) et les protéines partenaires du complexe PKA/ezrin/Cx43. Des approches par peptide arrays seront réalisées afin de préciser le partenaire de liaison ainsi que la séquence d'acides aminés minimale permettant l'ancrage des deux protéines. Le rôle fonctionnel des PDEs sur la Cx43 sera étudié en s'intéressant par western-blot à son statut de phosphorylation mais aussi par gap-FRAP, dans le but de quantifier et de visualiser l'impact des PDEs sur le complexe PKA/ezrin/Cx43 ainsi que sur le contrôle de la communication intercellulaire et sur l'échange du message fusogène.

3.2.3 Détermination du message fusogène

Les jonctions communicantes *via* la Cx43 sont indispensables à la fusion des trophoblastes (Cronier et al., 2003; Frendo et al., 2003a; Pidoux et al., 2010). Dans une nouvelle étude (Pidoux et al., 2012, *soumis pour publication* et voir chapitre V section III.3.2.1) nous avons mis en évidence la composition du complexe protéique intervenant dans le contrôle des communications intercellulaires indispensables pour l'induction de la fusion des trophoblastes, en revanche la nature du signal fusogène traversant les jonctions communicantes reste à ce jour non identifiée. Le laboratoire du Pr. E. Winterhager a publié récemment que les cellules issues de la lignée JEG3 (choriocarcinome) incapables de fusionner n'expriment pas la Cx43, en revanche lorsque les JEG3 expriment de manière constitutive la Cx43, elles retrouvent

leur capacité à fusionner (Dunk et al., 2012). A partir de cette observation, en s'appuyant sur nos derniers résultats et en collaboration avec le laboratoire du Pr. K. Tasken (Oslo, Norvège) nous réalisons des lignées stables JEG3 Cx43/TET-ON présentant différentes mutations de la Cx43 (dans le domaine de liaison à l'e_zrin et/ou dans le domaine de phosphorylation de la PKA mimant une Cx43 constitutivement active ou inactive). Ces constructions vont nous permettre de déterminer précisément l'impacte de chacune des mutations sur la localisation cellulaire de la Cx43 (immunolocalisation par confocal), sur le contrôle de la fusion cellulaire (tests de fusion), la communication intercellulaire (gap-FRAP) et la nature de la perméabilité aux solutés (message fusogène). En collaboration avec le Dr. P. Vincent (CNRS, Paris 6, Paris) nous utiliserons la technologie FRET associée à l'utilisation de 'Caged Probes' (Caged cAMP, Caged inositol 1,4,5-triphosphate et Caged Ca²⁺) et de microscopie confocal en 'live imaging' (Dr. J. Dompierre, CNRS, Gif) vont nous permettre de mesurer quantitativement et qualitativement mais de manière non physiologique la perméabilité de différents second messagers susceptibles de rentrer dans la composition du message fusogène traversant les différents mutants de la Cx43 que nous avons générés (Pidoux et al., 2012) au cours de la fusion.

Les cellules JEG3 Cx43/TET-ON, présentant différentes mutations de la Cx43 (voir Pidoux et al., 2012) seront co-transfectées par les 'Caged Probes' et par diverses biosenseurs sensibles à l'AMPc (TEpacVV et/ou AKAR4), au calcium (Premo Cameleon Calcium Sensor) ou à l'IP3 (LiBRAvIII ou LiBRAvN). La photoactivation des 'Caged Probes' dans des cellules trophoblastiques en contacts et exprimant le biosenseur, va permettre de suivre la libération du second messager dans le milieu intracellulaire, sa diffusion à la cellule voisine communicante et l'activation du biosenseur correspondant au second messager libéré.

Une seconde approche, plus physiologique prévoit comme précédemment de transfecter les cellules JEG3 Cx43/TET-ON présentant les différents mutants de la Cx43 (Pidoux et al., 2012) par les différents biosenseurs et d'appliquer une pipette de patch-clamp à la surface d'une cellule afin de la stimuler par de l'hCG ou de la forskolin (inducteurs fusogènes). Cette approche va nous permettre de suivre l'activation du ou des biosenseur(s) associée à l'induction de fusion et diffusant à la cellule voisine par les jonctions communicantes.

Ces approches vont nous permettre de déterminer la nature du message fusogène diffusant à travers les Cx43.

3.3 - Détermination de l'implication de l'AKAP18 dans la fusion cellule-cellule

3.3.1 Résultats acquis

Dans une étude préliminaire (voir Fig.10) nous avons observé que l'AKAP18 semble être impliquée dans le contrôle de la fusion. Les différentes isoformes de l'AKAP18 sont décrites comme étant associées soit à la membrane plasmique aux canaux calciques de type L ou associées à la protéine phospholamban au réticulum endoplasmique. L'AKAP18 a été montré comme indispensable dans la régulation de l'homéostasie calcique en ancrant la PKA de type II. Nous avons dans un premier temps confirmé l'effet du 'silencing' de l'AKAP18 sur la fusion des trophoblastes humains (Fig.12).

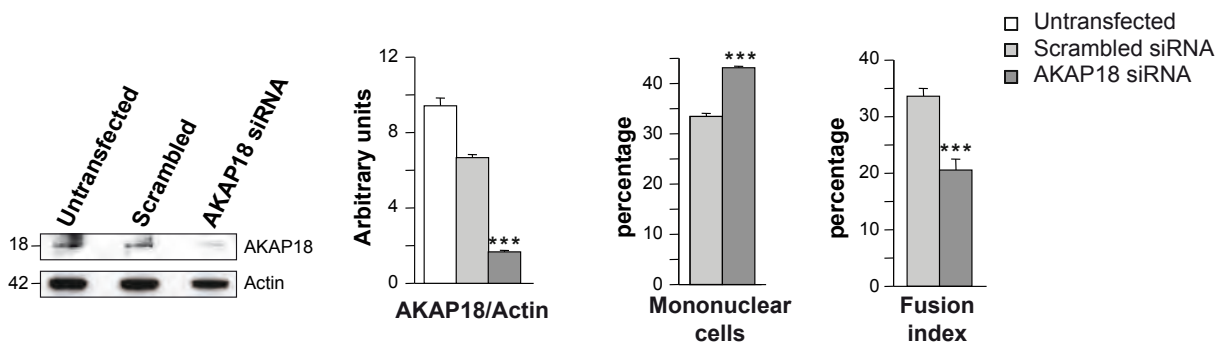


Fig.12: Effet des siRNAs AKAP18 sur la fusion des trophoblastes humains. (à gauche) Analyse par western-blot du niveau d'expression de l'AKAP18 et de l'actin dans des trophoblastes transfecté à 72h de culture ou non par des siRNA contrôle (scrambled) et siRNA spécifiques de l'AKAP18. Les histogrammes (à gauche) représentent le niveau d'expression par densitométrie de l'AKAP18 normalisé par le niveau d'actin. Les histogrammes de droites représentent l'effet des siRNA contrôles et AKAP18 sur la fusion des trophoblastes avec le pourcentage de cellules mononuclées et le pourcentage de l'index de fusion.

3.3.2 Perspectives

Nous allons approfondir nos études sur le rôle de l'AKAP18 dans la fusion des trophoblastes, pour cela nous allons nous intéresser à l'expression et la localisation intracellulaire de l'AKAP18 au cours du processus de fusion cellulaire (western-blot et immunocytofluorescence).

Une approche par pull-down ('tagged-AKAP18') suivie d'une analyse par spectrométrie de masse (MS) sera mise en place dans le but de d'identifier les partenaires protéiques associés à l'AKAP18 (protéines connues ou non comme impliquées dans la fusion, PDEs). Les protéines

d'intérêt identifiées par MS et associées à l'AKAP18 seront confirmées par co-immunoprécipitation et 'proximity ligand assay' (Duolink). Des études de 'peptide arrays' seront réalisées pour déterminer les séquences minimales d'acides aminés nécessaires pour l'interaction entre l'AKAP18 et ces partenaires protéiques.

L'AKAP18 a été montré dans plusieurs systèmes biologiques comme un régulateur de l'homéostasie calcique intracellulaire, nous nous intéresserons par conséquent aux modifications des flux calciques intracellulaires générés au cours de la fusion cellulaire et dans des trophoblastes contrôlés et ceux traités par des siRNA AKAP18. Ces approches expérimentales vont nous permettre de déterminer le rôle fonctionnel de l'AKAP18 et de ces partenaires protéiques dans la fusion des trophoblastes.

3.4 - Détermination de l'implication de l'AKAP450 dans la fusion cellule-cellule

De manière similaire à l'AKAP18, nous avons démontré par l'utilisation de siRNA spécifiques de l'AKAP450 que cette dernière était impliquée dans la fusion des trophoblastes (Fig.10). L'AKAP450, spécifique de la PKA de type II a été démontré dans différents modèles cellulaires comme indispensable à l'organisation et la régulation du cytosquelette et du centrosome. Le réseau de microtubules et le centrosome jouent un rôle important dans les processus de fusion cellulaire. Nous nous intéresserons à l'organisation du cytosquelette et à la localisation de l'AKAP450 au cours du processus de fusion des trophoblastes humains. Nous étudierons l'association de l'AKAP450 avec la réorganisation du cytosquelette au cours de la fusion cellulaire par des expériences de 'silencing' de l'AKAP450. Enfin nous utiliserons les mêmes stratégies d'étude que pour l'AKAP18 (voir 3.3.2) pour identifier les protéines partenaires de l'AKAP450 ainsi que son rôle direct dans la fusion des trophoblastes humains.

IV. Environnement scientifique

Le laboratoire Inserm U767 s'intéresse à un problème majeur de santé publique lié aux pathologies de la grossesse ainsi qu'aux effets toxiques des xénobiotiques et des médicaments sur le développement placentaire. Son directeur, le Dr. D. Evain-Brion dirige un groupe de 26 personnes incluant 3 DR, 2CR, 7 MCU/PHU/PUPH, 2 EI-HC, 2 postdocs, 4 doctorants, 4

étudiants en master, 3 TCN et 1 administratif. Elle possède plus de 155 publications originales (incluant des papiers dans Lancet, Biochem Biophys Res Commun, J Biol Chem, Mol Cell Biol, J Clin Inv, J Cell Sci, Endocrinology, J Immunol, PloS one, J Clin Endocrinol Metab), 2 brevets portant sur la culture primaire de cellules placentaires. Depuis 2007, elle dirige un réseau de thématique de recherche et de soins (RTRS) qui s'intéresse à la grossesse et à la prématurité. Ce RTRS a donné naissance à la fondation de coopération scientifique PremUP. En 2012, et pour une durée de 3 ans, l'U767 a obtenu deux projets financés par l'ANR. L'un spécifique sur le rôle des xénobiotiques dans le développement placentaire (en partenariat avec le laboratoire de toxicologie dirigé par le Pr O. Laprévotte, Paris Descartes). Le deuxième projet financé se propose d'étudier le rôle de l'Annexin 5 dans la réparation membranaire du syncytiotrophoblaste ainsi que la formation de microparticules syncytiales relarguées dans le sang maternel (en partenariat avec le laboratoire de biophysique du Pr. A. Brisson, Bordeaux, France).

L'unité Inserm U767 est reconnue pour ses contributions majeures dans la compréhension de la grossesse normale et pathologique. Le laboratoire cherche à comprendre la physiologie de la grossesse et de développer des approches de diagnostic précoces des pathologies de la grossesse d'origine placentaire (RCIU et pré-éclampsie). De plus le laboratoire reçoit l'assistance d'un échange fructueux avec plusieurs unités de gynécologie obstétrique des hôpitaux de Paris mais aussi d'hormonologie, lui permettant d'obtenir des placentas provenant de grossesses physiologiques et pathologiques.

Enfin, la création du RTRS PremUP permet le transfert de l'expertise aux plateformes techniques de PremUP et ainsi de bénéficier du réseau pour la validation de nouveaux marqueurs sériques des pathologies de la grossesse mais aussi la mise en place de nouvelles stratégies pour la prévention des naissances prématurées et aussi dans la prévention de grossesses associées à une "intoxication" par des xénobiotiques (médicaments, perturbateurs endocriniens ou polluants environnementaux). Dans les prochaines années, l'unité va emménager dans de nouvelles installations (1600 m²), le département "mère-enfant" (P2M) de la faculté des sciences pharmaceutiques de Paris Descartes dans le cadre du financement plan campus. Ce département sera constitué de différentes équipes de l'Inserm, de l'IRD et universitaires qui travailleront sur différentes thématiques mais complémentaires en périnatalité (placenta, prématurité, grossesse ...). La taille des nouvelles installations et la réputation de PremUP attireront des équipes 'ATIP/Avenir' et des professeurs étrangers pour les positions "chaires" PremUP. De plus le laboratoire possède une place importante au sein de l'IMTCE (Institut Médicament-Toxicologie-Environnement). Cette implication au sein de

l'IMTCE me permettra de bénéficier des compétences scientifiques de différentes équipes mais aussi d'avoir accès à plusieurs plateformes techniques (spectrométrie de masse, microscopie confocale, électronique et à balayage, RT-qPCR, phosphorimager, odyssey, biologie structurale, peptides et protéines array, peptides en solution et animalerie).

C'est dans ce cadre que l'Inserm U767 m'offre la possibilité de réaliser ce projet de recherche de manière indépendante et avec une petite équipe ('Cell Fusion') que je dirige. Mes connaissances en biochimie, biologie moléculaire et protéomique seront indispensables pour développer ce projet scientifique qui contribuera à développer l'excellence scientifique de l'Université Paris Descartes grâce à un projet original et à l'utilisation de technologies de pointe.

V. Faisabilité

Je vais développer ce projet au sein de l'équipe 'Cell Fusion' sur le site de l'université Paris Descartes qui inclut :

- L'IMTCE et ses différentes plateformes technologiques telles que: les équipes spécialisées en protéomique (Dr. MC. Menet) en microscopie confocale (Dr. B. Saubamea).
- Des collaborations actives avec les départements d'obstétrique des hôpitaux de Paris au sein du RTRS (Port Royal, Robert Debré, CHIC Créteil) qui me permettent d'obtenir en toute légalité (avec le consentement des patientes) et dans des conditions techniques appropriées des placentas humains.

L'IMTCE me donnera accès à des plateformes comprenant des équipements techniques et des installations d'imageries requis pour l'accomplissement de mon projet. Les bases d'une collaboration futur ont déjà été établis avec le Pr. M. Vidal (Paris Descartes) dans le but de réaliser les analyses par peptide array, indispensables à l'aboutissement des différents projets scientifiques.

Grâce à des résultats obtenus précédemment à l'unité l'Inserm U767, le laboratoire est au centre de collaborations intenses avec deux groupes majeurs français de la recherche sur les rétrovirus endogènes humains. Une des équipes est dirigée par le Dr. F. Mallet (UMR 2714

CNRS-bioMerieux). Ensemble, les deux équipes ont montré que la syncytin-1 était impliquée dans la fusion et la différenciation des trophoblastes humains. L'UMR 8122 CNRS "Rétrovirus Endogène et Eléments Rétroïdes des Eucaryotes Supérieurs" dirigée par le Dr. T. Heidmann constitue le deuxième groupe collaboratif. Les travaux collaboratifs antérieurs ont porté sur l'étude d'une nouvelle famille de rétrovirus endogène humain exprimé dans le trophoblaste humain: la syncytin-2. Pour ces deux rétrovirus endogènes humains rien n'est connu sur leur régulation post-traductionnelle cellulaire et leur possible implication dans des macrocomplexes protéiques fusogéniques.

Enfin je pourrai bénéficier de l'expertise, de conseils, d'échanges scientifiques et collaborations fructueuses avec les membres du "Club AMPc" dont je suis l'initiateur et co-organisateur avec le Dr. P. Vincent (UMR 7624, Paris V). Ce club a débuté en Juin 2011. Il regroupe différents laboratoires Parisiens et Français qui ont pour centre d'intérêt l'AMPc (UMR-S 769, Dr. R. Fischmeister; UMR-S 621, Dr. A-M. Lompre; UMR 8104, Pr. J. Bertherat; BFA EAC 4413, Pr. J. Cohen-Tannoudji; EA4479 Dr. F. Riquet; UMR 1048; Dr. F. Lezoualc'h et d'autres). Ce réseau se réunit tous les trois mois et permet de présenter, d'échanger scientifiquement sur des projets, les travaux en cours, d'avoir des retours objectifs sur les publications en pré-soumission ou dans l'utilisation d'outils spécifiques. Le succès de ce groupe est d'une part dû à son nombre croissant de participant (80 à ce jour) et d'autre part aux échanges de compétences, d'approches, d'outils (FRET, Flex Station, peptides) et aux collaborations scientifiques qui se sont instaurées entre les différents groupes. Nous souhaitons dans le futur demander une création de GDR spécifique.

En conclusion au cours de ma thèse j'ai été formé à l'étude du développement du placenta humain et plus particulièrement à la différenciation du trophoblaste et à ses fonctions hormonales. Au cours de mon post-doc, j'ai développé un projet qui m'a permis de me familiariser avec les dernières technologies utilisées pour l'étude des voies de signalisation liées à l'AMPc et à l'ancrage de la PKA avec notamment un aspect associé à la protéomique. Je suis de retour en France depuis Septembre 2009, où j'anime une petite équipe de recherche ('Cell Fusion') incluant une technicienne Inserm (TCN, F. Ferreira), une ingénieure d'étude hors-classe (IE-HC, Dr. P. Gerbaud) et un futur postdoc (Dr. S. Degrelle). Mon but est de créer au sein du département de périnatalité de l'université Paris Descartes, un groupe d'investigation indépendant sur le thème de la fusion cellulaire.

L'étude et les résultats obtenus sur les événements moléculaires intervenant dans le processus de fusion cellule-cellule observé au niveau des cellules trophoblastiques, placera l'Université Paris Descartes au premier plan dans ce domaine sur la scène internationale. En effet, du fait de la complexité des systèmes biologiques de fusion cellule-cellule ce processus biologique est très peu étudié. Mais les résultats obtenus et les approches utilisées pour mener à bien ce projet intéresseront la communauté scientifique dans les domaines de la fusion cellulaire (muscle, cancer, reproduction), de la signalisation cellulaire, mais aussi dans le domaine du placenta humain et du développement. La publication des données dans des journaux internationaux ainsi que la participation à des congrès internationaux, permettront d'accroître la visibilité du groupe mais aussi celui de l'Université dans la communauté scientifique. La caractérisation des mécanismes conduisant à la fusion et à la régénération des cellules dans le placenta humain fournira de nouvelles pistes pour comprendre et lutter contre les pathologies de la grossesse comme le RCIU ou la pré-éclampsie. Enfin, la caractérisation des événements moléculaires tels que les événements post-traductionnels (état de phosphorylation des protéines) impliqués dans le processus de fusion physiologique pourront fournir de nouvelles pistes pour comprendre, lutter et diagnostiquer les pathologies de la grossesse d'origines placentaires liées ou associées à un défaut de formation ou de régénération du syncytiotrophoblaste.

REFERENCES

- Alsat, E., J. Guibourdenche, D. Luton, F. Frankenne, and D. Evain-Brion. 1997. Human placental growth hormone. *Am J Obstet Gynecol.* 177:1526-1534.
- Alsat, E., J. Haziza, and D. Evain-Brion. 1993. Increase in epidermal growth factor receptor and its messenger ribonucleic acid levels with differentiation of human trophoblast cells in culture. *J Cell Physiol.* 154:122-128.
- Alsat, E., V. Mirlesse, C. Fondacci, M. Dodeur, and D. Evain-Brion. 1991. Parathyroid hormone increases epidermal growth factor receptors in cultured human trophoblastic cells from early and term placenta. *J Clin Endocr Metab.* 73:288-294.
- Alsat, E., P. Wyplosz, A. Malassiné, J. Guibourdenche, D. Porquet, C. Nessmann, and D. Evain-Brion. 1996. Hypoxia impairs cell fusion and differentiation process in human cytotrophoblast, in vitro. *J Cell Physiol.* 168:346-353.
- Blanchette-Mackie, E.J., N.K. Dwyer, T. Barber, R.A. Coxey, T. Takeda, C.M. Rondinone, J.L. Theodorakis, A.S. Greenberg, and C. Londos. 1995. Perilipin is located on the surface layer of intracellular lipid droplets in adipocytes. *J Lipid Res.* 36:1211-1226.
- Brasaemle, D.L., D.M. Levin, D.C. Adler-Wailes, and C. Londos. 2000a. The lipolytic stimulation of 3T3-L1 adipocytes promotes the translocation of hormone-sensitive lipase to the surfaces of lipid storage droplets. *Biochim Biophys Acta.* 1483:251-262.
- Brasaemle, D.L., B. Rubin, I.A. Harten, J. Gruia-Gray, A.R. Kimmel, and C. Londos. 2000b. Perilipin A increases triacylglycerol storage by decreasing the rate of triacylglycerol hydrolysis. *J Biol Chem.* 275:38486-38493.
- Chen, C.P., L.F. Chen, S.R. Yang, C.Y. Chen, C.C. Ko, G.D. Chang, and H. Chen. 2008. Functional characterization of the human placental fusogenic membrane protein syncytin 2. *Biol Reprod.* 79:815-823.
- Cipolat, S., O. Martins de Brito, B. Dal Zilio, and L. Scorrano. 2004. OPA1 requires mitofusin 1 to promote mitochondrial fusion. *Proc Natl Acad Sci U S A.* 101:15927-15932.
- Corbin, J.D., T.R. Soderling, and C.R. Park. 1973. Regulation of adenosine 3',5'-monophosphate-dependent protein kinase. I. Preliminary characterization of the adipose tissue enzyme in crude extracts. *J Biol Chem.* 248:1813-1821.
- Coutifaris, C., L. Kao, H. Sehdev, U. Chin, G. Babalola, O. Blaschuk, and J. Strauss 3d. 1991. E-cadherin expression during the differentiation of human trophoblasts. *Development.* 113:767-777.
- Cronier, L., J.L. Frendo, N. Defamie, G. Pidoux, G. Bertin, J. Guibourdenche, G. Pointis, and A. Malassine. 2003. Requirement of gap junctional intercellular communication for human villous trophoblast differentiation. *Biol Reprod.* 69:1472-1480.
- Darrow, B.J., V.G. Fast, A.G. Kleber, E.C. Beyer, and J.E. Saffitz. 1996. Functional and structural assessment of intercellular communication. Increased conduction velocity and enhanced connexin expression in dibutyryl cAMP-treated cultured cardiac myocytes. *Circ Res.* 79:174-183.
- Diviani, D., and J.D. Scott. 2001. AKAP signaling complexes at the cytoskeleton. *J Cell Sci.* 114:1431-1437.
- Duncan, R.E., M. Ahmadian, K. Jaworski, E. Sarkadi-Nagy, and H.S. Sul. 2007. Regulation of lipolysis in adipocytes. *Annu Rev Nutr.* 27:79-101.
- Dunk, C.E., A. Gellhaus, S. Drewlo, D. Baczyk, A.J. Potgens, E. Winterhager, J.C. Kingdom, and S.J. Lye. 2012. The Molecular Role of Connexin 43 in Human Trophoblast Cell Fusion. *Biology of reproduction.*
- Eaton, B., and S. Contractor. 1993. In vitro assessment of trophoblast receptors and placental transport mechanisms. In *The human placenta*. C.W. Redman, I.L. Sargent, and P.M. Starkey, editors. Blackwell Scientific Publication, London. 471-503.
- Fain, J.N., and J.A. Garcija-Sainz. 1983. Adrenergic regulation of adipocyte metabolism. *J Lipid Res.* 24:945-966.
- Fanning, A.S., B.J. Jameson, L.A. Jesaitis, and J.M. Anderson. 1998. The tight junction protein ZO-1 establishes a link between the transmembrane protein occludin and the actin cytoskeleton. *The Journal of biological chemistry.* 273:29745-29753.
- Feinman, M., H. Kliman, S. Caltabiano, and J.r. Strauss. 1986. 8 Bromo-3', 5'-adenosine monophosphate stimulates the endocrine activity of human cytotrophoblasts in culture. *J Clin Endocrinol Metab.* 63:1211-1217.
- Frendo, J.-L., L. Cronier, G. Bertin, J. Guibourdenche, M. Vidaud, D. Evain-Brion, and A. Malassine. 2003a. Involvement of connexin 43 in human trophoblast cell fusion and differentiation. *J Cell Sci.* 116:3413-3421.

- Frendo, J.-L., J. Guibourdenche, G. Pidoux, M. Vidaud, D. Luton, Y. Giovangrandi, D. Porquet, F. Muller, and D. Evain-Brion. 2004. Trophoblast Production of a Weakly Bioactive Human Chorionic Gonadotropin in Trisomy 21-Affected Pregnancy. *J Clin Endocrinol Metab.* 89:727-732.
- Frendo, J.-L., D. Olivier, V. Cheynet, J.-L. Blond, M. Vidaud, M. Rabreau, D. Evain-Brion, and F. Mallet. 2003b. Direct involvement of HERV-W Env glycoprotein in human trophoblast cell fusion and differentiation. *Mol Cell Biol.* 23:3566-3574.
- Frendo, J.-L., M. Vidaud, J. Guibourdenche, D. Luton, F. Muller, D. Bellet, Y. Giovangrandi, A. Tarrade, D. Porquet, P. Blot, and D. Evain-Brion. 2000. Defect of villous cytotrophoblast differentiation into syncytiotrophoblast in Down syndrome. *J Clin Endocrinol Metab.* 85:3700-3707.
- Frezza, C., S. Cipolat, O. Martins de Brito, M. Micaroni, G.V. Beznoussenko, T. Rudka, D. Bartoli, R.S. Polishuck, N.N. Danial, B. De Strooper, and L. Scorrano. 2006. OPA1 controls apoptotic cristae remodeling independently from mitochondrial fusion. *Cell.* 126:177-189.
- Gao, S., C. De Geyter, K. Kossowska, and H. Zhang. 2007. FSH stimulates the expression of the ADAMTS-16 protease in mature human ovarian follicles. *Mol Hum Reprod.* 13:465-471.
- Getsios, S., and C. MacCalman. 2003. Cadherin-11 modulates the terminal differentiation and fusion of human trophoblastic cells in vitro. *Dev Biol.* 257:41-54.
- Greenberg, A.S., J.J. Egan, S.A. Wek, N.B. Garty, E.J. Blanchette-Mackie, and C. Londos. 1991. Perilipin, a major hormonally regulated adipocyte-specific phosphoprotein associated with the periphery of lipid storage droplets. *J Biol Chem.* 266:11341-11346.
- Greenberg, A.S., J.J. Egan, S.A. Wek, M.C. Moos, Jr., C. Londos, and A.R. Kimmel. 1993. Isolation of cDNAs for perilipins A and B: sequence and expression of lipid droplet-associated proteins of adipocytes. *Proc Natl Acad Sci U S A.* 90:12035-12039.
- Handwerger, S. 1991. The physiology of placental lactogen in human pregnancy. *Endocrinology.* 12:329-336.
- Huppertz, B., and J.C. Kingdom. 2004. Apoptosis in the trophoblast--role of apoptosis in placental morphogenesis. *J Soc Gynecol Investig.* 11:353-362.
- Jameson, J., and A. Hollenberg. 1993. Regulation of chorionic gonadotropin gene expression. *Endocr Rev.* 14:203-221.
- Keryer, G., E. Alsat, K. Tasken, and D. Evain-Brion. 1998. Cyclic AMP-dependent protein kinases and human trophoblast cell differentiation in vitro. *J Cell Sci.* 111:995-1004.
- Kimmel, A.R., D.L. Brasaemle, M. McAndrews-Hill, C. Sztalryd, and C. Londos. 2009. Adoption of PERILIPIN as a unifying nomenclature for the mammalian PAT-family of intracellular, lipid storage droplet proteins. *J Lipid Res.* 51:468-471.
- Kliman, H., J. Nestler, E. Sermasi, J. Sanger, and J. Strauss III. 1986. Purification, characterization, and *in vitro* differentiation of cytotrophoblasts from human term placentae. *Endocrinology.* 118:1567-1582.
- Knerr, I., S.W. Schubert, C. Wich, K. Amann, T. Aigner, T. Vogler, R. Jung, J. Dotsch, W. Rascher, and S. Hashemolhosseini. 2005. Stimulation of GCMA and syncytin via cAMP mediated PKA signaling in human trophoblastic cells under normoxic and hypoxic conditions. *FEBS Lett.* 579:3991-3998.
- Levitzki, A. 1988. From epinephrine to cyclic AMP. *Science.* 241:800-806.
- Londos, C., D.L. Brasaemle, C.J. Schultz, J.P. Segrest, and A.R. Kimmel. 1999. Perilipins, ADRP, and other proteins that associate with intracellular neutral lipid droplets in animal cells. *Semin Cell Dev Biol.* 10:51-58.
- Malassine, A., J.-L. Frendo, and D. Evain-Brion. 2010. Trisomy 21- affected placentas highlight prerequisite factors for human trophoblast fusion and differentiation.. *Int J Dev Biol.* 54:475-482.
- Michel, J.J., and J.D. Scott. 2002. AKAP mediated signal transduction. *Annu Rev Pharmacol Toxicol.* 42:235-257.
- Midgley, A., G. Pierce, G. Denau, and J. Gosling. 1963. Morphogenesis of syncytiotrophoblast in vivo: an autoradiographic demonstration. *Science.* 141:350-351.
- Morrish, D., D. Bhardwaj, L. Dabbagh, H. Marusyk, and O. Siy. 1987. Epidermal growth factor induces differentiation and secretion of human chorionic gonadotropin and placental lactogen in normal human placenta. *J Clin Endocrinol Metab.* 65:1282-1290.
- Morrish, D., D. Bhardwaj, and M. paras. 1991. Transforming growth factor β 1 inhibits placental differentiation and human chorionic gonadotropin and human placental lactogen secretion. *Endocrinology.* 129:22-26.
- Morrish, D.W., Y. Kudo, I. Caniggia, J. Cross, D. Evain-Brion, M. Gasperowicz, M. Kokozidou, C. Leisser, K. Takahashi, and J. Yoshimatsu. 2007. Growth factors and trophoblast differentiation--workshop report. *Placenta.* 28 Suppl A:S121-124.
- Ogren, L., and F. Talamantes. 1994. The placenta as an endocrine organ: polypeptides. In *Physiology of reproduction*. E. Knobil and J. Neill, editors. Raven Press, New-York. 875-945.
- Pidoux, G., P. Gerbaud, S. Gnidehou, M. Grynberg, G. Geneau, J. Guibourdenche, D. Carette, L. Cronier, D. Evain-Brion, A. Malassine, and J.L. Frendo. 2010. ZO-1 is involved in trophoblastic cells differentiation in human placenta. *Am J Physiol Cell Physiol.* 298:C1517-1526.

- Pidoux, G., P. Gerbaud, V. Tsatsaris, O. Marpeau, F. Ferreira, G. Meduri, J. Guibourdenche, J. Badet, D. Evain-Brion, and J.-L. Frendo. 2007. Biochemical characterization and modulation of LH/CG-receptor during human trophoblast differentiation. *J Cell Physiol.* 212:26-35.
- Pierce, K.L., R.T. Premont, and R.J. Lefkowitz. 2002. Seven-transmembrane receptors. *Nat Rev Mol Cell Biol.* 3:639-650.
- Scott, J.D. 1991. Cyclic nucleotide-dependent protein kinases. *Pharmacol Ther.* 50:123-145.
- Scott, J.D., R.E. Stofko, J.R. McDonald, J.D. Comer, E.A. Vitalis, and J.A. Mangili. 1990. Type II regulatory subunit dimerization determines the subcellular localization of the cAMP-dependent protein kinase. *J Biol Chem.* 265:21561-21566.
- Shi, Q., Z. Lei, C. Rao, and J. Lin. 1993. Novel role of human chorionic gonadotropin in differentiation of human cytotrophoblasts. *endocrinology.* 132:1387-1395.
- Smith, F.D., and J.D. Scott. 2002. Signaling complexes: junctions on the intracellular information super highway. *Curr Biol.* 12:R32-40.
- Soderling, S.H., and J.A. Beavo. 2000. Regulation of cAMP and cGMP signaling: new phosphodiesterases and new functions. *Curr Opin Cell Biol.* 12:174-179.
- Souza, S.C., K.V. Muliro, L. Liscum, P. Lien, M.T. Yamamoto, J.E. Schaffer, G.E. Dallal, X. Wang, F.B. Kraemer, M. Obin, and A.S. Greenberg. 2002. Modulation of hormone-sensitive lipase and protein kinase A-mediated lipolysis by perilipin A in an adenoviral reconstituted system. *J Biol Chem.* 277:8267-8272.
- Sunahara, R.K., C.W. Dessauer, and A.G. Gilman. 1996. Complexity and diversity of mammalian adenylyl cyclases. *Annu Rev Pharmacol Toxicol.* 36:461-480.
- Sutherland, E.W., and T.W. Rall. 1958. Fractionation and characterization of a cyclic adenine ribonucleotide formed by tissue particles. *J Biol Chem.* 232:1077-1091.
- Tansey, J.T., A.M. Huml, R. Vogt, K.E. Davis, J.M. Jones, K.A. Fraser, D.L. Brasaemle, A.R. Kimmel, and C. Londos. 2003. Functional studies on native and mutated forms of perilipins. A role in protein kinase A-mediated lipolysis of triacylglycerols. *J Biol Chem.* 278:8401-8406.
- Tasken, K., B.S. Skalhegg, R. Solberg, K.B. Andersson, S.S. Taylor, T. Lea, H.K. Blomhoff, T. Jahnsen, and V. Hansson. 1993. Novel isozymes of cAMP-dependent protein kinase exist in human cells due to formation of RI alpha-RI beta heterodimeric complexes. *J Biol Chem.* 268:21276-21283.
- Wakelam, M. 1985. The fusion of myoblasts. *Biochem J.* 15:1-12.
- Wright, A., Y. Zhou, J.F. Weier, E. Caceres, M. Kapidzic, T. Tabata, M. Kahn, C. Nash, and S.J. Fisher. 2004. Trisomy 21 is associated with variable defects in cytotrophoblast differentiation along the invasive pathway. *Am J Med Genet A.* 130:354-364.
- Zamboni Zallone, A., A. Teti, and M. Primavera. 1984. Monocytes from circulating blood fuse in vitro with purified osteoclasts in primary culture. *J Cell Sci.* 66:335-342.

Biochemical Characterization and Modulation of LH/CG—Receptor During Human Trophoblast Differentiation

GUILLAUME PIDOUX,¹ PASCALE GERBAUD,¹ VASSILIS TSATSARIS,^{1,4} OLIVIER MARPEAU,¹ FATIMA FERREIRA,¹ GERI MEDURI,² JEAN GUIBOURDENCHE,^{1,3} JOSETTE BADET,¹ DANIELÈ EVAIN-BRION,¹ AND JEAN-LOUIS FRENDO^{1,5*}

¹INSERM, Université Paris, Paris, France

²INSERM, Le Kremlin-Bicêtre, France

³CHU Paris, Hôpital Robert Debré, Service d'Endocrinologie, Paris, France

⁴AP-HP, Hôpital Cochin, Maternité Port-Royal, Paris, France

⁵CNRS, Paris, France

Due to the key role of the human chorionic gonadotropin hormone (hCG) in placental development, the aim of this study was to characterize the human trophoblastic luteinizing hormone/chorionic gonadotropin receptor (LH/CG-R) and to investigate its expression using the *in vitro* model of human cytotrophoblast differentiation into syncytiotrophoblast. We confirmed by *in situ* immunocytochemistry and in cultured cells, that LH/CG-R is expressed in both villous cytotrophoblasts and syncytiotrophoblasts. However, LH/CG-R expression decreased during trophoblast fusion and differentiation, while the expression of hCG and hPL (specific markers of syncytiotrophoblast formation) increased. A decrease in LH/CG-R mRNA during trophoblast differentiation was observed by means of semi-quantitative RT-PCR with two sets of primers. A corresponding decrease (~60%) in LH/CG-R protein content was shown by Western-blot and immunoprecipitation experiments. The amount of the mature form of LH/CG-R, detected as a 90-kDa band specifically binding ¹²⁵I-hCG, was lower in syncytiotrophoblasts than in cytotrophoblasts. This was confirmed by Scatchard analysis of binding data on cultured cells. Maximum binding at the cell surface decreased from 3,511 to about 929 molecules/seeded cells with a *K*_d of 0.4–0.5 nM. Moreover, on stimulation by recombinant hCG, the syncytiotrophoblast produced less cyclic AMP than cytotrophoblasts, indicating that LH/CG-R expression is regulated during human villous trophoblast differentiation.

J. Cell. Physiol. 212: 26–35, 2007. © 2007 Wiley-Liss, Inc.

Human chorionic gonadotropin (hCG) belongs to a family of glycoprotein hormones, which includes lutropin (LH), thyrotropin (TSH) and follitropin (FSH). These hormones composed of two noncovalently linked subunits, alpha (α) and beta (β), are active on bicomplex form. The α-subunit is common to all glycoprotein hormones, whereas the β-subunits confer the hormonal specificity (Pierce and Parsons, 1981). Alpha hCG is encoded by a single gene and βhCG by six genes, one of which, *CGβ5*, is predominantly expressed in the placenta (Bo and Boime, 1992). HCG is essential for the initiation and maintenance of early pregnancy. After implantation, hCG is produced by the placenta and mainly by the trophoblast (Hoshina et al., 1985; Kliman et al., 1986; Muyan and Boime, 1997; Handschuh et al., 2007). It is used as a diagnostic marker of pregnancy.

The human placenta is characterized by extensive invasion of the trophoblast in the maternal uterus, creating direct trophoblast contact with maternal blood (haemochorial placentation). In early pregnancy, mononuclear cytotrophoblasts (CT) proliferate and invade the maternal endometrium to form the anchoring villi (Aplin, 1991). Cytotrophoblasts also differentiate into a multinucleated continuous layer known as the syncytiotrophoblast (ST). This cell layer, which covers the chorionic villi, is bathed by maternal blood in the intervillous spaces from early gestation (Richard, 1961; Midgley et al., 1963; Boyd and Hamilton, 1970; Benirschke and Kaufmann, 2000). This syncytiotrophoblast is

multifunctional, but its primary functions are exchange of oxygen, nutrients, removal of waste products and hormone production. The syncytiotrophoblast secretes hCG in large amounts, directly into the maternal blood bathing the chorionic villi in the intervillous space.

The mechanisms underlying villous trophoblast differentiation remain largely to be explored. Syncytiotrophoblast formation *in vivo* and *in vitro* arises from villous cytotrophoblast fusion and differentiation. Several factors modulate villous trophoblast differentiation, including EGF (epidermal growth factor) and

Guillaume Pidoux and Pascale Gerbaud are contributed equally to the work.

Contract grant sponsor: la Caisse d'Assurance Maladie des Professions Libérales Province.

*Correspondence to: Jean-Louis Frendo, INSERM U767, Faculté de Pharmacie, 4 Avenue de l'Observatoire, 75270 Paris, France.
E-mail: jean-louis.frendo@univ-paris5.fr

Received 3 July 2006; Accepted 22 November 2006

DOI: 10.1002/jcp.20995

EGF receptor expression (Morrish et al., 1987; Alsat et al., 1993), hypoxia (Alsat et al., 1996), cAMP-dependent protein kinase (PKA) (Keryer et al., 1998), granulocyte-macrophage stimulating factor (Garcia-Lloret et al., 1994), transforming growth factor β (TGF β) (Morrish et al., 1991) and oxidative stress due to overexpression of copper zinc superoxide dismutase (Frendo et al., 2000a, 2001). The molecular mechanisms underlying trophoblast membrane fusion are poorly understood. Proteins involved in cell adhesion (cadherin 11) (Getsios and MacCalman, 2003) and cell–cell communication (connexin 43) (Frendo et al., 2003a) are known to be directly involved. We recently demonstrated the direct involvement of syncytin 1, a human endogenous retroviral envelope glycoprotein (Frendo et al., 2003b), and the presence of syncytin 2, restricted to some villous cytotrophoblasts (Malassine et al., 2007). Several studies suggest that hCG stimulates villous trophoblast differentiation by acting on the LH/CG-R (Shi et al., 1993; Cronier et al., 1994; Yang et al., 2003). This receptor, which has seven transmembrane domains, belongs to the superfamily of G protein-coupled receptors (Pierce and Parsons, 1981; Loosfelt et al., 1989; McFarland et al., 1989; Minegishi et al., 1990). The LH/CG receptor gene has been cloned in pig, mouse, rat and human; in humans it is composed of 11 exons and 10 introns, and its coding region is over 60 kb long (Segaloff and Ascoli, 1993). HCG binding to its receptor activates adenylyl cyclase, phospholipase C and ion channels, which in turn control cellular cAMP, inositol phosphates, Ca²⁺ and other secondary messengers (Gudermann et al., 1992; Hipkin et al., 1992). The presence of LH/CG-R in human placenta was first described by Alsat (Alsat and Cedar, 1974) and has since been confirmed by other authors (Reshef et al., 1990; Lei and Rao, 1992). Inhibition of LH/CG-R expression by specific antisense oligodeoxynucleotides during cytotrophoblast culture results in time- and concentration-dependent inhibition of cytotrophoblast differentiation, showing that hCG, via its receptor, is an autocrine and paracrine regulator of human placental syncytiotrophoblast formation (Yang et al., 2003). Most of the studies actually done, have used transfected cells with cDNA from LH/CG-receptor in rat or mouse models. In human, the characterization and the modulation of LH/CG-R expression during syncytiotrophoblast formation is poorly documented. Here we used the physiological model of cultured primary human trophoblasts (Kliman et al., 1986; Frendo et al., 2000b), in which isolated mononuclear cytotrophoblasts differentiate and fuse to form a syncytiotrophoblast, which secretes large amounts of hCG and other pregnancy-related hormones. We used various methodological approaches to characterize the hCG/LH receptor, and observed its down-regulation during villous trophoblast differentiation. This was confirmed by in situ immunolocalization of the hCG receptor in sections of human placenta.

Materials and Methods

Placental tissue collection and trophoblast cell culture

These studies were performed in agreement with our local ethics committee and with written informed consent of patients. Third trimester placentas were obtained immediately after iterative Caesarian section from healthy mothers delivered at 35–39 weeks of amenorrhoea. First trimester placentas (7–12 weeks of gestation) were collected following legal voluntary interruption of pregnancy from women who gave their written informed consent. Cytotrophoblasts were isolated as previously described (Alsat et al., 1993). After sequential trypsin (0.25%)/DNase I digestion followed by Percoll gradient centrifugation (Frendo et al., 2003a), the cells were further purified by negative selection to obtain a trophoblast preparation not contaminated by other cells, by using a monoclonal anti-human leukocytic antigen A, B and C antibodies (VV6-32HL, Sera Lab, Crawley Down, UK) according to a published method (Schmon et al., 1991;

Cronier et al., 2002). This antibody reacts with most cell types (e.g., macrophages, fibroblasts, extravillous trophoblasts) but not with villous cyto- or syncytiotrophoblast. Cytotrophoblasts were diluted to a final density of 2.7×10^6 cells in 3 ml of minimum essential medium (MEM) containing 10% fetal calf serum (FCS). Cells were plated in 60-mm plastic dishes (TPP, Trasadingen, Switzerland) and incubated at 37°C in 5% CO₂. Cytokeratin 7 immunocytochemistry was performed to confirm the cytotrophoblastic nature of the attached cells: about 95–98% of the cells were positively stained.

Hormone assay

The hCG concentration was determined in culture medium after 24 and 72 h of culture by using an enzyme-linked fluorescence assay (Vidas System, BioMerieux, Marcy l'Etoile, France) with a detection limit of 2 mIU/ml. The hPL concentration was determined in fourfold-concentrated conditioned medium by using a method (Amerlex IRMA, GE Healthcare, Saclay, France) with a detection limit of 0.5 μ g/ml. All reported values are means \pm SEM of triplicate determinations.

Immunohistochemistry

Placental samples were obtained after first-trimester abortion. They were fixed by incubation in 4% formalin for 4–12 h at room temperature and then embedded in paraffin, dewaxed in xylene and rehydrated in ethanol/water. Immunostaining was performed with a universal streptavidin-peroxidase immunostaining kit (Peroxidase, Dako LSAB⁺ Kit, DAKO[®], Glostrup, Denmark). Nonspecific binding was blocked by incubation for 5 min in a blocking reagent containing 3% H₂O₂ and then in 3% serum albumin in PBS for 30 min. The sections were incubated with the primary antibody for 30 min at room temperature. The primary antibodies (Table 1) were polyclonal anti-human LH/CG-R (LHR-K15, Santa Cruz Biotechnology, Inc., Heidelberg, Germany, CA, at 2 μ g/ml), monoclonal anti-cytokeratin 7 (M7018, DAKO[®], at 1 μ g/ml), and polyclonal anti-hCG (A0231 against the beta subunit of hCG, DAKO[®], at 2 μ g/ml). Sections were washed in PBS and incubated with a biotinylated secondary antibody for 15 min. They were then washed three times in PBS and incubated with streptavidin conjugated to horseradish peroxidase for 15 min. The sections were washed in PBS and staining was detected by incubation for 30 sec with the DAB (3,3'-diaminobenzidine) chromogen. Controls were performed by incubating the sections with nonspecific IgG at the same concentration as the primary antibody. Successive pre-adsorptions of LH/CG-R antibody with trophoblastic cells in culture abrogate LH/CG-R immunodetection.

Immunocytochemistry

To detect desmoplakin, LH/CG-R, hCG, cytokeratin 7 and hPL, cultured cells were rinsed with PBS, fixed and permeabilized in methanol at -20°C for 8 min. Alternatively, cultured cells were fixed with 4% paraformaldehyde at 4°C for 20 min. After washing once with PBS, the remaining free aldehyde groups were blocked by adding 50 mM N HCl for 10 min. A polyclonal anti-desmoplakin (AHP320, Serotec, Oxford, UK, at 2.5 μ g/ml), two polyclonal anti-LH/CGR (LHR-K15 and LHR-H50, Santa Cruz Biotechnology, Inc., at 2 μ g/ml), two polyclonal anti-hCG (A0231, DAKO[®], at 2 μ g/ml and SC-7821, Santa Cruz Biotechnology, Inc., at 2 μ g/ μ l), a monoclonal

TABLE 1. Antibodies used for immunohistochemistry, immunocytochemistry and Western-blot

Antibody	Antigen	Isotype	Species	Source
M7018	Cytokeratin 7	IgG1 κ	Mouse	Dako
A0231	β hCG and total hCG	Polyclonal	Rabbit	Dako
A0137	hPL	Polyclonal	Rabbit	Dako
SC-25828	LHR (H50) extracellular domain 28–77	Polyclonal	Rabbit	Santa Cruz
SC-26341	LHR (K15) internal region	Polyclonal	Goat	Santa Cruz
AHP320	Desmoplakin	Polyclonal	Rabbit	Serotec
A5060	Actin	Polyclonal	Rabbit	Sigma-Aldrich

anti-cytokeratin 7 (M7018, DAKO[®], at 2.6 $\mu\text{g/ml}$), or a polyclonal anti-hPL (A0137, DAKO[®], at 1.6 $\mu\text{g/ml}$) was then applied (Table 1), followed by fluorescein isothiocyanate-labeled goat anti-mouse IgG, or fluorescein isothiocyanate-labeled goat anti-rabbit IgG (Jackson Immuno Research, Baltimore, MD, at 1:150), or Alexa 488-labeled donkey anti rabbit (Molecular probes, Inc., Eugene, OR, at 1:400), or Texas red labeled donkey anti goat (Jackson Immuno Research, at 1:400), or Cy^{TM3} goat anti-rabbit IgG, as previously described (Frendo et al., 2001). The controls, which consisted of omitting the primary antibody or applying the nonspecific IgG of the same isotype, were all negative.

Immunoblotting

Cell extracts were prepared as previously described (Alsat et al., 1996). Protein (70 μg) was solubilized in RIPA (radioimmunoprecipitation) buffer (50 mM Tris, 150 mM NaCl, 1% Triton X100, 1% deoxycholate, 0.1% SDS, pH 8), and stained markers were submitted to 7.5% SDS-PAGE and transferred to nitrocellulose sheets. Membranes were immunoblotted with two polyclonal antibodies against LH/CG-R, LHR-K15 (goat anti human, Santa Cruz Biotechnology, Inc.) and LHR-H50 (rabbit anti human, Santa Cruz Biotechnology, Inc.) at 2 $\mu\text{g/ml}$ each, and the specific band was revealed by chemiluminescence (West Pico Chemiluminescent, Pierce, Rockford, IL) after incubation with an anti-goat or anti-rabbit peroxidase-coupled antibody (Jackson Immuno Research). To detect actin, cyokeratin 7, hCG and hPL, we proceeded as described above, except that proteins were immunoblotted with rabbit polyclonal antibody at 0.7 $\mu\text{g/ml}$ for actin (Sigma-Aldrich, St. Louis, MO), rabbit polyclonal antibody at 0.4 $\mu\text{g/ml}$ for hCG and 0.32 $\mu\text{g/ml}$ for hPL (DAKO[®]) and mouse monoclonal antibody at 0.5 $\mu\text{g/ml}$ for cyokeratin 7 (DAKO[®]). Successive pre-adsorptions of LH/CG-R antibody with trophoblastic cells in culture abrogate LH/CG-R immunodetection in western-blot analysis.

Immunoprecipitation and ligand blotting

Protein G Plus-Agarose (Immuno precipitation Reagent, Santa Cruz Biotechnology, Inc.) was pre-mixed with a polyclonal antibody against human LHCG-R (K15, Santa Cruz Biotechnology, Inc.), or without antibody. Cells (1.0×10^6 /well) were seeded in six-well plates and cultured as previously described. After 24 h of culture, cells were washed with PBS and scraped free in ice-cold RIPA buffer. After sonication, the cellular lysate and debris were separated by centrifugation at 10,000g for 10 min at 4°C. The supernatant was transferred to the protein G-anti-human LHCG-R immunocomplex and incubated overnight at 4°C on a rocker platform, followed by four washes in RIPA buffer. Protein was eluted by heating at 60°C for 10 min in 1 \times electrophoresis sample buffer (Bio-Rad laboratories, Hercules, CA). Aliquots were submitted to 7.5% SDS-PAGE and transferred to nitrocellulose membranes. Membranes were exposed to antibody as previously described, or the blots were incubated with ¹²⁵I-hCG at 10⁻¹¹ M (Perkin-Elmer Life and Analytical Sciences, Inc., Waltham, MA) for 16 h at 4°C in the absence or presence of excess unlabeled hCG at 10⁻⁶ M (Organon SA, Puteaux, France). The blots were washed with PBS containing 0.1% Tween-20, then dried. Bound ¹²⁵I-hCG was visualized by autoradiography and analyzed by Cyclone (Storage phosphorImaging System, Hewlett Packard, France).

RNA extraction

Total RNA was extracted from trophoblastic cells after 24 or 72 h of culture by using the Trizol reagent (Invitrogen Life Technologies, Carlsbad, CA) and was stored at -80°C or at -20°C in 75% ethanol until use. The total RNA concentration was determined at 260 nm and RNA integrity was checked in 1% agarose gel. The relative LH/CG-R mRNA levels were determined by semi-quantitative reverse transcriptase-polymerase chain reaction (RT-PCR). The transcript level was normalized to the actin mRNA level (endogenous control).

RT-polymerase chain reaction

RNA samples were pretreated with DNase I using the RQ1 RNase-Free DNase kit (Promega, Inc., Madison, WI). Briefly, we used 5 U of RQ1 RNase-free DNase per 5 μg of RNA, we then added RQ1 RNase-free 10 \times reaction buffer and TE buffer. Mixture was incubated at 37°C for 30 min and the digestion was terminated by the RQ1 DNase stop solution. DNase was then inactivated by heating at 65°C for 10 min.

Complementary DNA was synthesized from 5 μg of total RNA. The reaction mixture had a final volume of 20 μl and contained 375 mM KCl, 250 mM Tris-HCl (pH 8.3), 15 mM MgCl₂, 0.1 M DTT, 40 U of RNAsin[®], 200 U of reverse transcriptase Superscript II (Invitrogen Life Technologies), 10 mM each dNTP and 200 ng of random primers (Invitrogen Life Technologies). Mixture of total RNA, DTT and random primers was heat at 65°C for 5 min. Annealing was run for 10 min at 25°C and primer extension for 50 min at 42°C. An aliquot of the reaction mixture (5 μl) was then made up to 45 μl with Taq polymerase buffer containing 1 U of Taq polymerase Platinum (Invitrogen Life Technologies). Before heating to 94°C (hot-start), 50 pmol of each specific primer was added. Amplification was run for 40 cycles for LH/CG-R and for 20 cycles for actin, consisting of 1 min at 94°C (denaturation), 1 min at 55°C (annealing) and 1 min at 72°C (extension). Oligonucleotide primers specific for the coding sequence of LH/CG-R (NM_000233) were used (Fig. 3A): P1 (+): 5'-CAAGCTTTTCAGAGGACTTAATGAGGTC-3'; P1 (-): 5'-AAAGCACAGCAGTGG CTGGGGTA-3'; P2 (+): 5'-TCGACTATCATTGCCTACC-3'; P2 (-): 5'-GGAGAAGACCTTCGTA ACAT-3'; Actin (NM_001101) (+): 5'-GTGGGGCGCCCCAGGCACCA-3'; Actin (-): 5'-CTCCTTA ATGTCACGCACGATTTTC-3'. Amplified products were analyzed by electrophoresis on 1.8% agarose gels and visualized by ethidium bromide staining.

Cloning and DNA sequencing of LH/CG-R from trophoblastic cells

PCR products were eluted from agarose gel by using the Macherey Nagel kit (NucleoSpin Extract II, MN, Hoerd, France) and purified DNA fragments were cloned into the pCRII-TOPO vector by using the TOPO-TA Cloning kit (Invitrogen Life Technologies). Positive clones were selected by PCR and were sequenced by Genome Express (Meylan, France). Both strands of DNA fragments were sequenced, using M13 reverse and M13 forward primers.

Intracellular cAMP determination

Cells (1.0×10^6 /well) were seeded in six-well plates and cultured as described above. After 24 or 72 h, cells were preincubated with 10 mM IBMX (3-isobutyl-1-methylxanthine) for 1 h to prevent cAMP degradation and were stimulated for 20 min with 10⁻⁸ M hCG (C6322, Sigma-Aldrich). Cells were frozen on dry ice and cAMP was extracted with ice-cold 65% ethanol. The extracts were dried and kept at -20°C until use. Cyclic AMP was assayed after acetylation by using a method (GE Healthcare, Saclay, France) based on the competition between unlabelled cAMP and a fixed quantity of ¹²⁵I-labelled cAMP for binding to a cAMP-specific antibody. Bound antibody was separated from free fraction by magnetic separation with a second antibody AmerlexTM-M preparation that is bound to magnetizable polymer particles. Separation of the antibody bound fraction is effected either by magnetic separation of the AmerlexTM-M suspension or decantation of the supernatant. The concentration of unlabelled cAMP in the sample was then determined by interpolation from a standard curve.

Binding assay and scatchard analyses

Trophoblastic cells (1.0×10^6 /well) were seeded in six-well plates and cultured as described above. After 24 or 72 h of culture the cells were washed five times and cultured in DMEM, 0.1% BSA for 2 h to dissociate any bound endogenous hCG. The cells were then washed and placed in 1 ml of DMEM containing 0.1% BSA and 1 mM HEPES, pH 7.3. Cells were incubated for 30 min at room temperature with 0.5 nM ¹²⁵I-hCG and an increasing concentration of unlabelled hCG (from 10⁻¹² M to 10⁻⁸ M, C6322, Sigma-Aldrich) on a shaker platform at 50 cycles/min. At the end of the incubation period the cells were washed and scraped free, and bound radioactivity was counted. Each assay was performed in triplicate. Data were analyzed by using the LIGAND fitting program (version 4.97; Munson and Rodbard, 1980). For Scatchard analysis, the results showing the number of labeled molecules associated with the cellular membrane were expressed in a number of molecule associated per seeded cells. For comparison between CT and ST experiments, nuclei were counted at 24 and 72 h of culture after staining with DAPI, as previously described in the immunocytochemistry section. We did not observe difference between the number of nuclei at 24 and 72 h of culture (CT are

nonproliferative cells and apoptosis or cellular loss account for about 4% (data not shown)).

^{125}I -labeled hCG was prepared using chloramine T as oxidant (Hunter and Greenwood, 1962). In a final volume of 20 μl , hCG (5 μg , 4.4 μM) was added to 0.5 mCi of Na^{125}I (Perkin-Elmer Life and Analytical Sciences; 17.4 Ci/mg, 11.5 μM) neutralized with 0.1 M Mops and poly(ethylene glycol) 1,000 (1%). The reaction in 25 mM

Mops buffer pH 7.2 was started by adding 100 μM chloramine-T for 3 min at room temperature and was stopped by adding 120 μM sodium bisulfite for 3 min and 2 mM NaI for 1 min. The volume was then adjusted to 0.5 ml with Mops-buffered saline (20 mM Mops, 130 mM NaCl, pH 7.2) containing 1 mg/ml BSA. Iodinated-hCG was desalted on a PD10 Sephadex G25-M column in the same buffer. Specific activity of ^{125}I -hCG was

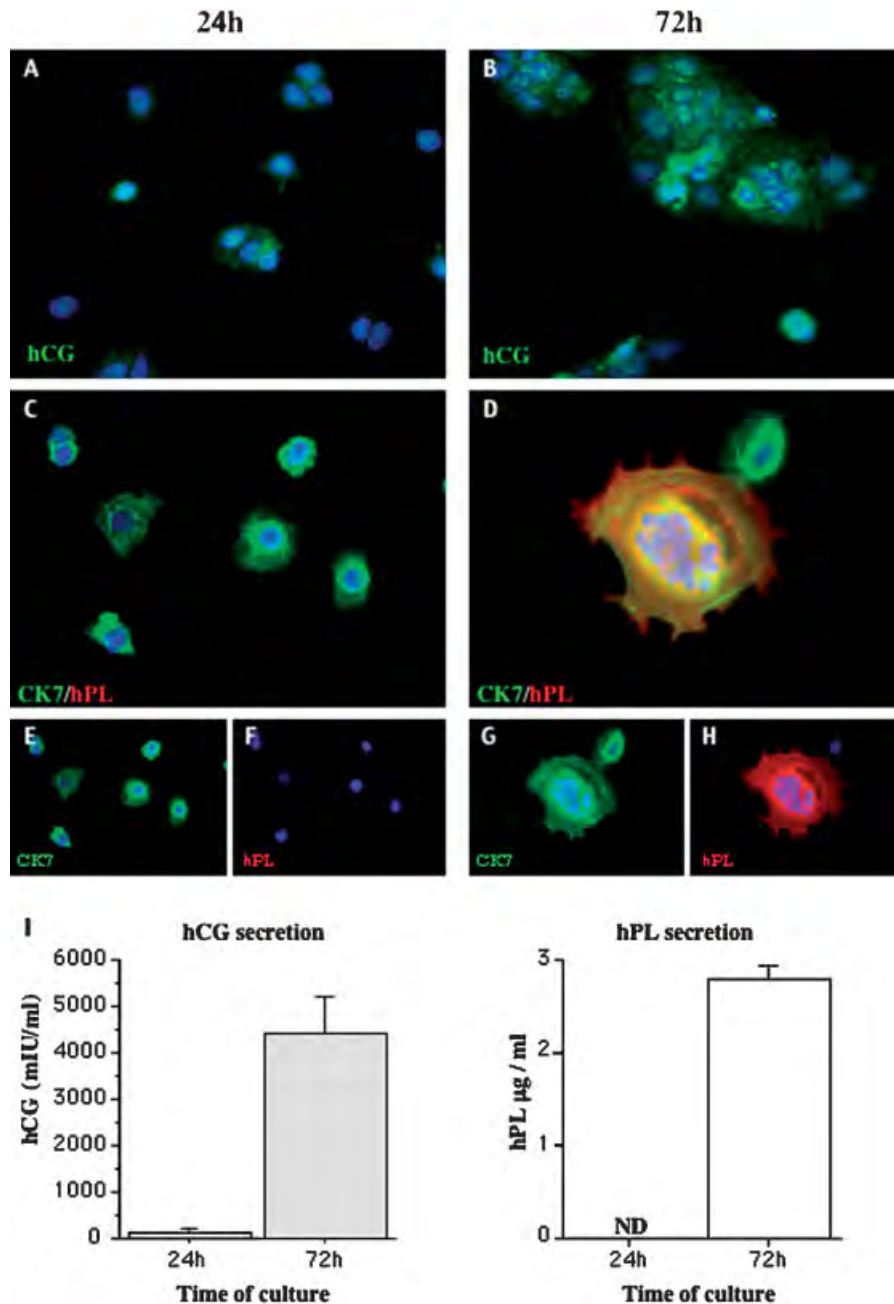


Fig. 1. In vitro human villous trophoblast differentiation. A,B: hCG immunodetection after 24 and 72 h of culture of villous cytotrophoblasts isolated from term placentas. At 24 h the cells are sparse or aggregated (A). At 72 h, they have fused to form the syncytiotrophoblast, characterized by multiple nuclei and a strong positive immunofluorescent staining for hCG (B). Nuclei were labeled with DAPI (blue fluorescence). C,D: Co-immunolocalization of cytokeratin 7 (in green) and hPL (in red) at 24 h (C) and 72 h of culture (D). Nuclei are stained blue with DAPI. HPL, known to be expressed mainly by the syncytiotrophoblast, was detected by immunostaining at 72 h (H) but not at 24 h of culture (F). Cytokeratin 7 immunostaining, was positive at 24 h (E) and 72 h (G). I: Levels of hCG and hPL (expressed respectively in milli-international units per milliliter and micrograms per milliliter of medium) secreted into the culture medium at the indicated times. Since cells were plated in triplicate (see Experimental procedures), hCG and hPL levels were determined for each plate. ND, nondetectable. Results are means \pm SEM of the three culture dishes. This figure illustrates one experiment representative of three. Scale for pictures (A–D) 1 cm = 30 μm . Scale for pictures (E–H) 0.5 cm = 30 μm .

2.1–2.4 Ci/ μ mol corresponding to about 1 atom of iodine per molecule hCG.

Statistical analysis

We used the StatView F-4.5 software package (Abacus Concepts, Inc., Cary, NC). Values are reported as means \pm SEM. Significant differences ($P < 0.05$) were identified by analysis of variance (ANOVA).

Results

Human villous trophoblast differentiation in vitro

We used the primary cell culture model of villous cytotrophoblasts isolated from term placenta (Kliman et al., 1986; Alsat et al., 1991). Figure 1 shows purified cytotrophoblasts cultured on plastic dishes for 24 and 72 h. Mononuclear cytotrophoblasts fused and formed multinucleated syncytiotrophoblasts, 72 h after plating (Kliman et al., 1986). Syncytiotrophoblast formation was associated with a significant increase in hCG and hPL levels in the culture medium (Fig. 1I). Concomitantly, immunostaining for hCG (Fig. 1A,B) and hPL (Fig. 1F,H) showed an increase in intensity during in vitro syncytiotrophoblast formation. hPL, expressed mainly by the syncytiotrophoblast (Handwerger, 1991), was detected by immunostaining at 72 h (Fig. 1D,H) but not at 24 h (Fig. 1C,F). Immunostaining of cytokeratin 7, expressed by trophoblastic cells (Blaschitz et al., 2000), was positive at 24 h (Fig. 1C,E) and 72 h (Fig. 1D,G).

These results showed that differentiation of isolated cytotrophoblasts into a syncytiotrophoblast is associated with an increase in the expression and secretion of hCG

and hPL, hormones mainly synthesized by the syncytiotrophoblast.

Decrease in LH/CG-R protein levels during in vitro trophoblast differentiation

As shown in Figure 2A,B, LH/CG-R was expressed by cultured cytotrophoblasts. The LH/CG-R immunostaining shown in this figure was obtained with the polyclonal antibody LHR-K15. Another antibody (LHR-H50) gave the same results (data not shown). LH/CG-R was expressed in both cytotrophoblasts (24 h) and syncytiotrophoblasts (72 h), with punctuate immunolabeling. LH/CG-R immunostaining appeared stronger in cytotrophoblasts than in syncytiotrophoblasts. Double immunostaining for LH/CG-R (LHR-50) and hCG (C-20) of trophoblasts cultured for 48 h (Fig. 2C,D respectively, merge Fig. 2E) illustrated the dynamics of the process. A mononucleated cytotrophoblast (Fig. 2C arrow head) expressed LH/CG-R, whereas aggregated trophoblasts showed and heterogenous immunostaining of both LH/CG-R and hCG (Fig. 2E). To validate this observation, Western-blot analysis was performed on extracts of cytotrophoblasts (24 h) and syncytiotrophoblasts (72 h) (Fig. 3A). At 24 and 72 h of culture, two major bands with molecular masses (estimated from SDS gels) of 65–75 kDa and 85–95 kDa were observed, as described in other cellular models and in mammalian cells transfected with LH/CG-R cDNA. In the literature, the 85–95 kDa band corresponds to the mature LH/CG-R present at the cell surface, and the 65–75 kDa band is the precursor of the cell-surface receptor (for review see Ascoli et al., 2002). Our results show that the expression of the mature LH/CG-R and its precursor (respectively designated m and p in Fig. 3A)

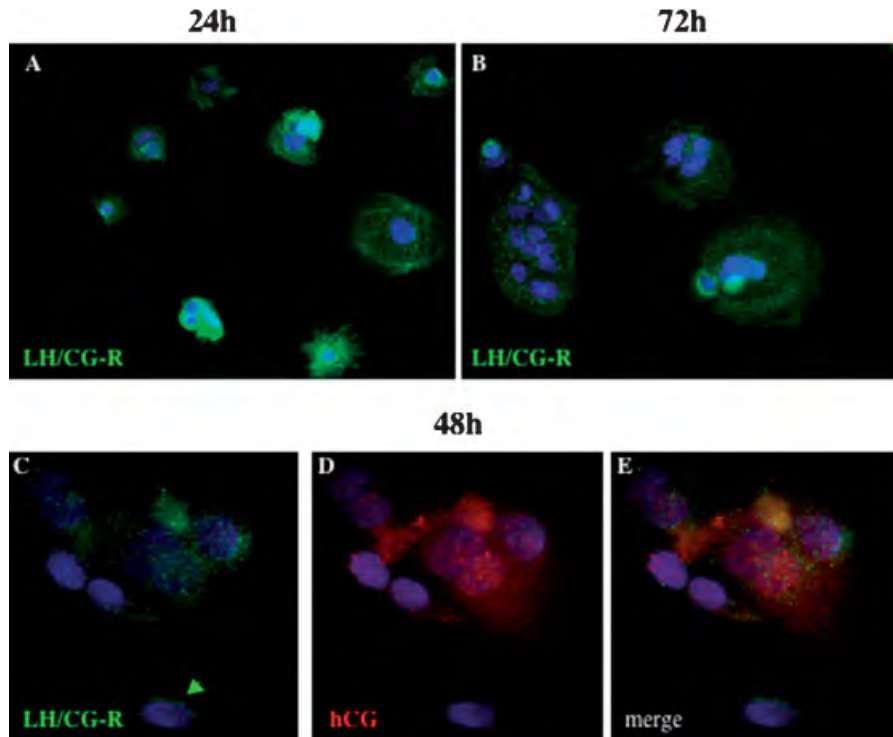


Fig. 2. LH/CG-R immunodetection during in vitro trophoblast differentiation. A,B: Immunostaining for LH/CG-R by using the polyclonal antibody LHR-K15 raised against the human LH/CG receptor. LH/CG-R was expressed in both cyto- (A; 24 h) and syncytiotrophoblasts (B; 72 h), albeit more strongly in cytotrophoblasts. E: Co-immunodetection of LH/CG-R and hCG by using the polyclonal antibodies LHR-H50 (C; in green) and hCG-C20 (D; in red) respectively at 48 h of culture. Single trophoblast (arrowed) was stained for LH/CG-R and aggregated trophoblasts were stained for both LH/CG-R and hCG. Nuclei were labeled with DAPI (blue fluorescence). Scale for pictures (A,B) 0.5 cm = 30 μ m; scale for pictures (C–E) 1 cm = 15 μ m.

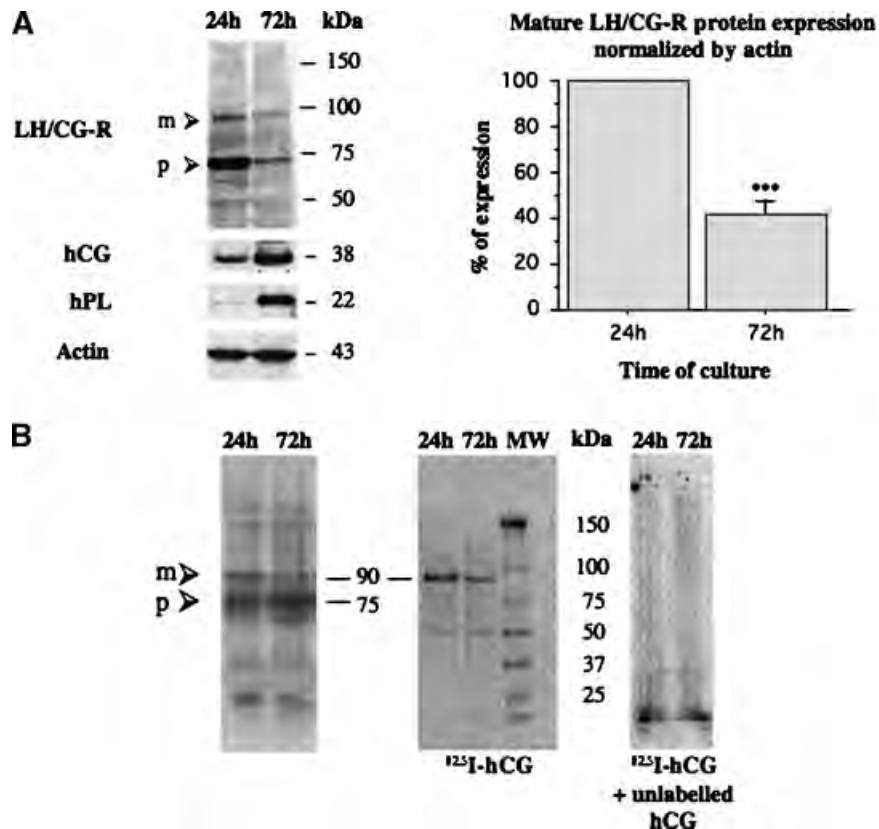


Fig. 3. LH/CG-R protein expression during in vitro trophoblast differentiation. **A,B:** Western-blot analyses (**A**) were performed using the same antibody on extracts from cytotrophoblasts (24 h) and syncytiotrophoblasts (72 h). At 24 and 72 h of culture, two major bands with molecular masses of 65–75 kDa, corresponding to the precursor (p) of the cell-surface receptor and 85–95 kDa, corresponding to the mature LH/CG-R (m) present at the cell surface, were observed. The histogram presents the normalization of mature LH/CG-R protein expression (m) by actin expression (43 kDa) (** $P < 0.0001$). Results are expressed as the mean \pm SEM of three culture dishes. In the same cellular extracts, decrease in precursor and mature LH/CG-R expression was concomitant with an increase in hCG (38 kDa) and hPL (22 kDa) expression. **B:** Immunoprecipitation and ligand-blot analysis. Cellular extracts were purified by immobilized anti-receptor antibody. Eluates were analyzed by SDS-PAGE and immunoblotting using the receptor-specific antibody. A 90 kDa band corresponding to the mature form of LH/CG-R (m) and a major band with a molecular mass of 75 kDa corresponding to the precursor (p) were observed. Incubation of the IP blot with labeled ^{125}I -hCG (10^{-11} M) revealed a major radioactive band at a molecular weight of 90 kDa, which was not detected when the blot was incubated with an excess of unlabeled hCG (10^{-6} M). Figures (A,B) illustrate one experiment representative of five.

decreases during cytotrophoblast differentiation. At the same time, actin expression remains constant. Normalization of mature LH/CG-R protein expression to actin expression showed a significant decrease ($58.6 \pm 6.7\%$; $P < 0.0001$) in cell-surface receptor expression. We obtained similar results with the two antibodies used (LHR-K15 and LHR-H50). Interestingly, in the same cellular extracts, the decrease in precursor and mature LH/CG-R expression coincided with an increase in hCG and hPL expression (Fig. 3A).

To further characterize LH/CG-R expression during trophoblast differentiation, we performed immunoprecipitation (IP) with anti-human LH/CG-R antibody (K15). Cellular extracts were purified by immobilized anti-receptor antibody (IP) and eluates were analyzed by SDS-PAGE and immunoblotting using the receptor-specific antibody (K15). A 90 kDa band corresponded to the mature form of LH/CG-R (m), and a major band of 75 kDa corresponded to the precursor (p).

To determine which molecular form of the receptor bound the hormone, we used ^{125}I -hCG in ligand-blot experiments (Fig. 3B). Incubation of the IP blot with ^{125}I -hCG (10^{-11} M) revealed a major band of 90 kDa. This band was absent when the blot was incubated with an excess of unlabeled hCG (10^{-6} M), showing that the 90-kDa LH/CG-R specifically binds the

hormone. In these conditions, ^{125}I -hCG binding to the mature form of the receptor (90 kDa) was lower in the syncytiotrophoblast than in cytotrophoblasts.

Decrease in LH/CG-R mRNA expression during in vitro trophoblast differentiation

We conducted semi-quantitative RT-PCR experiments with two different sets of primers (P1 and P2; for primer positions see Fig. 4A). To avoid contamination by genomic DNA, each primer was located on a separate exon and RNA extracts were pretreated with DNase I.

As shown in Figure 4B, amplification of the 647-bp and 282-bp fragments, obtained with primers P1 and P2 respectively, indicated that LH/CG-R mRNA was significantly less abundant in the syncytiotrophoblast (72 h) than in cytotrophoblasts (24 h). No significant difference was noted in the actin mRNA level. We obtained similar results with the two sets of primers. The amplification products were then purified from the agarose gel and cloned into the pCRII-TOPO vector. Sequencing confirmed that both the 647-bp and 282-bp fragments were part of the human LH/CG receptor. Normalization of LH/CG-R mRNA to actin mRNA after RT-PCR with primer sets P1 and P2 showed a significant

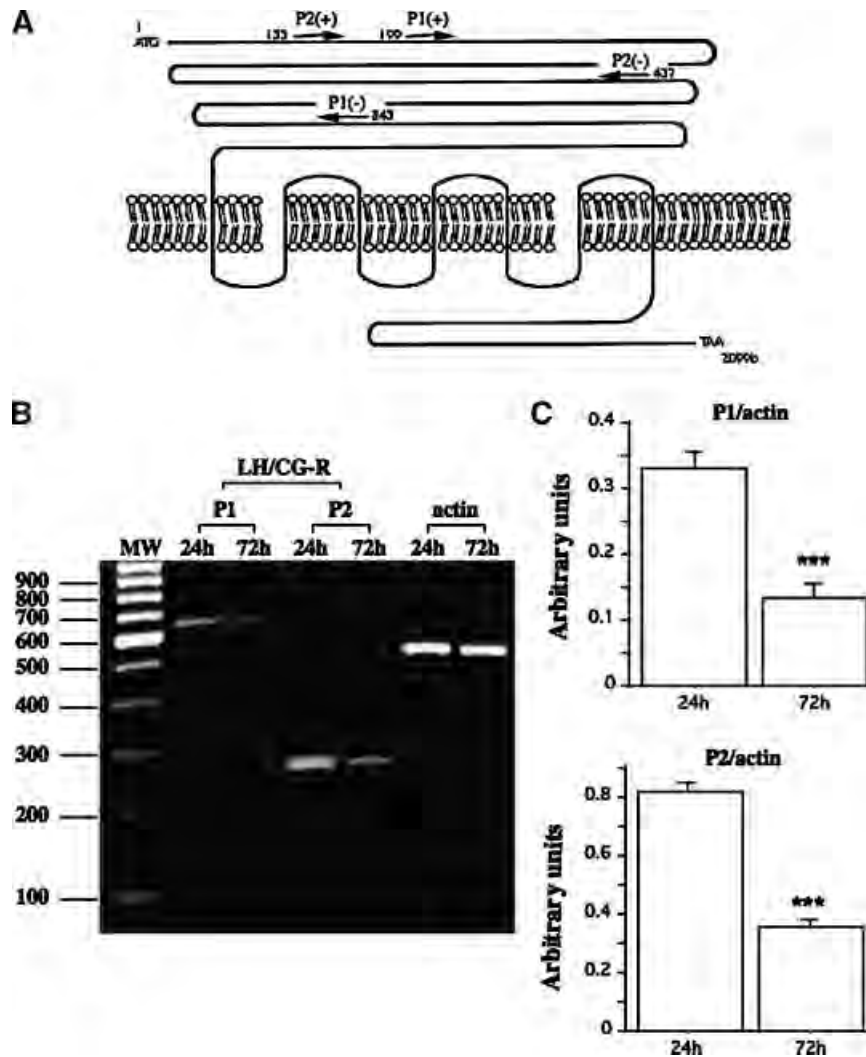


Fig. 4. LH/CG-R mRNA expression during in vitro trophoblast differentiation. **A:** Diagram showing the seven transmembrane domains of the LH/CG-receptor and the location of the primers sets used in this study. The two sets of primers (P1 and P2) are located on the extracellular domain. P1 amplifies a fragment of 647-bp in the exons 2–9 and P2 amplifies a fragment of 282-bp in the exons 1–5. **B:** Ethidium bromide-staining gel of one representative of five independent experiments. Semi-quantitative RT-PCR experiments with both the primers P1 and P2 shows respectively a 647-bp and a 282-bp amplified fragment. RT-PCR products were separated on 1.8% agarose gel and analyzed by densitometry. Sequencing confirmed that both the 647-bp and the 282-bp fragments are part of the LH/CG receptor. **C:** Histograms represent the normalization of LH/CG-R mRNA by actin mRNA after RT-PCR with primers sets P1 (upper histogram) and P2 (lower histogram). Data are expressed as mean \pm SEM of five independent experiments similar to the one shown in (B) bp: base pairs; *** $P < 0.0001$.

decrease in LH/CG-R mRNA levels during differentiation (Fig. 4C). With the P1 primers, LH/CG-R mRNA levels fell from 0.33 ± 0.01 at 24 h to 0.13 ± 0.01 at 72 h ($P < 0.0001$). A similar decrease was observed with the P2 primers (from 0.82 ± 0.02 at 24 h to 0.36 ± 0.01 at 72 h; $P < 0.0001$). Although the amplification product obtained with primers P2 appeared to be at least twice as abundant as that obtained with primers P1 (probably because the P2 amplicon is about half the length of the P1 amplicon), the size of the decrease in LH/CG-R levels at 72 h was similar with the two primer sets (respectively 2.5- and 2.3-fold).

Decrease in ^{125}I -hCG binding to cell-surface LH/CG-R during in vitro trophoblast differentiation

To confirm the decrease in LH/CG-R mRNA and protein levels, we performed binding saturation experiments with iodinated hCG at 24 and 72 h of culture (Fig. 5). Scatchard analysis of

binding data showed that the number of molecules bound per seeded cell at 24 h of culture (cytotrophoblasts) was 3511 ± 693 . After differentiation, at 72 h of culture, this number fell significantly ($P = 0.02$) to 929 ± 583 . No significant difference in kDa values was observed between 24 h (0.5 ± 0.1 nM) and 72 h (0.4 ± 0.1 nM).

LH/CG-R stimulation during in vitro trophoblast differentiation

In order to confirm the reduction in functional mature hCG receptor expression at the syncytiotrophoblast surface compared to the cytotrophoblast surface, we determined cAMP production in response to an effective hCG concentration for 20 min (Fig. 6). As cAMP is a second messenger for hCG signaling in trophoblastic cells, the decrease in LH/CG-R transcript and protein levels ought to be associated with a decrease in cAMP production. Determination of the

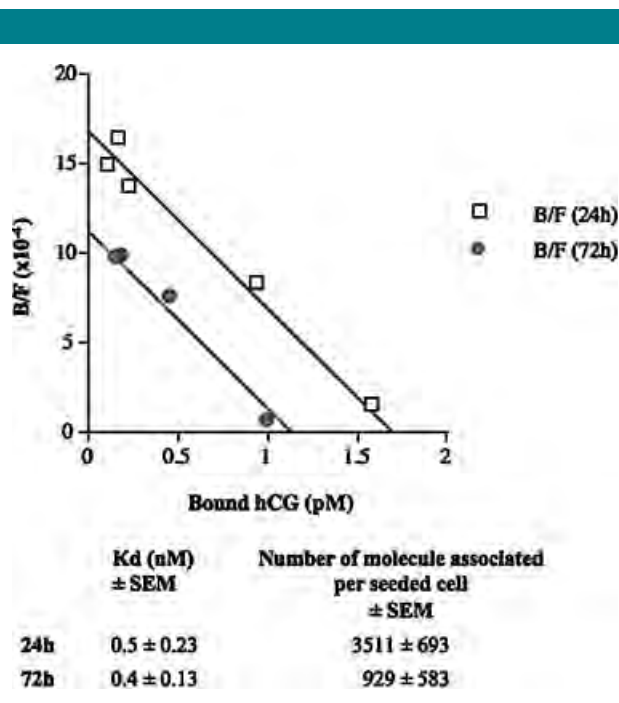


Fig. 5. Scatchard analyses of ^{125}I -hCG binding to trophoblasts during in vitro differentiation. Binding was performed for 30 min at room temperature, on cells at 24 h (\square) or 72 h (\bullet) of culture. The apparent dissociation constants (kDa) and the maximum number of molecules bound per mg of protein at 24 and 72 h of culture were calculated by the LIGAND program (lower table). Results are expressed as the mean \pm SEM of three experiments.

most effective hCG concentration was carried out by stimulating trophoblasts with 10^{-12} M to 10^{-6} M hCG; 10^{-8} M hCG was the most effective concentration (data not shown). As shown in Figure 6, hCG-stimulated cAMP production by trophoblasts was higher at 24 h than at 72 h of culture

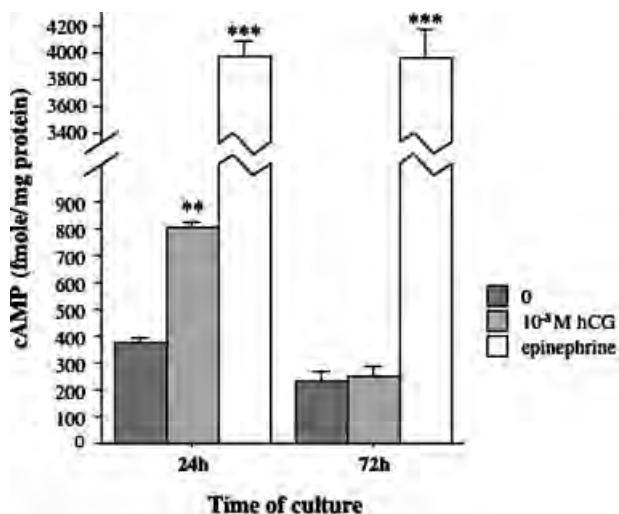


Fig. 6. Intracellular cAMP production after LH/CG-R stimulation during in vitro trophoblast differentiation. Stimulation of cells at 24 and 72 h of culture was performed with 10^{-8} M of hCG or with epinephrine (used as a positive control) for 20 min and compared to nonstimulated cells (0). ** $P < 0.005$ and *** $P < 0.0001$.

($P = 0.0021$). Trophoblast stimulation by hCG (10^{-8} M) at 24 h of culture induced at least a twofold increase in cAMP production compared to the basal level ($P = 0.0016$), but did not induce detectable cAMP production at 72 h of culture ($P = 0.7644$). In contrast, epinephrine (which stimulates cAMP production and is used as a positive control) induced similar cAMP production at 24 and 72 h of culture, indicating that the cells were functional and that the decrease in cAMP production observed at 72 h was not due to a defective cAMP pathway.

Immunolocalization of LH/CG-R in villous sections

These in vitro findings were confirmed by examining placental LH/CG-R expression in situ, on villous sections. First-trimester placenta was chosen because cytotrophoblasts are more abundant than at other stages of pregnancy and form a continuous layer.

LH/CG-R was detected in villous cytotrophoblasts and syncytiotrophoblasts. Use of a polyclonal antibody raised against the extracellular domain of human LH/CG-R showed that LH/CG-R is mainly expressed by the cytotrophoblast layer (Fig. 7A). Weaker staining was observed in the syncytiotrophoblast (ST). LH/CG-R was also expressed by perivascular cells (VC) of the villous core. We obtained similar results with two other monoclonal antibodies (LHR 29 and LHR 1055) which recognize two different epitopes of the extracellular domain of LH/CG-R (Vuhai-Luuthi et al., 1990; Méduri et al., 1997; data not shown). No staining was detected in negative control sections (Fig. 7D). Interestingly, strong hCG immunostaining was observed in the syncytiotrophoblast (Fig. 7B) while cytokeratin 7 was mainly located in the cytotrophoblast layer (Fig. 7C).

Taken together, these results strongly suggest that the expression of a functional cell-surface LH/CG-R decreases during cytotrophoblast differentiation into a syncytiotrophoblast.

Discussion

By using several complementary methods and a well-characterized in vitro model of human villous trophoblast differentiation, we clearly observed that LH/CG-R mRNA and protein expression is lower in syncytiotrophoblasts than in cytotrophoblasts and that this down-regulation is associated with an apparent decrease of receptor activation by its specific hormone. These results differ from those of two previous studies published by CV. Rao, who described stronger expression of LH/CG-R in syncytiotrophoblasts than in cytotrophoblasts (Reshef et al., 1990; Lei and Rao, 1992). This divergence may come from the use of different tools. Anti-human LH/CG-R antibodies were not available in the early 1990s, and most immunohistochemical and western-blotting studies used antibodies raised against the N-terminal part of the rat LH/CG receptor. The amino acid sequence identity between the rat and human receptors is 85%, with the strongest similitude in the transmembrane portion of the molecule and not in the N-terminal region (Segaloff and Ascoli, 1993). Moreover, experiments involving radiolabeled probes, such as northern blotting and in situ hybridization, used porcine cDNA with 88% sequence identity to the human sequence. In this study, we cloned PCR fragments of the human hCG/LH receptor from villous cytotrophoblasts and used antibodies specific for the human receptor.

HCG, which is produced in large amounts by the syncytiotrophoblast, plays an important role in cytotrophoblast differentiation into syncytiotrophoblast. An increasing number of studies have investigated the central role of hCG and its receptor in the trophoblastic differentiation process. Many authors have described down-regulation of LH/CG-R

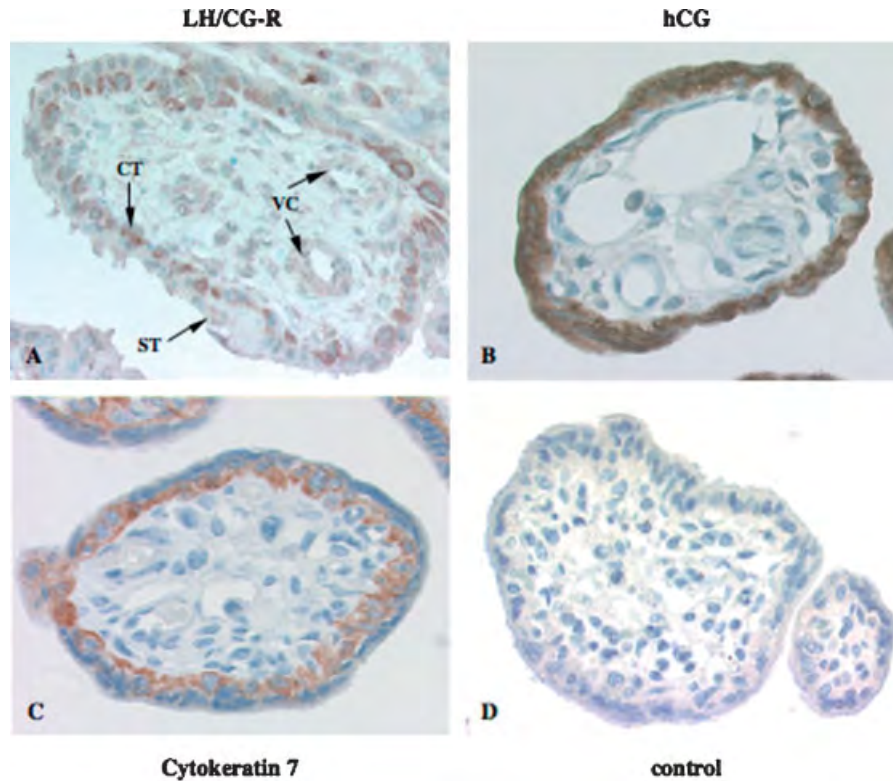


Fig. 7. Immunolocalization of LH/CG-R, hCG and cytokeratin 7 in villous sections. **A:** Immunohistochemical staining of LH/CG-R, using the polyclonal antibody (H50) raised against the extracellular domain. Villous cytotrophoblasts (CT), syncytiotrophoblast (ST) and perivascular cells (VC) of the villous core were positively stained. **B:** A strong immunostaining of hCG was observed in the syncytiotrophoblast. **C:** Immunostaining of cytokeratin 7 was mainly located in cytotrophoblasts layer. **D:** No staining was observed in control sections treated with nonspecific isotypic immunoglobulins.

expression by increasing concentrations of hCG. Indeed, exposure of ovarian or testicular cells expressing the endogenous LH/CG-R to a high concentration of hCG down-regulates cell-surface receptor expression. This coincides with a decrease in the abundance of LH/CG-R transcripts (Hu et al., 1990; LaPolt et al., 1990; Segaloff et al., 1990; Hoffman et al., 1991; Peegel et al., 1994). It is noteworthy in this respect that hCG is secreted in large amounts during syncytiotrophoblast formation. The decrease in cell-surface receptor expression was confirmed in our study by the clear decrease in cAMP production by the syncytiotrophoblast after stimulation by recombinant hCG. Interestingly, the decrease in cAMP production by the syncytiotrophoblast was not due to a loss of affinity or to weak binding between the receptor and its hormone, as we found no difference in LH/CG-R kd values between 24 and 72 h of culture. Moreover, Scatchard plots clearly showed that the maximum number of hCG molecules bound per seeded cell was significantly lower at 72 h of culture than at 24 h (~74%). This result confirms the decrease of LH/CG-R (~60%) observed by Western-blot analysis. The difference in LH/CG-R decrease (60% vs. 74%) may be due to the technical approaches used for the purpose. By Western-blot analysis, we quantified the mature form of the LH/CG-R in proteins from total cellular extracts. In binding experiments, we used living cells, meaning that only the mature form of the LH/CG-R present at the cell surface was quantified. Some mature forms internalized or present in the endosome might not be accessible to ^{125}I -hCG.

LH/CG-R desensitization has been described in rat ovary and is accompanied by a transient loss of responsiveness to LH, the receptor being temporarily uncoupled from its Gs protein (Segaloff et al., 1990). We observed here that syncytiotrophoblast stimulation by recombinant hCG (10^{-8} M) did not induce detectable cAMP production although the cAMP pathway was functional as shown by epinephrine stimulation. This loss of responsiveness to recombinant hCG may thus be due in part to cell-surface receptor desensitization. Western blotting showed that two major species of LH/CG-R with molecular masses of 65–75 kDa and 85–95 kDa were expressed by cytotrophoblasts and by syncytiotrophoblasts. Immunoprecipitation experiments and ligand blot analysis confirmed that the 65–75 kDa band was the intracellular precursor of the cell-surface receptor and that the 85–95 kDa band corresponded to mature LH/CG-R present at the cell surface, as shown by its ability to bind specifically labeled ^{125}I -hCG. Our results show that the expression of the mature LH/CG-R and its intracellular precursor decreased during cytotrophoblast differentiation. Furthermore, the precursor form seemed to be more strongly expressed than the mature form in trophoblastic cells. Most studies of these two forms of LH/CG-R have used mammalian cells transfected with the cDNA for the porcine, rat or human receptor (for review see Ascoli et al., 2002), but as shown here, primary cultured human trophoblasts may be an excellent model for studying the maturation of the intracellular precursor into the mature cell-surface protein. Recently, Pietila et al. (2005) using transfection models have shown that regulation of the

immature form into the mature form might be considered important in LH/CG-R expression.

In this study, we characterized for the first time, in a human physiological model, the expression and regulation of LH/CG-receptor. We demonstrate, both *in situ* and *in vitro*, that LH/CG-R is expressed by human cytotrophoblasts and, albeit to a lesser extent, by the syncytiotrophoblast. LH/CG-R expression thus seems to be regulated during villous trophoblast differentiation, and this regulation may involve down-regulation of the receptor by its ligand. Abnormal regulation of this process might be involved in trisomy 21-associated pregnancies, in which we recently observed an abnormal glycosylated form of hCG associated with defective syncytiotrophoblast formation (Frendo et al., 2000b, 2004). Abnormal syncytiotrophoblast formation might lead to complications such as preeclampsia and intrauterine growth retardation.

Acknowledgments

We thank Dr Fanny Lewin for her support and the staff of the Saint Vincent de Paul Obstetrics Department for providing us with placentas. This work was supported by la Caisse d'Assurance Maladie des Professions Libérales Province. GP was supported by a fellowship from Conseil Regional d'Ile-de-France, and J-LF by a grant from INSERM (Projet Avenir).

Literature Cited

- Alsat E, Cedar L. 1974. Mise en évidence d'une fixation spécifique de gonadotrophine chorionique humaine radio-iodée dans les tranches de placentas humains. *C R Acad Sci Paris* 278:2665–2668.
- Alsat E, Mirlesse V, Fondacci C, Dodeur M, Evain-Brion D. 1991. Parathyroid hormone increases epidermal growth factor receptors in cultured human trophoblastic cells from early and term placenta. *J Clin Endocrinol Metab* 73:288–294.
- Alsat E, Haziza J, Evain-Brion D. 1993. Increase in epidermal growth factor receptor and its messenger ribonucleic acid levels with differentiation of human trophoblast cells in culture. *J Cell Physiol* 154:122–128.
- Alsat E, Wyplosz P, Malassiné A, Guibourdenche J, Porquet D, Nessmann C, Evain-Brion D. 1996. Hypoxia impairs cell fusion and differentiation process in human cytotrophoblast, *in vitro*. *J Cell Physiol* 168:346–353.
- Aplin J. 1991. Implantation, trophoblast differentiation and haemochorial placentation: Mechanistic evidence *in vivo* and *in vitro*. *J Cell Sci* 99:681–692.
- Ascoli M, Fanelli F, Segaloff DL. 2002. The lutropin/choriogonadotropin receptor, a 2002 perspective. *Endocr Rev* 23:141–174.
- Benirschke K, Kaufmann P. 2000. *Pathology of the human placenta*. New-York: Springer-Verlag.
- Blaschitz A, Weiss U, Dohr G, Desoye G. 2000. Antibody reaction patterns in first trimester placenta: Implications for trophoblast isolation and purity screening. *Placenta* 21:733–741.
- Bo M, Boime I. 1992. Identification of the transcriptionally active genes of the chorionic gonadotrophin beta gene cluster *in vivo*. *J Biol Chem* 267:3179–3184.
- Boyd J, Hamilton W. 1970. *The human placenta*. Cambridge: Heffer and Sons.
- Cronier L, Bastide B, Herve JC, Deleze J, Malassiné A. 1994. Gap junctional communication during human trophoblast differentiation: Influence of human chorionic gonadotropin. *Endocrinology* 135:402–408.
- Cronier L, Defamie N, Dupays L, Theveniau-Ruissy M, Goffin F, Pointis F, Malassiné A. 2002. Connexin expression and gap junctional intercellular communication in human first trimester trophoblast. *Mol Hum Reprod* 8:1005–1013.
- Frendo J-L, Thérond P, Guibourdenche J, Bidart J-M, Vidaud M, Evain-Brion D. 2000a. Modulation of copper/zinc superoxide dismutase expression and activity with *in vitro* differentiation of human villous cytotrophoblast. *Placenta* 21:773–781.
- Frendo J-L, Vidaud M, Guibourdenche J, Luton D, Muller F, Bellet D, Giovagranti Y, Tarrade A, Porquet D, Blot P, Evain-Brion D. 2000b. Defect of villous cytotrophoblast differentiation into syncytiotrophoblast in Down's syndrome. *J Clin Endocrinol Metab* 85:3700–3707.
- Frendo J-L, Thérond P, Bird T, Massin N, Muller F, Guibourdenche J, Luton D, Vidaud M, Anderson WB, Evain-Brion D. 2001. Overexpression of copper zinc superoxide dismutase impairs human trophoblast cell fusion and differentiation. *Endocrinology* 142:3638–3648.
- Frendo J-L, Cronier L, Bertin G, Guibourdenche J, Vidaud M, Evain-Brion D, Malassiné A. 2003a. Involvement of connexin 43 in human trophoblast cell fusion and differentiation. *J Cell Sci* 116:3413–3421.
- Frendo J-L, Olivier D, Cheynet V, Blond J-L, Vidaud M, Rabreau M, Evain-Brion D, Mallet F. 2003b. Direct involvement of HERV-W Env glycoprotein in human trophoblast cell fusion and differentiation. *Mol Cell Biol* 23:3566–3574.
- Frendo J-L, Guibourdenche J, Pidoux G, Vidaud M, Luton D, Giovagranti Y, Porquet D, Muller F, Evain-Brion D. 2004. Trophoblast production of a weakly bioactive human chorionic gonadotropin in trisomy 21-affected pregnancy. *J Clin Endocrinol Metab* 89:727–732.
- García-Lloret M, Morrish DW, Wegmann TG, Honore L, Turner AR, Guilbert LJ. 1994. Demonstration of functional cytokine-placental interactions: CSF-1 and GM-CSF stimulate human cytotrophoblast differentiation and peptide hormone secretion. *Exp Cell Res* 214:46–54.
- Getsios S, MacCalman CD. 2003. Cadherin-11 modulates the terminal differentiation and fusion of human trophoblastic cells *in vitro*. *Dev Biol* 257:41–54.
- Gudermann T, Birnbaumer M, Birnbaumer L. 1992. Evidence for dual coupling of the murine luteinizing hormone receptor to adenylyl cyclase and phosphoinositide breakdown and Ca²⁺ mobilization. Studies with the cloned murine luteinizing hormone receptor expressed in L cells. *J Biol Chem* 267:4479–4488.
- Handschuh K, Guibourdenche J, Tsatsaris V, Guesnon M, Laurendeau I, Evain-Brion D, Fournier T. 2007. Human Chorionic Gonadotropin expression in human trophoblasts from early placenta: Comparative study between villous and extravillous trophoblastic cells. *Placenta* 28:175–184.
- Handwerger S. 1991. The physiology of placental lactogen in human pregnancy. *Endocrinology* 12:329–336.
- Hipkin RW, Sanchez-Yague J, Ascoli M. 1992. Identification and characterization of a luteinizing hormone/chorionic gonadotropin (LH/CG) receptor precursor in a human kidney cell line stably transfected with the rat luteal LH/CG-R complementary DNA. *Mol Endocrinol* 6:2210–2218.
- Hoffman YM, Peegel H, Sprock MJ, Zhang QY, Menon KM. 1991. Evidence that human chorionic gonadotropin/luteinizing hormone receptor down-regulation involves decreased levels of receptor messenger ribonucleic acid. *Endocrinology* 128:388–393.
- Hoshina M, Boothby M, Husa R, Pattillo R, Camel HM, Boime I. 1985. Linkage of human chorionic gonadotrophin and placental lactogen biosynthesis to trophoblast differentiation and tumorigenesis. *Placenta* 6:163–172.
- Hu ZZ, Tsai-Morris CH, Buczko E, Dufau ML. 1990. Hormonal regulation of LH receptor mRNA and expression in the rat ovary. *FEBS Lett* 274:181–184.
- Hunter WM, Greenwood FC. 1962. Preparation of iodine-131 labeled human growth hormone of high specific activity. *Nature* 194:495–496.
- Keryer G, Alsat E, Tasken K, Evain-Brion D. 1998. Cyclic AMP-dependent protein kinases and human trophoblast cell differentiation *in vitro*. *J Cell Sci* 111:995–1004.
- Kliman H, Nestler J, Sermasi E, Sanger J, Strauss J, III. 1986. Purification, characterization, and *in vitro* differentiation of cytotrophoblasts from human term placenta. *Endocrinology* 118:1567–1582.
- LaPolt PS, Oikawa M, Jia XC, Dargan C, Hsueh AJ. 1990. Gonadotropin-induced up- and down-regulation of rat ovarian LH receptor message levels during follicular growth, ovulation and luteinization. *Endocrinology* 126:3277–3279.
- Lei ZM, Rao CV. 1992. Gonadotropin receptors in human fetoplacental unit: Implications for hCG as an intracrine, paracrine and endocrine regulator of human trophoblast function. *Troph Res* 6:213–224.
- Loosfelt H, Misrahi M, Atger M, Saless R, Vu Hai-Luu Thi MT, Jolivet A, Guiochon-Mantel A, Sar S, Jallat B, Garnier J, et al. 1989. Cloning and sequencing of porcine LH-hCG receptor cDNA: Variants lacking transmembrane domain. *Science* 245:525–528.
- Malassiné A, Blaise S, Handschuh K, Lалуque H, Dupressoir A, Evain-Brion D, Heidmann T. 2007. Expression of the fusogenic HERV-FRD Env glycoprotein (syncytin 2) in human placenta is restricted to villous cytotrophoblastic cells. *Placenta* 28:185–191.
- McFarland KC, Sprengel R, Phillips HS, Kohler M, Roseblit N, Nikolics K, Segaloff DL, Seeburg PH. 1989. Lutropin-choriogonadotropin receptor: An unusual member of the G protein-coupled receptor family. *Science* 245:494–499.
- Midgley AR, Pierce GB, Denau GA, Gosling JR. 1963. Morphogenesis of syncytiotrophoblast *in vivo*: An autoradiographic demonstration. *Science* 141:350–351.
- Minegishi T, Nakamura K, Takakura Y, Miyamoto K, Hasegawa Y, Ibuki Y, Igarashi M. 1990. Cloning and sequencing of human LH/hCG receptor cDNA. *Biochem Biophys Res Commun* 172:1049–1054.
- Morrish DW, Bhardwaj D, Dabbagh LK, Marusyk H, Siy O. 1987. Epidermal growth factor induces differentiation and secretion of human chorionic gonadotropin and placental lactogen in normal human placenta. *J Clin Endocrinol Metab* 65:1282–1290.
- Morrish DW, Bhardwaj D, Paras MT. 1991. Transforming growth factor beta 1 inhibits placental differentiation and human chorionic gonadotropin and human placental lactogen secretion. *Endocrinology* 129:22–26.
- Munson PJ, Rodbard D. 1980. LIGAND: A versatile computerized approach for characterization of ligand-binding systems. *Anal Biochem* 107:220–239.
- Muyan M, Boime I. 1997. Secretion of chorionic gonadotropin from human trophoblasts. *Placenta* 18:237–241.
- Méduri G, Charneau N, Loosfelt H, Jolivet A, Spyrtatos F, Brailly S, Milgrom E. 1997. Luteinizing hormone/human chorionic gonadotropin receptors in breast cancer. *Cancer Res* 57:857–864.
- Peegel H, Randolph J, Jr., Midgley AR, Menon KM. 1994. *In situ* hybridization of luteinizing hormone/human chorionic gonadotropin receptor messenger ribonucleic acid during hormone-induced down-regulation and the subsequent recovery in rat corpus luteum. *Endocrinology* 135:1044–1051.
- Pierce JG, Parsons TF. 1981. Glycoprotein hormones: Structure and function. *Annu Rev Biochem* 50:465–495.
- Pietila EM, Tuusa JT, Apaja PM, Aatsinki JT, Hakalahti AE, Rajaniemi HJ, Petaja-Repo UE. 2005. Inefficient maturation of the rat luteinizing hormone receptor: A putative way to regulate receptor numbers at the cell surface. *J Biol Chem* 280:26622–26629.
- Reshef E, Lei ZM, Rao CV, Pridham DD, Chegini N, Luborsky JL. 1990. The presence of gonadotropin receptors in nonpregnant human uterus, human placenta, fetal membranes, and decidua. *J Clin Endocrinol Metab* 70:421–430.
- Richard R. 1961. Studies of placental morphogenesis I. Radioautographic studies of human placenta utilizing tritiated thymidine. *Proc Soc Exp Biol Med* 106:829–831.
- Schmon B, Hartmann M, Jones CJ, Desoye G. 1991. Insulin and glucose do not affect the glycogen content in isolated and cultured trophoblast cells of human term placenta. *J Clin Endocrinol Metab* 73:888–893.
- Segaloff DL, Ascoli M. 1993. The lutropin/choriogonadotropin receptor... 4 years later. *Endocr Rev* 14:324–347.
- Segaloff DL, Wang HY, Richards JS. 1990. Hormonal regulation of luteinizing hormone/chorionic gonadotropin receptor mRNA in rat ovarian cells during follicular development and luteinization. *Mol Endocrinol* 4:1856–1865.
- Shi QJ, Lei ZM, Rao CV, Lin J. 1993. Novel role of human chorionic gonadotropin in differentiation of human cytotrophoblasts. *Endocrinology* 132:1387–1395.
- Vuhai-Luuthi MT, Jolivet A, Jallat B, Saless R, Bidart JM, Houllier A, Guiochon-Mantel A, Garnier J, Milgrom E. 1990. Monoclonal antibodies against luteinizing hormone receptor. Immunohistochemical characterization of the receptor. *Endocrinology* 127:2090–2098.
- Yang M, Lei ZM, Rao ChV. 2003. The central role of human chorionic gonadotropin in the formation of human placental syncytium. *Endocrinology* 144:1108–1120.

Human Placental Development Is Impaired by Abnormal Human Chorionic Gonadotropin Signaling in Trisomy 21 Pregnancies

Guillaume Pidoux,* Pascale Gerbaud,* Olivier Marpeau, Jean Guibourdenche, Fatima Ferreira, Josette Badet, Danièle Evain-Brion, and Jean-Louis Frendo

Institut National de la Santé et de la Recherche Médicale (G.P., P.G., O.M., J.G., F.F., J.B., D.E.-B., J.-L.F.), Unité 767, Faculté des Sciences Pharmaceutiques et Biologiques (G.P., P.G., O.M., F.F., J.B., D.E.-B., J.-L.F.), and Centre National de la Recherche Scientifique (J.-L.F.), Université Paris Descartes, Paris F-75006, France; and Assistance Publique-Hôpitaux de Paris (J.G.), Hôpital Cochin, Service de Biochimie Hormonale, Paris F-75014, France

Placental development is markedly abnormal in women bearing a fetus with trisomy 21, with defective syncytiotrophoblast (ST) formation and function. The ST occurs from cytotrophoblast (CT) fusion and plays an essential role by secreting human chorionic gonadotropin (hCG), which is essential to placental development. In trisomy of chromosome 21 (T21) pregnancies, CTs do not fuse and differentiate properly into STs, leading to the secretion of an abnormal and weakly bioactive hCG. In this study we report for the first time, a marked decrease in the number of mature hCG receptor (LH/CG-R) molecules expressed at the surface of T21-affected CTs. The LH/CG-R seems to be functional based on sequencing that revealed no mutations or deletions and bind-

ing of recombinant hCG as well as endogenous hCG. We hypothesize that weakly bioactive hCG and lower LH/CG-R expression may be involved in the defect of ST formation. Interestingly, the defective ST formation is mimicked in normal CT cultures by using LH/CG-R small interfering RNA, which result in a lower hCG secretion. Furthermore, treatment of T21-affected CTs with recombinant hCG overcomes *in vitro* the T21 phenotype, allowing CTs to fuse and form a large ST. These results illustrate for the first time in trisomy 21 pathology, how abnormal endogenous hCG signaling impairs human placental development. (*Endocrinology* 148: 5403–5413, 2007)

THE HUMAN PLACENTA is characterized by extensive invasion of the trophoblast in the maternal uterus, creating direct trophoblast contact with maternal blood (hemochorial placentation). In early pregnancy, cytotrophoblasts (CTs) proliferate and invade the maternal endometrium to form the anchoring villi (1). CTs also differentiate into a continuous multinucleated layer known as the syncytiotrophoblast (ST).

Human chorionic gonadotropin (hCG) is produced by the trophoblast, and, especially, by the ST covering the chorionic villi and bathing in maternal blood (2). The ST plays an essential role during pregnancy by allowing fetomaternal exchanges and by secreting placental hormones into the maternal blood. *In vivo* and *in vitro*, the ST occurs from cytotrophoblastic cell fusion and differentiation. Numerous factors

regulate ST formation, in an autocrine or paracrine manner (for review, see Ref. 3), including hCG (4, 5), and oxidative stress related to overexpression of copper/zinc superoxide dismutase located on chromosome 21 (6, 7). The molecular mechanisms underlying CT fusion and differentiation are poorly understood, but proteins involved in cell adhesion (cadherin 11) (8) and cell-cell communication (connexin 43) (9) are directly involved. We also recently demonstrated the direct involvement of syncytin 1, a human endogenous retroviral envelope glycoprotein (10).

Very few of the genes involved in human placental development and trophoblast differentiation have been identified. In contrast, with the increasing number of transgenic and knockout mice and rats, many of the genes involved in murine placental development have been characterized (for review, see Ref. 11). However, results obtained in mice are difficult to extrapolate to humans, owing to the specific features of human placental development (3). For instance, hCG does not exist in mice and rats.

Anomalies in CT differentiation and cell fusion may lead to severe placental abnormalities. In trisomy 21-affected pregnancies, the CTs fuse poorly or tardily, and the resulting defect in ST formation is associated with a decrease in hCG synthesis and secretion (12). We recently demonstrated that hCG secreted by trisomy of chromosome 21 (T21)-affected CTs is abnormally glycosylated (13), and Fisher and colleagues (14) have described variable defects in CT differentiation along the invasive pathway.

T21, which causes the phenotype known as Down's syn-

First Published Online August 9, 2007

* G.P. and P.G. contributed equally to the work.

Abbreviations: Ab-hCG, Antihuman chorionic gonadotropin; Ab-LH/CG-R, anti-LH/chorionic gonadotropin receptor; CG-R, chorionic gonadotropin receptor; CT, cytotrophoblast; dsRNA, double-strand RNA; DTSSP, 3,3'-dithiobis [sulfosuccinimidyl-propionate]; DTT, dithiothreitol; hCG, human chorionic gonadotropin; Kd, dissociation constants; LHR, LH receptor; rhCG, recombinant human chorionic gonadotropin; RIPA, radioimmunoprecipitation assay; SDS, sodium dodecyl sulfate; SSC, sodium chloride and sodium citrate; siRNA, small interfering RNA; ST, syncytiotrophoblast; TSH, thyroid-stimulating hormone; T21, trisomy of chromosome 21.

Endocrinology is published monthly by The Endocrine Society (<http://www.endo-society.org>), the foremost professional society serving the endocrine community.

drome, is the major known genetic cause of mental retardation, affecting about one in 800 live births. Screening strategies to identify women at an increased risk for bearing a T21 fetus are based on maternal age, ultrasound signs, and maternal serum markers (15). Some of these markers, such as hCG, are of placental origin. The hCG level in maternal serum is abnormally elevated at 14–18 wk in pregnancies with a T21 fetus, for reasons that are largely unknown.

hCG belongs to the family of gonadotrophin hormones, which also includes LH, FSH, and thyroid-stimulating hormone (TSH) (16). These glycoprotein hormones are composed of two subunits, α and β . The α -subunit, common to the other gonadotrophin hormones, is a 92-amino acid polypeptide with two N-linked oligosaccharides. β -hCG is a 145-amino acid polypeptide with two N-linked oligosaccharides and four O-linked oligosaccharides (17). The action of hCG in stimulating CT fusion and differentiation is primarily mediated via the chorionic gonadotropin receptor (LH/CG-R), which can also bind human LH (4, 5, 18). When engaged by these hormones, the LH/CG-R couples to a number of G proteins, and activates adenylate cyclase, phospholipase C, and ion channels, thereby stimulating the cAMP and inositol phosphate-signaling cascades (19, 20). LH/CG-R, which has seven transmembrane domains, belongs to a subfamily of G protein-coupled receptors (21), also comprising the FSH receptor and TSH receptor. The human LH/CG-R gene has been assigned to chromosome 2p21 (22). Its coding region is over 60-kb long, and it has been cloned in pig, mouse, rat, and also human, in whom it is composed of 11 exons and 10 introns (16, 21, 23, 24). LH receptor (LHR) has been also cloned in fish (25–28), monkeys (29), bears (30), and many other species. The presence of LH/CG-R in human placenta was first described by Alsat and Cedar (31), and subsequently confirmed by other authors (32, 33). We recently showed that LH/CG-R expression is modulated during normal CT fusion and differentiation (34).

To understand better the defective ST formation occurring in T21-affected pregnancies, we studied the involvement of the abnormal hCG by examining its function and receptor interaction. We found that T21-affected pregnancy is associated with a low LH/CG-R expression and that the secreted abnormal hCG can bind to its receptor. This low LH/CG-R expression, together with the secretion of abnormal hCG, is involved in the defective ST formation because specific inhibition of LH/CG-R expression by small interfering RNAs (siRNAs) in normal CTs mimics the T21 phenotype (defective ST formation). More interestingly, treatment of T21-affected CTs *in vitro* with normal recombinant hCG (rhCG) overcomes the T21 phenotype, allowing CTs to fuse and form a large ST.

Materials and Methods

Placental tissue collection

French law allows termination of pregnancy with no gestational age limit when severe fetal abnormalities are present. Placentas were collected at termination, between 12- and 35-wk gestation (amenorrhea), in T21-affected pregnancies and gestational age-matched control pregnancies. Gestational age was confirmed by sonographic measurement of crown-rump length at 8- to 12-wk gestation. Control pregnancies were terminated because of severe bilateral or low obstructive uropathies, or

major cardiac abnormalities. The karyotype of placental cells was determined in all cases (free T21 or normal). The study was approved by our local ethics committee.

Trophoblast cell culture

CTs from normal and trisomic placentas were isolated as previously described (35). After sequential trypsin/DNase I digestion followed by Percoll gradient centrifugation, the cells were further purified by negative selection to obtain a trophoblast preparation not contaminated by other cells, using monoclonal antihuman leukocytic antigen A, B, and C antibodies (W6-32HL; Sera Lab, Crawley Down, UK) according to a published method (36, 37). This antibody reacts with most cell types (*e.g.* macrophages, fibroblasts, extravillous trophoblasts), but not with villous cytotrophoblast or STs. Cytokeratin 7 immunocytochemistry was used to confirm the cytotrophoblastic nature of attached cells. Of the cells, 95–98% were positively stained.

Hormone assay

The hCG concentration was determined in culture medium at 24 and 72 h using an enzyme-linked fluorescence assay (Vidas System; BioMerieux, Marcy l'Étoile, France) with a detection limit of 2 mU/ml. All values are the mean \pm SEM of triplicate determinations.

hCG biological activity assay

The biological activity of secreted hCG was tested on Leydig cells (MA-10 cells, a generous gift from Professor M. Ascoli, University of Iowa, Iowa City, IA) as previously described (38). hCG levels were first assayed in trophoblast culture medium. Various amounts of culture medium were added as previously described (13). The results were expressed as the progesterone concentration per number of cells for each hCG concentration added to the control and T21 trophoblast culture medium. Progesterone was assayed with the ACS180SE instrument (Bayer, Fernwald, Germany), a polyclonal antibody against hCG (A0231, rabbit antihuman, at 7 μ g/ml; Dako Denmark A/S, Glostrup, Denmark), and a polyclonal antibody against LH/CG-R (LHR H50, rabbit antihuman, at 2 μ g/ml; Santa Cruz Biotechnology, Inc., Santa Cruz, CA) to block the action of hCG on MA-10 cells.

Immunoblotting

Proteins (70 μ g) were solubilized in radioimmunoprecipitation assay (RIPA) buffer, submitted to 7.5% SDS-PAGE, and transferred to nitrocellulose membranes. The membranes were immunoblotted with a polyclonal antibody against human LH/CG-R (LHR-H50, rabbit antihuman; Santa Cruz Biotechnology, Inc.) at 2 μ g/ml, and the specific band was revealed by chemiluminescence (West Pico Chemiluminescent; Pierce, Rockford, IL) after incubation with an antirabbit peroxidase-coupled antibody (Jackson ImmunoResearch, West Grove, PA). Actin was immunoblotted with a rabbit polyclonal anti-actin antibody at 1:1000 (Sigma-Aldrich, St. Louis, MO).

Cross-linking and immunoprecipitation

3,3'-Dithiobis [sulfosuccinimidyl-propionate] (DTSSP) is a soluble, homobifunctional N-hydroxysuccinimide ester. This cross-linker is thiol-cleavable and primary amine reactive. N-hydroxysuccinimide ester reactions with primary amines form covalent amide bonds that result in the release of N-hydroxysuccinimide. To cleave the covalent bond, we used 10 mM dithiothreitol (DTT) at 37 C for 30 min.

Protein G Plus-Agarose (Immunoprecipitation Reagent; Santa Cruz Biotechnology, Inc.) was premixed with a polyclonal antibody to human LHCG-R (LHR-H50). Cells (10^6 per well) were seeded in six-well plates and cultured as previously described, except for overnight serum-free cultures. After 24-h culture, 2 mM DTSSP was added to the culture medium for 30 min at 25 C to cross-link hCG to LHCG-R. Stop solution [Tris/glycine 20 mM (pH 7.5)] was then added at 25 C for 15 min. The cells were then washed with PBS and scraped in ice-cold RIPA buffer. After sonication the cellular extract was transferred to the immunocomplex Protein G antibody to human LHCG-R, incubated overnight at 4 C, and washed four times in RIPA buffer. Proteins were reduced with

10 mM DTT (sufficient to cleave the covalent bond) and eluted by heating at 60 C for 10 min in 1× electrophoresis sample buffer (Bio-Rad Laboratories, Hercules, CA). Aliquots were submitted to 7.5% SDS-PAGE and transferred to nitrocellulose membranes. Immunoprecipitates were treated with antibodies as described previously.

RNA extraction and RT-PCR

Total RNA was extracted from trophoblastic cells after 24-h culture using the TRIzol reagent (Invitrogen Life Technologies, Carlsbad, CA). RT-PCR was performed as previously described (34) using specific oligonucleotide primers based on the coding sequence of the LH/CG-R (NM 000233) (see Fig. 3A): P1(+), 5'-CA GACTTTTGCATGGGGCTC-3'; P1(-), 5'-GTGGCAGTGGTCATAGACTACAC-3'; P2(+), 5'-GCATCT-GTAACACAGGCATC-3'; P2(-), 5'-CA TCTGGTTCAGGAGCACAT-3'; P3(+), 5'-CAAGCTTTCAGAGGACTTAATGAGGTC-3'; P3 (-), 5'-AAAGCACAGCAGTGGCTGGGGTA-3'; actin (NM 001101) (+), 5'-GTGGGGCGCCCCAGGCACCA-3'; and actin (-), 5'-CTCCTTAATG-TCACAGCATTTC-3'.

RNA samples pretreated with DNase I were also amplified as controls. Amplified products were analyzed by electrophoresis on 1.8% agarose gel, visualized with ethidium bromide, and transferred to membranes (GeneScreen; New England Nuclear Life Science Products, Inc., Boston, MA). The amplified cDNA was hybridized with three LH/CG-R-specific cDNA probes (P1, P2, and P3) radiolabeled with ³²P using a random priming method. P1 is specific for the LH/CG-R transmembrane and intracellular domains, and spans positions 1300–2099 (position 1 corresponds to the A of the ATG start codon of the LH/CG-R coding sequence). P2 and P3 were specific for the extracellular domain, located from positions 386–1055 and 199–845, respectively. After prehybridization for 4 h at 60 C in 50% deionized formamide, 1% sodium dodecyl sulfate (SDS), 2× sodium chloride and sodium citrate (SSC), 10% dextran sulfate, the membranes were hybridized at 60 C in the same buffer containing the specific LH/CG-R cDNA probes, and were washed at 55 C, twice in 2× SSC, 1% SDS for 30 min, 2× SSC containing 0.1% SDS for 30 min, and 2× SSC for 5 min. The membranes were analyzed by Cyclone (Storage Phosphor System; Hewlett Packard, Rungis, France).

Cloning and DNA sequencing of LH/CG-R

PCR products were eluted from agarose gel, cloned into the pCRII-TOPO vector, and sequenced as previously described (34).

Binding assay

Trophoblastic cells (10⁶ per well) were seeded in six-well plates and cultured as described previously. After 24-h culture, they were washed and placed 2 h in DMEM without fetal calf serum, then placed in 1 ml DMEM, 0.1% BSA, 1 mM HEPES. To determine the time of [¹²⁵I]-hCG incubation for maximum binding, we performed a time-course study at 25 C (from 10 min to 2 h) with 0.5 nM [¹²⁵I]-hCG. Thirty minutes was the most effective time, corresponding to maximum binding of [¹²⁵I]-hCG in trophoblastic cells (data not shown). For equilibrium binding experiments, the cells were incubated for 30 min at 25 C with 0.5 nM [¹²⁵I]-hCG and with increasing concentrations of unlabeled hCG (from 10⁻¹² to 10⁻⁸ M, C6322; Sigma-Aldrich). At the end of the incubation period, the cells were washed and scrapped, and bound radioactivity was counted. Assays were performed in triplicate. Data were analyzed by using the LIGAND fitting program (version 4.97) (39).

[¹²⁵I]-labeled hCG was prepared as described by Hunter and Greenwood (40), using chloramine T as the oxidative reagent, as previously described (34).

Intracellular cAMP determination

At 24-h culture, cells (10⁶ per well) were stimulated with increasing concentrations of hCG (from 10⁻¹² to 10⁻⁶ M, C6322) in the presence of 3-isobutyl-1-methylxanthine to prevent cAMP degradation. Cells were frozen on dry ice, and cAMP was extracted from with ice-cold 65% ethanol. The extracts were dried and kept at -20 C until use. cAMP concentrations were determined with an assay kit (Amersham Biosciences, Piscataway, NJ) as previously described (34). Assays were

performed in sextuplet. To determine the optimum time of cAMP accumulation under hCG stimulation, we performed a time-course study (from 5 min to 1 h) by stimulating trophoblasts with hCG (10⁻¹² to 10⁻⁶ M). The most effective stimulating time was 20 min (data not shown). We used a polyclonal antibody against hCG (A0231, rabbit antihuman, at 7 μg/ml; Dako) to block the action of hCG on trophoblasts.

LH/CG-R siRNA protocol

LH/CG-R siRNA was a Smartpool mix (four different LH/CG-R siRNAs pooled) purchased from Dharmacon (Lafayette, CO). SiRNA transfection was performed using the DharmaFECT 2 siRNA transfection reagent (Dharmacon) according to the manufacturer's protocol. Briefly, 5 μl (20 μM) LH/CG-R siRNA (M-003681) or scrambled siRNA (46–2629; Invitrogen Life Technologies) was diluted in 245 μl OPTI-MEM (Invitrogen Life Technologies), and 4 μl transfection reagent (DharmaFECT 2) was diluted in 246 μl OPTI-MEM. The two solutions were incubated for 5 min at room temperature, then combined and incubated for 20 min at room temperature. The mixture was added to the cells (2.0 × 10⁶ per well) and incubated for 48 h at 37 C in air-5% CO₂. After transfection the medium was removed and kept for hormone assay. Cells were collected and used for immunoblot analysis.

Transfection efficiency was determined by testing siRNA uptake by primary CT cultures. After 5-h culture, CTs were incubated with a fluorescein-labeled double-strand RNA (dsRNA) oligomer for 18 h, then washed three times in PBS, fixed at 24, 48, and 72-h culture, and analyzed by fluorescence microscopy. The dsRNA oligomer was taken up from the first 24 h (60% of cells were labeled), and the proportion of labeled cells then increased progressively with time (75% at 48 h, 85% at 72 h), whereas the number of dead cells after transfection remained constant (~10%) during the culture and at a very low rate. Nuclei were stained blue using the Hoechst 33342 reagent (Invitrogen Life Technologies). A dead cell reagent (ethidium homodimer-I, staining dead cells red) was used to assess cell viability after transfection, visually or quantitatively. Both reagents are fluorescent compounds that bind to DNA; however, Hoechst 33342 binds to DNA in living cells, whereas the dead cell reagent binds only to the DNA of dying cells. Transfected cells can be visualized by fluorescence microscopy, as they integrate the fluorescein-labeled dsRNA oligomer. This experiment enabled us to determine the optimum concentrations of siRNA and transfection reagents.

Statistical tests

Statistical analysis was performed using the StatView F-4.5 software package (Abacus Concepts, Inc., Berkeley, CA). Values are presented as mean ± SEM. Significant differences were identified using ANOVA, and *P* < 0.05 was considered significant.

Results

Defective ST formation in T21 cytotrophoblastic cells

Mononucleated CTs isolated from normal placenta aggregate and fuse to form a ST at 72-h culture. In contrast, CTs isolated from T21-affected placentas aggregate but fuse poorly, forming a few small STs after 3-d culture (Fig. 1A). With cells isolated from normal placenta, *in vitro* ST formation is associated with an increase in hCG secretion into the culture medium (Fig. 1B), from 7.4 ± 2.3 (in mIU/ml·10⁶ cells) at 24 h to 1089 ± 61 at 72 h. With cells isolated from T21-affected placentas, the defective ST formation is associated with a significant lower (*P* < 0.0001) hCG secretion into the culture medium compared with normal cells (16.8 ± 9.5 and 366 ± 28 mIU/ml·10⁶ cells at 24 and 72 h, respectively) (Fig. 1B).

Defective LH/CG-R expression in T21 cytotrophoblastic cells

hCG secretion by the ST is lower in T21 than normal cells. To evaluate the role of hCG and its receptor in ST formation,

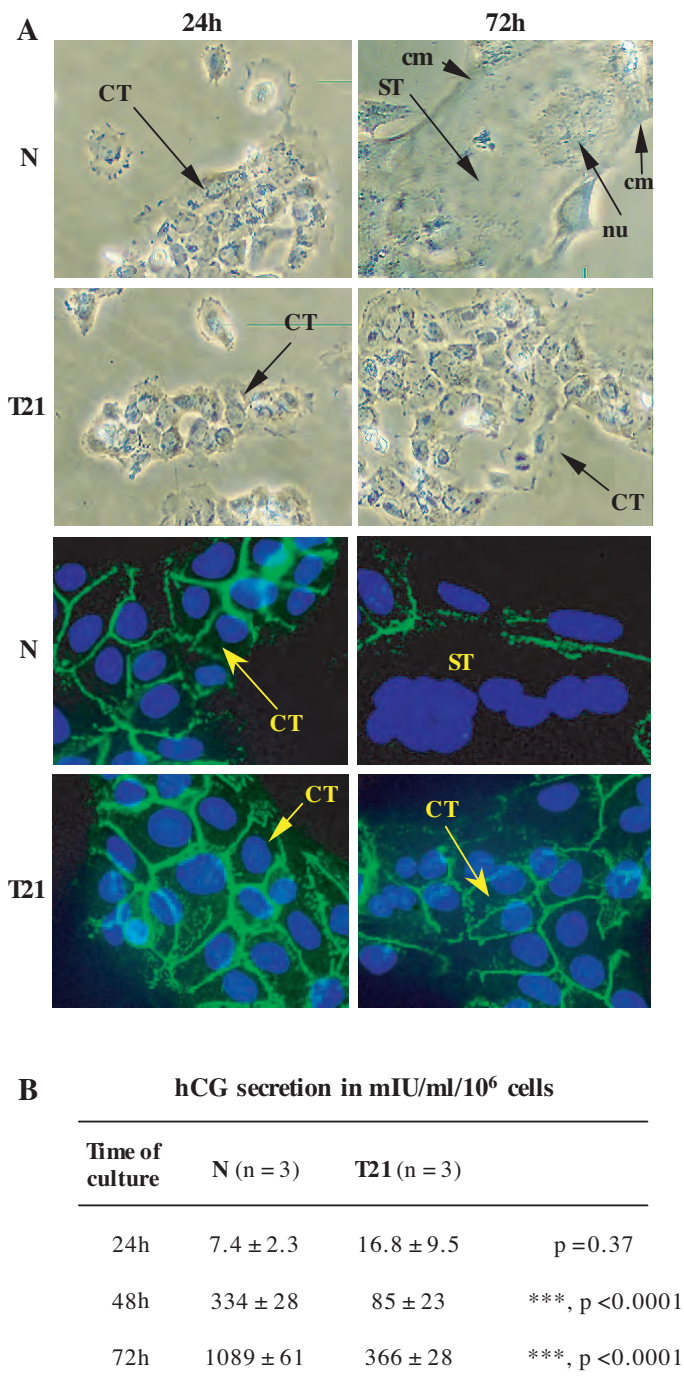


FIG. 1. Defective ST formation by T21 cytotrophoblastic cells. A, Differentiation of CTs into ST, at 24 and 72-h culture, with normal (N) and T21 cells. The cells were visualized by phase contrast microscopy (upper panel) and immunostaining (lower panel) of the cellular membrane (cm) with an anti-desmoplakin monoclonal antibody. Nuclei (nu) were counterstained by 4',6-diamidino-2-phenylindole. At 24-h culture, normal and T21-affected CTs had aggregated. At 72 h, normal CT had fused, as immunofluorescence staining of the cell boundaries disappeared, owing to the formation of a large syncytium (ST) containing many nuclei. T21 CTs were still aggregated and had not fused. B, hCG secretion into the culture medium at the indicated times, in normal (N) and T21-affected cell cultures. Results are means ± SEM of three culture dishes. This figure illustrates one experiment representative of three.

we first studied the expression of LH/CG-R mRNA in normal and T21-affected CTs at 24-h culture. We performed semiquantitative RT-PCR experiments with three sets of primers (P1, P2, and P3); positions are indicated in Fig. 2A. To avoid contamination by genomic DNA, each RNA extract was pretreated with DNase I. Moreover, the primers of pairs P2 and P3 were located on separated exons.

As shown in Fig. 2B, the 800, 660, and 647-bp fragments obtained with P1, P2, and P3, respectively, indicated that LH/CG-R mRNA was significantly less abundant in T21-affected CTs than in normal CTs. No significant difference was noted in the actin mRNA (control) level. To confirm the specificity of these RT-PCR results, amplification products were transferred to nylon membranes and hybridized with ³²P-radiolabeled probes. We used three probes specific for LH/CG-R, spanning the extracellular, transmembrane, and intracellular domains (for positions, see *Materials and Methods*). Hybridization confirmed the significant lower LH/CG-R mRNA expression in T21-affected CTs. No difference was noted with an actin-specific control probe.

Normalization of LH/CG-R mRNA to actin mRNA confirmed the decrease in LH/CG-R mRNA levels in T21-affected CTs (Fig. 2C). Using primer set P1, LH/CG-R mRNA levels were 1.23 ± 0.26 (in arbitrary units) in normal CTs compared with 0.6 ± 0.1 in T21-affected CTs ($P < 0.013$). A similar decrease was observed with primer sets P2 (1.20 ± 0.26 and 0.35 ± 0.06 ; $P < 0.034$) and P3 (1.42 ± 0.12 and 0.54 ± 0.28 ; $P < 0.043$). Interestingly, the relative expression was similar with the three primer sets (2.0-, 3.4-, and 2.6-fold, respectively).

We then used Western blot to determine LH/CG-R protein expression in extracts of normal and T21-affected CTs, using the polyclonal antibody LHR-H50 (Fig. 3A). Two major bands were observed: an 85- to 95-kDa band corresponding to the mature form of the LH/CG-R (noted "m" on Fig. 3A) present at the cell surface; and a 65- to 75-kDa band that is the precursor (noted "p") of the cell-surface receptor (34) (for review, see Ref. 41).

As shown in Fig. 3A, the mature form of LH/CG-R was far less abundant in T21-affected CTs than normal CTs, whereas no significant difference in actin expression was observed. Normalization of mature LH/CG-R protein expression to actin expression showed a significant difference (at least 68%) between normal CTs and T21-affected CTs (9.2 ± 0.7 and 2.9 ± 1.4 arbitrary units; $P < 0.0038$).

To confirm the decrease in LH/CG-R mRNA and protein levels, we performed binding experiments with [¹²⁵I]-hCG at 24-h culture of normal and T21-affected CTs (Fig. 3B). Scatchard analysis showed that the number of [¹²⁵I]-hCG molecules bound per normal CT (3511 ± 693) was significantly higher ($P < 0.04$) than that in T21-affected CTs (1124 ± 350). The difference in dissociation constants (Kd) values between normal CTs (0.5 ± 0.2 nM) and T21-affected CTs (0.4 ± 0.2 nM) was not statistically significant. These results indicate that T21 CTs express three times fewer LH/CG cell-surface receptors, than normal CTs. However, the LH/CG-R molecule expressed at the surface of T21 CT bound [¹²⁵I]-hCG with the same affinity as the LH/CG-R on normal CTs.

The reduced level of functional mature LH/CG-R at the cell surface of T21-affected CT was confirmed by measuring

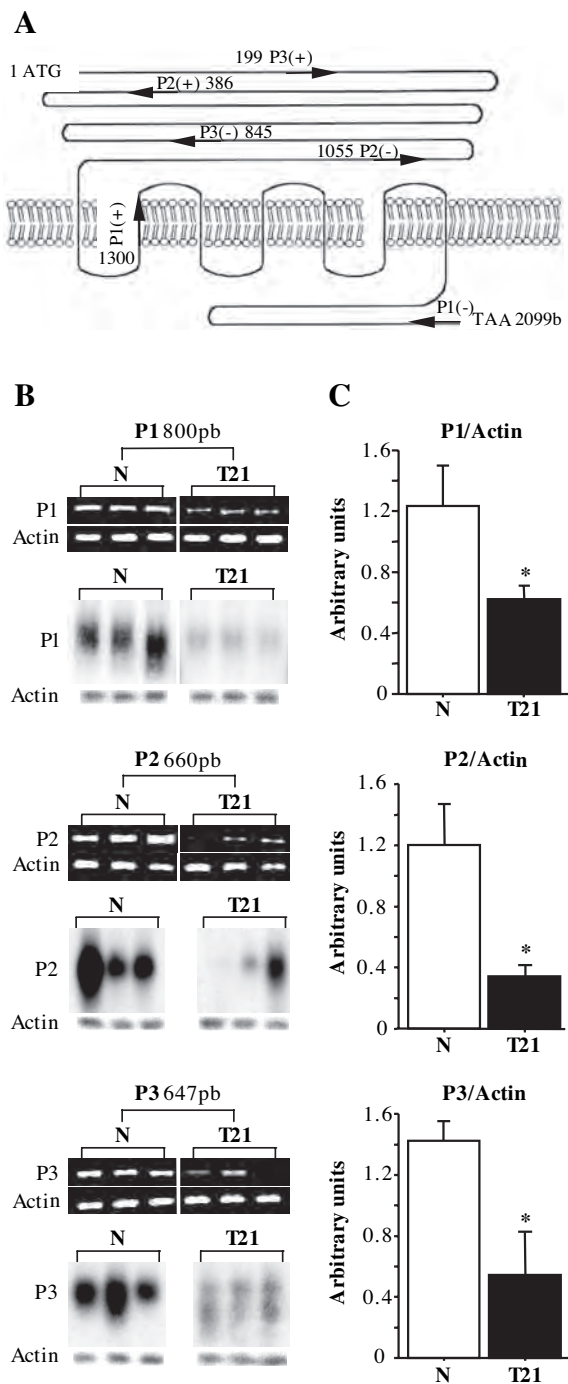


FIG. 2. Defective LH/CG-R mRNA expression in T21 cytotrophoblastic cells. **A**, Schematic representation of the LH/CG-R and location of primers used for this study. **B**, Ethidium bromide-staining gel after RT-PCR. Amplified products were separated on 1.8% agarose gel and analyzed by densitometry. Primers P1, P2, and P3 generate 800-, 660-, and 647-bp amplified fragments, respectively. Hybridization with ³²P-labeled specific probes confirmed that the amplified fragments were part of the LH/CG-R. RT-PCR was done with total mRNA extracted from CTs obtained from three normal (N) and three trisomic (T21) placentas. **C**, The histograms represent LH/CG-R mRNA normalized to actin mRNA after RT-PCR with primers P1, P2, and P3. The data are means ± SEM of four independent experiments similar to the one shown in **B**. *, *P* < 0.05.

cAMP production in response to increasing hCG concentrations, at 24-h culture. As shown in Fig. 3C, at 10⁻¹⁰ M hCG, corresponding to maximum cAMP accumulation, the ability of hCG to stimulate cAMP production in trophoblastic cells was significantly higher (*P* < 0.007) in normal CTs (222 ± 3 fmol/mg protein) than T21-affected CTs (164 ± 10 fmol/mg protein). Stimulation with epinephrine (used as a positive control) induced similar accumulation of intracellular cAMP in T21-affected CTs as in normal CTs, showing that the T21-affected CTs were viable and that the reduced cAMP production was not due to increased apoptosis of T21 cells or a defect in the cAMP pathway.

These results clearly show that LH/CG-R expression at the surface of trophoblastic cells is markedly reduced in T21-affected pregnancies.

Specific inhibition of LH/CG-R expression by siRNA inhibits syncytium formation and hCG secretion by normal cytotrophoblastic cells

We then tried to mimic with normal CTs what we observed in T21-affected CTs, by incubating normal CTs with LH/CG-R siRNA. As shown by Western blot analysis (Fig. 4B), LH/CG-R siRNA markedly reduced LH/CG-R protein expression. Normalization of LH/CG-R protein expression to actin expression showed 74% inhibition compared with cells transfected with scrambled siRNA (8.0 ± 0.1 arbitrary units; *P* < 0.002). A similar decrease (78% inhibition; *P* < 0.002) was also found when we compared control nontransfected cells with cells transfected with LH/CG-R siRNA. No difference was seen between nontransfected cells (control) and cells transfected with scrambled siRNA, indicating that transfection had no effect on the decreased receptor expression.

Specific inhibition of LH/CG-R expression by siRNA was associated with a strong decrease in CT fusion and differentiation. The histogram in Fig. 4A shows that there were more mononuclear cells (58.5 ± 0.2%) in cultures treated with LH/CG-R siRNA than in those incubated with scrambled siRNA (32.5 ± 0.1%; *P* < 0.005). Calculation of an apparent fusion index showed a 2.1-fold decrease in fusion (53.3 ± 7.1% scrambled siRNA-treated cells fused, compared with 25.0 ± 0.6% LH/CG-R siRNA-treated cells; *P* < 0.017). LH/CG-R siRNA treatment led to a decrease in the number and size of syncytia. Similar results were obtained when LH/CG-R siRNA-treated cells were compared with nontransfected control cells (data not shown).

Interestingly, the decrease in syncytium formation observed when normal cells were treated with LH/CG-R siRNA was associated with a decrease of syncytium function. As illustrated in Fig. 4C, hCG secretion into the culture medium was far lower with LH/CG-R siRNA-treated cells than with scrambled siRNA-treated cells (59% reduction) or control cells (66% reduction). This result was not due to a difference in cell viability after transfection because hCG secretion by control and scrambled siRNA-treated cells was similar.

These results point to a direct role of LH/CG-R in CT fusion and differentiation during ST formation.

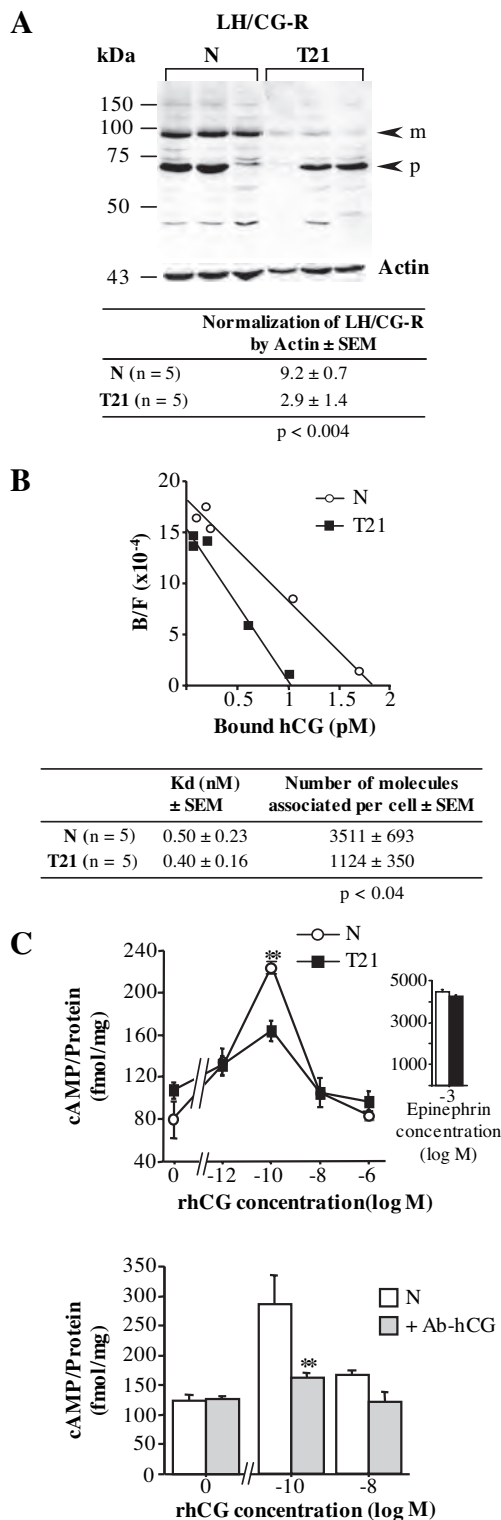


FIG. 3. Defective LH/CG-R protein expression in T21 cytotrophoblastic cells. **A**, Western blot analyses were performed with normal (N) and T21-affected trophoblast cell extracts. The polyclonal antibody LHR-H50 raised against the human LH/CG-R yielded two major bands on SDS-PAGE: a 65- to 75-kDa band corresponding to the LH/CG-R precursor (p) and a 85- to 95-kDa band corresponding to the mature LH/CG-R (m) expressed at the cell surface. The *table* shows mature LH/CG-R protein expression (m) normalized to actin expression (43 kDa). The results are the mean ± SEM of five culture dishes.

LH/CG-Rs of T21-affected trophoblasts bind endogenous weakly bioactive hCG

We have shown that T21-affected CTs bear a reduced number of LH/CG-Rs. We then analyzed the bioactivity of the endogenous hCG ligand using the well-established test of hCG function on MA-10 Leydig cells (38). hCG secreted into the culture medium at 72 h by normal ($n = 3$) and T21-affected trophoblasts ($n = 3$) was used to stimulate steroid production by Leydig cells, which constitutively express LH/CG-Rs. At equivalent hCG concentrations in the culture medium (from 2.5×10^{-11} to 10^{-10} M), the ability of hCG secreted by T21-affected trophoblasts to stimulate Leydig cell progesterone secretion was significantly decreased (Fig. 5A, *upper panel*). To emphasize this result, we quantified the production of intracellular cAMP by Leydig cells after stimulation with hCG from normal ($n = 3$) and T21 ($n = 3$) culture medium. In view of previous results, we used two hCG concentrations to stimulate Leydig cells: 0.1×10^{-11} M, which does not elicit progesterone secretion; and 5×10^{-11} M, which leads to maximal progesterone secretion. The histogram in Fig. 5A (*lower panel*) shows that stimulation with hCG secreted at 72-h culture by T21-affected trophoblasts was associated with significantly lower (at least 3-fold) cAMP production than was hCG secreted by normal trophoblasts (510 ± 64 vs. 1535 ± 61 fmol/mg of protein; $P < 0.0001$). Intracellular cAMP accumulation occurred after hCG stimulation because no cAMP production was detectable when the culture media were preincubated with anti-hCG (Ab-hCG) or anti-LH/CG-R (Ab-LH/CG-R) blocking antibodies before hCG stimulation. We obtained similar results when we used hCG secreted at 24 h by normal and T21-affected trophoblasts (data not shown).

This reduction in progesterone secretion and cAMP production after stimulation with hCG secreted by T21-affected trophoblasts was not due to lesser binding of this hormone to its receptor. Scatchard analysis (Fig. 5B) showed that hCG secreted by T21-affected trophoblasts bound to LH/CG-Rs expressed by Leydig cells with the same affinity ($K_d = 0.13 \pm 0.01$ nM) as hCG secreted by normal trophoblasts ($K_d = 0.15 \pm 0.07$ nM).

Our results clearly show that hCG secreted by T21-affected trophoblasts is less bioactive than normal hCG and that this is not due to deficient binding to the LH/CG-R, as expressed on Leydig cells. We then studied the interaction of the LH/CG-R expressed by T21-affected CTs with endogenous hCG secreted by the same cells. For this purpose we cultured

This illustrates one experiment representative of five. **B**, Scatchard analyses of [125 I]-hCG binding *in vitro* to normal and T21-affected trophoblasts. Binding was allowed to proceed for 30 min at room temperature, on normal (○) and T21-affected cells (■), after 24-h culture. Apparent K_d and the maximum number of molecules bound per cell were calculated with the LIGAND program (*table*). Results are means ± SEM of five experiments. **C**, Intracellular cAMP production by normal (○) and T21-affected cells (■) after stimulation with rhCG (10^{-12} to 10^{-6} M) or with a positive control reagent (epinephrine 10^{-3} M), compared with nonstimulated cells (0). To show the specificity of stimulation by hCG, we used an Ab-hCG blocking antibody. Stimulation of normal trophoblasts was performed with 10^{-10} and 10^{-8} M hCG in the presence or absence of the blocking hCG antibody. This illustrates one experiment representative of three. **, $P < 0.01$.

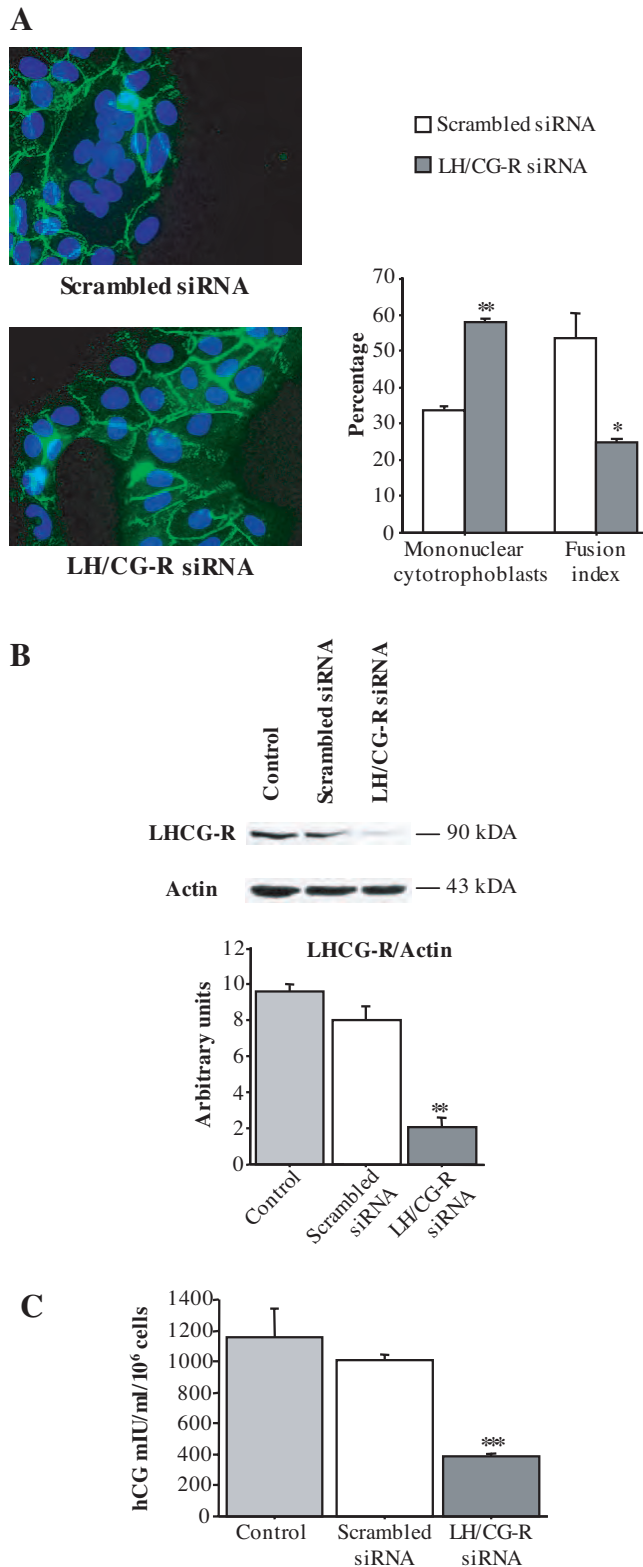


FIG. 4. This figure illustrates one experiment representative among five. Specific inhibition of LH/CG-R expression by siRNA reduces syncytium formation and hCG secretion by normal cytotrophoblastic cells. A, Normal CTs were transfected with scrambled or LH/CG-R-specific siRNA. The extent and number of syncytia were assessed by desmoplakin immunostaining and determining the number of 4',6-diamidino-2-phenylindole-stained nuclei. After 72-h culture, mono-

T21-affected CTs and cross-linked the endogenous hCG secreted into the culture medium to its receptor to form hCG-LH/CG-R complexes. These complexes were immunoprecipitated (Fig. 6) using an Ab-LH/CG-R polyclonal antibody (LHR-H50) and were then incubated in presence or absence of DTT. We used the DTSSP cross-linker agent, which is cleavable in the presence of DTT (used as a reducing agent). After immunoprecipitation the complexes were probed with an Ab-LH/CG-R antibody (Fig. 6, left). Without the reducing agent (-DTT), we observed a band at approximately 130 kDa, corresponding to hCG cross-linked to LH/CG-R. The presence of DTT (+DTT) disrupted the hormone-receptor complex, and the band at 130 kDa disappeared; a band corresponding to the receptor alone then appeared at 90 kDa. To ensure that the 130-kDa band corresponded to hCG-LH/CG-R complexes, we used an Ab-hCG polyclonal antibody to treat the previous immunoprecipitates (Fig. 6, right). In nondenaturing conditions, a 130-kDa band corresponding to hCG bound to the LH/CG-R, and a smaller band (40 kDa), corresponding to total hCG, was observed. In reducing conditions only the 40-kDa band was observed. No 130-kDa band was found as hCG-LH/CG-R complexes were disrupted. The interactions and complexes observed in these experiments were specific because no cross-reactions occurred in a range of control conditions (Fig. 6, lower).

These results show that T21 trophoblastic cells produce an abnormal hCG that is weakly bioactive but that can, nonetheless, bind its receptor LH/CG.

Defective ST formation by T21 cytotrophoblastic cells is overcome by rhCG treatment

Interestingly, as shown in Fig. 7A, addition of rhCG (10^{-8} M) to the culture medium of T21-affected CTs induced ST formation. T21 CTs cultured for 72 h contained twice as many mononuclear cells in control conditions ($76.2 \pm 0.6\%$) than when treated with rhCG ($39.3 \pm 0.9\%$; $P < 0.0001$). In other words, rhCG induced T21-affected CT differentiation and fusion because more than 60% of the cells participated in syncytia formation (*vs.* 23% untreated cells) (Fig. 7B). With T21 cells, the percentage of syncytia containing 10–50 nuclei increased from $1.6 \pm 0.3\%$ with untreated cells (controls) to $13.0 \pm 1.7\%$ with treated cells (+rhCG) ($P < 0.003$). In contrast, the proportion of mononuclear cells observed at 72-h culture of normal CTs was not affected by rhCG (+rhCG: $15.8 \pm 1.2\%$, -rhCG: $17.2 \pm 0.4\%$; Fig. 7B). Indeed, rhCG promoted the fusion of al-

nuclear cells were counted, and the fusion index was determined as $(N-S)/T$, where N is the number of nuclei in the syncytia, S the number of syncytia, and T the total number of nuclei counted. Results are expressed as percentages of the control fusion index. Larger syncytia were observed with cells treated with scrambled siRNA than with cells treated with LH/CG-R siRNA. B, Western blot analysis of LH/CG-R expression in lysates of untransfected cells (control) and cells transfected with scrambled siRNA or LH/CG-R siRNA. LH/CG-R was detected with polyclonal antibody LHR-H50 raised against the human LH/CG-R and standardized with an anti-actin polyclonal antibody. The histogram shows LH/CG-R protein expression normalized to actin expression. C, Levels of hCG secreted into the culture medium at 72 h by untransfected cells (control) and cells transfected with scrambled or LH/CG-R-specific siRNA. Results are expressed as the mean \pm SEM. *, $P < 0.05$. **, $P < 0.01$. ***, $P < 0.001$.

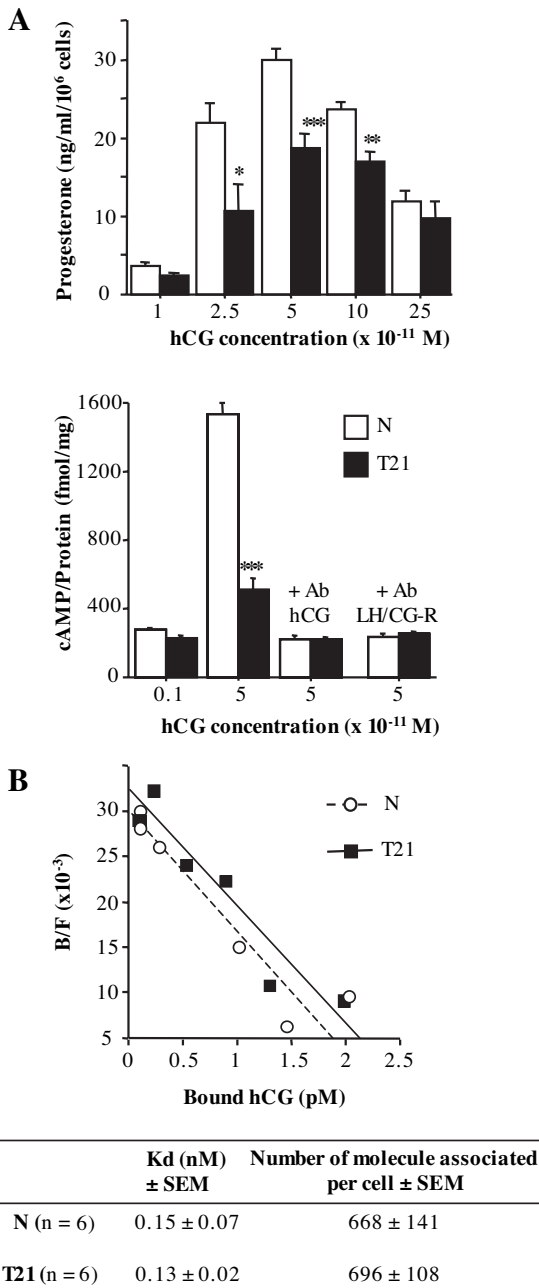


FIG. 5. hCG secreted by T21-affected trophoblast binds LH/CG-R but is weakly bioactive. A (Upper panel), MA-10 Leydig cells were stimulated with hCG secreted in the culture media of normal (N) and T21-affected cells. Various volumes of these media, corresponding to the indicated concentrations of hCG, were used to stimulate MA-10 cells. Progesterone was assayed in MA-10 culture medium 3 h later. To confirm the lesser bioactivity of T21 hCG, we determined the intracellular cAMP accumulation in MA-10 cells after stimulation with medium conditioned by normal (N) and T21-affected cells (lower panel). The specificity of stimulation by hCG was determined with Ab-hCG and Ab-LH/CG-R blocking antibodies. *, $P < 0.05$. **, $P < 0.01$. ***, $P < 0.001$. B, Scatchard analysis of [¹²⁵I]-hCG binding to LH/CG-Rs expressed by Leydig cells in the presence of hCG secreted by normal (○) and T21-affected cells (■). The apparent Kd and maximum number of molecules bound per cell (table) were calculated with the LIGAND program.

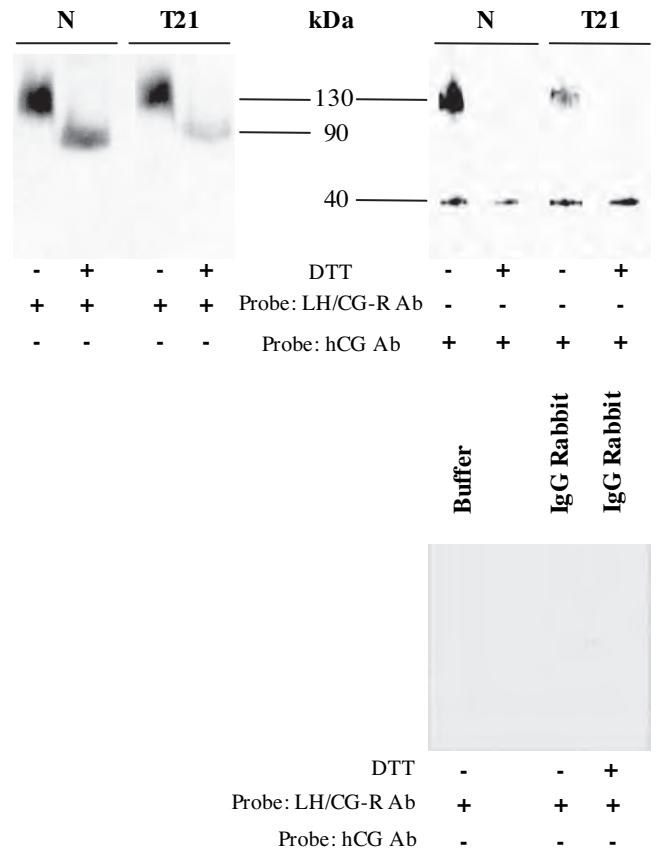


FIG. 6. LH/CG-R of T21-affected trophoblasts binds endogenous hCG. Endogenous hCG from normal (N) and trisomic (T21) cultures was cross-linked to its receptor using DTSSP, a reversible and cleavable (in reducing conditions) cross-linker. Cellular extracts were purified with immobilized LH/CG-R antibody (LHR H50) on protein G Plus-agarose. LH/CG-R-hCG complexes were analyzed by SDS-PAGE in reducing conditions in the presence or absence of DTT and probed with Ab-LH/CG-R antibody (+) (left panel) or Ab-hCG antibody (+) (right panel). When Ab-LH/CG-R was used as probe (left panel), in nonreducing conditions (–DTT), extracts of normal (N) and T21-affected cells contained a 130-kDa band corresponding to the hormone/receptor complex. In reducing conditions (+DTT), the hormone/receptor complexes were disrupted, and a 90-kDa band corresponding to LH/CG-R was observed. When Ab-hCG was used to probe the immunoblot (right panel), in nonreducing conditions (–DTT), hCG in the hormone/receptor complex (130 kDa) and free total hCG (40-kDa) were detected in extracts from normal (N) and T21-affected cells. In reducing conditions (+DTT), the hormone/receptor complexes were disrupted, and only free total hCG (40 kDa) was observed. The observed interactions and complexes were specific because no cross-reactions were seen between the buffer used for cell extract preparation and protein G agarose beads alone or between cell extracts and protein G agarose beads coated with rabbit IgG, in either reducing or nonreducing conditions (lower panel).

ready formed syncytia, producing larger syncytia (Fig. 7B); the percentage of syncytia containing more than 50 nuclei was significantly higher with treated cells than control cells ($P < 0.0001$).

These results show that the defective cell fusion and differentiation of T21-affected CTs may be overcome. More importantly, they show the key role of hCG in ST formation because the addition of rhCG to the T21 CT culture medium led to CT fusion and ST formation.

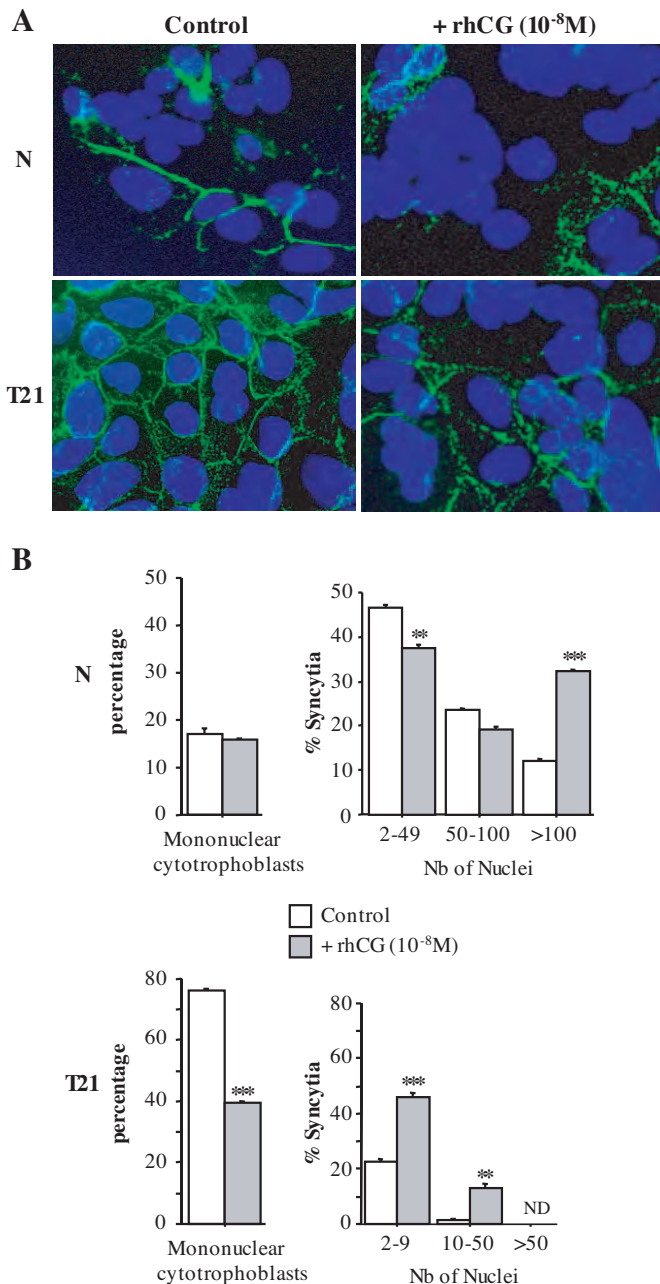


FIG. 7. ST formation in T21 cytotrophoblastic cells is induced by rhCG. A, Normal (N) and trisomic (T21) CTs were cultured for 72 h in the presence (+rhCG) or absence (control) of 10⁻⁸ M rhCG. After 72-h culture, the cells were immunostained with an anti-desmoplakin monoclonal antibody, and the nuclei were counterstained with 4',6-diamidino-2-phenylindole. B, Mononuclear cells were counted, and the distribution of nuclei was evaluated as follows: 100 syncytia were scored, and the nuclei were counted in each syncytium. Data (from one representative experiment among five) are expressed as the distribution of the number of nuclei per syncytium. Results are expressed as the mean ± SEM. **, P < 0.01. ***, P < 0.001. Nb, number; ND, nondetectable.

Discussion

Placental development is severely abnormal in women bearing a T21 fetus, with defective ST formation and function leading to the secretion of an abnormal hyperglycosylated hCG (12, 13). We show here, for the first time, that treatment

of T21-affected CTs with normal or rhCG restores their capacity to form a ST. This reversal of the T21 phenotype indicates that T21 CTs have all the equipment required to fuse and differentiate. Thus, the abnormal CT fusion and differentiation observed in T21-affected pregnancies may be due to impaired hCG signaling. This is supported by our observation that specific inhibition of LH/CG-R expression by siRNA in normal CTs mimics the T21 phenotype (defective ST formation).

In this study we clearly show that LH/CG-R expression, present at the cell surface of the cells, was far lower on T21-affected CTs than normal CTs, as shown by using several complementary methods and a well-characterized model of human villous trophoblast differentiation *in vitro*. LH/CG-R mRNA and protein levels were lower in T21 cells, as also observed *in situ* by immunohistochemical studies (data not shown).

These results are in line with those reported by Nicolaides and colleagues (42), who demonstrated in total placental extracts that LH/CG-R expression was significantly lower in T21 pregnancies than in of controls, whereas Rao and colleagues (43) described stronger expression of LH/CG-R in T21 placentas. This divergence may stem from the use of different approaches and tools. Rao and colleagues quantified LH/CG-R immunostaining in total samples of placental villous tissue and, thus, may have overestimated LH/CG-R expression because the receptor is also expressed in Hofbauer and endothelial cells in villous stromal tissue (44, 45) and by intermediate trophoblasts (46). Moreover, experiments with radiolabeled probes, such as *in situ* hybridization, use porcine cDNA that shares only 88% of the human sequence. In this study we designed specific probes for the human LH/CG-R in normal and T21-affected villous CTs. In addition, we quantified the mature form of the receptor expressed at the CT surface, whereas the other authors quantified all LH/CG-R isoforms.

Scatchard plots clearly showed that the maximum number of hCG molecules bound per cell was significantly lower on T21-affected CTs than normal CTs. This lower cell-surface receptor expression by T21-affected CTs was confirmed by the lower cAMP production observed after stimulation with rhCG. This decrease in cAMP production was not due to a loss of receptor affinity for the recombinant hormone because rhCG was able to bind to LH/CG-R on both normal and T21-affected CTs with the same apparent affinity (same Kd values). Apart from the smaller number of LH/CG-R molecules expressed at the surface of T21-affected CTs, the LH/CG-R seems to be normal because sequencing revealed no mutations or deletions. Moreover, the receptor was functional and able to signal after stimulation with rhCG. Indeed, replacing the abnormal endogenous hCG by the recombinant hormone in T21-affected CT cultures enhanced ST formation. This also implied that a functional hormone is necessary for ST formation. In other words, the secretion of abnormal hCG by T21-affected cells might be responsible for the defective CT differentiation. We have previously shown that hCG is hyperglycosylated in T21 pregnancies by using different lectins (13). Indeed, mRNA levels of two enzymes involved in the glycosylation pathway, sialyl-transferase-1 (which adds a sialyl group to antennary structures) and fucosyl-trans-

ferase-1 (which adds a fucose to the first N-acetyl-glucosamine of glycoproteins), were significantly higher in cultured trophoblasts isolated from trisomy 21 placenta (13). We show here that it is biologically less functional on cytotrophoblast differentiation. We also demonstrate here that this abnormal hormone is able to bind its receptor.

One particularly interesting result is the differential effect of rhCG on normal and T21-affected mononuclear CTs (Fig. 1C). rhCG did not reduce the percentage of normal unfused mononuclear CTs but rather induced the fusion of already formed syncytia with one another, leading to huge STs containing more than 100 nuclei. In contrast, rhCG induced the differentiation of T21 CTs into an ST. At 24-h culture, the percentage of unfused CTs was higher than in normal placenta, suggesting that their maturation or differentiation is delayed. rhCG enhanced CT fusion and differentiation into ST, possibly through the induction of LH/CG-R expression at the CT surface. A similar form of regulation has been described for epidermal growth factor, which up-regulates epidermal growth factor-receptor mRNA and protein expression in human prostate cancer (47). Another possible explanation is that, in T21, despite the lower LH/CG-R expression, the level of expression is still sufficient (above a critical threshold of receptor density required to induce differentiation), and the defective differentiation is due to the abnormal secreted hCG molecules. By removing the latter from the culture medium and replacing them with rhCG, we restored the CT fusion and differentiation process. However, even after stimulation with rhCG, the rate of fusion was never as high as that observed with normal cells, whether or not they were treated with rhCG. This difference may be due to the lower number of LH/CG-R molecules expressed at the surface of T21 CTs. Indeed, our results show that LH/CG-R is directly involved in human trophoblast cell fusion and differentiation because its inhibition by specific siRNA reduces trophoblast cell fusion. It appears that the hCG-LH/CG-R system acts as a positive feedback system. If hCG signaling is intact, then ST formation is increased and hCG production as well, resulting in increased ST formation.

Screening strategies used to identify women at an increased risk for bearing a T21 fetus are partly based on maternal serum markers such as hCG. The hCG level in maternal serum is elevated during T21 pregnancies, for reasons that remain largely unknown. We demonstrate that, despite this increase, the autocrine/paracrine effects of hCG on the placenta are severely impaired, owing to a loss of hormone function and reduced expression of the mature form of the LH/CG-R at the cell surface. The conjunction of these two phenomena results in inadequate receptor-mediated signaling, leading to hCG accumulation in maternal serum. Abnormal receptor expression leading to hormone accumulation has already been described in various systems (48–50).

The main clinical relevance of this report is that it shows the significance of hCG in establishing and maintaining placental and fetal development during human pregnancy. We clearly demonstrate that, in pregnancies associated with a T21 fetus, the placenta secretes an abnormal and weakly bioactive hCG molecule that cannot correctly stimulate CT differentiation. In addition, the subnormal expression of

functional LH/CG-R protein in the placenta of T21 pregnancies may have far-reaching consequences. For instance, the rate of spontaneous abortion is high in T21-affected pregnancies. Aneuploidy might alter the fetal cells' ability to differentiate properly. The morphological, phenotypic, and functional differences among T21-affected trophoblastic cells may explain why a significant number of pregnancies end in spontaneous miscarriage.

Acknowledgments

We thank Dr. Fanny Lewin for her support and the staff of the Saint Vincent de Paul Obstetrics Department for providing us with placentas.

Received May 3, 2007. Accepted July 31, 2007.

Address all correspondence and requests for reprints to: Dr. Jean-Louis Frendo, Institut National de la Santé et de la Recherche Médicale, Unité 767, Faculté de Pharmacie, 4 Avenue de l'Observatoire, 75270 Paris, France. E-mail: jean-louis.frendo@univ-paris5.fr.

This work was supported by la Caisse d'Assurance Maladie des Professions Libérales Province. G.P. was supported by a fellowship from Conseil Régional d'Ile-de-France and J.-L.F. by a grant from Institut National de la Santé et de la Recherche Médicale (Projet Avenir).

Disclosure Statement: The authors have nothing to declare.

References

1. Red-Horse K, Zhou Y, Genbacev O, Prakobphol A, Foulk R, McMaster M, Fisher SJ 2004 Trophoblast differentiation during embryo implantation and formation of the maternal-fetal interface. *J Clin Invest* 114:744–754
2. Bo M, Boime I 1992 Identification of the transcriptionally active genes of the chorionic gonadotropin β gene cluster in vivo. *J Biol Chem* 267:3179–3184
3. Malassiné A, Frendo J-L, Evain-Brion D 2003 A comparison of placental development and endocrine functions between the human and mouse model. *Hum Reprod Update* 9:531–539
4. Cronier L, Bastide B, Hervé J-C, Delèze J, Malassiné A 1994 Gap junctional communication during human trophoblast differentiation: influence of human chorionic gonadotropin. *Endocrinology* 135:402–408
5. Shi Q, Lei Z, Rao CV, Lin J 1993 Novel role of human chorionic gonadotropin in differentiation of human cytotrophoblasts. *Endocrinology* 132:1387–1395
6. Frendo J-L, Théron P, Guibourdenche J, Bidart J-M, Vidaud M, Evain-Brion D 2000 Modulation of copper/zinc superoxide dismutase expression and activity with in vitro differentiation of human villous cytotrophoblasts. *Placenta* 21:773–781
7. Frendo J-L, Théron P, Bird T, Massin N, Muller F, Guibourdenche J, Luton D, Vidaud M, Anderson W, Evain-Brion D 2001 Overexpression of copper zinc superoxide dismutase impairs human trophoblast cell fusion and differentiation. *Endocrinology* 142:3638–3648
8. Getsios S, MacCalman C 2003 Cadherin-11 modulates the terminal differentiation and fusion of human trophoblastic cells in vitro. *Dev Biol* 257:41–54
9. Frendo J-L, Cronier L, Bertin G, Guibourdenche J, Vidaud M, Evain-Brion D, Malassiné A 2003 Involvement of connexin 43 in human trophoblast cell fusion and differentiation. *J Cell Sci* 116:3413–3421
10. Frendo J-L, Olivier D, Cheynet V, Blond J-L, Vidaud M, Rabreau M, Evain-Brion D, Mallet F 2003 Direct involvement of HERV-W Env glycoprotein in human trophoblast cell fusion and differentiation. *Mol Cell Biol* 23:3566–3574
11. Rossant J, Cross J 2001 Placental development: lessons from mouse mutants. *Nat Rev Genet* 2:538–548
12. Frendo J-L, Vidaud M, Guibourdenche J, Luton D, Muller F, Bellet D, Giovannardi Y, Tarrade A, Porquet D, Blot P, Evain-Brion D 2000 Defect of villous cytotrophoblast differentiation into syncytiotrophoblast in Down's syndrome. *J Clin Endocrinol Metab* 85:3700–3707
13. Frendo J-L, Guibourdenche J, Pidoux G, Vidaud M, Luton D, Giovannardi Y, Porquet D, Muller F, Evain-Brion D 2004 Trophoblast production of a weakly bioactive human chorionic gonadotropin in trisomy 21-affected pregnancy. *J Clin Endocrinol Metab* 89:727–732
14. Wright A, Zhou Y, Weier JF, Caceres E, Kapidzic M, Tabata T, Kahn M, Nash C, Fisher SJ 2004 Trisomy 21 is associated with variable defects in cytotrophoblast differentiation along the invasive pathway. *Am J Med Genet A* 130:354–364
15. Bogart M, Pandian M, Jones O 1987 Abnormal maternal serum chorionic gonadotropin levels in pregnancies with fetal chromosome abnormalities. *Prenat Diagn* 7:623–630
16. Pierce J, Parsons T 1981 Glycoprotein hormones: structure and function. *Annu Rev Biochem* 50:465–495
17. O'Connor J, Birken S, Lustbader J, Krichevsky A, Chen Y, Canfield R 1994

- Recent advances in the chemistry and immunochemistry of human chorionic gonadotropin: impact on clinical measurements. *Endocr Rev* 15:650–683
18. Yang M, Lei Z, Rao C 2003 The central role of human chorionic gonadotropin in the formation of human placental syncytium. *Endocrinology* 144:1108–1120
 19. Gudermann T, Birnbaumer M, Birnbaumer L 1992 Evidence for dual coupling of the murine luteinizing hormone receptor to adenylyl cyclase and phosphoinositide breakdown and Ca²⁺ mobilization. Studies with the cloned murine luteinizing hormone receptor expressed in L cells. *J Biol Chem* 267:4479–4488
 20. Hipkin R, Sanchez-Yague J, Ascoli M 1992 Identification and characterization of a luteinizing hormone/chorionic (LH/CG) receptor precursor in a human kidney cell line stably transfected with the rat luteal LH/CG receptor complementary DNA. *Mol Endocrinol* 6:2210–2218
 21. McFarland K, Sprengel R, Phillips H, Kohler M, Rosembly N, Nikolics K, Segaloff D, Seeburg P 1989 Lutropin-choriogonadotropin receptor: an unusual member of the G protein-coupled receptor family. *Science* 245:494–499
 22. Rousseau-Merck M, Misrahi M, Atger M, Loosfelt H, Milgrom E, Berger R 1990 Localization of the human luteinizing hormone/choriogonadotropin receptor gene (LHCGR) to chromosome 2p21. *Cytogenet Cell Genet* 54:77–79
 23. Loosfelt H, Misrahi M, Atger M, Saless R, Vu Hai-Luu Thi M, Jolivet A, Guiochon-Mantel A, Sar S, Jallal B, Garnier J 1989 Cloning and sequencing of porcine LH-hCG receptor cDNA: variants lacking transmembrane domain. *Science* 245:525–528
 24. Minegishi T, Nakamura K, Takakura Y, Miyamoto K, Hasegawa Y, Ibuki Y, Igarashi M 1990 Cloning and sequencing of human LH/hCG receptor cDNA. *Biochem Biophys Res Commun* 172:1049–1054
 25. Rocha A, Gomez A, Zanuy S, Cerda-Reverter JM, Carrillo M 2007 Molecular characterization of two sea bass gonadotropin receptors: cDNA cloning, expression analysis, and functional activity. *Mol Cell Endocrinol* 272:63–76
 26. Maugars G, Schmitz M 2006 Molecular cloning and characterization of FSH and LH receptors in Atlantic salmon (*Salmo salar* L.). *Gen Comp Endocrinol* 149:108–117
 27. Kumar RS, Ijiri S, Trant JM 2001 Molecular biology of channel catfish gonadotropin receptors: 1. Cloning of a functional luteinizing hormone receptor and preovulatory induction of gene expression. *Biol Reprod* 64:1010–1018
 28. Kwok HF, So WK, Wang Y, Ge W 2005 Zebrafish gonadotropins and their receptors: I. Cloning and characterization of zebrafish follicle-stimulating hormone and luteinizing hormone receptors—evidence for their distinct functions in follicle development. *Biol Reprod* 72:1370–1381
 29. Zhang F, Rannikko A, Manna P, Fraser H, Huhtaniemi I 1997 Cloning and functional expression of the luteinizing hormone receptor complementary deoxyribonucleic acid from the marmoset monkey testis: absence of sequences encoding exon 10 in other species. *Endocrinology* 138:2481–2490
 30. Howell-Skalla L, Bunick D, Bleck G, Nelson RA, Bahr JM 2000 Cloning and sequence analysis of the extracellular region of the polar bear (*Ursus maritimus*) luteinizing hormone receptor (LHr), follicle stimulating hormone receptor (FSHr), and prolactin receptor (PRLr) genes and their expression in the testis of the black bear (*Ursus americanus*). *Mol Reprod Dev* 55:136–145
 31. Alsat E, Cedar L 1974 [Demonstration of a specific fixation of radio-iodinated human chorionic gonadotropin (HCG I-125) in fragments of human placentas]. *C R Acad Sci Hebd Seances Acad Sci D* 278:2665–2668 (French)
 32. Reshef E, Lei Z, Rao C, Pridham D, Chegini N, Luborsky J 1990 The presence of gonadotropin receptors in nonpregnant human uterus, human placental, fetal membranes, and decidua. *J Clin Endocrinol Metab* 70:421–430
 33. Lei Z, Rao C, Ackerman D, Day T 1992 The expression of human chorionic gonadotropin/human luteinizing hormone receptors in human gestational trophoblastic neoplasms. *J Clin Endocrinol Metab* 74:1236–1241
 34. Pidoux G, Gerbaud P, Tsatsaris V, Marpeau O, Ferreira F, Meduri G, Guibourdenche J, Badet J, Evain-Brion D, Frendo J-L 2007 Biochemical characterization and modulation of LH/CG-receptor during human trophoblast differentiation. *J Cell Physiol* 212:26–35
 35. Alsat E, Haziza J, Evain-Brion D 1993 Increase in epidermal growth factor receptor and its messenger ribonucleic acid levels with differentiation of human trophoblast cells in culture. *J Cell Physiol* 154:122–128
 36. Schmon B, Hartmann M, Jones CJ, Desoye G 1991 Insulin and glucose do not affect the glycogen content in isolated and cultured trophoblast cells of human term placenta. *J Clin Endocrinol Metab* 73:888–893
 37. Cronier L, Defamie N, Dupays L, Théveniau-Ruissy M, Goffin F, Pointis F, Malassiné A 2002 Connexin expression and gap junctional intercellular communication in human first trimester trophoblast. *Mol Hum Reprod* 8:1005–1013
 38. Ascoli M 1981 Characterization of several clonal lines of cultured Leydig tumor cells: gonadotropin receptors and steroidogenic responses. *Endocrinology* 108:88–95
 39. Munson P, Rodbard D 1980 Ligand: a versatile computerized approach for characterization of ligand-binding systems. *Anal Biochem* 107:220–239
 40. Hunter W, Greenwood F 1962 Preparation of iodine-131 labelled human growth hormone of high specific activity. *Nature* 194:495–496
 41. Ascoli M, Fanelli F, Segaloff D 2002 The lutropin/choriogonadotropin receptor, a 2002 perspective. *Endocr Rev* 23:141–174
 42. Banerjee S, Smallwood A, Chambers A, Papageorgiou A, Loosfelt H, Spencer K, Campbell S, Nicolaides K 2005 A link between high serum levels of human chorionic gonadotropin and chorionic expression of its mature functional receptor (LHCGR) in Down's syndrome pregnancies. *Reprod Biol Endocrinol* 3:25–39
 43. Jauniaux E, Bao S, Eblen A, Li X, Lei Z, Meuris S, Rao C 2000 hCG concentration and receptor gene expression in placental tissue from trisomy 18 and 21. *Mol Hum Reprod* 6:5–10
 44. Sonoda N, Katabuchi H, Tashiro H, Ohba T, Nishimura R, Minegishi T, Okamura H 2005 Expression of variant luteinizing hormone/chorionic gonadotropin receptors and degradation of chorionic gonadotropin in human chorionic villous macrophages. *Placenta* 26:298–307
 45. Toth P, Lukacs H, Gimes G, Sebestyen A, Pasztor N, Paulin F, Rao C 2001 Clinical importance of vascular LH/hCG receptors—a review. *Biol Reprod* 1:5–11
 46. Tao Y, Lei Z, Hofmann G, Rao C 1995 Human intermediate trophoblasts express chorionic gonadotropin/luteinizing hormone receptor gene. *Biol Reprod* 53:899–904
 47. Seth D, Shaw K, Jazayeri J, Leedman P 1998 Complex post-transcriptional regulation of EGF-receptor expression by EGF and TGF- α in human prostate cancer cells. *Br J Cancer* 80:657–669
 48. Ying H, Furuya F, Zhao L, Araki O, West BL, Hanover JA, Willingham MC, Cheng SY 2006 Aberrant accumulation of PTTG1 induced by a mutated thyroid hormone β receptor inhibits mitotic progression. *J Clin Invest* 116:2972–2984
 49. Dorman SE, Holland SM 1998 Mutation in the signal-transducing chain of the interferon- γ receptor and susceptibility to mycobacterial infection. *J Clin Invest* 101:2364–2369
 50. de Roux N, Milgrom E 2001 Inherited disorders of GnRH and gonadotropin receptors. *Mol Cell Endocrinol* 179:83–87

ZO-1 is involved in trophoblastic cell differentiation in human placenta

Guillaume Pidoux, Pascale Gerbaud, Sédami Gnidehou, Michael Grynberg, Graziello Geneau, Jean Guibourdenche, Diane Carette, Laurent Cronier, Danièle Evain-Brion, André Malassiné and Jean-Louis Frendo

Am J Physiol Cell Physiol 298:1517-1526, 2010. First published Mar 3, 2010;
doi:10.1152/ajpcell.00484.2008

You might find this additional information useful...

This article cites 52 articles, 30 of which you can access free at:

<http://ajpcell.physiology.org/cgi/content/full/298/6/C1517#BIBL>

Updated information and services including high-resolution figures, can be found at:

<http://ajpcell.physiology.org/cgi/content/full/298/6/C1517>

Additional material and information about *AJP - Cell Physiology* can be found at:

<http://www.the-aps.org/publications/ajpcell>

This information is current as of June 8, 2010 .

ZO-1 is involved in trophoblastic cell differentiation in human placenta

Guillaume Pidoux,^{1,2,6*} Pascale Gerbaud,^{1,2,6*} Sédami Gnidehou,^{1,2} Michael Grynberg,^{1,2} Graziello Geneau,³ Jean Guibourdenche,^{1,2,4,6} Diane Carette,^{2,7} Laurent Cronier,³ Danièle Evain-Brion,^{1,2,6} André Malassiné,^{1,2,6} and Jean-Louis Frendo^{1,2,5,6}

¹Institut National de la Santé et de la Recherche Médicale (INSERM), U767, Paris; ²Université Paris Descartes, Paris;

³Institut de Physiologie et Biologie Cellulaires, Centre National de la Recherche Scientifique (CNRS) Unité Mixte de Recherche 6187, Université de Poitiers, Poitiers; ⁴Assistance Publique - Hôpitaux de Paris, Hôpital Cochin, Maternité Port-Royal, Paris; ⁵CNRS, Paris; ⁶PremUp, Paris; and ⁷INSERM, U895, Paris, France

Submitted 23 September 2008; accepted in final form 24 February 2010

Pidoux G, Gerbaud P, Gnidehou S, Grynberg M, Geneau G, Guibourdenche J, Carette D, Cronier L, Evain-Brion D, Malassiné A, Frendo JL. ZO-1 is involved in trophoblastic cell differentiation in human placenta. *Am J Physiol Cell Physiol* 298: C1517–C1526, 2010. First published March 3, 2010; doi:10.1152/ajpcell.00484.2008.—Trophoblastic cell-cell fusion is an essential event required during human placental development. Several membrane proteins have been described to be directly involved in this process, including connexin 43 (Cx43), syncytin 1 (Herv-W env), and syncytin 2 (Herv-FRD env glycoprotein). Recently, zona occludens (ZO) proteins (peripheral membrane proteins associated with tight junctions, adherens junctions, and gap junctions) were shown to be involved in mouse placental development. Moreover, zona occludens 1 (ZO-1) was localized mainly at the intercellular boundaries between human trophoblastic cells. Therefore the role of ZO-1 in the dynamic process of human trophoblastic cell-cell fusion was investigated using primary trophoblastic cells in culture. In vitro as in situ, ZO-1 was localized mainly at the intercellular boundaries between trophoblastic cells where its expression substantially decreased during differentiation and during fusion. At the same time, Cx43 was localized at the interface of trophoblastic cells and its expression increased during differentiation. To determine a functional role for ZO-1 during trophoblast differentiation, small interfering RNA (siRNA) was used to knock down ZO-1 expression. Cytotrophoblasts treated with ZO-1 siRNA fused poorly, but interestingly, decreased Cx43 expression without altering the functionality of trophoblastic cell-cell communication as measured by relative permeability time constant determined using gap-FRAP experiments. Because kinetics of Cx43 and ZO-1 proteins show a mirror image, a potential association of these two proteins was investigated. By using coimmunoprecipitation experiments, a physical interaction between ZO-1 and Cx43 was demonstrated. These results demonstrate that a decrease in ZO-1 expression reduces human trophoblast cell-cell fusion and differentiation.

zona occludens 1; connexin 43; placenta; trophoblast differentiation; cell fusion

CELL-CELL FUSION IS ESSENTIAL for embryonic and fetal development and for cell differentiation, but few specialized human cell types can fuse together and differentiate into multinucleated cell (for review, see Ref. 40). This process is involved in the formation of myotubes (7, 37, 52), osteoclasts (54), and the syncytiotrophoblast (18). Additionally, cell fusion participates in tissue repair and may be important to cancer development and progression (33). The cell-cell fusion process can be summarized like this: first, the cells must leave the proliferative

stage and express genes and proteins involved in the fusion process. Second, the cells must recognize and interact with their fusion partner allowing efficient communication and signal exchange. This dynamic process must be tightly regulated and coordinated at each stage for successful fusion to occur.

In the human placenta, the cytotrophoblastic cells of the floating chorionic villi remain attached to the villous basement membrane, forming a monolayer of epithelial cells. These cells proliferate and differentiate by fusion to form a syncytiotrophoblast that covers the entire surface of the villus (Fig. 1, A and B) (32, 42). This syncytiotrophoblast plays a major role throughout pregnancy, since it is the site of numerous placental functions including ion, nutrient and gas exchanges, removal of waste products, and synthesis of steroid and peptide hormones required for fetal growth and development (16, 39). This process of cell-cell fusion can be reproduced in vitro. Purified cytotrophoblastic cells isolated from human placentas aggregate and then fuse, forming the multinucleated syncytiotrophoblast with pregnancy-specific hormonal production (i.e., the human chorionic gonadotropin hormone: hCG) (32). Using this physiological model, we have previously demonstrated the direct involvement of human endogenous retroviral envelope Herv-W (syncytin 1) (19), gap junctional intercellular communication (11) via connexin 43 (Cx43) (18, 34) in the cytotrophoblastic cell fusion. In other models, phosphatidylserine flip (1), cadherin 11 (22), caspase 8 (6), CD98 (13), and ADAM12 (38) were also implicated.

Trophoblast fusion is a multifactorial and dynamic process that remains poorly understood, and the identification of other prerequisite factors needs to be assessed. A protein or macromolecular complex directly involved in trophoblastic cell fusion is required to be localized at the cellular membrane, and the silencing or knockdown of these proteins should induce an inhibition or decrease of cell fusion.

Recently, zona occludens 1 (ZO-1) was demonstrated to be localized mainly in cytotrophoblastic cells and at the intercellular boundaries between cytotrophoblastic cells and between cyto- and syncytiotrophoblasts (36). Furthermore, the role of zona occludens proteins in early development has been recently established using a knockout mouse model (53). Interestingly, deficiency of ZO-1 in knockout mice induced defects in mouse placental development, mainly in the formation of vascular trees and in chorioallantoic fusion (29).

ZO-1 has originally been identified at tight junctions, which form a network inside cells. This structure is only present at the intersection between two cells at the cell-cell contact zone. ZO-1 is a 220-kDa membrane protein, colocalized with the

* G. Pidoux and P. Gerbaud contributed equally to this work.

Address for reprint requests and other correspondence: J. -L. Frendo, INSERM U767, Faculté de Pharmacie, 4, Avenue de l'Observatoire, F-75270 Paris, France (e-mail: jean-louis.frendo@univ-paris5.fr).

transmembrane proteins claudins and occludin (4, 48). Later, ZO-1 was demonstrated and identified as adherens junctions that zip cells together and thereby maintains cell and tissue polarity. Furthermore, these junctions anchor the cytoskeleton, allowing the formation of macrocomplexes at the plasma membrane. A growing number of both structural and regulatory proteins that associate with the different domains of ZO proteins have been identified, including multiple connexins. A recent study using nuclear magnetic resonance demonstrated that the interaction of Cx43 with ZO-1 occurs through the last 20 amino acids in the extreme carboxyl terminus of Cx43 and the second PDZ domain of ZO-1 (25, 47).

The aim of this study was to analyze ZO-1 involvement in trophoblastic cell-cell fusion process. We have first immunolocalized ZO-1 in situ and in vitro during trophoblast differentiation. Interestingly, Cx43 was the only connexin detected in trophoblastic cells of the human chorionic villi (8, 10, 30, 34). Therefore, the kinetics of ZO-1 and Cx43 expression during the process of differentiation was investigated. We used small interfering RNA (siRNA) to determine the influence of ZO-1 expression on cell fusion followed by morphological analysis (desmoplakin immunostaining) and by measuring hCG production. Interactions between ZO-1 and Cx43 were analyzed by coimmunoprecipitation and immunofluorescence. The influence of ZO-1 knockdown on gap junction-mediated intercellular communication was investigated using a gap-FRAP approach. We demonstrate here that ZO-1 is required for trophoblastic cell-cell fusion in human placental development.

MATERIALS AND METHODS

Placental tissue collection and trophoblastic cell culture. These studies were performed in agreement with our local ethics committee (Comité de Protection des Personnes: CPP -Île-de-France III) and with written consent of patients. For immunohistological localization, second-trimester placentas were collected at the time of termination of pregnancy at 12–19 wk of gestation (in weeks of amenorrhea). For trophoblast cell culture, placentas were obtained immediately after caesarian section from healthy mothers with uncomplicated pregnancies delivered at 35–39 wk of amenorrhea. Cytotrophoblasts were isolated as previously described (2). After sequential trypsin/DNase I digestion followed by Percoll gradient centrifugation, cytotrophoblasts were diluted to a final density of 2.7×10^6 cells in 3 ml minimum essential medium containing 10% fetal calf serum. Cells were plated in 60-mm plastic dishes (TPP, Trasadingen, Switzerland) and incubated at 37°C in 5% CO₂ atmosphere. About 95–98% of the cells were positively stained by cytokeratin 7, confirming the trophoblastic nature of these cells.

Hormone assay. The hCG concentration was determined in culture medium after 24 and 72 h of culture by using an enzyme-linked

fluorescence assay (Vidas System, BioMerieux, Marcy l'Etoile, France) with a detection limit of 2 mU/ml. Values are means \pm SE of triplicate determinations.

Immunolocalization. For immunohistological localization, samples of second-trimester placental tissues were fast frozen in isopentane cooled in a liquid nitrogen bath and stored at -80°C . For ZO-1, Cx43, and desmoplakin detection, cultured cells and frozen sections were fixed for 10 min in methanol at -20°C . They were then washed three times in PBS and incubated in a blocking solution consisting of 1% Triton X-100 and 2% bovine serum albumin (BSA) in PBS at room temperature for 30 min. Specimens were incubated overnight at 4°C in an appropriate dilution of primary antibodies (Table 1) in PBS and 1% BSA for direct fluorescence, as specified in the figure legends. The secondary antibodies fluorescein isothiocyanate-labeled donkey anti-rabbit IgG or Cy goat anti-mouse IgG (1:150; Jackson ImmunoResearch, Baltimore, MD) were used as previously described (10, 20). ZO-1 immunostaining was performed with a universal streptavidin-peroxidase kit (Dako, Glostrup, Denmark). The controls, which consisted of omitting the primary antibody or applying the nonspecific IgG of the same isotype, were all negative.

Immunoblotting. Cell extracts were prepared as previously described (3). Protein (70 μg) was solubilized in RIPA buffer (50 mM Tris, 150 mM NaCl, 1% NP-40, and 50 mM *N*-octyl- β -D-glucoside, pH 8) with 1 \times protease and phosphatase inhibitors (Calbiochem-Novagen), separated by 4–12% SDS-PAGE, and transferred to nitrocellulose membranes. Membranes were immunoblotted with a monoclonal antibody against ZO-1 at 0.5 $\mu\text{g}/\text{ml}$, and the specific band was revealed by chemiluminescence (West Pico Chemiluminescent Substrate; Pierce, Rockford, IL) after incubation with an anti-mouse peroxidase-coupled antibody. To detect actin, p53, and Cx43, we proceeded as described above, except that proteins were immunoblotted with rabbit polyclonal antibody at 3.5 $\mu\text{g}/\text{ml}$ for actin, rabbit polyclonal antibody at 1 $\mu\text{g}/\text{ml}$ for p53, and rabbit polyclonal antibody at 0.5 $\mu\text{g}/\text{ml}$ for Cx43 (Sigma-Aldrich, St. Louis, MO). Successive preadsorptions of Cx43, ZO-1, and p53 antibodies with trophoblastic cells in culture abrogate Cx43, ZO-1, and p53 immunodetection in Western blot analysis. To analyze phosphorylated Cx43, samples were separated on 5–15% SDS-PAGE, electroblotted onto a polyvinylidene difluoride membrane (PVDF Immobilon-P, Millipore), and analyzed by Western blotting with anti-Cx43 (1:250, BD Biosciences) and anti- α -tubulin (1:200, Santa Cruz Biotechnology, Santa Cruz, CA) antibodies.

Immunoprecipitation. Immunoprecipitation was performed using Carboxyl-Ademeads 0213 (Ademtech SA-Pessac, France) according to the manufacturer's protocol. The Carboxyl-Ademeads (3%) were resuspended and washed in 1 \times activation buffer (Adem-Buffer 10101). Beads were activated with EDC [1-ethyl-3-(3-dimethylaminopropyl) carbodiimide hydrochloride (at 4 mg/ml), which reacts with the carboxylic acid groups to form an amine-reactive intermediate. After incubation for 10 min at 40°C, 5 μg of ZO-1 polyclonal antibody (0.2 $\mu\text{g}/\mu\text{l}$; Zymed) or Cx43 polyclonal antibody (0.25 $\mu\text{g}/\mu\text{l}$, Santa Cruz Biotechnology) or a nonspecific mouse IgG (Jackson ImmunoResearch) was added per milligram of activated particles.

Table 1. Antibodies used in this study

Antibody	Antigen	Isotype	Species	Concentration, $\mu\text{g}/\text{ml}$	Source
33-9100	Zona occludens 1	IgG1k	Mouse	0.5	Zymed (San Francisco, CA)
61-7300	Zona occludens 1	Polyclonal	Rabbit	0.25	Zymed
610062	Connexin 43	IgG1	Mouse	0.25	BD Biosciences (Franklin Lakes, NJ)
sc-9059	Connexin 43	Polyclonal	Rabbit	1	Santa Cruz Biotechnology (Santa Cruz, CA)
C6219	Connexin 43	Polyclonal	Rabbit	0.06	Sigma-Aldrich (St. Louis, MO)
7001	p53	Polyclonal	Rabbit	1	Dako (Glostrup, Denmark)
AHP320	Desmoplakin	Polyclonal	Rabbit	2.5	Serotec (Cergy, France)
A2066	α -Tubulin	Polyclonal	Rabbit	0.35	Sigma-Aldrich
sc-12462	Actin	Polyclonal	Rabbit	1	Santa Cruz Biotechnology

Table 2. siRNA used in this study

siRNA	Access No.	Target Sequence
siRNA scrambled		5'-GGGAAGACAGAACUUGUACUCUAAAA-3' 3'-CCCUUCUGUCUUGAACAUAGAUUUU-5'
siRNA p53	NM_000546	5'-AAACUCAUGUUCAGACAGAAGGGU-3' 3'-UUUUGAGUACAAGUUCUGUCUCCCA-5'
siRNA ZO-1 1681	NM_003257	5'-CCAUCUGAUGGUGUCCUACCUAUU-3' 3'-GGUAGACUACCACAGGAUGGAUUA-5'
siRNA ZO-1 2137	NM_003257	5'-GGGCUCUUGGCUUGCUAUUCGAAUU-3' 3'-CCCGAGAACCGAAGCAUAGCUUAA-5'
siRNA ZO-1 5518	NM_003257	5'-CCUUCACCUUUAGAUAAAAGAGAAA-3' 3'-GGAAGGUGGAAUUCUUAUUUCUUU-5'

siRNA, small interfering RNA; ZO, zona occludens.

The complex was incubated for 2 h at 37°C under shaking, followed by incubation for 30 min at 37°C in the presence of BSA solution (0.5 mg/ml). The beads were washed with 1× storage buffer (Adem-Buffer 10201) twice and resuspended at a concentration of 1%. Cells (2.7×10^6 /well) were seeded in 60-mm plastic dishes and cultured as previously described. After 24 h of culture, cells (5×10^6) were washed with PBS and scraped free in ice-cold RIPA buffer with protease inhibitors. After sonication, the cellular lysate and debris were separated by centrifugation at 10,000 g for 10 min at 4°C. The supernatant was transferred to the antibody-coated beads immunocomplex and incubated overnight at 4°C on a rocker platform. Proteins were eluted by heating at 60°C for 10 min in 1× electrophoresis sample buffer (Bio-Rad, Hercules, CA). Eluates were separated by 4–12% SDS-PAGE and transferred to nitrocellulose membranes. Membranes were then exposed to ZO-1 monoclonal antibody (Zymed) and Cx43 rabbit polyclonal antibody (Sigma-Aldrich), as previously described.

ZO-1 siRNA protocol. We have used the BLOCK-iT RNAi kit (Invitrogen Life Technologies) to optimize the transfection efficiency and siRNA uptake in primary cytotrophoblast cultures. Briefly, after 5 h of culture, cytotrophoblasts were incubated with the fluorescein-labeled double-stranded RNA (dsRNA) oligomer. Cells were washed three times in PBS, fixed, and analyzed by fluorescence microscopy at 24, 48, and 72 h of culture. Nuclei were stained by a mix of Hoechst 33342 (staining living cells) and Dead Cell reagent (ethidium homodimer-I, staining dead cells). Three different ZO-1 siRNA (1681, 2137, and 5518), a random siRNA (scrambled), and a positive control siRNA (p53) were purchased from Invitrogen Life Technologies (see Table 2). Briefly, 20 μM of each siRNA were diluted in OPTI-MEM (Invitrogen Life Technologies) and mixed with the transfection reagent (Lipofectamine 2000, Invitrogen Life Technologies). The mixture was added to the cells (2.0×10^6 cells/well) and incubated for 48 h at 37°C in 5% CO₂ atmosphere. Medium was removed and kept for

subsequent hormone analysis. Proteins were extracted and protein expression was analyzed by Western blot using an anti-ZO-1, p53, or Cx43 antibodies as previously described. The most efficient decrease of ZO-1 expression was obtained with ZO-1 siRNA 2137.

Syncytium formation analysis. Syncytium formation was followed by fixing and immunostaining cells so that the distribution of desmoplakin and nuclei in cells (DAPI staining) could be observed (18). The staining of desmoplakin present at the intercellular boundaries in aggregated cells progressively disappears as the syncytium is formed. After 72 h of culture, mononuclear cells and the number of nuclei in syncytia were counted and then the fusion index ($(N - S)/T$) was determined. N is the number of nuclei in the syncytia, S is the number of syncytia, and T is the total number of nuclei counted.

Gap-FRAP method. The degree of cell-cell communication between human trophoblastic cells was measured by means of the gap-FRAP method (51) on a confocal microscope (FV 1000 Olympus IX-81, Tokyo, Japan). After being washed, cultured trophoblastic cells were loaded for 15 min at room temperature in Tyrode solution (in mM: 144 NaCl, 5.4 KCl, 2.5 CaCl₂, 1 MgCl₂, 0.3 NaH₂PO₄, 5 HEPES, and 5.6 glucose, pH 7.4) containing the membrane-permeate molecule 6-carboxyfluorescein diacetate (Sigma Chemicals, St. Louis, MO) (7 μg/ml in 0.25% DMSO). The highly fluorescent and membrane-impermeable 6-carboxyfluorescein moiety is released and accumulates within cells. After the excess of extracellular fluorogenic ester was washed off to avoid further loading, the fluorescence of some selected cells adjacent to others cells was photobleached by applying strong light pulses from an argon laser set at 405 nm. Digital images of the fluorescent emission excited at 488 nm by weak laser pulses were recorded at regular intervals for 9 min (each time period = 30 s) and stored for subsequent analysis. In each experiment, one labeled, isolated cell was left unbleached as a reference for the loss of fluorescence due to repeated scanning and dye leakage. In case of the presence of cytoplasmic bridges, the fluorescence recovery is charac-

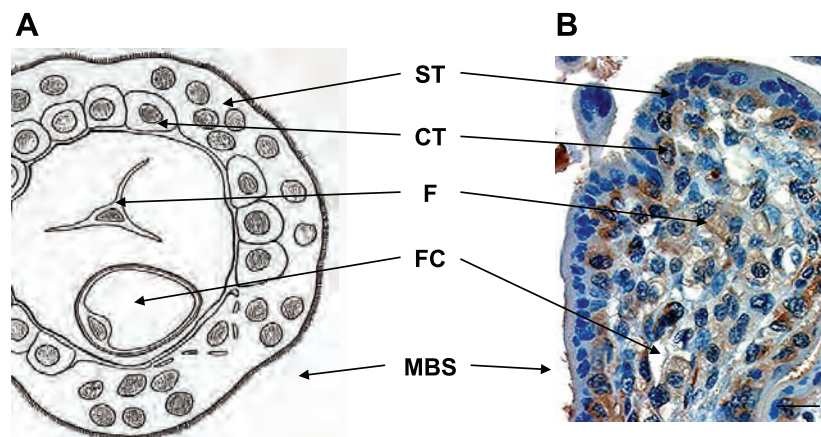


Fig. 1. Zona occludens (ZO)-1 localization in human chorionic villi. **A:** in human placenta, the chorionic floating villi are in direct contact with the maternal blood in the maternal blood space (MBS) consisting of cytotrophoblasts (CT) and syncytiotrophoblast (ST) surrounding a core of mesenchymal cells including fetal vessels. F, fibroblasts; FC, fetal capillary. **B:** immunohistochemical analysis of ZO-1 in chorionic villi of second-trimester placenta (mouse monoclonal antibody). ZO-1 immunostaining was observed in cytotrophoblasts, in some fibroblasts, and in fetal capillaries of the mesenchymal chore. Scale bar, 10 μm.

terized by a fast steplike course which is not prevented by an exposure to a known junctional uncoupler like heptanol (9, 12). An estimation of the relative permeability of the gap junctions is given by the diffusion rate constant k determined from recovery curves using the following equation: $(F_i - F_t)/(F_i - F_0) = e^{-kt}$, where F_i , F_t , and F_0 are fluorescence intensities before bleaching, at time t and at $t = 0$, respectively.

Statistical analysis. We used the StatView F-4.5 software package (Abacus Concepts). Values are reported as means \pm SE. Significant differences ($P < 0.05$) were identified by analysis of variance.

RESULTS

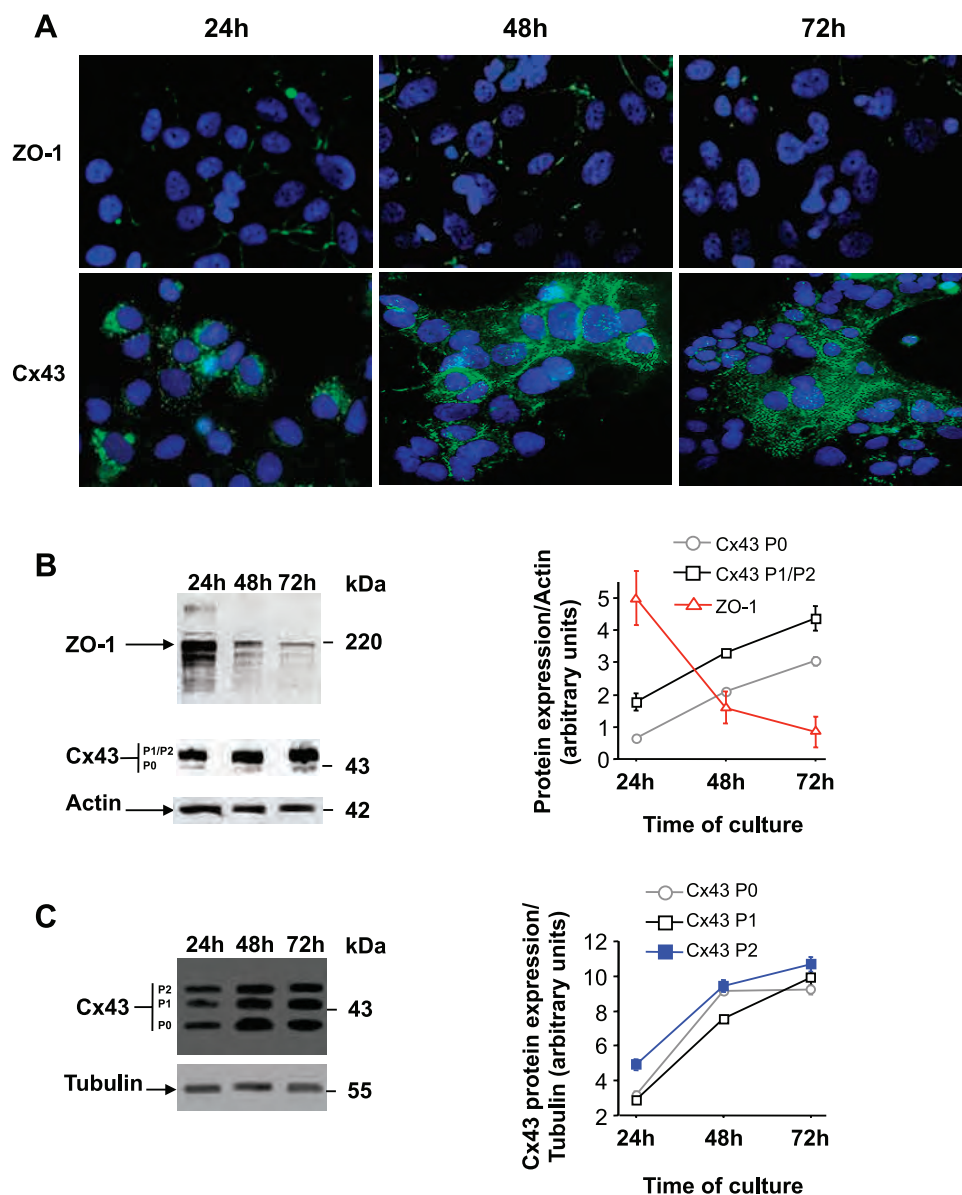
ZO-1 immunolocalization in human chorionic villi. In situ, using streptavidin peroxidase immunostaining, ZO-1 was detected mainly at the level of cytotrophoblastic cells (Fig. 1B).

Evolution of ZO-1 and Cx43 expression during in vitro cytotrophoblast differentiation. In culture, purified cytotrophoblasts from human placenta began to extend protrusions and pseudopodia to make initial contacts with neighboring cells.

Later, groups of cytotrophoblastic cells in close apposition present an aspect consistent with an aggregation stage. Finally, large multinucleated cells with syncytia characteristics can be observed (18, 32). After 24 h, a strong ZO-1 immunofluorescence was observed at the intercellular contact between aggregated cells (Fig. 2A). The ZO-1 immunofluorescence progressively disappears as the syncytiotrophoblast is formed (Fig. 2A). In the meantime, a weak punctuated Cx43 immunofluorescence was observed after 24 h of culture. This immunofluorescence increased during differentiation (at 48 and 72 h). No fluorescence was observed on controls using the nonspecific IgG of the same isotype (data not shown).

Western blot analysis was performed on trophoblastic extracts after 24, 48, and 72 h of culture. The expression of ZO-1 protein (with an estimated molecular mass from SDS gels of 220 kDa) decreased during cytotrophoblast differentiation. Normalization of ZO-1 protein expression to actin showed a significant decrease at 48 h (1.34 ± 0.45 arbitrary units; $P <$

Fig. 2. ZO-1 and connexin 43 (Cx43) expression during in vitro trophoblastic cell fusion and differentiation. **A:** immunofluorescence localization of ZO-1 (rabbit polyclonal antibody) and Cx43 (rabbit polyclonal antibody) in villous trophoblastic cells in culture. ZO-1 immunofluorescence was observed at the intercellular boundaries of aggregated cells after 24 h. After 48 and 72 h, ZO-1 immunofluorescence was observed at the border of cytotrophoblastic cells, which were still in contact with the syncytiotrophoblast. A weak punctuated Cx43 immunofluorescence was observed after 24 h. This immunofluorescence increased during differentiation (48 and 72 h). Nuclei were labeled with DAPI. Scale for pictures: 0.5 cm = 15 μ m. **B:** immunoblotting of ZO-1 and Cx43 after 1, 2, and 3 days of culture. Western blot analysis, using a ZO-1 monoclonal antibody and a Cx43 polyclonal antibody, shows a decrease in ZO-1 protein expression, while at the same time, Cx43 expression increases (unphosphorylated form P0 as well as the phosphorylated forms P1 and P2). The histogram presents the normalization of ZO-1 and the different status of Cx43 (P0 and P1/P2) expression by actin expression. **C:** immunoblotting of Cx43 after 24, 48, and 72 h of culture. Western blot analysis by using a Cx43 monoclonal antibody presents an increase of all forms (P0, P1, and P2) of Cx43 protein expression. The histogram presents the normalization of Cx43 protein expression by tubulin expression. Results are expressed as means \pm SE of three culture dishes. One experiment representative of five is illustrated.



0.009) and 72 h (0.81 ± 0.44 arbitrary units; $P < 0.002$) compared with 24 h of culture (3.85 ± 0.70 arbitrary units) (Fig. 2B).

Cx43 is a phosphoprotein, which can be differentially phosphorylated. Cx43 has multiple electrophoretic isoforms when analyzed by SDS-PAGE: a faster-migrating form corresponding to a nonphosphorylated form also called P0 and at least two slower-migrating forms, commonly termed P1 and P2 (for review, see Ref. 46). Since it has been described that phosphorylation affects both the structure and the function of Cx43 and leads to changes in localization, interacting protein partners, and channel functionality (46), we decided to check the nonphosphorylated and phosphorylated forms of Cx43. All forms of Cx43 (unphosphorylated P0, phosphorylated P1 and P2) increased during cytotrophoblast differentiation (Fig. 2, B and C). As presented in Fig. 2B, the normalization of Cx43 protein expression by actin showed a significant increase after 48 h (1.92 ± 0.063 arbitrary units; $P < 0.001$ for P0; 3.07 ± 0.04 arbitrary units; $P < 0.001$ for P1/P2) and 72 h (2.84 ± 0.10 arbitrary units; $P < 0.001$ for P0; 4.2 ± 0.32 arbitrary units; $P < 0.001$ for P1/P2) compared with 24 h of culture (0.76 ± 0.07 arbitrary units for P0 and 1.75 ± 0.2 arbitrary

units for P1/P2). However, in these experiments, we failed to properly separate the P1/P2 forms.

Figure 2C presents a high-resolution gel allowing us to determine the kinetics of the P0, P1, and P2 forms during the differentiation and fusion process.

P0, P1, and P2 forms of Cx43 separated by Western blot analysis from cell lysates after 24, 48, and 72 h of culture were normalized by α -tubulin. Graph in Fig. 2C shows a significant increase of Cx43 expression during the cell fusion process whatever its phosphorylation status.

Specific inhibition of ZO-1 expression by siRNA. To investigate the involvement of ZO-1 in human cytotrophoblast fusion, we used a siRNA strategy. First, the efficient uptake of siRNA by cytotrophoblast cells was analyzed by adding fluorescein-labeled dsRNA oligomer to the cell culture. The dsRNA oligomer (green) was taken up during the first 24 h (65% of labeled cells), and the proportion of labeled cells increased progressively (74% at 48 h and 83% at 72 h). A very low rate (13%) of dead cells (red) was observed after transfection and remained constant during the culture period (Fig. 3A). Next, the efficiency and specificity of ZO-1 siRNA treatment to block the production of ZO-1 protein was analyzed. Three

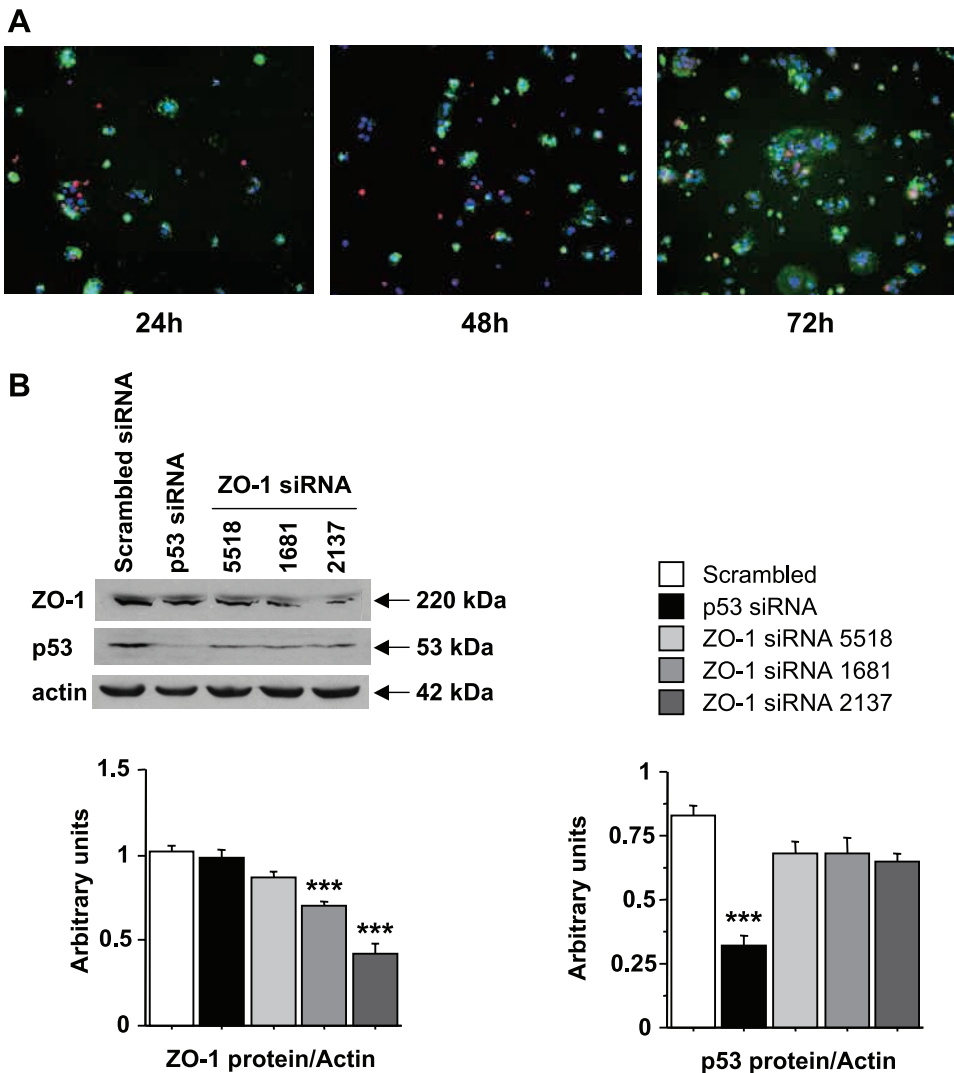


Fig. 3. Specific inhibition of ZO-1 expression by small interfering RNA (siRNA). A: visualization of efficiency in siRNA uptake by cytotrophoblastic cells in culture. Five hours after plating, cytotrophoblasts were incubated with a fluorescein-labeled double-stranded RNA (dsRNA) oligomer. Cells were fixed at 24, 48, and 72 h of culture and analyzed by fluorescence microscopy. Intensely fluorescent green cells have internalized the siRNA. Dead cells were stained in red by using ethidium homodimer-I, and living cells were stained in blue by using Hoechst 33342 reagent. Scale for pictures: 0.1 cm = 15 μ m. B: effect of siRNA oligonucleotides on ZO-1 expression. Five hours after plating, cytotrophoblasts were incubated with three different ZO-1 siRNA: ZO-1 siRNA 1681, ZO-1 siRNA 2137, and ZO-1 siRNA 5518, or with a scrambled siRNA or with a p53-specific siRNA. At 72 h of culture, ZO-1, p53, and actin proteins were analyzed by Western blot. Histograms present the normalization of ZO-1 and p53 protein expression by actin expression. One experiment representative of five is illustrated in B. Results are expressed as means \pm SE; *** $P < 0.001$.

different ZO-1 siRNA oligonucleotides were designed and incubated with cytotrophoblastic cells (Table 2). As shown by Western blot analysis in Fig. 3B, ZO-1 siRNA 1681 and 2137 decreased ZO-1 protein expression, whereas ZO-1 siRNA 5518 did not present a significant effect. Normalization of ZO-1 protein expression with actin showed a 31.4% inhibition by ZO-1 siRNA 1681 (0.7 ± 0.01 arbitrary units; $P < 0.001$) compared with cells transfected with scrambled siRNA (1.02 ± 0.02 arbitrary units) and siRNA 2137 more efficiently decreased (60.8% of inhibition; 0.4 ± 0.06 arbitrary units; $P < 0.001$) ZO-1 protein expression. Cells transfected with p53 siRNA, used as a specificity control, did not present a decrease in ZO-1 protein expression (Fig. 3B) but a decrease in p53 protein expression. Normalization of p53 protein expression with actin showed 62.5% of inhibition with the p53 siRNA (0.3 ± 0.04 arbitrary units; $P < 0.001$) compared with scrambled siRNA (0.8 ± 0.03 arbitrary units), whereas no significant decrease in p53 was shown in the cells transfected with siRNA specific to ZO-1. The most efficient ZO-1 siRNA 2137 was used for the following experiments.

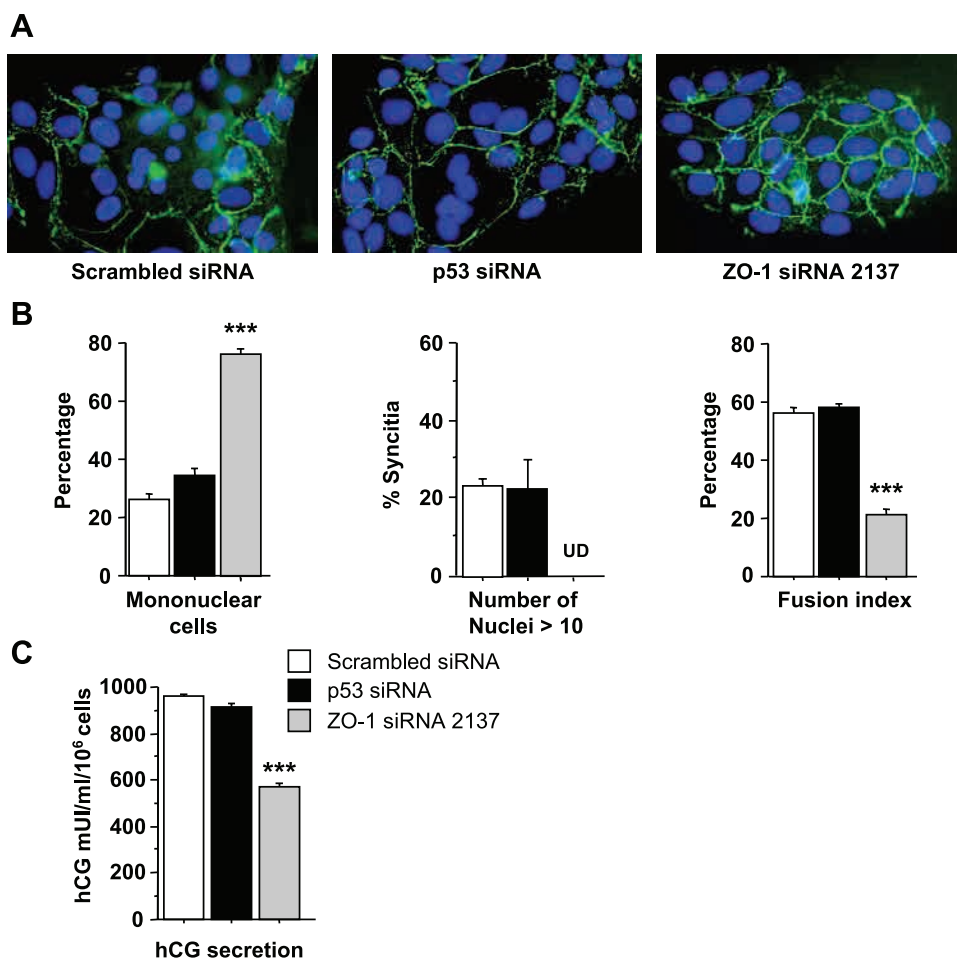
Effects of ZO-1 siRNA on morphological and functional trophoblast differentiation. After 72 h of culture, cells treated with siRNA 2137 showed an aggregated phenotype, suggesting that inhibition of ZO-1 expression delayed cell fusion (Fig. 4A). Indeed, these cells exhibited the same phenotype as normal cells at 24 h. No effects were observed with scrambled and p53 siRNA.

A morphological method was also used to analyze the effect of siRNA (Fig. 4B). When cells were treated with ZO-1 siRNA 2137 for 72 h, a larger number of mononuclear cells were present ($76 \pm 2.2\%$; $P < 0.001$) than in cultures incubated with scrambled siRNA ($26.3 \pm 1.9\%$), or p53 siRNA ($34.2 \pm 2\%$) (Fig. 4B, left). After 72 h of culture, around 25% of the syncytia contained more than 10 nuclei (18). In cultures treated with ZO-1 siRNA 2137, no syncytia containing 10 nuclei or more were found, while in cells treated with scrambled siRNA, $23.2 \pm 2\%$ of syncytia contained 10 or more nuclei, like in cells treated with p53 siRNA ($22.1 \pm 7\%$) (Fig. 4B, center). Moreover, the cell fusion index analysis, which reflects the global cell-cell fusion process, demonstrated that ZO-1 siRNA decreased the number and size of syncytia formed (Fig. 4B, right).

In vitro, hCG secretion increases during trophoblast cell fusion (17, 32). Cells treated with ZO-1 siRNA 2137 secreted significantly less hCG at 72 h than cells treated with scrambled or p53 siRNA (Fig. 4C).

Because Cx43 increased during trophoblastic cell differentiation (Fig. 2B), its expression was analyzed after ZO-1 siRNA treatment (Fig. 5A). All forms of Cx43 protein expression (P0 and P1/P2) were significantly lower in cells treated with ZO-1 siRNA compared with cells treated with scrambled siRNA (control). The gap junction functional coupling between trophoblastic cells was analyzed using the gap-FRAP technique (51). Figure 5B shows the typical changes in the

Fig. 4. Effect of ZO-1 siRNA 2137 on morphological and functional differentiation of trophoblastic cells. **A:** after 5 h of culture, normal cytotrophoblasts were transfected with scrambled siRNA, p53 siRNA, or ZO-1 siRNA 2137. After 72 h of culture, the cells were fixed, immunostained with anti-desmoplakin antibody, and counterstained with DAPI. Large syncytia were observed in cells treated with scrambled or p53 siRNA as immunofluorescent staining disappeared when cells have fused. By contrast, immunofluorescent staining can be observed at the boundaries between aggregated cytotrophoblastic cells treated with ZO-1 siRNA 2137. Scale for pictures: 0.3 cm = 15 μ m. **B:** when cells were treated with ZO-1 siRNA 2137, after 72 h of culture, a larger number of mononuclear cells were present than in cultures incubated with scrambled siRNA or p53 (left). No syncytia containing 10 nuclei or more were found, while in cells treated with scrambled or p53 siRNA, syncytia containing 10 or more nuclei were present (center). Cell fusion index analysis demonstrates that ZO-1 siRNA decreases the number and size of syncytia formed (right). **C:** human chorionic gonadotropin hormone (hCG) secretion in the presence of scrambled, p53, or ZO-1 siRNA. Levels of hCG (expressed in milli-international units per milliliter of medium and per number of cells) secreted into the culture medium at 72 h of culture are shown. UD, undetectable. Results are expressed as means \pm SE; *** $P < 0.001$. One experiment representative of five is illustrated.



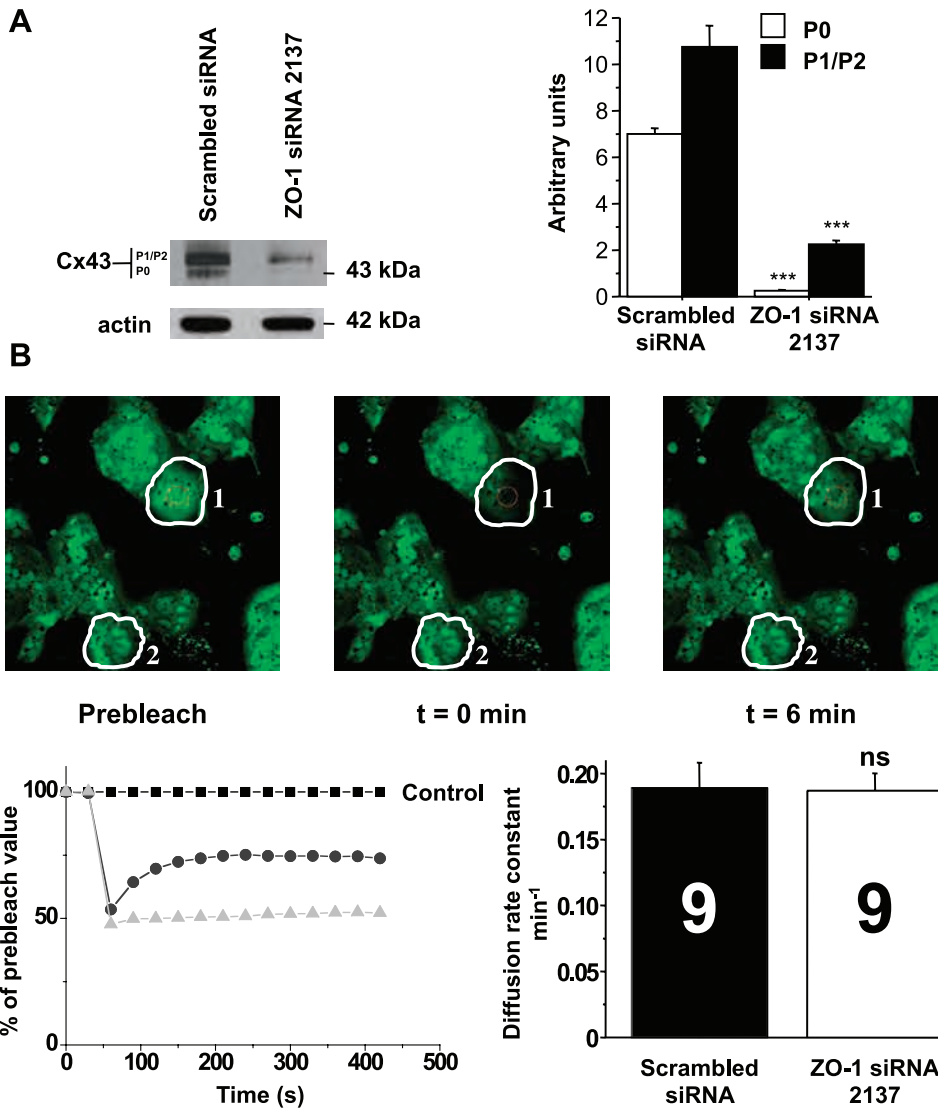


Fig. 5. Effects of ZO-1 siRNA on Cx43 expression and gap junctional intercellular communication. *A*: Cx43 protein expression. Five hours after plating, cytotrophoblasts were incubated 48 h with ZO-1 siRNA 2137 or with a scrambled siRNA. At 72 h of culture, proteins were extracted and Cx43 expression was analyzed by Western blot by using a rabbit polyclonal antibody. Histograms present the normalization of the different forms of Cx43 protein expression (P0 and P1/P2) by actin. Results are expressed as means \pm SE and are representative of five experiments. *** $P < 0.001$. *B*: functional coupling in human villous trophoblastic cells. Digital images of fluorescence distribution in syncytiotrophoblasts during gap-FRAP experiment: Prebleach, just after photobleach [time (t) = 0] and after fluorescence redistribution ($t = 6$ min). Polygon 1 represents the photobleached, tested cell, and polygon 2 represents an unbleached control cell (■) for correction of the loss of fluorescence due to repeated scanning and dye leakage. Examples of corrected recovery curves are expressed as the percentage of prebleach value. When the bleached cell was interconnected by open gap junction channels to unbleached contiguous cells, a fluorescence recovery following a slow exponential time course was measured (●). In contrast, the fluorescence intensity remained unchanged during the 6 min of the experiment (▲) in case of the absence of cell-to-cell communication with neighboring cells. Histogram shows the diffusion rate constant k measured only for coupled trophoblastic cells, in scrambled condition, or after siRNA treatment. Numbers of investigated cells are indicated inside the bars; NS, not significant.

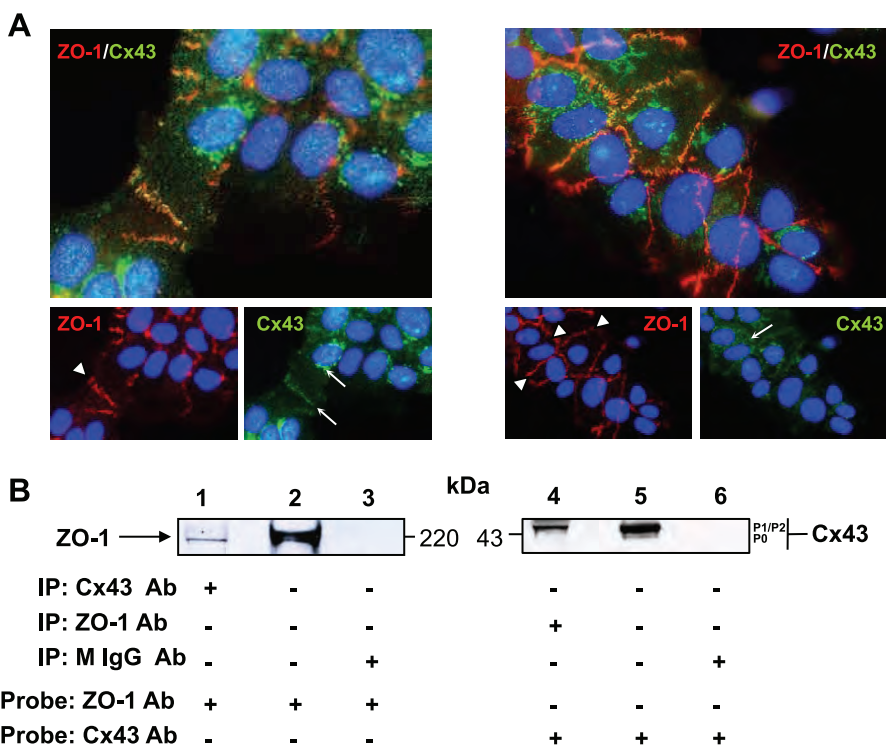
fluorescence intensity of selected cells within a field before and after photobleaching. The corresponding fluorescence recovery curves allow the measurement of the relative permeability constant k (min^{-1}). The presence of ZO-1 siRNA 2137 in the culture medium did not affect the relative permeability constant of interconnected cells compared with control (Fig. 5B). Indeed, the decrease of ZO-1 expression did not alter the functionality of cell-cell communication between trophoblastic cells.

ZO-1 and Cx43 colocalization and coimmunoprecipitation. Because the kinetics of Cx43 and ZO-1 proteins show a mirror image, it was interesting to ascertain whether the two proteins were associated during differentiation. Moreover, Cx43 expression was affected by the ZO-1 siRNA, indicating that ZO-1 and Cx43 interact to stabilize each other and that loss of ZO-1 expression is due to destabilization of a supramolecular complex. Therefore, a potential association between Cx43 and ZO-1 was investigated by coimmunolocalization and coimmunoprecipitation at 48 h after plating, when these two proteins are mainly coexpressed (Fig. 6, A and B). ZO-1 was only localized at the intercellular boundaries between aggregated

cells (arrowhead). A punctuated Cx43 fluorescence was observed at the membrane level and in the cytoplasm, mainly around the nucleus (arrow). As shown in the merged image, the red ZO-1 fluorescence is associated with the green Cx43 fluorescence only at the level of some intercellular contacts, as evidenced by the presence of yellow fluorescence (Fig. 6A). In some areas, only ZO-1 fluorescence was observed.

Coimmunoprecipitation studies were carried out to further explore ZO-1 and Cx43 association. Cellular lysates were purified by immobilized anti-Cx43 antibody or anti-ZO-1 antibody on magnetic beads. After immunoprecipitation, complexes were analyzed by SDS-PAGE and probed by using the ZO-1 antibody or the Cx43 antibody specifically. After immunoprecipitation with Cx43 antibody, complexes were probed with an anti-ZO-1 antibody (Fig. 6B, lane 1). A band at ~ 220 kDa, corresponding to ZO-1, was present (Fig. 6B, lane 2). Conversely, immunoprecipitation with ZO-1 antibody, followed by immunoblotting with an anti-Cx43 antibody, showed a band at 43 kDa corresponding to the Cx43 (Fig. 6B, lane 4) as well as in positive control where P0, P1, and P2 can be observed (Fig. 6B, lane 5). Interestingly, in trophoblastic cells,

Fig. 6. ZO-1 and Cx43 colocalization and coimmunoprecipitation in human trophoblastic cells. **A:** coimmunolocalization of ZO-1 monoclonal antibody (red) and Cx43 rabbit polyclonal antibody (green) on aggregated cytotrophoblasts at 48 h of culture. As shown in the merged images, ZO-1 immunofluorescence is associated with Cx43 immunofluorescence at the level of intercellular contacts, as evidenced by the presence of yellow fluorescence (*left and right*). Punctuated green Cx43 fluorescence was observed in the cytoplasm, and in some areas, only red ZO-1 immunofluorescence was observed at the borders of adjacent cells. Scale for pictures: 0.5 cm = 15 μ m. **B:** immunoprecipitation analysis. Cellular extracts were purified by immobilized rabbit polyclonal anti-Cx43 (*lane 1*) and mouse monoclonal anti-ZO-1 (*lane 4*) antibodies. Eluates (*lanes 1 and 4*) and lysates (which serve as positive control; *lanes 2 and 5*) were analyzed by SDS-PAGE and immunoblotting using the ZO-1-specific rabbit polyclonal antibody (*lanes 1, 2, and 3*) and the Cx43-specific rabbit polyclonal antibody (*lanes 4, 5, and 6*). Bands at 220 kDa were observed (*lanes 1 and 2*) corresponding to ZO-1 protein. A band with ~43 kDa molecular mass was observed (*lanes 4 and 5*) corresponding to the Cx43. Interactions and complexes observed are specific since no cross-reactions were visualized between cell extracts and beads coated with a nonspecific IgG. One experiment representative of five is illustrated in *B*.



ZO-1 seems to interact with phosphorylated forms P1/P2 of Cx43. No cross-reactions were observed in controls showing the specificity of the interactions (Fig. 6*B*, *lanes 3 and 6*).

These results demonstrate that ZO-1 and Cx43 are associated during trophoblastic cell aggregation.

DISCUSSION

In this study, we showed for the first time that ZO-1 knockdown decreased cell-cell fusion and subsequent trophoblast differentiation as established by morphological and biochemical data.

Very few genes involved in human placental development and trophoblast differentiation have been identified. In contrast, with the increasing number of transgenic and knockout mice and rats, many of the genes involved in murine placental development have been characterized (for review, see Ref. 43). However, the results obtained in mice are difficult to extrapolate to humans, owing to the specific features of human placental development (35).

We demonstrated that in chorionic villi, ZO-1 was localized mainly in cytotrophoblastic cells (immunostaining) and at the intercellular boundaries between cytotrophoblastic cells and between cyto- and syncytiotrophoblasts (immunofluorescence). This localization was previously described (36) and correlates well with the expected localization of a protein involved in the fusion process.

We have used an *in vitro* model of cultured villous trophoblastic cells to study some aspects of the cell-cell fusion dynamic process. *In vitro*, ZO-1 was localized only at the intercellular boundaries and its expression drastically decreased during 2 and 3 days of culture. Cx43 expression was also localized at the interface of trophoblastic cells and increased during trophoblast differentiation. It appears that after

48 h of culture, ZO-1 and Cx43 colocalized only at the intercellular boundaries of aggregated cells.

Morphological and functional analyses using desmoplakin immunostaining and hCG secretion demonstrated that treatment with ZO-1 siRNA decreased trophoblastic cell-cell fusion. Furthermore, Cx43 expression was significantly decreased. Indeed, Cx43 expression analyzed by Western blot consists of Cx43 expressed in the cytoplasm and at the intercellular membrane contacts. Effectively, ZO-1 siRNA treatment decreases Cx43 expression, suggesting a decrease in the number of functional gap junction. However, the measure of a functional cell-cell communication shows that some gap junctions are still present and functional. Gap-FRAP analysis, used here, only determined the relative permeability (k^{-1}) of gap junction still present, and the presence of ZO-1 siRNA in the culture medium did not affect this permeability constant compared with control. Therefore, it is concluded that ZO-1 decreases the content of Cx43 but does not affect the functionality of gap junctions.

Moreover, by using coimmunoprecipitation experiments, we demonstrated the physical interaction between ZO-1 and active phosphoforms of Cx43 in aggregated cytotrophoblastic cells.

Over the past two decades, evidence has accumulated that Cx43 interacts with partner proteins: chaperones, scaffolding proteins, kinases, phosphatases, and other cell signaling molecules (for review, see Ref. 27). Among these partner proteins, ZO-1 has been demonstrated to interact with multiple connexins and particularly with Cx43 (14, 25, 28, 45, 50). Different roles have been proposed for the interaction of ZO-1 and Cx43. Changes in Cx43 and ZO-1 interaction have been noted during remodeling of gap junctions in different cell types (5, 14, 26, 44). Modulation of Cx43 and ZO-1 interactions may also be involved in gap junction formation, localization, and activity

(15, 24, 28, 47, 49). A role in internalization and remodeling of Cx43 in response to intracellular changes (5) and in targeting for endocytosis (44) was also demonstrated. However, COOH-terminal tagging or mutation of Cx43 abolishes ZO-1 interaction but truncated or tagged Cx43 form gap junction plaques. These plaques seem to be larger than those formed by native Cx43, which might point to a function of ZO-1 in gap junction turnover (23).

Our present experimental approach does not allow to specify the role of the Cx43/ZO-1 association in trophoblastic cell fusion, and other studies are required. To provide proof of the involvement of ZO-1 in fusion by binding to Cx43, mutations of the PDZ domain of the Cx43 COOH terminus should be performed on choriocarcinoma cells. However, only BeWo cells are able to fuse in the presence of cAMP to form a multinucleated syncytium, and the last step of differentiation, the gathering of nuclei into a central area, is missing. In addition, these cells are transformed and some trophoblastic functions are not present (31).

In our physiological model of trophoblastic primary cultures, ZO-1 expression is observed to be predominant during the aggregation of cytotrophoblastic cells and decreased drastically with cell fusion, while Cx43 expression is concomitantly increased throughout aggregation and fusion. It is conceivable that cells must be joined by tight junctions and adherens junctions (via ZO-1) before establishing gap junctions, gap junction communication (via Cx43), and to initiate cell-cell fusion. Indeed, it is evident from gene inactivation for ZO-1 using siRNA that, in the absence of ZO-1 expression, a significant decrease in Cx43 was observed, suggesting that ZO-1 expression may be a prerequisite for Cx43 expression. Since Cx43 expression is associated with trophoblastic cell differentiation, the decrease in Cx43 expression after ZO-1 siRNA treatment resulted in a large number of nonaggregated mononuclear cells.

In conclusion, cell fusion is the limiting step in human villous trophoblast differentiation. To get proteins at the correct place at the right time is a logistical challenge for cell-cell fusion, and this knowledge is necessary to clarify this dynamic process. Recently, several proteins have been implicated (Herv-W, Cx43, CD98, cadherin 11), and studies are still required to clarify the interactions between the different factors as well as the kinetics of their expression. In this study, we showed for the first time that ZO-1 is one of the components involved. Pathological models, such as cytotrophoblasts isolated from T21-affected placentas in which cell fusion and syncytiotrophoblast formation are defective (21, 41), should help to further our understanding of the cell-cell fusion process.

ACKNOWLEDGMENTS

We thank Dr. Nikolaus G. Oberprieler for constructive comments. We thank Dr. Fanny Lewin for support and the staff of the Saint Vincent de Paul Obstetrics Department for providing us with placentas.

GRANTS

This work was supported by la Caisse d'Assurance Maladie des Professions Libérales Province. Guillaume Pidoux was supported by a fellowship from Conseil Regional d'Ile-de-France and Jean-Louis Frendo by a grant from INSERM (Projet Avenir).

DISCLOSURES

No conflicts of interest, financial or otherwise, are declared by the authors.

REFERENCES

1. Adler R, Ng A, Rote N. Monoclonal antiphosphatidylserine antibody inhibits intercellular fusion of the choriocarcinoma line. *JAR. Biol Reprod* 53: 905–910, 1995.
2. Alsat E, Haziza J, Evain-Brion D. Increase in epidermal growth factor receptor and its messenger ribonucleic acid levels with differentiation of human trophoblast cells in culture. *J Cell Physiol* 154: 122–128, 1993.
3. Alsat E, Wyplosz P, Malassiné A, Guibourdenche J, Porquet D, Nessmann C, Evain-Brion D. Hypoxia impairs cell fusion and differentiation process in human cytotrophoblast, in vitro. *J Cell Physiol* 168: 346–353, 1996.
4. Anderson JM, Stevenson BR, Jesaitis LA, Goodenough DA, Mooseker MS. Characterization of ZO-1, a protein component of the tight junction from mouse liver and Madin-Darby canine kidney cells. *J Cell Biol* 106: 1141–1149, 1988.
5. Barker RJ, Price RL, Gourdie RG. Increased association of ZO-1 with connexin43 during remodeling of cardiac gap junctions. *Circ Res* 90: 317–324, 2002.
6. Black S, Kadyrov M, Kaufmann P, Ugele B, Emans N, Huppertz B. Syncytial fusion of human trophoblast depends on caspase 8. *Cell Death Differ* 11: 90–98, 2004.
7. Chen EH, Olson EN. Towards a molecular pathway for myoblast fusion in *Drosophila*. *Trends Cell Biol* 14: 452–460, 2004.
8. Cronier L, Bastide B, Defamie N, Niger C, Pointis G, Gasc J, Malassine A. Involvement of gap junctional communication and connexin expression in trophoblast differentiation of the human placenta. *Histol Histopathol* 16: 285–295, 2001.
9. Cronier L, Bastide B, Hervé JC, Delèze J, Malassiné A. Gap junctional communication during human trophoblast differentiation: influence of human chorionic gonadotropin. *Endocrinology* 135: 402–408, 1994.
10. Cronier L, Defamie N, Dupays L, Théveniau-Ruissy M, Goffin F, Pointis F, Malassiné A. Connexin expression and gap junctional intercellular communication in human first trimester trophoblast. *Mol Hum Reprod* 8: 1005–1013, 2002.
11. Cronier L, Frendo JL, Defamie N, Pidoux G, Bertin G, Guibourdenche J, Pointis G, Malassine A. Requirement of gap junctional intercellular communication for human villous trophoblast differentiation. *Biol Reprod* 69: 1472–1480, 2003.
12. Cronier L, Herve J, Deleze J, Malassine A. Regulation of gap junctional communication during human trophoblast differentiation. *Microsc Res Tech* 38: 21–28, 1997.
13. Dalton P, Christian HC, Redman CW, Sargent IL, Boyd CA. Membrane trafficking of CD98 and its ligand galectin 3 in BeWo cells—implication for placental cell fusion. *FEBS J* 274: 2715–2727, 2007.
14. Defamie N, Mograbi B, Roger C, Cronier L, Malassine A, Brucker-Davis F, Fenichel P, Segretain D, Pointis G. Disruption of gap junctional intercellular communication by lindane is associated with aberrant localization of connexin43 and zonula occludens-1 in 42GPA9 Sertoli cells. *Carcinogenesis* 22: 1537–1542, 2001.
15. Duffy HS, Ashton AW, O'Donnell P, Coombs W, Taffet SM, Delmar M, Spray DC. Regulation of connexin43 protein complexes by intracellular acidification. *Circ Res* 94: 215–222, 2004.
16. Eaton B, Contractor S. In vitro assessment of trophoblast receptors and placental transport mechanisms. In: *The Human Placenta*, edited by Redman CW, Sargent IL, and Starkey PM. London: Blackwell Scientific, 1993, p. 471–503.
17. Feinman MA, Kliman HJ, Caltabiano S, Strauss JF 3rd. 8-Bromo-3',5'-adenosine monophosphate stimulates the endocrine activity of human cytotrophoblasts in culture. *J Clin Endocrinol Metab* 63: 1211–1217, 1986.
18. Frendo JL, Cronier L, Bertin G, Guibourdenche J, Vidaud M, Evain-Brion D, Malassine A. Involvement of connexin 43 in human trophoblast cell fusion and differentiation. *J Cell Sci* 116: 3413–3421, 2003.
19. Frendo JL, Olivier D, Cheynet V, Blond JL, Vidaud M, Arbreaux M, Evain-Brion D, Mallet F. Direct involvement of HERV-W Env glycoprotein in human trophoblast cell fusion and differentiation. *Mol Cell Biol* 23: 3566–3574, 2003.
20. Frendo JL, Théron P, Bird T, Massin N, Muller F, Guibourdenche J, Luton D, Vidaud M, Anderson W, Evain-Brion D. Overexpression of

- copper zinc superoxide dismutase impairs human trophoblast cell fusion and differentiation. *Endocrinology* 142: 3638–3648, 2001.
21. **Frendo JL, Vidaud M, Guibourdenche J, Luton D, Muller F, Bellet D, Giovangrandi Y, Tarrade A, Porquet D, Blot P, Evain-Brion D.** Defect of villous cytotrophoblast differentiation into syncytiotrophoblast in Down syndrome. *J Clin Endocrinol Metab* 85: 3700–3707, 2000.
 22. **Getsios S, MacCalman C.** Cadherin-11 modulates the terminal differentiation and fusion of human trophoblastic cells in vitro. *Dev Biol* 257: 41–54, 2003.
 23. **Giepmans BN.** Gap junctions and connexin-interacting proteins. *Cardiovasc Res* 62: 233–245, 2004.
 24. **Giepmans BN, Hengeveld T, Postma FR, Moolenaar WH.** Interaction of c-Src with gap junction protein connexin-43. Role in the regulation of cell-cell communication. *J Biol Chem* 276: 8544–8549, 2001.
 25. **Giepmans BN, Moolenaar WH.** The gap junction protein connexin43 interacts with the second PDZ domain of the zona occludens-1 protein. *Curr Biol* 8: 931–934, 1998.
 26. **Gilleron J, Fiorini C, Carette D, Avondet C, Falk MM, Segretain D, Pointis G.** Molecular reorganization of Cx43, Zo-1 and Src complexes during the endocytosis of gap junction plaques in response to a non-genomic carcinogen. *J Cell Sci* 121: 4069–4078, 2008.
 27. **Herve JC, Bourmeyster N, Sarrouilhe D.** Diversity in protein-protein interactions of connexins: emerging roles. *Biochim Biophys Acta* 1662: 22–41, 2004.
 28. **Hunter AW, Barker RJ, Zhu C, Gourdie RG.** Zonula occludens-1 alters connexin43 gap junction size and organization by influencing channel accretion. *Mol Biol Cell* 16: 5686–5698, 2005.
 29. **Katsuno T, Umeda K, Matsui T, Hata M, Tamura A, Itoh M, Takeuchi K, Fujimori T, Nabeshima YI, Noda T, Tsukita S, Tsukita S.** Deficiency of zonula occludens-1 causes embryonic lethal phenotype associated with defected yolk sac angiogenesis and apoptosis of embryonic cells. *Mol Biol Cell* 19: 2465–2475, 2008.
 30. **Kibschull M, Gellhaus A, Winterhager E.** Analogous and unique functions of connexins in mouse and human placental development. *Placenta* 29: 848–854, 2008.
 31. **King A, Thomas L, Bischof P.** Cell culture models of trophoblast II: trophoblast cell lines—a workshop report. *Placenta* 21, Suppl A: S113–S119, 2000.
 32. **Kliman HJ, Nestler JE, Sermasi E, Sanger JM, Strauss JF 3rd.** Purification, characterization, and in vitro differentiation of cytotrophoblasts from human term placentae. *Endocrinology* 118: 1567–1582, 1986.
 33. **Larsson LI, Bjerregaard B, Talts JF.** Cell fusions in mammals. *Histochem Cell Biol* 129: 551–561, 2008.
 34. **Malassine A, Cronier L.** Involvement of gap junctions in placental functions and development. *Biochim Biophys Acta* 1719: 117–124, 2005.
 35. **Malassine A, Frendo JL, Evain-Brion D.** A comparison of placental development and endocrine functions between the human and mouse model. *Hum Reprod Update* 9: 531–539, 2003.
 36. **Marzioni D, Banita M, Felici A, Paradinas FJ, Newlands E, De Nictolis M, Muhlhauer J, Castellucci M.** Expression of ZO-1 and occludin in normal human placenta and in hydatidiform moles. *Mol Hum Reprod* 7: 279–285, 2001.
 37. **Mege R, Goudou D, Giaume C, Nicolet M, Rieger F.** Is intercellular communication via gap junctions required for myoblast fusion? *Cell Adhes Commun* 2: 329–343, 1994.
 38. **Morrish DW, Kudo Y, Caniggia I, Cross J, Evain-Brion D, Gasperowicz M, Kokozidou M, Leisser C, Takahashi K, Yoshimatsu J.** Growth factors and trophoblast differentiation—workshop report. *Placenta* 28, Suppl A: S121–S124, 2007.
 39. **Ogren L, Talamentes F.** The placenta as an endocrine organ: polypeptides. In: *Physiology of Reproduction*, edited by Knobil E and Neill J. New York: Raven, 1994, p. 875–945.
 40. **Oren-Suissa M, Poddilewicz B.** Cell fusion during development. *Trends Cell Biol* 17: 537–546, 2007.
 41. **Pidoux G, Gerbaud P, Marpeau O, Guibourdenche J, Ferreira F, Badet J, Evain-Brion D, Frendo JL.** Human placental development is impaired by abnormal human chorionic gonadotropin signaling in trisomy 21 pregnancies. *Endocrinology* 148: 5403–5413, 2007.
 42. **Richard R.** Studies of placental morphogenesis I. Radioautographic studies of human placenta utilizing tritiated thymidine. *Proc Soc Exp Biol Med* 106: 829–831, 1961.
 43. **Rossant J, Cross J.** Placental development: lessons from mouse mutants. *Nat Rev Genet* 2: 538–548, 2001.
 44. **Segretain D, Fiorini C, Decrouy X, Defamie N, Prat JR, Pointis G.** A proposed role for ZO-1 in targeting connexin 43 gap junctions to the endocytic pathway. *Biochimie* 86: 241–244, 2004.
 45. **Singh D, Solan JL, Taffet SM, Javier R, Lampe PD.** Connexin 43 interacts with zona occludens-1 and -2 proteins in a cell cycle stage-specific manner. *J Biol Chem* 280: 30416–30421, 2005.
 46. **Solan JL, Lampe PD.** Connexin43 phosphorylation: structural changes and biological effects. *Biochem J* 419: 261–272, 2009.
 47. **Sorgen PL, Duffy HS, Sahoo P, Coombs W, Delmar M, Spray DC.** Structural changes in the carboxyl terminus of the gap junction protein connexin43 indicates signaling between binding domains for c-Src and zonula occludens-1. *J Biol Chem* 279: 54695–54701, 2004.
 48. **Stevenson BR, Siliciano JD, Mooseker MS, Goodenough DA.** Identification of ZO-1: a high molecular weight polypeptide associated with the tight junction (zonula occludens) in a variety of epithelia. *J Cell Biol* 103: 755–766, 1986.
 49. **Toyofuku T, Akamatsu Y, Zhang H, Kuzuya T, Tada M, Hori M.** c-Src regulates the interaction between connexin-43 and ZO-1 in cardiac myocytes. *J Biol Chem* 276: 1780–1788, 2001.
 50. **Toyofuku T, Yabuki M, Otsu K, Kuzuya T, Hori M, Tada M.** Direct association of the gap junction protein connexin-43 with ZO-1 in cardiac myocytes. *J Biol Chem* 273: 12725–12731, 1998.
 51. **Wade M, Trosko J, Schindler M.** A fluorescence photobleaching assay of gap junction-mediated communication between human cells. *Science* 232: 525–528, 1986.
 52. **Wakelam M.** The fusion of myoblasts. *Biochem J* 15: 1–12, 1985.
 53. **Xu J, Kausalya PJ, Phua DC, Ali SM, Hossain Z, Hunziker W.** Early embryonic lethality of mice lacking ZO-2, but not ZO-3, reveals critical and nonredundant roles for individual zonula occludens proteins in mammalian development. *Mol Cell Biol* 28: 1669–1678, 2008.
 54. **Zamboni Zallone A, Teti A, Primavera M.** Monocytes from circulating blood fuse in vitro with purified osteoclasts in primary culture. *J Cell Sci* 66: 335–342, 1984.

Mesenchymal Activin-A Overcomes Defective Human Trisomy 21 Trophoblast Fusion

Pascale Gerbaud,* Guillaume Pidoux,* Jean Guibourdenche, Niroshani Pathirage, Jean Marc Costa, Josette Badet, Jean-Louis Frenedo, Padma Murthi, and Danièle Evain-Brion

Institut National de la Santé et de la Recherche Médicale (P.G., G.P., J.G., J.B., J.-L.F., P.M., D.E.-B.), Unité 767; Université Paris Descartes (P.G., G.P., J.G., J.B., J.-L.F., P.M., D.E.-B.), Faculté des Sciences Pharmaceutiques et Biologiques, and Fondation PremUP (P.G., G.P., J.G., D.E.-B.), Paris 75006, France; Department of Perinatal Medicine Pregnancy Research Centre and University of Melbourne (N.P., P.M.); Department of Obstetrics and Gynaecology, Royal Women's Hospital, Parkville, Victoria 3052, Australia; and Laboratoire Cerba (J.M.C.), Cergy Pontoise 95066, France

Placental development is markedly abnormal in trisomy 21 (T21) pregnancies. We hypothesized that abnormal paracrine cross talk between the fetal mesenchymal core and the trophoblast might be involved in the defect of syncytiotrophoblast formation and function. In a large series of primary cultured human cytotrophoblasts isolated from second-trimester control (n = 44) and T21 placentae (n = 71), abnormal trophoblast fusion and differentiation was observed in more than 90% of T21 cases. We then isolated and cultured villous mesenchymal cells from control (n = 10) and T21 placentae (n = 8) and confirmed their fetal origin. Conditioned medium of control mesenchymal cells overcame the abnormal trophoblast fusion of T21 cytotrophoblasts by activating the TGF β signaling pathway, as shown by the phosphospecific protein microarray analysis and the use of TGF β signaling pathway antagonists. Using protein arrays, we further analyzed the cytokines present in the conditioned medium from control and T21 mesenchymal cells. Activin-A was identified as strongly secreted by cells from both sources, but at a significantly ($P < 0.01$) lower level in the case of T21 mesenchymal cells. Recombinant activin-A stimulated T21 trophoblast fusion. Blocking activin-A antibody inhibited the fusion induced by conditioned medium and exogenous activin-A. Furthermore, follistatin, an activin-A binding protein largely secreted by T21 mesenchymal cells, inhibited the conditioned medium fusogenic activity. These results show that the defective trophoblast fusion and differentiation associated with T21 can be overcome *in vitro* and reveal the key role of the fetal mesenchymal core in human trophoblast differentiation. (**Endocrinology** 152: 0000–0000, 2011)

The chorionic villus is the structural and functional unit of the human placenta. Its mesenchymal core is covered by cytotrophoblastic cells forming a monolayer of epithelial cells attached to the villous basement membrane. These cells proliferate and differentiate by fusion, forming a syncytiotrophoblast that covers the entire surface of the villus, which bathes in the maternal blood (1). The syncytiotrophoblast plays a major role in fetomaternal exchanges throughout pregnancy, because it is the site

of numerous placental functions including ion, nutrient, and gas exchanges, removal of waste products, and synthesis of steroid and peptide hormones required for fetal growth and development (2, 3). This cell fusion process can be reproduced *in vitro*. Purified cytotrophoblastic cells isolated from human placentae aggregate and then fuse, forming the multinucleated syncytiotrophoblast producing pregnancy-specific hormones [human chorionic gonadotropin (hCG) and human placental lactogen (hPL)]

ISSN Print 0013-7227 ISSN Online 1945-7170

Printed in U.S.A.

Copyright © 2011 by The Endocrine Society

doi: 10.1210/en.2011-1193 Received May 3, 2011. Accepted September 6, 2011.

* P.G. and G.P. contributed equally to this work.

Abbreviations: CMC-CM, Control mesenchymal cell-conditioned medium; hCG, human chorionic gonadotropin; hPL, human placental lactogen; LAP, latency-associated peptide; MMP, matrix metalloproteinase; PI3K, phosphatidylinositol 3-kinase; PKA, protein kinase A; T21, chromosome 21 trisomy; T21MC-CM, T21 mesenchymal cell-conditioned medium.

(4). Using this physiological model, we have previously demonstrated the direct involvement of the endogenous retroviral envelope protein Herv-W (syncytin-1) (5), gap junctional intercellular communication (6) via connexin 43 (7, 8), and the connexin 43-associated zona occludens-1 protein in cytotrophoblastic cell fusion (9). Studies with other models have also shown the involvement of phosphatidylserine flip (10), cadherin 11 (11), caspase 8 (12), 4F2 cell-surface antigen heavy chain (13), and disintegrin and metalloproteinase domain-containing protein 12 precursor (14) in this process.

Chromosome 21 trisomy (T21), which causes Down's syndrome, is the leading genetic cause of mental retardation and affects about one in 800 live births. Although antenatal T21 screening is based on maternal serum markers of placental origin, little is known about placental development in this aneuploid disorder. Syncytiotrophoblast formation is defective in T21 placentae. Cultured cytotrophoblasts isolated from T21 placentae aggregate but fuse poorly or belatedly (15, 16). This abnormal trophoblast fusion is related to superoxide dismutase 1 (*SOD-1*) gene overexpression (17) and to the secretion of hyperglycosylated hCG with low bioactivity (18). A predominance of two-layered mononuclear cytotrophoblasts is observed in T21 placentae compared with controls (19, 20).

A number of factors promoting or inhibiting cytotrophoblastic cell fusion and differentiation have been described (21). These include epidermal growth factor (22, 23), which acts through a membrane tyrosine kinase receptor, and activin (24) acting through a combination of type I and II transmembrane serine/threonine kinase receptors that stimulate trophoblast differentiation, whereas *TGF β 1* (25) and *TNF α* (26) are known inhibitors of trophoblast differentiation. The monomeric activin binding protein follistatin has been shown to regulate/inhibit the effects of activin by forming an inactive complex. Follistatin has been described in human placenta (27) and shown to neutralize the effects of activin on the endocrine activities of cytotrophoblastic cells (27, 28). Several studies have also confirmed the importance of hCG and its membrane receptor in syncytiotrophoblast formation (29–31). Binding of hCG to its receptor activates adenylate cyclase, phospholipase C, and ion channels, which in turn control cellular cAMP, inositol phosphates, Ca^{2+} , and other second messengers (32, 33). cAMP, via cAMP-dependent protein kinases [protein kinase A (PKA)], promotes cytotrophoblast fusion *in vitro* (34), and also elevates mRNA levels of the fusogenic protein syncytin-1 in cultured trophoblasts (5).

Possible cross talk between trophoblastic and mesenchymal cells may play a major role in placental develop-

ment but has rarely been explored (35–38). In this study, we identified activin-A as a soluble paracrine factor involved in the cross talk between trophoblastic and mesenchymal cells in normal and T21 placentae regulating the trophoblastic cell fusion.

Materials and Methods

Materials

The following were purchased from the indicated commercial sources: monoclonal antibodies anti-CD14 (PN6602622), anti-CD34 (IM0786), and antivimentin (IM1919) from Beckman Coulter Company, Marseille, France; anti-CD45 (31251A) from PharMingen International, San Diego, CA; anti-CD90 (ASO2) from Dianova, Hamburg, Germany; monoclonal antibody anti-CD31 (M0823) and anti-cytokeratin 7 (M7018) and rabbit polyclonal antibody anti-hPL (A0137) from Dako, Glostrup, Denmark; rabbit polyclonal antibody anti-actin (A2066) and monoclonal antibody antidesmoplakin (D1286) from Sigma-Aldrich, St. Louis, MO; human activin-A (338-AC) and monoclonal antibody anti-activin-A (MAB3381) from R&D Systems Europe, Lille, France; follistatin (F1175) from Sigma-Aldrich St. Louis, MO; 8-Br cAMP (B7880) and H89 dihydrochloride hydrate (B1427) from Sigma-Aldrich, St. Louis, MO; chelerythrine (C2932), herbimycin A (H6649), SB 525334 (S8822), A-83-01 (A5480), Tyr23 (T7165), *Clostridium difficile* B (C4102) from Sigma-Aldrich St. Louis, MO; signaling pathway antagonists LY294002 (440202), Gö6976 (6976), and Y27632 (688000) from Calbiochem La Jolla, CA; *TGF β* signaling phospho-antibody array (PTG176) from Full Moon Biosystems, Inc., Sunnyvale, CA; and RayBio arrays (AAH-CYT-8) from RayBiotech, Inc., Norcross, GA.

Placenta collection

Second-trimester placentae were collected during termination of pregnancies at 12–25 wk of amenorrhea from T21 and non-T21 gestational-age-matched samples referred to as control throughout this study. Gestational age was confirmed by ultrasound measurement of crown-rump length at 8–12 wk. Fetal Down's syndrome was diagnosed by karyotyping of amniotic fluid cells, chorionic villi cells, or fetal blood cells. Termination of the control pregnancies was indicated for severe bilateral or low obstructive uropathy or major cardiac abnormalities. Conventional and molecular cytogenetic analyses were performed on cultured trophoblastic cells (free trisomy 21 or normal karyotype) as previously described (39). A total of 71 T21-affected placentae (37 male and 34 female fetuses) and 44 gestational-age-matched control placentae (17 males and 27 females) were used for cell culture experiments. These biological samples were obtained after informed patient written consent and approval from our local ethics committee (CCPPRB, Paris Cochin, no. 18-05, Paris, France).

Trophoblast cell culture

Villous cytotrophoblasts from second-trimester placentae were isolated and purified as previously described (40). Cells were plated to a final density of 140,000 cells/cm².

Isolation and culture of mesenchymal cells

Mesenchymal cells were isolated by further trypsin-deoxyribonuclease digestion steps of the same second-trimester villi from control and T21 placentae used for trophoblastic cell isolation. Cells isolated by digestions 6–7 were pooled, diluted to a final density of 150,000 cells/cm² in 0.15 ml in supplemented DMEM (10% fetal calf serum, 2 mM glutamine, 100 IU/ml penicillin, and 100 µg/ml streptomycin). They were used after five passages. Conventional and molecular cytogenetic analyses were applied to cultured mesenchymal cells to detect chromosomes 21 and Y (39). To avoid contamination by cells of maternal origin, we used only control gestational-age-matched XY mesenchymal cells and XY mesenchymal cells harboring a free T21. Mesenchymal cells were used after five passages to avoid any trophoblastic cell contamination, and similar activin-A production was observed in cells derived between passages 2 and 7. Control mesenchymal cell-conditioned medium (CMC-CM) and T21 mesenchymal cell-conditioned medium (T21MC-CM) were collected and centrifuged at 200 × g for 10 min at 4 C; supernatants were kept frozen at –20 C until used.

Mesenchymal cell characterization

Mesenchymal cells were fixed, permeabilized as previously described (40), and characterized by indirect immunofluorescence staining using antibodies anti-CD14 (6 µg/ml), anti-CD31 (4 µg/ml), anti-CD34 (4 µg/ml), anti-CD45 (6 µg/ml), anti-CD90 (2.5 µg/ml), antivimentin (2.5 µg/ml), anti-cytokeratin 7 (2 µg/ml), and A488-labeled goat antimouse IgG (3 µg/ml). Controls (omission of the primary antibody or use of a nonspecific IgG of the same isotype) were all negative.

Trophoblast fusion assay

Syncytium formation was followed by monitoring the cellular distribution of desmoplakin and nuclei. The fusion index (9) were determined as previously described (30, 34).

Cells were cultured for 18 h after plating and treated with 1 mM 8-Br cAMP, 3 µM H89 dihydrochloride hydrate, recombinant human activin-A, or recombinant human follistatin. TGFβ signaling pathway antagonists were used on trophoblastic cells at their respective IC₅₀: LY 294002 (5 µM), Gö6976 (100 nM), tyrphostin 23 (Tyr23, 50 µM), chelerytrine (50 µM), herbimycin A (12 µM), A-83-01 (90 nM), SB 525334 (28 nM), and *C. difficile* B (50 pM). Cell viability after treatment was quantified with Trypan blue (41). To neutralize the bioactivity of activin-A, 5 ng/ml recombinant activin-A or CMC-CM was incubated with 2 µg/ml monoclonal antihuman activin-A antibody or with 1 µg/ml human recombinant follistatin for 1 h at 37 C and then added to cultured T21 cytotrophoblasts.

Phosphospecific protein microarray analysis for TGFβ signaling

Phosphospecific protein microarrays were performed according to the manufacturer's instructions. Protein microarray analysis was applied to trophoblast cells derived from T21 (n = 3) and matched control placentae (n = 3) treated with CMC-CM for 0, 20, and 60 min. Briefly, T21 placentae (n = 3) or control placentae (n = 3) were pooled, respectively. Cell lysate (100 µg protein) was collected in 50 µl reaction mixture and labeled with 1.5 µl biotin/DMF (*N,N*-dimethylformamide, 10 µg/µl). The bound biotinylated proteins were detected with Cy3-streptavi-

din (0.5 mg/ml), and the signal intensity was determined on a Typhoon Imager (model 9410; GE Healthcare, Piscataway, NJ) using ImageJ software (Rasband, W.S., National Institutes of Health, Bethesda, MD). The immunoreactivity of phosphoprotein was analyzed by subtracting the background and normalizing to the positive markers provided on the same slide. Then the relative protein intensity of each spot and for each membrane was illustrated using Adobe Photoshop software version CS3.

Intracellular cAMP assay

Cells (2.8 × 10⁶) were plated in 60-mm dishes and cultured as described above. After 24 h, the cells were preincubated with 10 mM isobutylmethylxanthine for 1 h to prevent cAMP degradation and were then stimulated for 20 or 60 min with CMC-CM. Intracellular cAMP was assayed as previously described (30).

Protein array

Media conditioned for 24 h by subconfluent mesenchymal cells isolated from T21 placentae (T21MC-CM, n = 5) or controls (CMC-CM, n = 5) were pooled and concentrated 4-fold on Amicon Ultra-15 columns. RayBio arrays were used to detect cytokines, and the membranes were processed according to the manufacturer's recommendation. Briefly, the membranes were blocked and incubated with biotin-conjugated antibodies and finally incubated with horseradish peroxidase-conjugated streptavidin.

Chemiluminescence was detected with a LAS-1000 device (Fujifilm), and the data were digitized and analyzed with ImageQuant software in volume integration mode (Molecular Dynamics, Sunnyvale, CA). By subtracting the background staining and normalizing to the positive controls on the same membrane, relative protein densities for each membrane were obtained, and the fold difference in protein concentration was calculated.

Hormone assays

hCG concentration was determined in triplicate in culture medium after 72 h of culture using an immunoassay developed on the Advia Centaur XP system (Siemens Healthcare Diagnostic, Deerfield, IL) (detection limit of 2 mIU/ml).

Activin-A concentration was determined in triplicate in cell-conditioned medium of T21 (n = 8) and control (n = 10) placental mesenchymal cell cultures, using the activin-A assay kit (MCA1426KZZ) from R&D Systems Europe (detection limit <78 pg/ml). Follistatin concentration was determined in triplicate in culture medium of T21 (n = 5) and control (n = 5) placental mesenchymal cell cultures, using the human follistatin assay kit (DFN00) from R&D Systems Europe (detection limit <29 pg/ml).

Immunoblotting

Cell extracts were prepared as previously described (42). The membranes were immunoblotted with a rabbit polyclonal antibody against hPL (2 µg/ml) or with a mouse antibody against human activin-A (0.5 µg/ml); the specific band was detected by chemiluminescence (West Pico Chemiluminescent; Pierce, Rockford, IL) after incubation with an antirabbit or antimouse peroxidase-coupled antibody according to the primary antibody. Actin was used as housekeeping control, and the membranes were immunoblotted using a rabbit polyclonal anti-actin antibody (A2066; 0.5 µg/ml) and detected with an antirabbit peroxidase-coupled antibody.

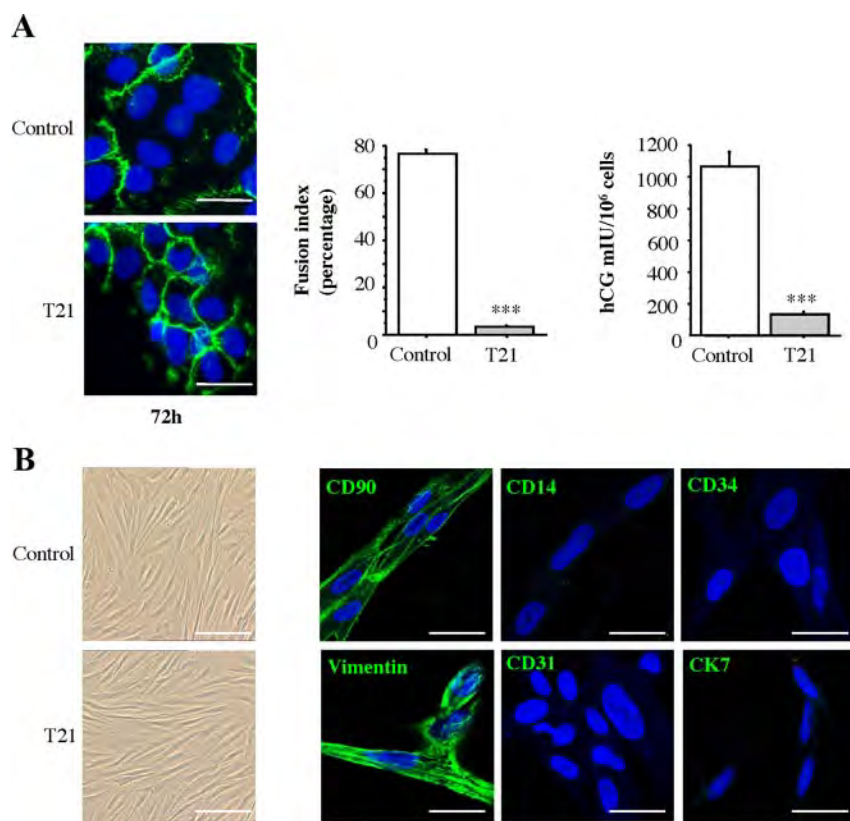


FIG. 1. *In vitro* differentiation of trophoblastic cells and characterization of mesenchymal cells from control and T21 placentae. **A, left panel,** Trophoblastic cells isolated from control and T21 placentae were cultured for 72 h, fixed, and immunostained for desmoplakin (green), and nuclei were counterstained with 4',6-diamidino-2-phenylindole; **middle panel,** cell fusion processes are represented as fusion index histogram, with results are expressed as the mean \pm SEM of four independent experiments (***, $P < 0.001$); **right panel,** level of hCG secreted into culture medium, with results expressed as the mean \pm SEM of 10 independent experiments (***, $P < 0.001$). **B, left panel,** Mesenchymal cells isolated from control and T21 placentae were visualized by phase-contrast microscopy; **right panel,** cells were immunostained (green) for fibroblast markers (CD90 and vimentin) and were negative for macrophage (CD14), hematopoietic stem cell (CD34), endothelial (CD31, CD34), and trophoblastic cell markers (CK7); nuclei were counterstained with 4',6-diamidino-2-phenylindole. Scale bars, 1 cm = 15 μ m (immunostaining) and 1 cm = 30 μ m (phase-contrast microscopy). CD90, Thy-1 membrane glycoprotein precursor; CD14, monocyte differentiation antigen CD14 precursor; CD34, hematopoietic progenitor cell antigen; CD31, platelet endothelial cell adhesion molecule precursor; CK7, cytokeratin 7.

Statistical analysis

The StatView F-4.5 software package (Abacus Concepts, Inc., Berkeley, CA) was used for statistical analysis. Statistical differences between groups were evaluated using Student's unpaired *t* test or ANOVA, as appropriate. *Post hoc* analysis (Tukey) was used for individual comparisons and to generate *P* values that are stated in the figure legends. The sample size and significance level is shown in the figure legends for each graph. All data are presented as means \pm SEM unless otherwise stated. A value of $P < 0.05$ was considered statistically significant.

Results

Cultured T21 cytotrophoblastic cells do not fuse and differentiate poorly *in vitro*

During a 4-yr period, we collected 71 second-trimester placentae with T21 and 44 gestational-age-matched con-

trol placentae with a normal karyotype. Villous cytotrophoblastic cells were isolated and cultured *in vitro* for 3 d (4). We found that mononucleated cytotrophoblastic cells isolated from control placentae aggregated and fused to form a syncytiotrophoblast after 72 h culture (Fig. 1A). This was associated with a large increase in hCG secretion into the culture medium, from 7.4 ± 2.3 mIU/ 10^6 cells at 24 h to 1015 ± 31 mIU/ 10^6 cells at 72 h. In contrast, in 67 of 71 cultures of cytotrophoblastic cells isolated from T21 placentae, cytotrophoblastic cells aggregated but fused inefficiently, forming only a few small syncytiotrophoblasts after 3 d of culture; the majority of the cells remained aggregated (Fig. 1A). Four cultures of cytotrophoblastic cells isolated from T21 placentae were able to fuse to form a syncytiotrophoblast. The fusion index was significantly lower in trophoblastic cells isolated from T21 placentae ($P < 0.001$, Fig. 1A). This defective syncytiotrophoblast formation was associated with significantly lower ($P < 0.001$) hCG secretion into the culture medium compared with control cells (2.8 ± 1 and 166 ± 12 mIU/ 10^6 cells at 24 h and 72 h; Fig. 1A).

Characterization of control and T21 placental mesenchymal cells

Mesenchymal cells and cytotrophoblasts were isolated and purified from the same placental villi. The fetal

origin of the mesenchymal cells was determined by conventional and molecular cytogenetic analyses. We confirmed the presence or absence of three chromosomes 21 and a Y chromosome. No difference in the shape (Fig. 1B) or growth rate (data not shown) of control and T21 mesenchymal cells was observed. After five passages, subconfluent control and T21 mesenchymal cells were allowed to condition the culture medium for 24 h. As illustrated in Fig. 1B, the mesenchymal cells used in this study stained positively for CD90 and vimentin (fibroblast markers) and negatively for CD14 (macrophage marker), CD31 (endothelial cell marker), CD34 (endothelial and hematopoietic stem cell marker), and cytokeratin 7 (trophoblastic cell marker).

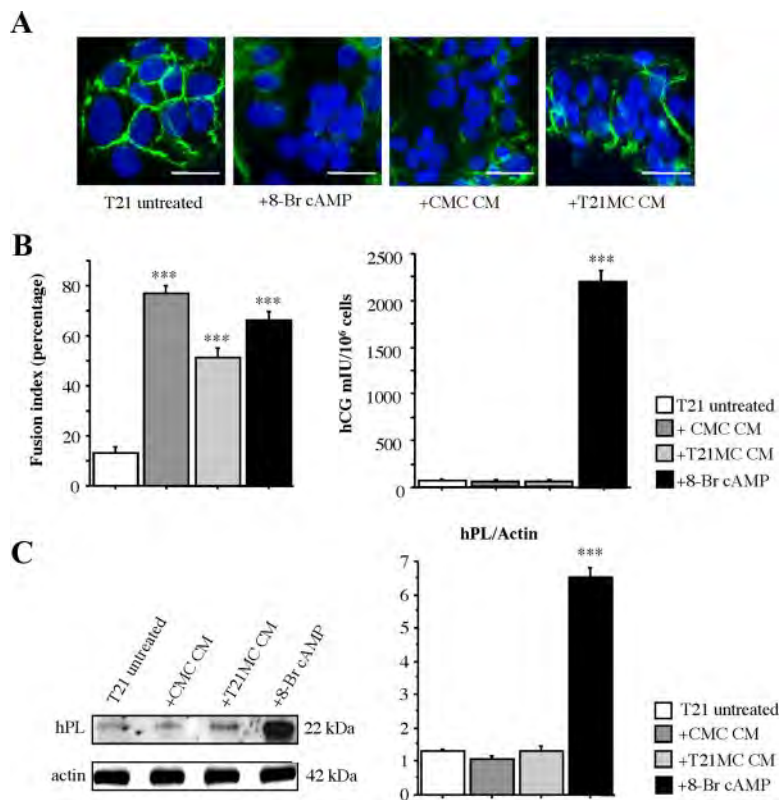


FIG. 2. Effect of 8-Br cAMP and mesenchymal cell-conditioned medium on T21 cytotrophoblast cell fusion. A, T21 trophoblastic cells cultured for 18 h were stimulated with 8-Br cAMP, CMC-CM, or T21MC-CM. Cells were immunostained for desmoplakin (green), and nuclei were counterstained with 4',6-diamidino-2-phenylindole. Scale bar, 1 cm = 15 μ m. B, left panel, Effects of 8-Br cAMP, CMC-CM, and T21MC-CM on the cell fusion process after 72 h culture are represented as fusion index histogram; right panel, levels of hCG detected in the medium of untreated cells and cells treated with 8-Br cAMP, CMC-CM, or T21MC-CM are represented by histogram. Results are expressed as the mean \pm SEM of three independent experiments (***, $P < 0.001$). C, Immunoblot analysis of hPL and actin levels in trophoblastic cells treated with 8-Br cAMP, CMC-CM, or T21MC-CM. Histogram represents the levels of hPL assessed by densitometry scanning of immunoblot and normalized to actin levels in the same blots.

Mesenchymal cell-conditioned medium induces T21 trophoblastic cell fusion

We confirmed that 8-Br cAMP stimulated T21-cytotrophoblast fusion (30, 31), as shown by the significant ($P < 0.001$) increase in the fusion index (Fig. 2, A and B). Mesenchymal cell-conditioned medium also induced T21-cytotrophoblast fusion. Indeed, T21-cytotrophoblast cultured for 72 h contained five times more mononuclear cells in control conditions ($58.2 \pm 0.6\%$) than after treatment with CMC-CM ($11.3 \pm 0.9\%$; $P < 0.001$) (data not shown). Medium conditioned by control mesenchymal cells induced T21-cytotrophoblast fusion, with approximately 75% of nuclei participating in syncytia formation (*vs.* 12% in untreated cells) (Fig. 2B). Interestingly, T21MC-CM induced syncytia formation as well, but only 50% of nuclei participated ($P < 0.001$ *vs.* T21 untreated cells). Thus, mesenchymal cells secrete soluble factors that are able to induce syncytialization.

Mesenchymal cell-conditioned medium does not stimulate trophoblast hormone secretion

Stimulation of syncytiotrophoblast formation by soluble factors of mesenchymal origin was not accompanied by secretion of the hormones specifically synthesized by the syncytiotrophoblast, contrary to the effect induced by 8-Br cAMP (Fig. 2B).

hCG secretion increased from 75 ± 3 mIU/10⁶ cells in untreated condition to 2000 ± 23 mIU/10⁶ cells in the presence of 8-Br cAMP at 72 h culture ($P < 0.001$). No increase in hCG secretion was observed when T21-cytotrophoblast cells were cultured with mesenchymal cell-conditioned medium for 72 h (Fig. 2B).

hPL was weakly detected in T21 trophoblastic cells at 72 h culture using immunoblot despite the formation of a syncytiotrophoblast in contrast to T21 cells treated with 8-Br cAMP (Fig. 2C; $P < 0.001$). No increase in hPL was observed when T21 cytotrophoblasts were cultured with mesenchymal cell-conditioned medium (Fig. 2C).

Thus, the production of mesenchymal cell-derived soluble factors that induced syncytialization was not accompanied by the increase in hormones of pregnancy (hCG and hPL), as usually observed during syncytium formation.

hormones of pregnancy (hCG and hPL), as usually observed during syncytium formation.

TGF β signaling but not cAMP signaling is involved in the stimulation of T21 trophoblast cell fusion by mesenchymal cell-derived soluble factors

Two major signaling pathways have been implicated in trophoblastic cell fusion: the cAMP signaling pathway and signaling associated with TGF β and EGF. T21 trophoblastic cells were cultured with H89 (a specific inhibitor of the cAMP-dependent protein kinase), either alone or together with control or T21MC-CM. H89 had no effect on the fusion index of cells treated with mesenchymal cell-conditioned medium (Fig. 3A). Likewise, no significant difference in intracellular cAMP levels between trophoblastic cells from control and T21 placentae was observed after incubation for 20 or 60 min with mesenchymal cell-conditioned medium (Fig. 3B). The results ruled out involvement of the cAMP signaling

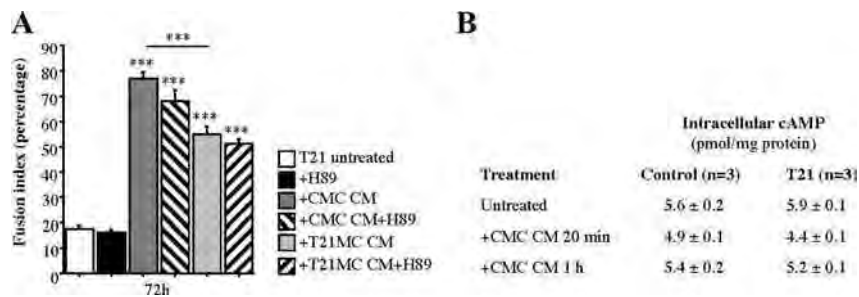


FIG. 3. Signaling pathways involved in the mesenchymal cell-conditioned medium inducing fusion of T21 cytotrophoblasts. A, Effect of H89 on the fusion of T21 cytotrophoblasts induced by mesenchymal cell-conditioned medium is represented as a fusion index histogram after 72 h culture. Results are expressed as the mean \pm SEM of three independent experiments (***, $P < 0.001$). B, Intracellular cAMP quantification by control and T21 cytotrophoblastic cells (T21) after stimulation for 20 min or 1 h with CMC-CM. Results are expressed as the mean \pm SEM of three different cultures from cells isolated from control and T21 placentae.

pathway. We then used an antibody microarray strategy to determine which proteins of the TGF β signaling pathway induced cell fusion. T21 cytotrophoblasts were stimulated with CMC-CM for 20 or 60 min. As illustrated in Fig. 4A, some proteins showed an increase in phosphorylation or expression after 20 min, suggesting a role in syncytialization. After 60 min stimulation, these candidate proteins returned mostly to their basal level of expression. These proteins were regrouped

(group I–VII) based on their known interactions described in the literature, with group I corresponding to the TGF β family members and their receptors. CMC-CM activated via the TGF β receptor (group I), the Rac-cdc43/p21-activated kinase 1/c-Abl pathway (group II), the phosphatidylinositol 3-kinase (Pi3K)/akt/mammalian target of rapamycin pathway (group III), and the adaptor proteins Shc (group IV). PKC (group V), the MAPK signaling pathway (MKK6/p38; group VI), and some Smad family proteins (group VII) were also activated. The Ras and RhoA pathways did not seem to be involved.

Thus, CMC-CM appeared to activate specific downstream effectors of the TGF β signaling pathway.

Effect of specific TGF β signaling pathway inhibition on trophoblastic cell fusion induced by CMC-CM

To identify which downstream effectors of the TGF β signaling pathway were involved in the trophoblastic cell fusion induced by CMC-CM, we used specific inhibitors. T21 cytotrophoblasts were

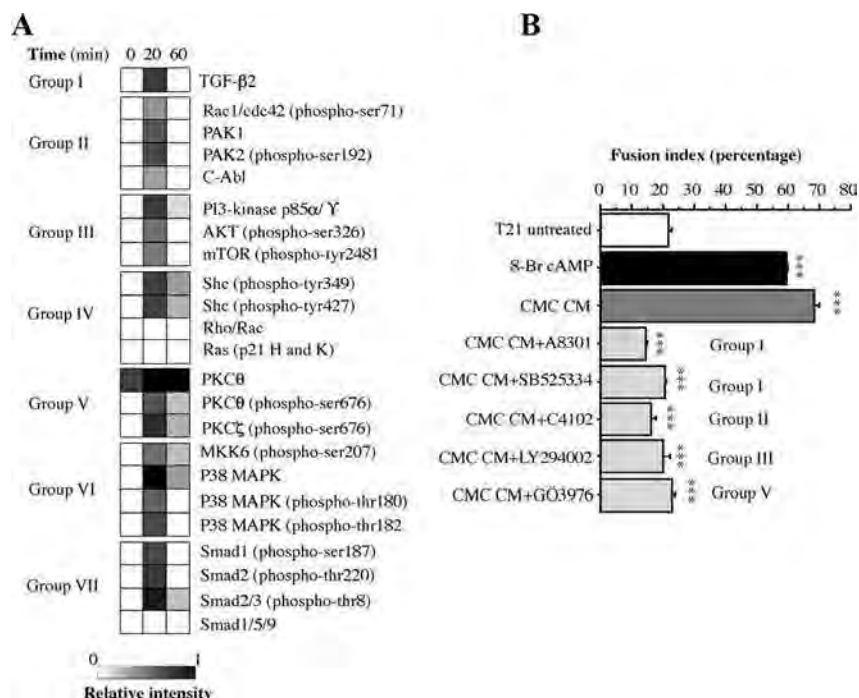


FIG. 4. Impact of specific TGF β inhibitors on the T21 cytotrophoblasts cell fusion induced by mesenchymal cell-conditioned medium. (A) Heat map depicting differences in phosphorylation state or expression of the TGF β signaling dynamics proteins of T21 cytotrophoblasts after stimulation for 20 min or 1 h with CMC-CM. (B) Effect of specific TGF β inhibitor on the fusion of T21 cytotrophoblasts induced by mesenchymal cell-conditioned medium is represented as fusion index histogram after 72 h of culture. Results are expressed as the mean \pm SEM of $n = 3$ independent experiments (***, $P < 0.001$).

cultured with CMC-CM to induce cell fusion, and the impact of specific inhibitors was measured in a fusion assay (Fig. 4B). TGF β receptor (ALK4, -5, and -7) inhibitors (A-83-01 and SB 525334), specifically from group I, presented a 50% reduction of fusion index ($P < 0.001$) compared with cells treated with CMC-CM or with 8-Br cAMP. This observation was also made by the use of specific TGF β 1 and - β 2 blocking antibodies (data not shown). Interestingly, the *C. difficile* B (a group II inhibitor, Rho/Rac/Cdc42 antagonist; C4102), a p inhibitor (group III inhibitor, LY294002), and a PKC antagonist (group V antagonist, Gö6976) presented as well a significant inhibition in cell fusion (up to 50%) induced by CMC-CM ($P < 0.001$). Finally, the use of group VI inhibitors (tyrosine kinase inhibitors Tyr23 and herbimycin A) and another PKC antagonist (group V, chelerythrine) presented an inhibition in cell fusion as well (data not shown).

Protein array analysis of conditioned medium identifies activin-A as largely produced by mesenchymal cells

To identify soluble paracrine factors produced by control and T21 mesenchymal cells, cytokine arrays were applied to control and T21MC-CM. Six soluble factors showed markedly different signal intensities between control and T21 (Fig. 5A). These factors were activin-A, a growth factor (TGF β 2), latency-associated peptide (LAP), a cytokine and its receptor (IL-18 receptor IIB) and matrix metalloproteinases (MMP1 and MMP3). Semiquantitative analyses showed approximately 2-fold higher TGF β 2, IL-18 receptor IIB, and MMP1 protein levels and 4- to

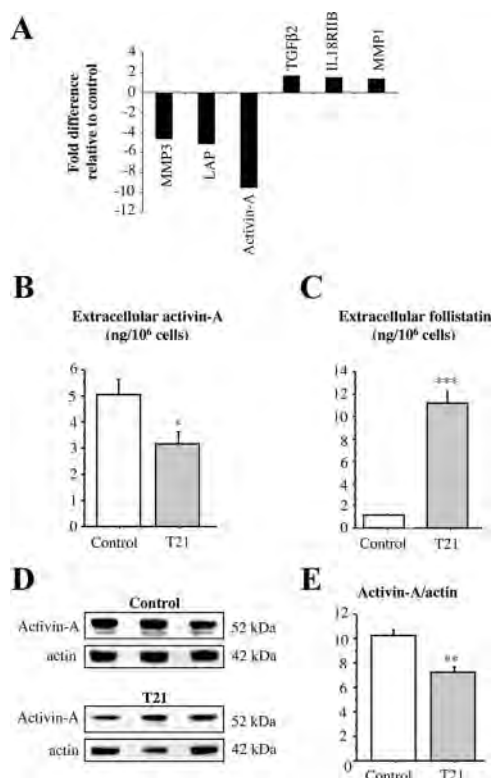


FIG. 5. Activin-A is produced and secreted by mesenchymal cells. A, Cytokine array of conditioned medium from control and T21 mesenchymal cells. Conditioned medium of human mesenchymal cells isolated from control ($n = 5$) or T21 ($n = 5$) placentae were pooled and analyzed by RayBio human cytokine arrays (AAH-CYT-8). Results are expressed as fold difference in T21 mesenchymal cells supernatant relative to control supernatant. B, Levels of activin-A in control and T21MC-CM measured by ELISA. Results are expressed as the mean \pm SEM of different cell cultures (control $n = 10$; T21 $n = 8$). *, $P < 0.05$. C, Levels of follistatin in control and T21MC-CM measured by ELISA. Results are represented as the mean \pm SEM of different cell cultures (control $n = 5$; T21 $n = 5$; ***, $P < 0.001$). D, Immunoblot analysis of activin-A and actin expression in lysates of control mesenchymal cells and T21 mesenchymal cells. E, Histogram representing the levels of activin-A assessed by densitometry scanning of immunoblot and normalized to actin levels in the same blots. Results are expressed as the mean \pm SEM of three different cultures from mesenchymal cells isolated from control and T21 placentae. **, $P < 0.01$.

10-fold lower MMP3, LAP, and activin-A levels in T21 mesenchymal cell culture supernatants than in controls.

T21 mesenchymal cells secrete less activin-A than control mesenchymal cells

As shown in Fig. 5B, activin-A levels measured with an ELISA were significantly higher in CMC-CM (5 ± 0.5 ng/10⁶ cells) than in T21MC-CM (3 ± 0.4 ng/10⁶ cells; $P < 0.05$). Interestingly, the extracellular amount of follistatin, the activin biological antagonist, quantified by ELISA (Fig. 5C) presented a 10-fold significant increase in T21MC-CM compared with control (11.2 ± 1.1 and 1.3 ± 0.1 ng/10⁶ cells, respectively; $P < 0.001$).

Immunoblotting showed significantly ($P < 0.01$) lower activin levels in T21 cell extracts than in control cell extracts (Fig. 5, D and E). Moreover, the amount of extracellular follistatin produced by control and T21 cytotrophoblastic cells were observed to be nonsignificant and as low as the CMC-CM production (0.38 ± 0.1 and 1.1 ± 0.3 ng/10⁶ cells, respectively; data not shown).

Activin-A present in mesenchymal cell-conditioned medium stimulates T21 trophoblast fusion

We first showed that recombinant activin-A stimulated syncytiotrophoblast formation (Fig. 6A). Three concentrations of activin-A (from 1–50 ng/ml) were tested (data not shown). In the presence of 5 ng/ml recombinant activin-A, the fusion index of the cells increased from $16 \pm 2\%$ to $70 \pm 2\%$ (Fig. 6A). This increase was not associated with a significant increase in hCG (data not shown). An

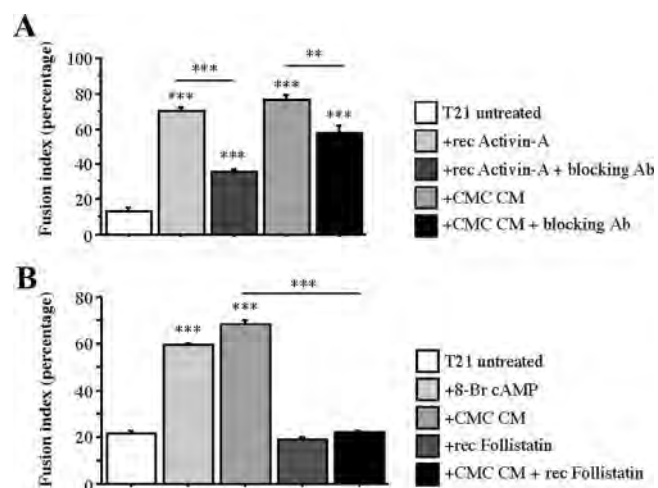


FIG. 6. Activin-A stimulates T21 cytotrophoblast fusion and differentiation. A, Effect of recombinant activin-A or CMC-CM with or without activin-A blocking antibody on T21 trophoblast cell fusion at 72 h culture is represented as fusion index. Results are expressed as the mean \pm SEM of four independent experiments. **, $P < 0.01$; ***, $P < 0.001$. B, Effect of 8-Br cAMP, recombinant follistatin, or CMC-CM on T21 trophoblast cell fusion at 72 h culture is represented as fusion index. Results are expressed as the mean \pm SEM of four independent experiments. ***, $P < 0.001$.

activin-blocking antibody partially inhibited the effect of exogenous activin-A on trophoblast fusion (fusion index was $70 \pm 2\%$ with activin-A alone and $38 \pm 1\%$ with activin-A and the blocking antibody; $P < 0.001$). The blocking antibody also significantly inhibited ($P < 0.001$) the effect of CMC-CM on T21 trophoblastic cell fusion (fusion index was $78 \pm 2\%$ with CMC-CM and $58 \pm 2\%$ with CMC-CM plus the blocking antibody; Fig. 6A). Finally, follistatin, first known as a potent biological inhibitor of activin and then described as an activin-binding protein, was used to confirm the role of activin-A in the cell fusion induced by mesenchymal cell-conditioned medium. The presence of follistatin (Fig. 6B) did not modify the fusion index compared with T21 untreated cells (19 ± 2 and $21.5 \pm 2\%$, respectively). However, T21 trophoblastic cells treated with a human recombinant follistatin ($1 \mu\text{g/ml}$) and mesenchymal cell-conditioned medium (Fig. 6B) presented a significant reduction (46% ; $P < 0.001$) of fusion index ($23 \pm 1\%$) compared with T21 trophoblastic cells treated with mesenchymal cell-conditioned medium alone ($69 \pm 2\%$).

Discussion

Numerous histomorphological studies of chorionic villi obtained after miscarriage or termination of pregnancy during the first trimester of pregnancy have shown qualitative differences between control and T21 pregnancies (43–49). T21 is associated with villous hypovascularity, intrastromal cytotrophoblastic cells, persistence of nucleated red blood cells, and abnormalities of the trophoblastic layer, suggesting a delay in villous maturation. Few studies have focused on second-trimester placentae (50). Here we used primary cultures of villous trophoblastic cells isolated from second-trimester control and T21 placentae. We confirm in this large and unique collection of samples that syncytiotrophoblast formation is defective and hCG secretion is subnormal in T21 placentae. T21 cytotrophoblastic cells adhered well in culture (data not shown) and aggregated but fused poorly or not at all.

This abnormal fusion and differentiation of trophoblastic cells isolated from T21 placentae was overcome *in vitro*. As previously shown (30, 31), 8-Br cAMP and biosynthetic hCG induced T21 trophoblast fusion and differentiation. It is well established that agents that increase cellular levels of cAMP promote cytotrophoblast fusion *in vitro* (34). Here we report for the first time that medium conditioned by mesenchymal cells can overcome the abnormal fusion of T21 cytotrophoblasts in a cAMP-independent manner. cAMP acts through several effectors, including PKA, exchange protein activated by

cAMP, and cyclic nucleotide-gated ion channels (51). We found that the specific cAMP-dependent protein kinase inhibitor H89 had no effect on trophoblastic cell fusion induced by mesenchymal cell-derived factors. This suggests that a signaling pathway other than the one activated by PKA is involved in trophoblastic cell fusion (30, 31, 34). Moreover, the noninvolvement of PKA in this process is confirmed by the absence of any increase in intracellular cAMP during trophoblastic cell fusion induced by conditioned medium. This also rules out the involvement of other cAMP-downstream effectors such as exchange protein activated by cAMP, which was recently shown to be involved in trophoblastic cell fusion (52).

The *in vitro* reversibility of abnormal T21 trophoblast differentiation points to abnormal regulation of the dynamic process leading to cell-cell fusion and differentiation rather than to a defect of major factors involved in trophoblast fusion and differentiation due to the genetic defect. To fuse *in vitro*, trophoblastic cells must exit the proliferative stage, express genes and proteins involved in the fusion process, and then recognize and interact with their fusion partners. This dynamic process is likely to be finely regulated and coordinated.

In vivo, cytotrophoblastic cells are in close contact with the underlying mesenchymal core. The villous chorionic core is composed of mesenchymal cells, Hofbauer macrophages (35), and fetal vessels. It is possible that the mesenchymal core plays a major role in villous development (35). Indeed, macrophage-conditioned medium has been shown to stimulate syncytiotrophoblast formation, an effect associated with a large increase in hCG secretion (53). Directional contact between the cytotrophoblast and syncytium is important for regulating the relative abundance of the two cell populations (54). Previous studies have shown that the extracellular matrix deposited by fibroblasts and mesenchymal cell-derived IGF-I stimulate trophoblast migration into the anchoring villi (37, 38).

We used mesenchymal cells derived only from male placentae and confirmed the presence of three chromosomes 21 and a Y chromosome. We also obtained XX cells not affected by T21 and therefore of maternal origin. These cells may be endothelial progenitor cells circulating in the intervillous space or endothelial cells coating the basal plate (55, 56). Only the cells of placental origin expressed fibroblastic markers.

Despite their similar growth rates and shapes, control and T21 mesenchymal cells produced different levels of cytokines and other soluble factors. The secretion of three factors was significantly lower in T21 mesenchymal cells. MMP3 is strongly expressed in the placenta and involved in matrix degradation and trophoblast invasion (for review see Ref. 57). It is also expressed by skin fibroblasts

(58) and gingival fibroblasts (59); its expression is increased in inflammatory processes (60). LAP was also significantly lower in T21MC-CM. TGF β is secreted as latent complexes, consisting of mature dimeric growth factor, the LAP, and a distinct gene product, latent TGF β binding protein. The secreted complex is targeted to specific locations in the extracellular matrix by the appropriate latent TGF β binding protein. The latent complex subsequently needs to be activated (61). Together, these results are in keeping with transcriptomic analysis of T21 tissues (62) and suggest that the modulation, composition, and maintenance of the extracellular matrix secreted by mesenchymal cells might be altered in T21 pregnancies and contribute to the delayed placental maturation.

Mesenchymal cell-conditioned medium stimulated the TGF β signaling pathway as indicated by activation of specific downstream effectors such as Pi3K, tyrosine kinases, and PKC and an increase in Smad2 and Smad3 phosphorylation, suggesting that members of the TGF β family are present in this medium. Interestingly, proteins shown to be activated on protein arrays under stimulation with mesenchymal cell-conditioned medium were all found to be involved in the cell fusion process by using specific TGF β signaling pathway antagonists, confirming the concordance of the data obtained from these two approaches. Then, it becomes complicated to define precisely which downstream effectors of the TGF β signaling pathway could be responsible for the cell fusion. Indeed, this process could be induced by cross talk between these effectors as presented in several systems or by the activation of multiple downstream effectors as suggested here by the effects of TGF β signaling pathway antagonists on cell fusion. Interestingly, TGF β 1 has been shown to inhibit trophoblastic cell differentiation (25), whereas activin (24), a TGF β family member, has been described to stimulate the cell fusion process. In this work, activin-A was found to be differentially secreted between control and T21 mesenchymal cells. Activin, initially identified as a regulator of the biosynthesis and secretion of FSH by the anterior pituitary, has numerous biological roles in proliferation, differentiation, apoptosis, metabolism, homeostasis, immune function, wound repair, and endocrine functions (63, 64). Activin has also a critical role in human embryonic stem cell pluripotency and in endoderm differentiation (65). Activin-A signals are transmitted through two transmembrane serine/threonine kinase receptors, type I and type II activin receptors, in target cells (66). The type I receptor is phosphorylated and activated by type II receptor kinase. Activin-specific smads, Smad2 and -3, are phosphorylated by the activated type I receptor. In the nucleus, Smad2 and -3 complexes recruit additional

transcriptional activators and repressors to regulate target genes.

In the placenta, activin is produced by cytotrophoblast cells (67, 68), which also possess activin receptors (69) and therefore appear to be a major local regulator of placental development (70). Previous studies have shown that activin addition stimulates hCG and progesterone secretion by isolated cytotrophoblast cells in culture (71). In this study, we found that exogenous activin-A strongly stimulated the fusion of T21 cytotrophoblastic cells in culture. This effect was not specific to aneuploid trophoblastic cells, because it was also observed on control cytotrophoblasts isolated from second-trimester and term placentae (data not shown). Interestingly, CMC-CM accelerated the cell fusion process of control cytotrophoblasts, pointing to the presence in the cell medium of a fusogenic and paracrine compound produced by the mesenchymal cells. We used in this study the well-established biological model of defective fusion observed in T21 cytotrophoblastic cells to easily characterize and quantify the fusogenic effect of the mesenchymal cell-conditioned medium. The intensity of the activin-A stimulatory effect on T21 trophoblast fusion was similar to that of cAMP and biosynthetic hCG. However, the stimulation of trophoblast fusion by activin-A was not associated with an increase of either hCG or hPL secretion. These results conflicted with those of previous studies, possibly because we used biosynthetic activin-A and not purified activin from porcine origin (72) or because we used purified villous cytotrophoblasts and not a mixed population of trophoblastic cells (71). Moreover, follistatin inhibited the T21 cytotrophoblastic cell fusion induced by mesenchymal cell-conditioned medium, whereas follistatin had no effect in cell fusion by itself, pointing again to the potential role of activin-A as a mesenchymal paracrine factor involved in cytotrophoblastic cell fusion.

Activins are dimeric proteins comprising two β -subunits and containing a backbone of a cysteine-knot fold, with the monomers linked by a single covalent disulfide bond (63). Inhibin and activin share a common β -subunit, inhibin constituting a dimer of a related α -subunit linked to the β -subunit (73). Thus, regulation of α -subunit biosynthesis and dimerization with the β -subunit can alter activin biosynthesis in cells that synthesize both subunits, such as ovarian granulosa cells (74). We therefore checked for the presence of inhibin-A. The assays developed on the Access-System (Beckman) did not detect inhibin-A in control or T21MC-CM. Similarly, immunoblot of mesenchymal cell lysates detected no inhibin-A (data not shown).

In conclusion, this study highlights that trophoblast fusion, differentiation, and therefore regeneration depend on different signaling events arising from the mesenchy-

mal core of the villi. Interestingly, activin, which seems to play a major role in embryonic stem cell differentiation, appears from these *in vitro* studies to be a potential major regulator of trophoblast differentiation during the second trimester of pregnancy. The well-established model of T21 trophoblastic and placental mesenchymal cells should help to decipher the mechanisms of abnormal cell behavior in T21 as well as paracrine cross talk involved in placental development.

Acknowledgments

We thank Dr. Fanny Lewin for her support and the staff of the Saint Vincent de Paul, Port Royal, Robert Debré, and Beaujon Obstetrics Departments for providing us with placentae. We thank Fatima Ferreira for her expertise in trophoblastic cell cultures. We thank Dr. P. Chafey from the proteomic platform of the Institut Cochin and the use of the Typhoon 9400.

Address all correspondence and requests for reprints to: Guillaume Pidoux, Institut National de la Santé et de la Recherche Médicale Unité 767, 4 Avenue de l'Observatoire, 75006 Paris, France. E-mail: guillaume.pidoux@parisdescartes.fr.

This work was supported by Institut National de la Santé et de la Recherche Médicale and la Caisse d'Assurance Maladie des Professions Libérales Province. G.P. was supported by a fellowship from PremUP Foundation.

Disclosure Summary: The authors have nothing to disclose.

References

- Benirschke K, Kaufmann P 2000 Pathology of the human placenta. New York: Springer-Verlag
- Eaton B, Contractor S 1993 In vitro assessment of trophoblast receptors and placental transport mechanisms. In: Redman CW, Sargent IL, Starkey PM, eds. The human placenta. London: Blackwell Scientific; 471–503
- Ogren L, Talamantes F 1994 The placenta as an endocrine organ: polypeptides. In: Knobil E, Neill J, eds. Physiology of reproduction. New York: Raven Press; 875–945
- Kliman H, Nestler J, Sermasi E, Sanger J, Strauss 3rd J 1986 Purification, characterization, and *in vitro* differentiation of cytotrophoblasts from human term placentae. *Endocrinology* 118:1567–1582
- Frendo JL, Olivier D, Cheynet V, Blond JL, Bouton O, Vidaud M, Rabreau M, Evain-Brion D, Mallet F 2003 Direct involvement of HERV-W Env glycoprotein in human trophoblast cell fusion and differentiation. *Mol Cell Biol* 23:3566–3574
- Cronier L, Frendo JL, Defamie N, Pidoux G, Bertin G, Guibourdenche J, Pointis G, Malassiné A 2003 Requirement of gap junctional intercellular communication for human villous trophoblast differentiation. *Biol Reprod* 69:1472–1480
- Frendo J-L, Cronier L, Bertin G, Guibourdenche J, Vidaud M, Evain-Brion D, Malassiné A 2003 Involvement of connexin 43 in human trophoblast cell fusion and differentiation. *J Cell Sci* 116:3413–3421
- Malassiné A, Cronier L 2005 Involvement of gap junctions in placental functions and development. *Biochim Biophys Acta* 1719:117–124
- Pidoux G, Gerbaud P, Gniddehou S, Grynberg M, Geneau G, Guibourdenche J, Carette D, Cronier L, Evain-Brion D, Malassiné A, Frendo JL 2010 ZO-1 is involved in trophoblastic cells differentiation in human placenta. *Am J Physiol Cell Physiol* 298:C1517–C1526
- Adler RR, Ng AK, Rote NS 1995 Monoclonal antiphosphatidylserine antibody inhibits intercellular fusion of the choriocarcinoma line, JAR. *Biol Reprod* 53:905–910
- Getsios S, MacCalman CD 2003 Cadherin-11 modulates the terminal differentiation and fusion of human trophoblastic cells *in vitro*. *Dev Biol* 257:41–54
- Black S, Kadyrov M, Kaufmann P, Ugele B, Emans N, Huppertz B 2004 Syncytial fusion of human trophoblast depends on caspase 8. *Cell Death Differ* 11:90–98
- Dalton P, Christian HC, Redman CW, Sargent IL, Boyd CA 2007 Membrane trafficking of CD98 and its ligand galectin 3 in BeWo cells: implication for placental cell fusion. *FEBS J* 274:2715–2727
- Morrish DW, Kudo Y, Caniggia I, Cross J, Evain-Brion D, Gasperowicz M, Kokozidou M, Leisser C, Takahashi K, Yoshimatsu J 2007 Growth factors and trophoblast differentiation: workshop report. *Placenta* 28(Suppl A):S121–S124
- Frendo JL, Vidaud M, Guibourdenche J, Luton D, Muller F, Bellet D, Giovagranti Y, Tarrade A, Porquet D, Blot P, Evain-Brion D 2000 Defect of villous cytotrophoblast differentiation into syncytiotrophoblast in Down's syndrome. *J Clin Endocrinol Metab* 85:3700–3707
- Massin N, Frendo JL, Guibourdenche J, Luton D, Giovagranti Y, Muller F, Vidaud M, Evain-Brion D 2001 defect of syncytiotrophoblast formation and human chorionic gonadotropin expression in Down's syndrome. *Placenta* 22(Suppl A):S93–S97
- Frendo JL, Therond P, Guibourdenche J, Vidaud M, Evain-Brion D 2002 Implication of copper zinc superoxide dismutase (SOD-1) in human placenta development. *Ann NY Acad Sci* 973:297–301
- Frendo JL, Guibourdenche J, Pidoux G, Vidaud M, Luton D, Giovagranti Y, Porquet D, Muller F, Evain-Brion D 2004 Trophoblast production of a weakly bioactive human chorionic gonadotropin in trisomy 21-affected pregnancy. *J Clin Endocrinol Metab* 89:727–732
- Oberweiss D, Gillerot Y, Koulischer L, Hustin J, Philippe E 1983 [The placenta in trisomy in the last trimester of pregnancy]. *J Gynecol Obstet Biol Reprod (Paris)* 12:345–349 (French)
- Roberts L, Sebire NJ, Fowler D, Nicolaides KH 2000 Histomorphological features of chorionic villi at 10–14 weeks of gestation in trisomic and chromosomally normal pregnancies. *Placenta* 21:678–683
- Malassiné A, Frendo JL, Evain-Brion D 2010 Trisomy 21-affected placentas highlight prerequisite factors for human trophoblast fusion and differentiation. *Int J Dev Biol* 54:475–482
- Alsat E, Haziza J, Evain-Brion D 1993 Increase in epidermal growth factor receptor and its messenger ribonucleic acid levels with differentiation of human trophoblast cells in culture. *J Cell Physiol* 154:122–128
- Morrish DW, Bhardwaj D, Dabbagh LK, Marusyk H, Siy O 1987 Epidermal growth factor induces differentiation and secretion of human chorionic gonadotropin and placental lactogen in normal human placenta. *J Clin Endocrinol Metab* 65:1282–1290
- Song Y, Keelan J, France JT 1996 Activin-A stimulates, while transforming growth factor β 1 inhibits, chorionic gonadotrophin production and aromatase activity in cultured human placental trophoblasts. *Placenta* 17:603–610
- Morrish DW, Bhardwaj D, Paras MT 1991 Transforming growth factor β 1 inhibits placental differentiation and human chorionic gonadotropin and human placental lactogen secretion. *Endocrinology* 129:22–26
- Leisser C, Saleh L, Haider S, Husslein H, Sonderegger S, Knöfler M

- 2006 Tumour necrosis factor- α impairs chorionic gonadotrophin β -subunit expression and cell fusion of human villous cytotrophoblast. *Mol Hum Reprod* 12:601–609
27. Petraglia F, Gallinelli A, Grande A, Florio P, Ferrari S, Genazzani AR, Ling N, DePaolo LV 1994 Local production and action of follistatin in human placenta. *J Clin Endocrinol Metab* 78:205–210
 28. Caniggia I, Lye SJ, Cross JC 1997 Activin is a local regulator of human cytotrophoblast cell differentiation. Activin is a local regulator of human cytotrophoblast cell differentiation. *Endocrinology* 138:3976–3986
 29. Shi QJ, Lei ZM, Rao CV, Lin J 1993 Novel role of human chorionic gonadotropin in differentiation of human cytotrophoblasts. *Endocrinology* 132:1387–1395
 30. Pidoux G, Gerbaud P, Marpeau O, Guibourdenche J, Ferreira F, Badet J, Evain-Brion D, Frendo JL 2007 Human placental development is impaired by abnormal human chorionic gonadotropin signaling in trisomy 21 pregnancies. *Endocrinology* 148:5403–5413
 31. Pidoux G, Gerbaud P, Tsatsaris V, Marpeau O, Ferreira F, Meduri G, Guibourdenche J, Badet J, Evain-Brion D, Frendo JL 2007 Biochemical characterization and modulation of LH/CG-receptor during human trophoblast differentiation. *J Cell Physiol* 112:26–35
 32. Gudermann T, Birnbaumer M, Birnbaumer L 1992 Evidence for dual coupling of the murine luteinizing hormone receptor to adenylyl cyclase and phosphoinositide breakdown and Ca^{2+} mobilization. Studies with the cloned murine luteinizing hormone receptor expressed in L cells. *J Biol Chem* 267:4479–4488
 33. Hipkin RW, Sánchez-Yagüe J, Ascoli M 1992 Identification and characterization of a luteinizing hormone/chorionic (LH/CG) receptor precursor in a human kidney cell line stably transfected with the rat luteal LH/CG receptor complementary DNA. *Mol Endocrinol* 6:2210–2218
 34. Keryer G, Alsat E, Tasken K, Evain-Brion D 1998 Cyclic AMP-dependent protein kinases and human trophoblast cell differentiation in vitro. *J Cell Sci* 111:995–1004
 35. Aplin JD 2010 Developmental cell biology of human villous trophoblast: current research problems. *Int J Dev Biol* 54:323–329
 36. Lacey H, Haigh T, Westwood M, Aplin JD 2002 Mesenchymally-derived insulin-like growth factor 1 provides a paracrine stimulus for trophoblast migration. *BMC Dev Biol* 2:5
 37. Chen CP, Aplin JD 2003 Placental extracellular matrix: gene expression, deposition by placental fibroblasts and the effect of oxygen. *Placenta* 24:316–325
 38. Aplin JD, Jones CJ, Harris LK 2009 Adhesion molecules in human trophoblast: a review. I. Villous trophoblast. *Placenta* 30:293–298
 39. Brisset S, Aboura A, Audibert F, Costa JM, L'Herminé AC, Gautier V, Frydman R, Tachdjian G 2003 Discordant prenatal diagnosis of trisomy 21 due to mosaic structural rearrangements of chromosome 21. *Prenat Diagn* 23:461–469
 40. Frendo JL, Théron P, Bird T, Massin N, Muller F, Guibourdenche J, Luton D, Vidaud M, Anderson WB, Evain-Brion D 2001 Overexpression of copper zinc superoxide dismutase impairs human trophoblast cell fusion and differentiation. *Endocrinology* 142:3638–3648
 41. Freshney R 1987 Culture of animal cells: a manual of basic technique. New York.: Alan RI Liss
 42. Alsat E, Wyplosz P, Malassiné A, Guibourdenche J, Porquet D, Nessmann C, Evain-Brion D 1996 Hypoxia impairs cell fusion and differentiation process in human cytotrophoblast, in vitro. *J Cell Physiol* 168:346–353
 43. Honoré LH, Dill FJ, Poland BJ 1976 Placental morphology in spontaneous human abortions with normal and abnormal karyotypes. *Teratology* 14:151–166
 44. Geisler M, Kleinebrecht J 1978 Cytogenetic and histologic analyses of spontaneous abortions. *Hum Genet* 45:239–251
 45. Jauniaux E, Hustin J 1992 Histological examination of first trimester spontaneous abortions: the impact of materno-embryonic interface features. *Histopathology* 21:409–414
 46. van Lijnschoten G, Arends JW, Leffers P, De La Fuente AA, Van Der Looij HJ, Geraedts JP 1993 The value of histomorphological features of chorionic villi in early spontaneous abortion for the prediction of karyotype. *Histopathology* 22:557–563
 47. Salafia C, Maier D, Vogel C, Pezzullo J, Burns J, Silberman L 1993 Placental and decidual histology in spontaneous abortion: detailed description and correlations with chromosome number. *Obstet Gynecol* 82:295–303
 48. Genest DR, Roberts D, Boyd T, Bieber FR 1995 Fetoplacental histology as a predictor of karyotype: a controlled study of spontaneous first trimester abortions. *Hum Pathol* 26:201–209
 49. Silvestre E, Cusi V, Borrás M, Antich J 1996 Cytogenetic and morphologic findings in chorionic villi from spontaneous abortions. *Birth Defects Orig Artic Ser* 30:353–357
 50. Qureshi F, Jacques SM, Johnson MP, Hume RF Jr, Kramer RL, Yaron Y, Evans MI 1997 Trisomy 21 placentas: histopathological and immunohistochemical findings using proliferating cell nuclear antigen. *Fetal Diagn Ther* 12:210–215
 51. Pidoux G, Taskén K 2010 Specificity and spatial dynamics of PKA signaling organized by A kinase anchoring proteins. *J Mol Endocrinol* 44:271–284
 52. Yoshie M, Kaneyama K, Kusama K, Higuma C, Nishi H, Isaka K, Tamura K 2010 Possible role of the exchange protein directly activated by cyclic AMP (Epac) in the cyclic AMP-dependent functional differentiation and syncytialization of human placental BeWo cells. *Hum Reprod* 25:2229–2238
 53. Khan S, Katabuchi H, Araki M, Nishimura R, Okamura H 2000 Human villous macrophage-conditioned media enhance human trophoblast growth and differentiation in vitro. *Biol Reprod* 62:1075–1083
 54. Forbes K, Westwood M, Baker PN, Aplin JD 2008 Insulin-like growth factor I and II regulate the life cycle of trophoblast in the developing human placenta. *Am J Physiol Cell Physiol* 294:C1313–C1322
 55. Ahenkorah J, Hottor B, Byrne S, Bosio P, Ockleford CD 2009 Immunofluorescence confocal laser scanning microscopy and immuno-electron microscopic identification of keratins in human materno-foetal interaction zone. *J Cell Mol Med* 13:735–748
 56. Pavlov N, Hatzi E, Bassaglia Y, Frendo JL, Evain Brion D, Badet J 2003 Angiogenin distribution in human term placenta, and expression by cultured trophoblastic cells. *Angiogenesis* 6:317–330
 57. Knofler M, Simmons DG, Lash GE, Harris LK, Armant DR 2008 Regulation of trophoblast invasion: a workshop report. *Placenta* 29(Suppl A):S26–S28
 58. Hazane F, Valenti K, Sauvaigo S, Peinnequin A, Mouret C, Favier A, Beani JC 2005 Ageing effects on the expression of cell defence genes after UVA irradiation in human male cutaneous fibroblasts using cDNA arrays. *J Photochem Photobiol B* 79:171–190
 59. Cury PR, de Araújo VC, Canavez F, Furuse C, Leite KR, de Araújo NS 2007 The effect of epidermal growth factor on matrix metalloproteinases and tissue inhibitors of metalloproteinase gene expression in cultured human gingival fibroblasts. *Arch Oral Biol* 52:585–590
 60. Nah SS, Ha E, Mun SH, Won HJ, Chung JH 2008 Effects of melittin on the production of matrix metalloproteinase-1 and -3 in rheumatoid arthritic fibroblast-like synoviocytes. *J Pharmacol Sci* 106:162–166
 61. Hyytiäinen M, Penttinen C, Keski-Oja J 2004 Latent TGF- β binding proteins: extracellular matrix association and roles in TGF- β activation. *Crit Rev Clin Lab Sci* 41:233–264
 62. Conti A, Fabbrini F, D'Agostino P, Negri R, Greco D, Genesio R, D'Armiento M, Olla C, Paladini D, Zannini M, Nitsch L 2007 Altered expression of mitochondrial and extracellular matrix genes in the heart of human fetuses with chromosome 21 trisomy. *BMC Genomics* 8:268
 63. Xia Y, Schneyer AL 2009 The biology of activin: recent advances in structure, regulation and function. *J Endocrinol* 202:1–12

64. **Chen YG, Wang Q, Lin SL, Chang CD, Chuang J, Ying SY** 2006 Activin signaling and its role in regulation of cell proliferation, apoptosis, and carcinogenesis. *Exp Biol Med* (Maywood) 231:534–544
65. **Xu RH, Sampsel-Barron TL, Gu F, Root S, Peck RM, Pan G, Yu J, Antosiewicz-Bourget J, Tian S, Stewart R, Thomson JA** 2008 NANOG is a direct target of TGF β /activin-mediated SMAD signaling in human ESCs. *Cell Stem Cell* 3:196–206
66. **Harrison CA, Gray PC, Vale WW, Robertson DM** 2005 Antagonists of activin signaling: mechanisms and potential biological applications. *Trends Endocrinol Metab* 16:73–78
67. **Petraglia F, Woodruff TK, Botticelli G, Botticelli A, Genazzani AR, Mayo KE, Vale W** 1992 Gonadotropin-releasing hormone, inhibin, and activin in human placenta: evidence for a common cellular localization. *J Clin Endocrinol Metab* 74:1184–1188
68. **Debieve F, Pampfer S, Thomas K** 2000 Inhibin and activin production and subunit expression in human placental cells cultured in vitro. *Mol Hum Reprod* 6:743–749
69. **Schneider-Kolsky ME, Manuelpillai U, Waldron K, Dole A, Wallace EM** 2002 The distribution of activin and activin receptors in gestational tissues across human pregnancy and during labour. *Placenta* 23:294–302
70. **Natale DR, Hemberger M, Hughes M, Cross JC** 2009 Activin promotes differentiation of cultured mouse trophoblast stem cells towards a labyrinth cell fate. *Dev Biol* 335:120–131
71. **Steele GL, Currie WD, Yuen BH, Jia XC, Perlas E, Leung PC** 1993 Acute stimulation of human chorionic gonadotropin secretion by recombinant human activin-A in first trimester human trophoblast. *Endocrinology* 133:297–303
72. **Petraglia F, Vaughan J, Vale W** 1989 Inhibin and activin modulate the release of gonadotropin-releasing hormone, human chorionic gonadotropin, and progesterone from cultured human placental cells. *Proc Natl Acad Sci USA* 86:5114–5117
73. **Vale W, Rivier C, Hsueh A, Campen C, Meunier H, Bicsak T, Vaughan J, Corrigan A, Bardin W, Sawchenko P, Petraglia F, Yu J, Plotsky P, Spiess J, Rivier J** 1988 Chemical and biological characterization of the inhibin family of protein hormones. *Recent Prog Horm Res* 44:1–34
74. **Antenos M, Stemler M, Boime I, Woodruff TK** 2007 N-linked oligosaccharides direct the differential assembly and secretion of inhibin α - and β A-subunit dimers. *Mol Endocrinol* 21:1670–1684

Optic atrophy 1 is an A-kinase anchoring protein on lipid droplets that mediates adrenergic control of lipolysis

Guillaume Pidoux^{1,2,7,8}, Oliwia Witczak^{1,2,3,7},
Elisabeth Jarnæss^{1,2,9}, Linda Myrvold^{1,2,3,10},
Henning Urlaub^{4,5}, Anne Jorunn Stokka^{1,2},
Thomas Küntziger⁶ and Kjetil Taskén^{1,2,*}

¹Centre for Molecular Medicine Norway, Nordic EMBL Partnership, University of Oslo, Oslo, Norway, ²Biotechnology Centre, University of Oslo, Oslo, Norway, ³Faculty of Health Sciences, Oslo and Akershus University College of Applied Sciences, Oslo, Norway, ⁴Max Planck Institute for Biophysical Chemistry, Bioanalytical Mass Spectrometry Group, Göttingen, Germany ⁵Bioanalytics, Department of Clinical Chemistry, University Medical Center Göttingen, Göttingen, Germany and ⁶Institute of Basic Medical Sciences, University of Oslo, Oslo, Norway

Adrenergic stimulation of adipocytes yields a cAMP signal that activates protein kinase A (PKA). PKA phosphorylates perilipin, a protein localized on the surface of lipid droplets that serves as a gatekeeper to regulate access of lipases converting stored triglycerides to free fatty acids and glycerol in a phosphorylation-dependent manner. Here, we report a new function for optic atrophy 1 (OPA1), a protein known to regulate mitochondrial dynamics, as a dual-specificity A-kinase anchoring protein associated with lipid droplets. By a variety of protein interaction assays, immunoprecipitation and immunolocalization experiments, we show that OPA1 organizes a supramolecular complex containing both PKA and perilipin. Furthermore, by a combination of siRNA-mediated knockdown, reconstitution experiments using full-length OPA1 with or without the ability to bind PKA or truncated OPA1 fused to a lipid droplet targeting domain and cellular delivery of PKA anchoring disruptor peptides, we demonstrate that OPA1 targeting of PKA to lipid droplets is necessary for hormonal control of perilipin phosphorylation and lipolysis.

The EMBO Journal advance online publication, 7 October 2011; doi:10.1038/emboj.2011.365

Subject Categories: membranes & transport; cellular metabolism

Keywords: cAMP; cell signalling; lipolysis; OPA1; perilipin

Introduction

In the fed state, the normal physiological response of white adipose tissue (WAT) to insulin involves generation of triacylglycerol (TAG) from free, nonesterified fatty acids (FFA) and glycerol and storage of TAG in intracellular lipid droplets. Lipid droplets consist of a hydrophobic core of TAG, surrounded by a phospholipid and cholesterol monolayer to which numerous proteins are attached. In the fasting state, stimulation of β -adrenergic receptors (β -ARs) with catecholamines either through sympathetic nervous control (noradrenalin), or through hormonal stress responses (adrenalin) or triggering of glucagon receptors on adipocytes initiate a precisely regulated process of lipolysis, which liberates FFA and glycerol to be used as energy substrates by other tissues. The activation of lipolysis proceeds by generation of cAMP leading to activation of protein kinase A (PKA). Subsequently, PKA phosphorylates perilipin (PAT-family member perilipin 1, *PLIN1*; see Kimmel *et al*, 2009 for review of nomenclature), a protein localized on the surface of the TAG-containing lipid droplets. Perilipin serves as a gatekeeper that controls access of lipases to lipid droplets in a phosphorylation-dependent fashion (Fain and Garcija-Sainz, 1983; Greenberg *et al*, 1991, 1993; Blanchette-Mackie *et al*, 1995). In the absence of any stimulus, unphosphorylated perilipin on the surface of lipid droplets blocks access of lipases, thus protecting TAG from lipolysis. Upon phosphorylation, perilipin alters conformation allowing lipases to access lipid droplets and degrade TAG (Brasaemle *et al*, 2000b; Souza *et al*, 2002; Tansey *et al*, 2003). Hence, at times of stress, exercise or fasting, hormone-induced lipolysis is triggered by making lipid droplets accessible for lipases and liberated FFA serves as a fuel for the peripheral tissues of the body (such as the heart and skeletal muscle) (Londos *et al*, 1999; Brasaemle *et al*, 2000a). Furthermore, PKA phosphorylates hormone-sensitive lipase (HSL), which was the first substrate for PKA shown to be regulated in hormone-induced lipolysis. HSL was until recently thought to be the enzyme responsible for hydrolysis of stored TAG and to control the rate-limiting step in regulation of lipolysis (Fain and Garcija-Sainz, 1983). However, HSL null-mutant mice clearly demonstrated that HSL is dispensable as a substantial fraction of catecholamine-stimulated lipolysis as well as basal lipolysis remain unaffected (Osuga *et al*, 2000; Wang *et al*, 2001; Haemmerle *et al*, 2002). Even more recent studies have identified desnutrin/adipocyte triglyceride lipase (ATGL) as the most important enzyme for degradation of TAG (Zimmermann *et al*, 2003, 2004; Jenkins *et al*, 2004; Villena *et al*, 2004). TAG hydrolase (TGH) may also contribute to non-HSL TAG lipolysis (Soni *et al*, 2004). Desnutrin/ATGL and TGH are, however, not regulated by phosphorylation. Together with the fact that HSL is dispensable in catecholamine-stimulated lipolysis, these results point to the gatekeeper function of perilipin as an important regulatory mechanism. However, HSL appears

*Corresponding author. Centre for Molecular Medicine Norway, Nordic EMBL Partnership and Biotechnology Centre, University of Oslo, PO Box 1125, Blindern, 0317 Oslo, Norway. Tel.: +47 2284 0505; Fax: +47 2284 0506; E-mail: kjetil.tasken@biotek.uio.no

⁷These authors contributed equally to this work

⁸Present address: INSERM U767 and PremUp, Université Paris Descartes, Paris F-75006, France

⁹Present address: Axis-Shield ASA, Oslo, Norway

¹⁰Present address: Oslo University Hospital, Oslo, Norway

Received: 24 July 2011; accepted: 7 September 2011

to be the only enzyme degrading diacylglycerol to FFA and monoacylglycerol, which is then hydrolysed to FFA and glycerol by monoglyceride lipase, but these reactions proceed comparably faster than the TAG hydrolysis, which remains the rate-limiting step in the control of lipolysis (Giudicelli *et al*, 1974; Tornqvist and Belfrage, 1976; Fredrikson *et al*, 1986).

The localization of PKA holoenzyme within the cell is controlled by interactions between the regulatory (R) subunit dimer of PKA and A-kinase anchoring proteins (AKAPs) (Diviani and Scott, 2001; Michel and Scott, 2002; Tasken and Aandahl, 2004). AKAPs target pools of PKA type I and type II (distinguished by the type I or type II R subunit, RI or RII) to distinct subcellular loci and facilitate discrete spatial and temporal control of phosphorylation of specific substrates. They also scaffold supramolecular signalling complexes with multiple signalling enzymes. All AKAPs contain an A-kinase-binding (AKB) domain and a unique targeting domain directing the PKA–AKAP complex to defined subcellular structures, membranes or organelles (Carr *et al*, 1992; Wong and Scott, 2004; Gold *et al*, 2006; Kinderman *et al*, 2006; Pidoux and Tasken, 2010).

Some studies have suggested the presence of AKAPs associated with lipid droplets to trigger lipolysis by discrete control of perilipin phosphorylation (Zhang *et al*, 2005; Bridges *et al*, 2006). However, no AKAP targeting a pool of PKA to lipid droplets and controlling the induction of lipolysis via phosphorylation of perilipin has been identified to date. In this study, we show that the previously identified mitochondrial protein optic atrophy 1 (OPA1) also functions as a dual-specificity AKAP (binding both type I and type II PKA) associated with lipid droplets. Mutations in the *opa1* gene is the predominant cause of autosomal dominant optic atrophy, a progressive form of bilateral blindness caused by loss of retinal ganglion cells and atrophy of the optic nerve (Alexander *et al*, 2000; Delettre *et al*, 2000). Previous studies have shown OPA1 to be a dynamin-related GTPase required for mitochondrial fusion, and regulation of apoptosis and localized both on the inner membrane of mitochondria and on cristae (Sesaki *et al*, 2003; Cipolat *et al*, 2004; Frezza *et al*, 2006; Ishihara *et al*, 2006). Here, we report the presence of OPA1 in adipocytes, where it is associated with both mitochondria and lipid droplets. We find that OPA1 forms a complex with PKA and perilipin on lipid droplets. Finally, we assign a new function to OPA1 by showing that it is involved in the control of lipolysis in response to adrenergic stimuli by anchoring a pool of PKA that phosphorylates perilipin and thereby triggers lipolysis.

Results

OPA1 is an AKAP associated with lipid droplets

To assess the effect of PKA anchoring in adrenergic regulation of lipolysis, 3T3-L1 cells were differentiated into adipocytes and transfected with constructs directing expression of a HA-tagged soluble fragment of AKAP-Lbc encompassing the PKA-binding site (Ht31 anchoring disruptor) or the corresponding control construct with proline substitutions (Ht31-P) that does not bind PKA (Ct in Figure 1A). Subsequently, transfected cells were stimulated with isoproterenol to activate PKA and perilipin phosphorylation status examined in immunoprecipitates from total cell extracts using an

anti-RRXpS/T antibody detecting phosphorylated PKA substrates (Figure 1A). While isoproterenol-induced perilipin phosphorylation was observed in Ht31-P-transfected cells, expression of the Ht31 anchoring disruptor abolished phosphorylation without affecting the level of immunoprecipitated perilipin. This suggests that an AKAP targets PKA to facilitate discrete adrenergic control of perilipin phosphorylation. In search of an AKAP for perilipin, lipid droplets were purified by sucrose gradient fractionation of lysates from differentiated 3T3-L1 adipocytes and lipid droplet protein extracts submitted to overlay with radiolabelled RII in the absence and presence of Ht31 anchoring disruptor peptide (Figure 1B). Five bands with molecular masses of ~110, 90, 75, 50 and 40 kDa detected by RII-overlay and competed by Ht31 peptide appeared to be enriched in lipid droplets compared with cell lysates from 3T3-L1 cells. Proteins in the regions of corresponding mobility from parallel lanes in the gel were excised, subjected to tryptic digestion and analysed by mass spectrometry (Supplementary Table S1).

Curation of lists of identified proteins from several experiments and bioinformatic analysis to identify proteins with putative PKA-binding sites resulted in a list of nine AKAP candidates. Libraries of overlapping peptides covering the putative PKA-binding sites of the candidates were synthesized on solid phase and subjected to RII-overlay in the absence and presence of Ht31 peptide (Figure 1C). The amphipathic helix AKB from AKAP-KL was included as a positive control. This analysis identified a sequence in the C-terminal part of a protein called OPA1 that bound RII in an Ht31-dependent manner. This suggests that OPA1 is a putative AKAP and that, in addition to its mitochondrial localization, OPA1 can also be associated with lipid droplets in adipocytes. To confirm and extend these results, the C-terminal part of the OPA1 sequence mapped in Figure 1C was synthesized as 19 mer overlapping peptides with 1-amino-acid offset on solid phase and analysed for PKA binding by RI- and RII-overlay with or without Ht31. This identified a sequence binding both RI and RII in the C-terminal part of OPA1 (amino acids 940–958; Figure 1D). Modelling the sequence of amino acids 940–958 in OPA1 as an α -helix in a helical wheel configuration suggested that the AKB sequence is an amphipathic helix with one clearly defined hydrophobic face and a negatively charged polar face, which is characteristic of AKB regions in AKAPs (Figure 1E, left). Furthermore, proline substitutions in the sequence (V942P, I945P, L949P; peptide OPA1 940–958-3P) that distort the α -helical configuration abolished binding to PKA (Figure 1E, right).

We have previously developed an amplified luminescence ligand proximity assay (AlphaScreen) based on RI binding to D-AKAP1 that can be used to characterize AKB regions in AKAPs as competitors (Stokka *et al*, 2006; Jarnaess *et al*, 2008). Since OPA1 appeared to bind both RI and RII, we used this RI competition binding platform to evaluate the binding properties of OPA1. As shown in Figure 1F, a peptide corresponding to amino acids 940–958 in OPA1 as well as Ht31 competed RI binding to D-AKAP1 with IC_{50} -values of 8.1 ± 0.13 and $9.5 \pm 0.16 \mu\text{M}$, respectively, in line with earlier observations with RI using this assay (Jarnaess *et al*, 2008). In contrast, the OPA1 940–958-3P control peptide was not able to compete the D-AKAP-RI interaction confirming the observation in Figure 1E. Taken together, our results suggest

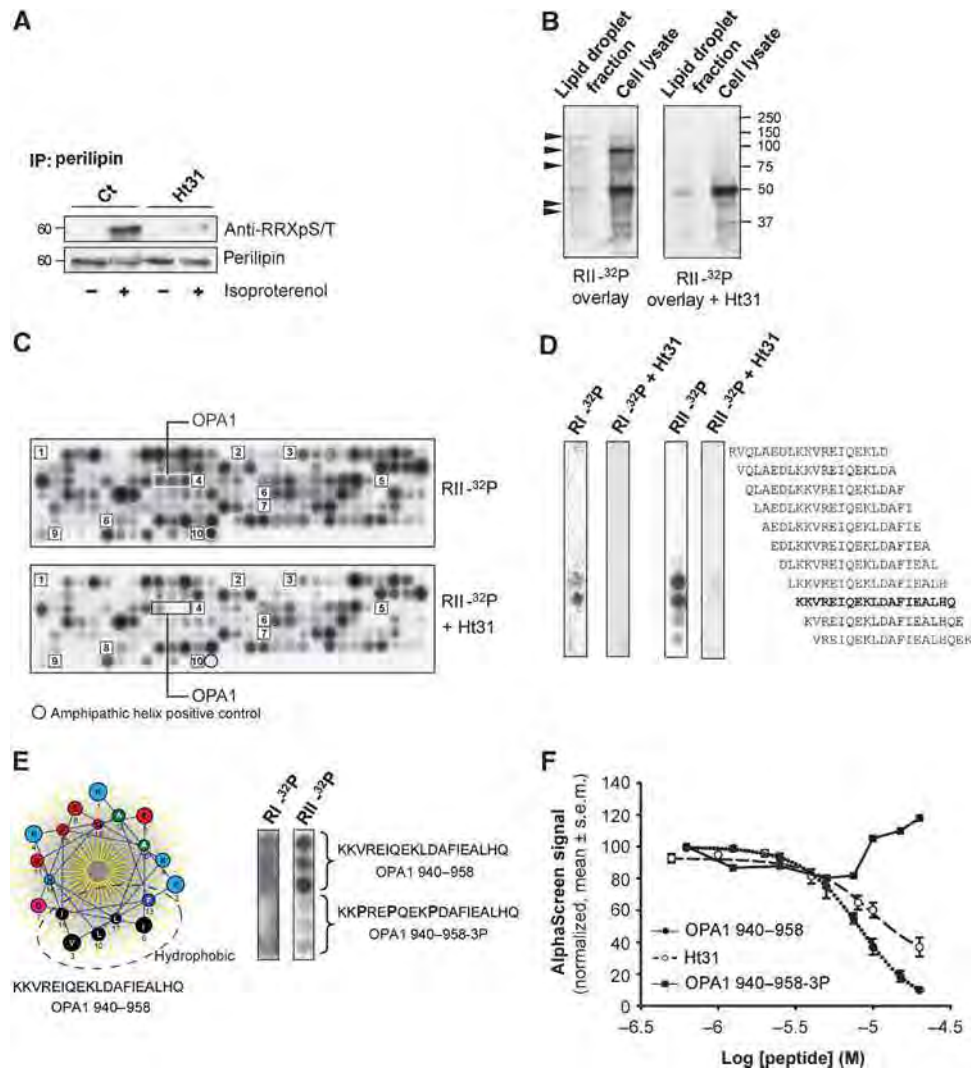


Figure 1 OPA1 is an AKAP associated with lipid droplets. (A) Perilipin was immunoprecipitated from extracts of 3T3-L1 fibroblasts differentiated into adipocytes, transfected with a mammalian expression vector encoding Ht31 or Ht31-P (Ct), and stimulated with or without isoproterenol (+, -). Perilipin phosphorylation status was assessed by immunoblotting for phosphorylated PKA substrates (anti-RRXpS/T antibody) and perilipin. (B) Purified lipid droplets and total cell lysates from 3T3-L1 adipocytes were subjected to a solid phase binding assay using ³²P-radiolabelled RII (RII-overlay) as a probe in the absence (left panel) or presence (right panel) of the Ht31 anchoring disruptor peptide (500 nM). Arrows indicate regions with putative AKAPs, which were excised from parallel lanes, and analysed by mass spectrometry. (C) Relevant parts of the sequences of putative AKAPs identified by mass spectrometry were printed on solid phase as overlapping 20 mer peptides (3 amino acid offset) and subjected to RII-overlay in the absence (upper panel) or presence (lower panel) of Ht31 (500 nM). Putative AKAP sequences as identified by numbers on the array are (Swissprot database entry in parenthesis): 1, Dip2b (Q3UH60); 2, Matrin3 (Q9ROU5); 3, OPA1 (P58281); 4, LONP (Q8CGK3); 5, LETM1 (Q9Z210); 6, Hsp90b1 (P08113); 7, importin subunit β 1 (P70168); 8, unknown protein product; 9, nuclear myosin 1 β (Q9ERB6); 10, AKAP-KL amphipathic helix (positive control). (D) RI- or RII-overlay in the absence or presence of Ht31 anchoring disruptor peptide (500 nM) of array of immobilized OPA1 19 mer peptides (1 amino acid offset). Bold sequence: PKA-R-binding region in OPA1. (E) α -Helical wheel representation of the PKA-R binding sequence contained within amino acids 940-958 of OPA1 (left). Dashed line indicates a hydrophobic region. R-overlays of the immobilized OPA1 940-958 substituted sequence with three prolines introduced (OPA1 940-958-3P) (right). (F) Concentration-dependent competition of RI α interaction with GST-D-AKAP1 (20 nM each) by OPA1 940-958 (●), HT31 (○) and OPA1 940-958-3P (■) peptides in a ligand proximity assay (AlphaScreen). Data represent mean \pm s.e.m. of three independent experiments performed in duplicate. Figure source data can be found in Supplementary data.

that OPA1 is an AKAP with a PKA-binding domain encompassing amino acids 940-958 in the C-terminal part of the protein that can bind both RI and RII.

Kinetics of the OPA1-PKA interaction

We next determined the rate and affinity constants of the OPA1-PKA association. Real-time analyses were carried out by surface plasmon resonance (SPR) technology (Figure 2). Specifically, cAMP-free RI and RII were immobilized on the surface of a CM5 sensor chip coated with 8-AHA-cAMP and a

purified, MBP-fused full-length OPA1 protein (containing the AKB region) was injected over the surfaces. The sensorgrams of MBP-OPA1 binding to RI and RII loaded surfaces (Figure 2A and C, respectively) as well as the corresponding steady-state binding isotherms (Figure 2B and D) clearly demonstrated a concentration-dependent binding with nanomolar affinities for both RI ($K_D = 12.5 \pm 2.8$ nM) and RII ($K_D = 14.0 \pm 1.4$ nM) and with K_D -values consistently somewhat lower for RI than for RII in all experiments. Furthermore, in contrast to observations made with other

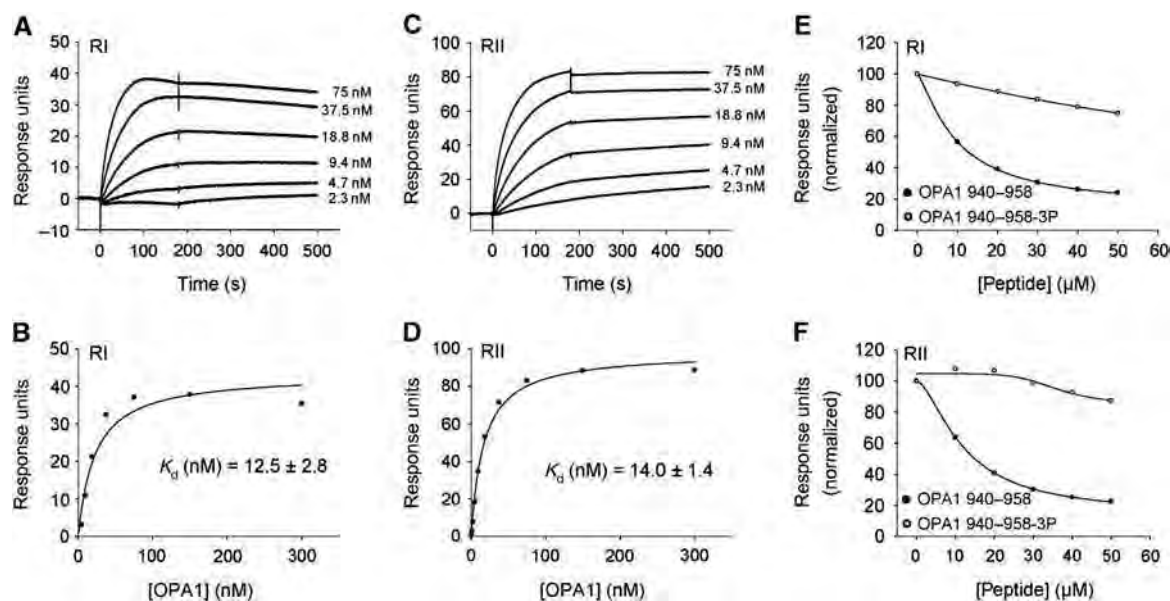


Figure 2 Studies of the OPA1-RI and OPA1-RII interaction. (A, C) SPR studies of the MBP-OPA1 binding to immobilized PKA-RI (A) or PKA-RII (C) on a sensor chip coated with 8-aminohexylamino-cAMP. MBP-OPA1 at concentrations indicated was injected for 180 s and the dissociation phase was monitored for 300 s. The graphs are representative of three independent experiments performed on different sensor surfaces. (B, D) Steady-state binding of the increasing MBP-OPA1 concentrations obtained from (A, C). The affinity constant was derived assuming a 1:1 binding in a Langmuir model using a global fit analyses algorithm provided in the BIACore T100 evaluation software. (E, F) Qualitative surface competition experiments with the OPA1 940-958 peptide. In all, 75 nM MBP-OPA1 was injected on a surface with captured PKA-RI (E) or PKA-RII (F) in the presence or absence of increasing concentrations (10–50 μ M) of the OPA1 940-958 or the OPA1 940-958-3P peptide. Both peptides were also injected without AKAP present and the binding response obtained in the absence of an AKAP present were subtracted in the graph shown. The graphs show one representative experiment of three independent experiments performed on different sensor surfaces.

RI-binding AKAPs, which typically display a faster off-rate for RI, the on- and off-rates of RI and RII binding to OPA1 were similar (RI: $K_a = 6.6 \times 10^5$ /M/s, $K_d = 3.7 \times 10^{-4}$ /s; RII: $K_a = 1.1 \times 10^6$ /M/s, $K_d = 4.4 \times 10^{-4}$ /s). Binding of MBP-OPA1 to RI and RII was displaced in the presence of increasing concentrations (10–50 μ M) of the OPA1 940-958 peptide characterized in Figure 1F (Figure 2E and F), whereas no displacement was observed with the proline-substituted OPA1 940-958-3P peptide. These results suggest that OPA1 may be a true dual-specificity AKAP.

OPA1 and PKA colocalize on lipid droplets in 3T3-L1 adipocytes

OPA1 expression in brown adipose tissue (BAT) and WAT, liver, muscle and 3T3-L1 adipocytes was analysed by immunoblotting (Figure 3A). This showed high levels of expression of three different forms in BAT and 3T3-L1 adipocytes whereas only the high and low molecular weight isoforms were detected at lower levels of expression in WAT. Liver and muscle also expressed OPA1 isoforms of different mobility. In contrast, perilipin was only expressed in adipose tissue and 3T3-L1 adipocytes. The level of expression of OPA1 could relate to the number of mitochondria, for example, in BAT versus WAT as OPA1 is previously reported to be localized in mitochondria.

The expression of OPA1 was next analysed during differentiation of 3T3-L1 preadipocytes into adipocytes (Figure 3B). Whereas the expression of the different R isoforms RI α , RII β remained constant during the differentiation process, the expression of OPA1 was upregulated somewhat prior to or concomitantly with the appearance of perilipin, which could indicate regulation of OPA1 during

adipocyte development by transcription factors such as PPAR γ to match that of other lipid droplet proteins. In contrast, mitochondrial proteins such as mitofusin 2 were not regulated with the same kinetics or amplitude, suggesting that the observed regulation of OPA1 is not just a function of an increase in the number of mitochondria.

The subcellular localization of OPA1 versus perilipin and PKA in adipocytes was analysed by dual-immunofluorescent labelling followed by laser confocal analysis and the extent of overlap was measured using line plot profile and intensity correlation coefficient-based analysis (Bolte and Cordelieres, 2006). OPA1 showed extensive colocalization with perilipin on lipid droplets (Figure 3C–E'; $R = 0.91$). Moreover, studies of the localization of PKA type I (RI α) and type II (RII β) in 3T3-L1 adipocytes demonstrated RI α to have strong colocalization with perilipin on the surface of lipid droplets (Figure 3F–H'; $R = 0.85$). In contrast, RII β appeared more localized in the cytoplasm and showed only partial overlap with perilipin on lipid droplets (Figure 3I–K'; $R = 0.67$). In agreement with previous studies, the localization of HSL was found to be mainly in the cytoplasm, but showed also some extent of colocalization with perilipin on lipid droplets (Figure 3L–N'; $R = 0.76$) (Londos *et al*, 1999; Brasaemle *et al*, 2000a).

To explore the possibility of a direct physical interaction between OPA1 and RI α on lipid droplets, we next solubilized the lipid droplet protein content of differentiated 3T3-L1 cells in a buffer containing detergent and *N*-octyl- β -D-glucoside. Immunoprecipitation of OPA1 revealed the presence of both perilipin and OPA1 in the precipitate (Figure 4A). The reverse immunoprecipitation experiment using a perilipin antibody likewise showed coprecipitation of OPA1 (Figure 4B). Interestingly, immunoprecipitation of RI α coprecipitated

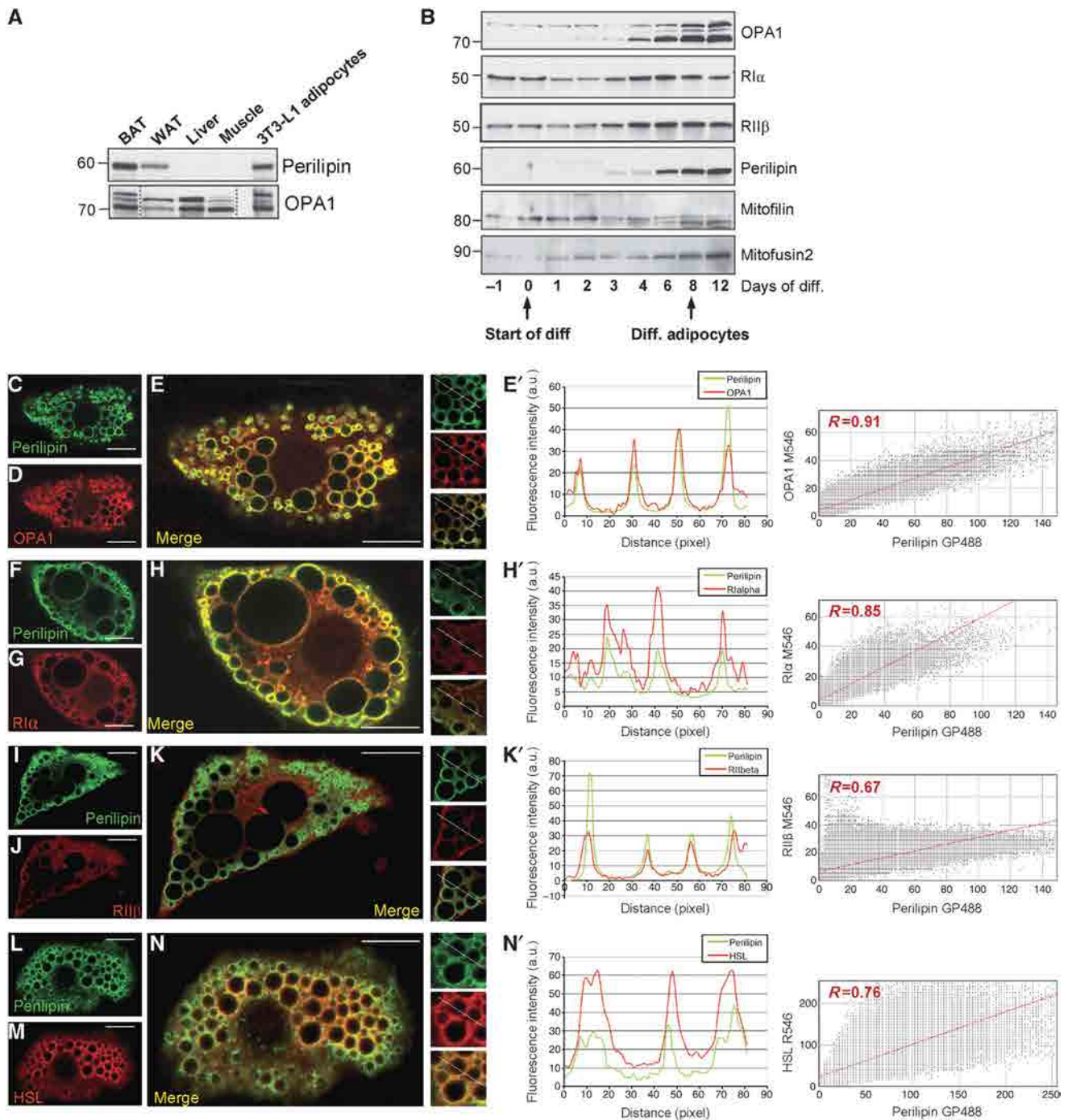


Figure 3 OPA1 is expressed in adipocytes and colocalizes with RI α on lipid droplets. (A) Distribution of OPA1 and perilipin in indicated mouse tissues and 3T3-L1 adipocytes by immunoblotting. Dotted lines indicate that an area between the displayed lanes was removed. Shown lanes are from a single gel and exposure. (B) Expression of OPA1, RI α , RII β , perilipin, mitofilin and mitofusin 2 during the differentiation of 3T3-L1 into adipocytes by immunoblotting. (C–N') 3T3-L1 adipocytes were immunostained for perilipin (green; C, F, I, L) in combination with OPA1 (red; D), RI α (red; G), RII β (red; J) and HSL (red; M). Merged pictures are shown in (E, H, K, N), respectively. Line plot and correlation analysis of colocalization of perilipin with OPA1 (E'), RI α (H'), RII β (K') and HSL (N') are also shown. Plot profiles (middle) show for both channels the variation in fluorescence intensity along line indicated in white in detailed area. Scatter plots (right) show pixel distribution whereby the intensities of a given pixel in the green and red images correspond to the x- and y-coordinate, respectively. Correlation coefficients (R) of overlaps are indicated. Scale bar: 20 μ m. Figure source data can be found in Supplementary data.

OPA1 (Figure 4C) and conversely, RI α was detected in OPA1 immunoprecipitates (Figure 4D). In contrast, RII β could not be coprecipitated with OPA1 from 3T3-L1 cells (not shown), indicating either that it does not bind in the presence of RI or that the fraction associated with OPA1 is below the level of

detection. Moreover, HSL and phospho-HSL were not detected after immunoprecipitation of OPA1 in adipocytes (Figure 4E). Together, our results indicate that OPA1 forms a complex with perilipin and RI α on lipid droplets in 3T3-L1 adipocytes.

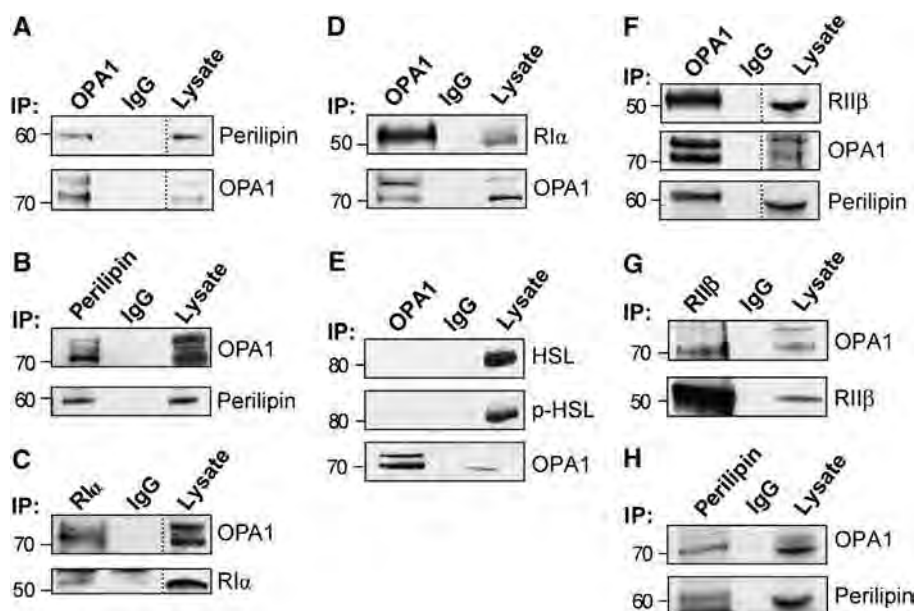


Figure 4 OPA1 organizes a supramolecular complex containing PKA and perilipin. (A–C) Lysates from 3T3-L1 adipocytes were subjected to immunoprecipitation with OPA1 antibody (A, D, E), perilipin (B) and RI α (C). Immunoprecipitates and corresponding lysates were analysed by immunoblotting for the presence of the indicated proteins. (F, G, H) Lysates from mouse WAT were subjected to immunoprecipitation with OPA1 (F), RII β (G) or perilipin (H) antibodies and analysed for the presence of OPA1, RII β and perilipin by immunoblotting. Dotted lines indicate lanes combined from a single gel and exposure. Figure source data can be found in Supplementary data.

While 3T3-L1 adipocytes appear to have an abundance of PKA type I and RI is associated with OPA1, WAT from wild-type mice has been reported to contain mainly PKA type II that regulates lipolysis and with RII β being the predominant RII subunit (Cummings *et al*, 1996; Cederberg *et al*, 2001). Therefore, we also examined the pool of PKA associated with OPA1 in total protein extracts from WAT. Here, we found that RII (Figure 4F and G) and not RI (not shown) coimmunoprecipitated with OPA1 and *vice versa*, which is compatible with the notion of OPA1 as a dual-specificity AKAP where the association with type I or type II PKA is determined by the availability of the two isozymes. Furthermore, OPA1 forms a complex with perilipin also in WAT (Figure 4F and H).

OPA1 distribution between lipid droplets and mitochondria

As reports on OPA1 localization and function in cells without lipid droplets describe a mitochondria-associated protein involved in mitochondrial fusion (Cipolat *et al*, 2004; Ishihara *et al*, 2006), it was important to examine the distribution of OPA1 between lipid droplets and mitochondria in adipocytes. Immunostaining of 3T3-L1 adipocytes with perilipin as a marker of lipid droplets was performed together with transfection of the targeting domain of the MDDX28 helicase tagged with the fluorescent protein mCherry (construct Δ MDDX28mCherry) as a marker of the inner mitochondrial membrane, or with immunostaining for mitofusin 2 as a marker of the outer mitochondrial membrane. Laser confocal analysis and intensity correlation coefficient-based analysis revealed little overlap between the lipid droplet marker and mitochondrial markers (Figure 5A–F; Supplementary Figure S1A and B; $R=0.22$ and 0.43 , respectively). In contrast, transfection of 3T3-L1 adipocytes with a construct directing the expression of the full-length OPA1 tagged with green fluorescent protein (GFP-FL-OPA1[#]) showed specific import

of the tagged OPA1 to lipid droplets as evident from a strong overlap with perilipin immunostaining as a marker for lipid droplets (Figure 5G–I; Supplementary Figure S1C; $R=0.89$), whereas comparably lower intensity signals were detected over mitochondria. This, together with the extensive colocalization of endogenous OPA1 with perilipin (Figure 3C–E; $R=0.91$) strongly suggest that OPA1 distribution in adipocytes is not strictly limited to mitochondria and that the main fraction is targeted to lipid droplets together with perilipin.

To determine in more detail the distribution of OPA1 between mitochondria and lipid droplets in adipocytes, post-nuclear supernatants were fractionated by sucrose gradient centrifugation to separate light components with high lipid content such as liposomes from cytoplasm and organelles with comparably higher density. Immunoblotting of the resulting fractions (Figure 5J) and quantification by densitometry of the relative distribution from several experiments (Figure 5K) showed perilipin exclusively in fraction 1 corresponding to the lipid droplet position in the density gradient. In contrast, mitochondrial markers for the inner membrane (mitofilin), outer membrane (mitofusin 2) and mitochondrial matrix (pyruvate dehydrogenase E1 β subunit) were mainly localized in the bottom fractions, although 10% of mitofilin, 5% of mitofusin 2 and 4% of pyruvate dehydrogenase E1 β subunit were also found in the top fraction. These mitochondrial contaminations observed in the lipid droplets fraction could represent mitochondrial membranes from ruptured mitochondria or possibly intact mitochondria weakly associated with lipid droplets. Interestingly, although OPA1 is reported to be a mitochondrial protein in other cell types, its distribution in 3T3-L1 adipocytes with >80% in the top fractions and <20% in the bottom fractions is distinctly different from the distribution of the mitochondrial markers in the same experiments. Altogether our results strongly suggest that a significant portion of OPA1 is associated with

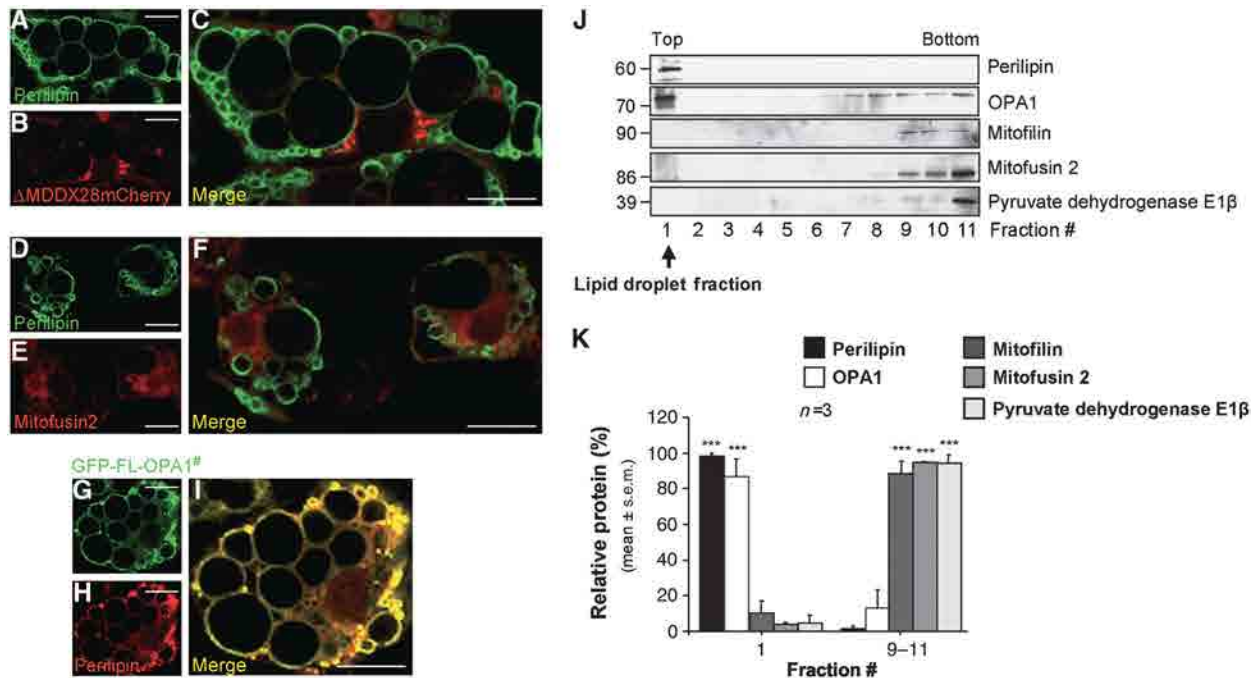


Figure 5 OPA1 distribution between lipid droplets and mitochondria. (A–I) 3T3-L1 adipocytes were untransfected (D–F) or transfected with mitochondrial marker Δ MDDX28mCherry (red; B) or GFP-OPA1 (green; G) and subsequently immunostained for perilipin (green; A, D and red; H) alone or in combination with mitofusin2 antibody (red; E). Corresponding merged pictures are shown in (C, F, I). Scale bar: 20 μ m. (J) Lipid droplets were purified from 3T3-L1 adipocytes by sucrose gradient centrifugation. Fractions were examined by immunoblotting for distribution of perilipin, OPA1, mitofilin (mitochondrial inner membrane marker), mitofusin 2 (mitochondrial outer membrane marker) or pyruvate dehydrogenase E1 β subunit (mitochondrial matrix marker). Arrow indicates the mobility of the lipid droplet fraction in the sucrose gradient. One representative experiment of three is shown. (K) Relative distribution of the perilipin, OPA1, mitofilin, mitofusin2 and pyruvate dehydrogenase E1 β subunit in fraction 1 (lipid droplet fraction) versus fractions 9–11 (mitochondria). Results are expressed as the mean \pm s.e.m. of $n = 3$ independent experiments ($***P < 0.001$). Figure source data can be found in Supplementary data.

the lipid droplet fraction in a mitochondria-independent manner. Furthermore, we also observed a strong colocalization between lipid droplets (perilipin immunolabelling) and GFP-FL-OPA1 (Figure 5G and H; Supplementary Figures S1C and S2A–C') and GFP-FL-OPA1 with three proline substitutions (V942P, I945P, L949P) inside the AKB domain (GFP-OPA1[#] AKBmut) (Supplementary Figure S2D–F'). In addition, deletion of the OPA1 mitochondrial targeting sequence (amino acids 1–87; Δ MTS) as defined in several reports (Misaka *et al*, 2002; Olichon *et al*, 2002; Satoh *et al*, 2003; Kita *et al*, 2009) or deletion of the 30 first critical amino acids of the MTS (Δ 1–30) abolish targeting of OPA1 to lipid droplets as well as mitochondria (Supplementary Figure S2G–P'). Furthermore, deletion of the 57 last amino acids of the MTS (Δ 30–87) also reduced targeting of OPA1 to both lipid droplets and mitochondria, although to a greater extent for the mitochondrial localization (Supplementary Figure S2Q–V'; $R = 0.48$ versus $R = 0.26$). These observations suggest that the MTS in OPA1 is important for the targeting of OPA1 also to lipid droplets and that an independent lipid droplet targeting sequence cannot readily be defined.

OPA1 is implicated in the adrenergic control of lipolysis

To address the function of OPA1 as a putative AKAP for perilipin, we employed a combined strategy of RNA interference and rescue with wild-type or modified forms of OPA1 and examined the effect on adrenergic regulation of lipolysis. First, 3T3-L1 adipocytes were transfected with specific OPA1 siRNA or scrambled control, incubated for 24 h, retransfected

with OPA1 siRNA and incubated for another 48 h. As shown by immunoblot analysis (Figure 6A), siRNA-mediated knockdown of OPA1 markedly reduced OPA1 protein level by $\sim 85\%$ after 48–72 h of culture compared with cells transfected with scrambled siRNA ($P < 0.025$, $n = 3$, see also Supplementary Figure S3A). No difference was seen between control-transfected and untransfected cells, indicating that the method of transfection did not interfere with OPA1 expression nor was it toxic to the differentiated adipocytes. The expression of $R1\alpha$, $R11\beta$ and HSL remained constant in cells that received OPA1 siRNA, indicating that removal of OPA1 does not affect other components of the PKA signalling pathway. Interestingly, perilipin expression was significantly reduced after siRNA-mediated knockdown of OPA1 by up to 75% at 48 h and 55% at 72 h post-transfection (Supplementary Figure S3B; $P < 0.05$). The effect of OPA1 knockdown on perilipin expression may indicate that OPA1 and perilipin interact to stabilize each other and that loss of perilipin expression could result from destabilization of a supramolecular complex. Interestingly, expression of the PAT-family protein ADRP (perilipin 2), but not TIP47 (perilipin 3), appeared to increase two- to three-fold at 48 h, maybe as a rescue mechanism for perilipin downregulation to help preserve lipid droplets (Supplementary Figure S4).

Knockdown of OPA1 protein expression was associated with a significant decrease in isoproterenol-induced glycerol release from 3T3-L1 adipocytes with little adrenergic induction of lipolysis and a 60% reduction in glycerol release compared with scrambled control at 5 or 10 nM isoproterenol

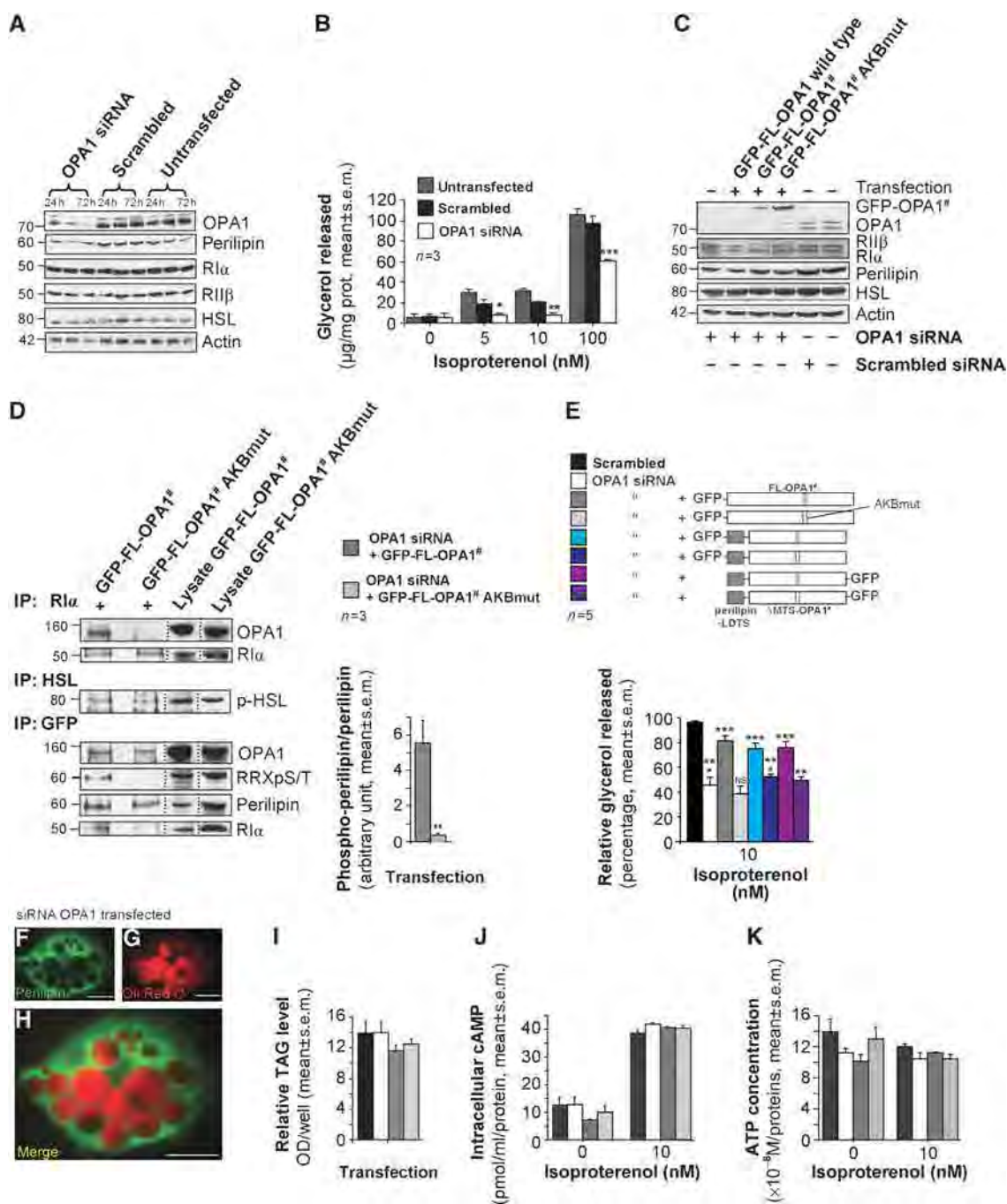


Figure 6 OPA1 is involved in the adrenergic control of lipolysis. (A) Immunoblot analysis of OPA1, perilipin, RI α , RII β , HSL and actin levels in 3T3-L1 adipocytes transfected with OPA1 siRNA or scrambled control after 24, 48 or 72 h of culture. (B) Glycerol release from 3T3-L1 adipocytes after siRNA transfection and stimulation with isoproterenol (5, 10 and 100 nM) for 2 h. (C) Detection by immunoblot of OPA1, GFP-FL-OPA1, perilipin, RI α , RII β , HSL and actin in 3T3-L1 adipocytes transfected with OPA1-specific siRNA or scrambled control and retransfected with wild-type OPA1-FL-GFP, siRNA-insensitive OPA1-FL-GFP (GFP-FL-OPA1^{WT}) or siRNA-insensitive OPA1-GFP 940-958-3P (GFP-FL-OPA1^{AKBmut}) plasmids, after 72 h of culture. (D; left panel) Lysates from 3T3-L1 adipocytes incubated with OPA1 siRNA and GFP-FL-OPA1^{WT} plasmid or GFP-FL-OPA1^{AKBmut} were subjected to immunoprecipitation with RI α , HSL or GFP antibodies. Lysate and precipitate were analysed for the presence of OPA1, RI α , perilipin, phospho-perilipin (PKA substrate antibody (anti-RRXpS/T)) and phospho-HSL. Dotted lines indicate lanes combined from a single gel and exposure. (D; right panel) The histogram shows levels of phosphorylated perilipin quantified by densitometry relative to total perilipin levels. (E) Amount of glycerol released in the media (percent of maximal) of 3T3-L1 adipocytes during 2 h of stimulation by 10 nM isoproterenol after transfection and incubation with OPA1 siRNA and GFP-FL-OPA1^{WT}, GFP-FL-OPA1^{AKBmut} or LDTs- Δ MTS-OPA1 chimeric expression vectors for 72 h. (Top) Schematic depiction of constructs. Open box: OPA1 full-length (FL-OPA1^{WT}) or deleted of the MTS (Δ MTS-OPA1^{WT}); light grey/dotted box: functional or mutated AKB domain (940-958-3P; AKBmut); dark grey box: perilipin lipid droplet targeting sequence (perilipin-LTDS). (F-H) 3T3-L1 adipocytes were immunostained for perilipin after OPA1 siRNA transfection (green; F) in combination with Oil Red O (marker of TAG; red; G). (H) Merged picture. Scale bar: 20 μ m. (I) Intracellular TAG content, (J) intracellular cAMP content and (K) intracellular ATP concentration of 3T3-L1 adipocytes 3 days after incubation with OPA1 siRNA and GFP-FL-OPA1^{WT} plasmid or GFP-FL-OPA1^{AKBmut} plasmid. Results represent mean \pm s.e.m. of $n = 3$ independent experiments except for (E) where $n = 5$ (** $P < 0.01$; *** $P < 0.001$; * $P < 0.05$ and NS, not significant). Figure source data can be found in Supplementary data.

(Figure 6B). The inhibition of isoproterenol-induced lipolysis by OPA1 knockdown was partially overcome at 100 nM where only 37% inhibition compared with control was observed probably because the high cAMP activates PKA over longer distances inside the cell reducing the requirement for AKAP targeting. For this reason, further studies of the effect of manipulation of OPA1 levels on lipolysis were conducted at concentrations around EC_{50} (10–30 nM). To rescue cells with OPA1 knockdown, 3T3-L1 adipocytes were first transfected with OPA1 siRNA to remove endogenous OPA1. This was followed by transfection with mammalian expression vectors encoding wild-type full-length OPA1 fused to green fluorescent protein (GFP-FL-OPA1), GFP-OPA1 made insensitive to functional siRNA (GFP-FL-OPA1[#]) or GFP-FL-OPA1[#] with three proline substitutions (V942P, I945P, L949P) inside the AKB domain (GFP-FL-OPA1[#] AKBmut), which should abolish binding of both type I and type II PKA as shown in Figures 1E and F and 2E and F. Whereas cells transfected with an expression vector directing the transcription of an siRNA-sensitive OPA1 did not regain OPA1 expression, adipocytes transfected with vectors directing the expression of siRNA-insensitive GFP-FL-OPA1[#] or GFP-FL-OPA1[#] AKBmut presented expression of a GFP-FL-OPA1 fusion protein (Figure 6C). Furthermore, colocalization with lipid droplets was confirmed for both these constructs by perilipin immunofluorescent labelling (Figure 5G–I; Supplementary Figures S1C and S2D–F'). While the expression of RI α , RIIB and HSL remained constant, the expression of perilipin was also found to be decreased in cells transfected with OPA1 siRNA (75% reduction) as previously observed in Figure 6A and in Supplementary Figure S3B, and there was a tendency to reversal of this effect in cells where OPA1 expression was rescued (Supplementary Figure S3C; $P=0.07$).

To assess the ability of the exogenously introduced GFP-FL-OPA1 to form a complex with endogenous PKA and perilipin, immunoprecipitations were performed from cell lysates of adipocytes cotransfected with OPA1 siRNA and siRNA-resistant GFP-FL-OPA1[#] or GFP-FL-OPA1[#] AKBmut (Figure 6D, left). Immunoprecipitation with RI α revealed the presence of GFP-FL-OPA1 in the precipitate from cells transfected with a vector encoding GFP-FL-OPA1[#] but not from cells expressing GFP-FL-OPA1[#] AKBmut, whereas RI α was precipitated in both cases. Together with the GFP immunoprecipitation experiment, where RI only coprecipitated with GFP-FL-OPA1[#] and not GFP-FL-OPA1[#] AKBmut, this indicates that OPA1 with three proline substitutions in the PKA-binding site does not interact with PKA *in situ*. However, immunoprecipitation with GFP antibody showed the presence of GFP-FL-OPA1 and perilipin in precipitates from cells expressing either GFP-FL-OPA1[#] or GFP-FL-OPA1[#] AKBmut, indicating that both the wild-type and substituted protein localize normally and interact with perilipin as also shown in the colocalization studies (Figure 5G–I; Supplementary Figures S1C and S2D–F'). Interestingly, the basal phosphorylation state of perilipin as observed with an anti-RXXpS/T antibody was found to be reduced by >90% in immunoprecipitates from cells reconstituted with GFP-FL-OPA1[#] AKBmut as compared with cells expressing GFP-FL-OPA1[#] (Figure 6D, right panel; $P<0.0025$). This suggests that the absence of PKA anchored to OPA1 affects basal levels of perilipin phosphorylation. Finally, immunoprecipitation of HSL revealed the presence of the same levels of phospho-

HSL in precipitates from both GFP-FL-OPA1[#] and GFP-FL-OPA1[#] AKBmut-transfected cells, indicating that the ability of OPA1 to bind PKA does not influence the basal phosphorylation state of HSL.

Isoproterenol-induced lipolysis in cells reconstituted with OPA1 was next assessed as glycerol release in the media from 3T3-L1 adipocytes transfected with OPA1 siRNA and either GFP-FL-OPA1[#] or GFP-FL-OPA1[#] AKBmut (Figure 6E). In the presence of 10 nM isoproterenol, a robust glycerol release was observed in cells that had received scrambled siRNA (solid bar), whereas significantly less glycerol was released in cultures treated with OPA1 siRNA (open bar, 51% reduction, $P<0.001$) as also seen in Figure 6B. Moreover, when GFP-FL-OPA1[#] was expressed in cells with knockdown of endogenous OPA1, the isoproterenol-induced glycerol release was increased two-fold compared with OPA1 knockdown cells and adrenergic regulation was partially restored ($P<0.001$). In contrast, expression of GFP-FL-OPA1[#] AKBmut in OPA1 knockdown cells did not restore isoproterenol-induced glycerol release (57.8% reduction compared with cells transfected with scrambled siRNA, $P<0.001$) and was not significantly different from the level of glycerol release in OPA1 knockdown cells. The fact that GFP-FL-OPA1 expression did not completely rescue the effect of OPA1 knockdown on isoproterenol-induced lipolysis may be due to transfection efficiency of the mammalian expression vector, which was lower than that of the siRNA as observed by GFP fluorescence compared with fluorescence of FITC-labelled siRNA in separate experiments (data not shown).

To examine the role of OPA1 in the control of lipolysis independently of its mitochondrial localization, we next engineered chimeric constructs consisting of the lipid droplet targeting sequence from perilipin (LDTS; amino acids 233–366, notably without any of the four PKA phosphorylation sites as Ser 276 inside the sequence was changed to Ala) (Subramanian *et al*, 2004) fused to OPA1 deleted of the MTS (Δ MTS-OPA1[#]) that directs the localization of wild-type OPA1 to both mitochondria and lipid droplets (Supplementary Figure S2G–V') with or without the AKB mutated (perilipin-LDTS Δ MTS-OPA1[#] or perilipin-LDTS Δ MTS-OPA1[#] AKBmut) and fused to green fluorescent protein in the N- or C-terminal position (see Figure 6E, top for design of fusion proteins). Expression of the chimeric proteins in the absence of endogenous OPA1 revealed colocalization with lipid droplets as evident from correlation analysis of GFP fluorescence with perilipin immunolabelling (correlation coefficients of $R=0.63$ – 0.66 , see Supplementary Figure S3D–F' for analysis of perilipin-LDTS Δ MTS-OPA1[#] AKBmut-GFP and perilipin). In the absence of endogenous OPA1 expression, the two chimeric LDTS- Δ MTS-OPA1 proteins with a functional AKB domain were able to restore isoproterenol-induced glycerol release (both $P<0.001$) compared with OPA1 knockdown cells whereas expression of chimeric constructs with a mutant AKB domain did not (Figure 6E). These data strongly suggest that LD-targeted OPA1 with a functional AKB domain is able to confer adrenergic regulation of perilipin phosphorylation by localizing of PKA independently of the mitochondrial pool of OPA1.

To control for the possibility that changes in glycerol release observed upon manipulations of OPA1 levels were not due merely to changes in the stored amount of TAG available for lipolysis or an effect on lipid droplet integrity,

lipid droplets of OPA1 knockdown cells were examined by immunostaining with perilipin antibody (Figure 6F and H, green) in combination with Oil Red O staining for TAG (Figure 6G and H, red). Lipid droplets in OPA1 knockdown cells were intact and with normal TAG stores. Furthermore, the level of TAG stored in adipocytes after siRNA-mediated OPA1 knockdown and reconstitution with exogenous OPA1 were quantified by staining cell cultures with Oil Red O, washing, extracting the remaining Oil Red O in isopropanol and measuring optical density (Figure 6I). No significant difference in TAG content was observed in adipocytes after siRNA knockdown or OPA1 expression compared with cells transfected with scrambled siRNA. To ensure that siRNA-mediated knockdown and reconstitution experiment did not affect the β -adrenergic signalling pathway or integrity and function of mitochondria, we measured the intracellular cAMP production and the ATP concentration in adipocytes before and after isoproterenol stimulation. Whereas a clear increase of cAMP was observed after stimulation with 10 nM isoproterenol compared with basal levels, no significant difference in intracellular cAMP production was observed after the different transfections (Figure 6J). Moreover, no differences in ATP concentration were observed in cells after siRNA-mediated knockdown and reconstitution experiments (Figure 6K).

Together, our knockdown and reconstitution experiments suggest that OPA1 plays a key role in the regulation of lipolysis by coordinating a signal complex on lipid droplets containing both PKA and perilipin where discretely controlled phosphorylation of perilipin regulates access of lipases to the lipid stores upon adrenergic stimuli.

The dual-specificity AKAP OPA1 permits both type I and type II PKA to regulate lipolysis

A typical feature of AKAP-coordinated phosphorylation events regulating physiological processes is that displacement of the anchored pool of PKA by anchoring disruptor peptides should block regulation by cAMP. The prototypic anchoring disruptor peptide Ht31 derived from AKAP-Lbc (Carr *et al*, 1992) has been extensively used for this type of experiment by offering soluble binding sites for PKA and was already in Figure 1A shown to disrupt isoproterenol-induced perilipin phosphorylation. Ht31 disrupts anchoring of type II PKA, but at somewhat higher concentrations also competes anchoring of type I PKA (Herberg *et al*, 2000; Gold *et al*, 2006; Ruppelt *et al*, 2007). More recently, the development of the high-affinity, isoform-specific anchoring disruptors RI anchoring disruptor (RIAD) and SuperAKAP-IS has provided tools to specifically delineate effects mediated by type I or type II PKA (Carlson *et al*, 2006; Gold *et al*, 2006). Here, we used the tool box of anchoring disruptor peptides to further characterize the AKAP coordinating adrenergic control of lipolysis. First,

conditions for peptide loading of differentiated adipocytes were established by incubating 3T3-L1 adipocytes with FITC-labelled, poly-arginine-tagged RIAD and SuperAKAP-IS peptides at different concentrations and for different time periods. Maximal peptide loading was observed at 120 min (Figure 7A and B, respectively). Furthermore, an optimal peptide concentration of 30 μ M was determined by toxicity testing (data not shown). The effect of anchoring disruptors on lipolysis was next analysed by glycerol-release assay. Adipocytes preincubated with Ht31 peptide presented significantly decreased glycerol release after stimulation with 30 or 100 nM isoproterenol compared with mock loaded cells (42% reduction, $P < 0.005$; 92% reduction, $P < 0.001$, respectively) (Figure 7C). In contrast, 3T3-L1 adipocytes incubated separately with either RIAD (Figure 7D) or SuperAKAP-IS peptide (Figure 7E) did not show any significant differences in lipolysis compared with the effect of the corresponding scrambled peptides. However, incubation with a combination of RIAD and SuperAKAP-IS peptides (Figure 7F; 30 μ M each) effectively blocked isoproterenol-induced glycerol release (74 and 97% decrease at 30 and 100 nM isoproterenol compared with scrambled control with both peptides, $P < 0.001$). Our results are compatible with the notion derived from the kinetic data on the PKA-OPA1 association in Figure 2 that OPA1 is a true dual-specificity AKAP that permits both type I and type II PKA to bind and regulate lipolysis (see Figure 7G for depiction of effect of various anchoring disruptors). From this notion it can be derived that if both type I and type II PKA are available for binding to OPA1 (although RI appears to be the preferred binding partner in 3T3-L1 cells), only the combination of RIAD and SuperAKAP-IS would compete binding of both forms of PKA and block adrenergic regulation of lipolysis. This is consistent with our observations of hormonally regulated lipolysis in the presence of various anchoring disruptors (Figure 7F and G, bottom right panel).

Discussion

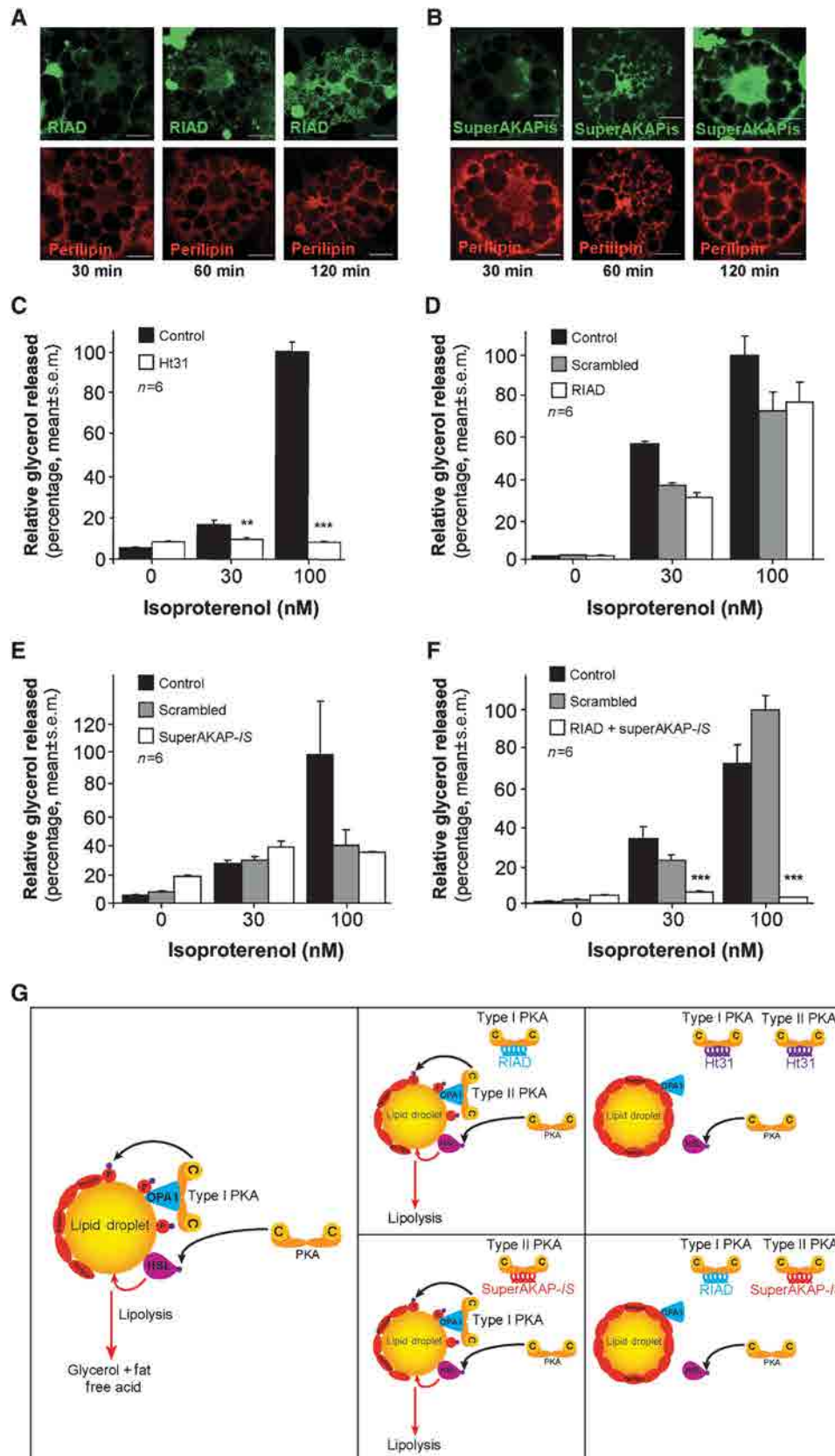
Here, we report the identification of OPA1 as an AKAP for perilipin. OPA1, normally found in mitochondria in other cell types, is expressed at increasing levels during adipocyte differentiation and targeted to lipid droplets where it organizes a supramolecular complex with both PKA and perilipin. We show that OPA1 is necessary for discrete control of perilipin phosphorylation and lipolysis.

The observation that adipocytes expressing the Ht31 anchoring disruptor lacked perilipin phosphorylation upon adrenergic stimulation indicated that AKAP-mediated targeting of PKA was necessary for perilipin phosphorylation. This prompted us to search for an AKAP for perilipin. Several AKAPs have already been identified in adipocytes (Chaudhry *et al*, 2002; Nomura *et al*, 2002; Tao *et al*, 2003; Zhang *et al*,

Figure 7 The dual-specificity function of OPA1 allows redundancy in the anchored PKA isozyme regulating lipolysis. (A, B) Time-dependent (30, 60 or 120 min) peptide loading of 3T3-L1 adipocytes with RIAD-FITC (A, green; upper row) or SuperAKAP-IS-FITC (B, green; upper row) at 15 μ M each. Subsequently, 3T3-L1 adipocytes were immunostained for perilipin (red; A, B, lower rows). Scale bar: 20 μ m. (C–F) Effect of anchoring disruptor peptides in isoproterenol-regulated lipolysis were studied by measuring the amount of glycerol released into media of 3T3-L1 adipocytes after incubation with Ht31 (C), RIAD (D), SuperAKAP-IS (E) or RIAD and SuperAKAP-IS peptides together (F). Stimulation was accomplished by incubation with 30 or 100 nM isoproterenol for 2 h at 72 h of culture. Results are expressed as the mean \pm s.e.m. of $n = 6$ independent experiments ($***P < 0.001$ and $**P < 0.01$). (G) Schematic illustration of the effect of specific anchoring disruptor peptides on lipolysis. (Left) Model of OPA1 as an AKAP organizing activation of lipolysis upon adrenergic stimulation. (Middle row) Model for effect of RIAD or SuperAKAP-IS on lipolysis. (Right row) Effect of Ht31 or RIAD and SuperAKAP-IS together on adrenergic regulation of lipolysis.

2005; Bridges *et al*, 2006). According to Tao *et al* (2003), a complex formed of the β -AR, an AKAP and PKA is involved in receptor internalization, resensitization and recycling of the

β -AR in adipocytes. Although some observations suggested that the association between β -AR and PKA in adipocytes is mediated by AKAP150 or gravin (Fraser *et al*, 2000; Tao *et al*,



2003), Zhang *et al* (2005) proposed the involvement of a yet unidentified AKAP. Moreover, the compartmentalization of HSL with AKAP150 and PKA has been described to be required for the induction of lipolysis by controlling HSL phosphorylation (Nomura *et al*, 2002), but the importance of this observation is challenged by the more recent reports that HSL is dispensable in catecholamine-stimulated lipolysis. A more recent work proposed D-AKAP1 as a major adipocyte PKA-binding protein and discussed the possibility of D-AKAP1 as a lipid droplet AKAP, but failed to convincingly demonstrate an association with lipid droplets and did not show data to support any functional effect of D-AKAP1 (Bridges *et al*, 2006). Furthermore, Chaudhry *et al* (2002) showed that D-AKAP1 is associated with mitochondria in differentiated adipocytes. In summary, no AKAP has previously been clearly shown to be associated with lipid droplets and to be involved in the regulation of the lipolytic process.

We report here for the first time that OPA1 is a dual-specificity AKAP targeted to lipid droplets in adipocytes. An amphipathic helix AKB domain localized in the C-terminal part of OPA1 is able to bind both type I and type II PKA with low nanomolar affinities. While most dual-specificity AKAPs appear to have lower affinity for type I than for type II PKA due to a faster off-rate of RI (Herberg *et al*, 2000), OPA1 appears to display equal affinities for both isozymes or even a slightly higher affinity for type I PKA. Our kinetic analysis demonstrated that this was due to similar on- and off-rates of both isozymes. When the affinity of an AKAP for type I and type II PKA is similar, the availability of the two isozymes would be expected to determine association. Indeed, in 3T3-L1 cells that express both RI α and RII β , we observed that PKA type I associated with OPA1 and controlled lipolysis. In contrast, OPA1 was associated with RII β in WAT, where it is the predominantly expressed R subunit and where type II PKA has been reported to control lipolysis (Beebe *et al*, 1984; Robinson-Steiner *et al*, 1984). Whether lipolysis is controlled by type I or type II PKA is clearly important as K_{act} for the two isozymes differ (50–100 and 200–400 nM for type I and type II, respectively). This, in turn, affects the sensitivity to catecholamine-stimulated lipolysis as illustrated in the RII β null-mutant mice where rescue by upregulation of RI α provides a type I PKA to control lipolysis and results in lean mice (Cummings *et al*, 1996). Furthermore, regulation of RI α levels may be a means to control adipocyte sensitivity to cAMP-regulated lipolysis. This is illustrated in mice with high levels of expression of FoxC2 that controls RI α expression resulting in mice protected against diet-induced obesity and insulin resistance (Cederberg *et al*, 2001).

OPA1 is earlier reported to be expressed in different cell types with phenotypes of mutations in the *opa1* gene related to its function in the nervous system. Here, we show that OPA1 is expressed in WAT and BAT and upregulated during adipocyte differentiation at a time consistent with its regulation by adipocyte-specific transcription factors such as PPAR γ . The dynamin-related GTPase OPA1 is reported to be targeted to the mitochondrial membrane in different cell types including adipocytes (Misaka *et al*, 2002; Olichon *et al*, 2002; Satoh *et al*, 2003; Kita *et al*, 2009) and involved in mitochondrial fusion and apoptosis through mitochondrial cristae remodelling (Olichon *et al*, 2003; Cipolat *et al*, 2004; Frezza *et al*, 2006; Ishihara *et al*, 2006). By transfection of

COS-7 cells with the 30, 60 or 90 N-terminal amino acids of the OPA1 MTS fused to the N-terminal end of EGFP, amino acids 30–90 of the MTS were shown to be important for the mitochondrial location (Misaka *et al*, 2002; Olichon *et al*, 2002; Satoh *et al*, 2003; Kita *et al*, 2009). In contrast, our immunolocalization and cell fractionation studies in adipocytes revealed that a substantial fraction of OPA1 is associated with lipid droplets and that amino acids 1–30 of the OPA1 MTS appeared to be required for OPA1 to access lipid droplets. Furthermore, deletion of amino acids 30–87 also reduced lipid droplet targeting of OPA1, although not to the same extent as its mitochondrial targeting. The differences in subcellular distribution may reflect that the lipophilic nature of the OPA1 membrane targeting domain favour its association with lipid droplets in cell types where these are available. Transport of OPA1 to lipid droplets may occur via a direct route to lipid droplets in parallel with the mitochondrial targeting (dual targeting) or by an indirect route via mitochondria. While the observation that deletion of the full 90 amino acids of the OPA1 MTS lead to loss of both and lipid droplet targeting may point towards the mitochondrial transit route, the fact that lipid droplet targeting was lost also upon deletion of the first 30 amino acids of the MTS that have been shown to be less important for mitochondrial targeting may indicate distinct targeting mechanisms. However, the targeting mechanism could not be readily defined and requires future investigation in more detail.

Two recent papers indicate that OPA1 may be redistributed from mitochondria to membrane tubulations extending from mitochondria (Ban *et al*, 2010) or lost during ER stress (Zhang *et al*, 2008), indicating some mobility of OPA1. It is interesting to speculate that OPA1 localized on both mitochondria and lipid droplets could coordinate the positioning of lipid droplets in close proximity to mitochondria to facilitate the supply of FFA from lipolysis to mitochondria for ATP synthesis. Silencing of mitochondrial fusion proteins such as mitofusin 2 in adipocytes lead to accumulation of lipid droplets, whereas silencing of fission proteins such as Drp1 is responsible of a decrease in TAG content (Kita *et al*, 2009), indicating interplay between mitochondrial dynamics and lipid storage in adipocytes. Our findings indicate that the silencing of OPA1 has a distinct effect as it does not impact lipid droplet accumulation or lipid content of adipocytes, but affects the adrenergic regulation of the lipolysis.

In addition to binding PKA, our data also showed that OPA1 bound perilipin, consistent with observations made with other macromolecular complexes organized by AKAPs that include the substrate for PKA as well as other signalling enzymes (Tasken and Aandahl, 2004; Wong and Scott, 2004). While preliminary data indicate a direct interaction between OPA1 and perilipin, the molecular determinants for interaction and possible presence of other signalling enzymes in the OPA1-scaffolded macromolecular complex remain to be investigated. Furthermore, the function of OPA1 in adipocyte mitochondria and the possibility of OPA1 functioning as an AKAP also in mitochondria in different cell types would be interesting to pursue in future studies.

By silencing and reconstitution experiments, we demonstrated a central role for OPA1 in catecholamine-stimulated lipolysis. siRNA-mediated knockdown of OPA1 induced a decrease in isoproterenol-induced lipolysis, while reconstitution experiments with siRNA-resistant wild-type OPA1

rescued this effect. Moreover, reconstitution experiments using a mutated construct substituted in the AKB domain, so that it cannot associate with PKA, did not rescue isoproterenol-induced lipolysis. Finally, reconstitution experiments with OPA1 deleted of its mitochondrial and lipid droplet targeting sequences but fused to a lipid droplet targeting domain also reconstituted adrenergic regulation of lipolysis when the AKB domain was present. Recent work revealed that loss of function of OPA1 increased mitochondrial fragmentation without altering bioenergetics or increasing apoptosis (Spinazzi *et al*, 2008), which would indicate that the loss of isoproterenol-stimulated lipolysis observed after OPA1 silencing in adipocytes is not due to induction of apoptosis. Nor was this lack in response to adrenergic stimulation due to a deficiency in substrate for lipolysis, as we observed no decrease in lipid droplet TAG content. Together with the reconstitution experiments, this indicates that it is the loss of PKA from the perilipin/OPA1 macromolecular complex, which prevents perilipin phosphorylation. The silencing of OPA1 and reconstitution experiments had no effect on HSL phosphorylation, supporting the hypothesis of another AKAP controlling the HSL phosphorylation state (Nomura *et al*, 2002). The silencing of OPA1 also led to a decrease in perilipin protein levels consistent with the notion that absence of one of the partners of the complex could destabilize the remainder. Indeed, it has been confirmed recently in other models that the knockdown of a protein may affect the stability of other protein partners present in the same supramolecular complex (Oswald *et al*, 2009). Here, however, perilipin levels appeared to be rescued by an upregulation of ADRP (Supplementary Figure S4), in line with earlier studies (Tansey *et al*, 2001).

We employed a strategy of PKA displacement using anchoring disruptor peptides to confirm the presence and role of a dual-specificity AKAP in regulation of lipolysis. Our results obtained with Ht31 are in agreement with a previous study showing decreased catecholamine-stimulated lipolysis in cells loaded with Ht31 (Nomura *et al*, 2002; Zhang *et al*, 2005). Furthermore, we show that RIAD and SuperAKAP-IS that selectively displace either type I or type II PKA did not inhibit isoproterenol-stimulated lipolysis when added separately, whereas the combination reduced regulation of lipolysis to the same extent as Ht31. These results allow us to propose a model to explain the adrenergic control of lipolysis (Figure 7G). In 3T3-L1 adipocytes, OPA1 is located in a supramolecular complex associated with lipid droplets, which keeps type I PKA preferentially in close proximity to perilipin to control its phosphorylation state during adrenergic stimulation. Phosphorylation of perilipin through the OPA1/PKA complex stimulates lipolysis by allowing access of lipases to TAG in lipid droplets. Interestingly, it is necessary to block the dual-specificity function of OPA1 to abolish stimulation of lipolysis as there is redundancy with respect to the use of different PKA isoforms, although the use of PKA type I versus PKA type II affects the sensitivity of the process to catecholamines.

In addition to control the supply of energy in the fed versus the fasting state, control of lipolysis is important to provide FFA for hepatic synthesis of TAG-containing lipoproteins. Furthermore, alterations in lipolysis are frequently observed in obesity, which is increasing rapidly in the industrialized part of the world and constitutes a growing medical problem.

Obesity, characterized primarily by an excess of WAT, results in metabolic syndrome, which encompasses insulin resistance and hypertension and leads to type II diabetes, atherosclerosis and cardiovascular disease (Kahn *et al*, 2000; Unger, 2003). At the cellular level, obesity leads to a pathological accumulation of TAG and an enlargement of adipocyte size, as well as increased numbers of adipocytes. Consequently, understanding the regulation of lipolysis and its dysregulation are highly interesting in the context of obesity.

In summary, we report a new function for the OPA1 protein as a dual-specificity AKAP associated with lipid droplets in adipocytes whose role is to coordinate a supramolecular signal complex at the surface of lipid droplets. We provide direct evidence that OPA1 mediates the adrenergic control of lipolysis by providing PKA in close proximity of perilipin to regulate its phosphorylation state and thereby control lipolysis.

Materials and methods

Cell culture

3T3-L1 cells (ATCC) were cultured as described previously (Enrique-Tarancon *et al*, 1998) (see Supplementary data).

Protein sample preparation and immunoblot analysis

Total cell lysates were prepared in lysis buffer (see Supplementary data) and proteins were resolved by SDS-PAGE and blotted onto nitrocellulose membranes. The resulting filters were immunoblotted with antibodies to OPA1 (0.25 µg/ml; BD Biosciences), perilipin (1:1000; Fitzgerald Industries from both rabbit and guinea pig), HSL (1:1000; Cell Signaling), phospho-HSL (1:1000; Cell Signaling), PKA-R1α (0.25 µg/ml; BD Biosciences), PKA-R1β (0.25 µg/ml; BD Biosciences), phospho-PKA substrate (anti-RRXpS/T, 1:2000, Cell Signaling), mitofilin (1:2000; AbCam), mitofusin2 (1 µg/ml; AbCam), pyruvate dehydrogenase E1β subunit (1 µg/ml; AbCam) ADRP and TIP47 (1/1000 each; gift from Dr KT Dalen). After incubation with appropriate HRP-conjugated secondary antibody, blots were developed by using Supersignal West Pico substrate (Pierce).

Immunoprecipitation

Protein A/G plus agarose (Santa Cruz Biotechnology) was absorbed with antibody against OPA1 (BD Biosciences), perilipin (Fitzgerald Industries) or PKA-R1α or -R1β (both BD Biosciences) or left without antibody. Total cell lysates were prepared as above, added to the protein A/G agarose immunocomplex and incubated overnight at 4 °C on a rocker platform. Immunocomplexes were washed five times in lysis buffer before SDS-PAGE and immunoblotting with the indicated antibodies.

Lipid droplet purification

Lipid droplets were purified as described previously (Brasaemle *et al*, 2004) (see Supplementary data).

R-overlays

R-overlays were performed as described previously (Hausken *et al*, 1998) by using ³²P-labelled recombinant RII or RI (A98S) substituted to allow autophosphorylation (Durgerian and Taylor, 1989) (see Supplementary data).

Immunolocalization studies

Immunofluorescence staining was performed on differentiated 3T3-L1. Cells were fixed for 15 min in 3% paraformaldehyde, permeabilized for 15 min with 0.1% saponin and blocked for 20 min in 3% fatty acid-free BSA, 0.2 M glycine and 0.1% saponin. Primary antibodies anti-OPA1 (2.5 µg/ml; BD Biosciences), anti-perilipin (1:100; Fitzgerald Industries from guinea pig), anti-HSL (1:100; Cell Signaling), anti-PKA-R1α (2.5 µg/ml; BD Biosciences), anti-PKA-R1β (2.5 µg/ml; BD Biosciences) and mitofusin2 (20 µg/ml; AbCam) were prepared in PBS with 0.01% Tween 20 (PBS-T), 3% BSA, 0.1% saponin and incubated overnight at 4 °C. Cells were next incubated with the appropriate fluorochrome-conjugated

secondary antibodies (Alexa Fluor 488 and Alexa Fluor 546 (1:1000; Invitrogen)) in PBS-T, 0.1% saponin for 1 h. Controls without primary antibody or with nonspecific IgG of the same isotype were all negative (data not shown). See also Supplementary data.

siRNA, mammalian expression vectors and transfection

siRNA transfection was performed using Lipofectamine 2000 CD reagent (Invitrogen) according to the manufacturer's protocol. See also Supplementary data.

The mammalian transfection vectors were introduced into 3T3-L1 adipocytes by using Fugene 6 transfection reagent (Roche) according to the manufacturer's protocol. See also Supplementary data.

Lipolysis assay

Differentiated 3T3-L1 cells were incubated in DMEM (without phenol red) containing 2% fatty acid-free BSA overnight. Cells were stimulated in fresh media with or without isoproterenol (5–100 nM) for lipolysis assays. After 2 h of incubation, 50 μ l of medium was withdrawn and used for the assay. Glycerol levels were determined using the Free Glycerol Determination Kit (Sigma-Aldrich) according to the manufacturer's instruction.

Statistics

Quantitative data are presented as mean \pm s.e.m. Differences were identified by analysis of variance and considered significant when $P < 0.05$. See also Supplementary data.

References

- Alexander C, Votruba M, Pesch UE, Thiselton DL, Mayer S, Moore A, Rodriguez M, Kellner U, Leo-Kottler B, Auburger G, Bhattacharya SS, Wissinger B (2000) OPA1, encoding a dynamin-related GTPase, is mutated in autosomal dominant optic atrophy linked to chromosome 3q28. *Nat Genet* **26**: 211–215
- Ban T, Heymann JA, Song Z, Hinshaw JE, Chan DC (2010) OPA1 disease alleles causing dominant optic atrophy have defects in cardiolipin-stimulated GTP hydrolysis and membrane tubulation. *Hum Mol Genet* **19**: 2113–2122
- Beebe SJ, Holloway R, Rannels SR, Corbin JD (1984) Two classes of cAMP analogs which are selective for the two different cAMP-binding sites of type II protein kinase demonstrate synergism when added together to intact adipocytes. *J Biol Chem* **259**: 3539–3547
- Blanchette-Mackie EJ, Dwyer NK, Barber T, Coxey RA, Takeda T, Rondinone CM, Theodorakis JL, Greenberg AS, Londos C (1995) Perilipin is located on the surface layer of intracellular lipid droplets in adipocytes. *J Lipid Res* **36**: 1211–1226
- Bolte S, Cordelieres FP (2006) A guided tour into subcellular colocalization analysis in light microscopy. *J Microsc* **224**: 213–232
- Brasaemle DL, Dolios G, Shapiro L, Wang R (2004) Proteomic analysis of proteins associated with lipid droplets of basal and lipolytically stimulated 3T3-L1 adipocytes. *J Biol Chem* **279**: 46835–46842
- Brasaemle DL, Levin DM, Adler-Wailes DC, Londos C (2000a) The lipolytic stimulation of 3T3-L1 adipocytes promotes the translocation of hormone-sensitive lipase to the surfaces of lipid storage droplets. *Biochim Biophys Acta* **1483**: 251–262
- Brasaemle DL, Rubin B, Harten IA, Gruia-Gray J, Kimmel AR, Londos C (2000b) Perilipin A increases triacylglycerol storage by decreasing the rate of triacylglycerol hydrolysis. *J Biol Chem* **275**: 38486–38493
- Bridges D, MacDonald JA, Wadzinski B, Moorhead GB (2006) Identification and characterization of D-AKAP1 as a major adipocyte PKA and PPI binding protein. *Biochem Biophys Res Commun* **346**: 351–357
- Carlson CR, Lygren B, Berge T, Hoshi N, Wong W, Tasken K, Scott JD (2006) Delineation of type I protein kinase A-selective signaling events using an RI anchoring disruptor. *J Biol Chem* **281**: 21535–21545
- Carr DW, Hausken ZE, Fraser ID, Stofko-Hahn RE, Scott JD (1992) Association of the type II cAMP-dependent protein kinase with a human thyroid RII-anchoring protein. Cloning and characterization of the RII-binding domain. *J Biol Chem* **267**: 13376–13382
- Cederberg A, Gronning LM, Ahren B, Tasken K, Carlsson P, Enerback S (2001) FOXC2 is a winged helix gene that counteracts obesity, hypertriglyceridemia, and diet-induced insulin resistance. *Cell* **106**: 563–573
- Chaudhry A, Zhang C, Granneman JG (2002) Characterization of RII(beta) and D-AKAP1 in differentiated adipocytes. *Am J Physiol Cell Physiol* **282**: C205–C212
- Cipolat S, Martins de Brito O, Dal Zilio B, Scorrano L (2004) OPA1 requires mitofusin 1 to promote mitochondrial fusion. *Proc Natl Acad Sci USA* **101**: 15927–15932
- Cummings DE, Brandon EP, Planas JV, Motamed K, Idzerda RL, McKnight GS (1996) Genetically lean mice result from targeted disruption of the RII beta subunit of protein kinase A. *Nature* **382**: 622–626
- Delettre C, Lenaers G, Griffoin JM, Gigarel N, Lorenzo C, Belenguer P, Pelloquin L, Grosgeorge J, Turc-Carel C, Perret E, Astarie-Dequeker C, Lasquellec L, Arnaud B, Ducommun B, Kaplan J, Hamel CP (2000) Nuclear gene OPA1, encoding a mitochondrial dynamin-related protein, is mutated in dominant optic atrophy. *Nat Genet* **26**: 207–210
- Diviani D, Scott JD (2001) AKAP signaling complexes at the cytoskeleton. *J Cell Sci* **114**: 1431–1437
- Durgerian S, Taylor SS (1989) The consequences of introducing an autophosphorylation site into the type I regulatory subunit of cAMP-dependent protein kinase. *J Biol Chem* **264**: 9807–9813
- Enrique-Tarancon G, Marti L, Morin N, Lizcano JM, Unzeta M, Sevilla L, Camps M, Palacin M, Testar X, Carpeno C, Zorzano A (1998) Role of semicarbazide-sensitive amine oxidase on glucose transport and GLUT4 recruitment to the cell surface in adipose cells. *J Biol Chem* **273**: 8025–8032
- Fain JN, Garcija-Sainz JA (1983) Adrenergic regulation of adipocyte metabolism. *J Lipid Res* **24**: 945–966
- Fraser ID, Cong M, Kim J, Rollins EN, Daaka Y, Lefkowitz RJ, Scott JD (2000) Assembly of an A kinase-anchoring protein-beta(2)-adrenergic receptor complex facilitates receptor phosphorylation and signaling. *Curr Biol* **10**: 409–412
- Fredrikson G, Tornqvist H, Belfrage P (1986) Hormone-sensitive lipase and monoacylglycerol lipase are both required for complete degradation of adipocyte triacylglycerol. *Biochim Biophys Acta* **876**: 288–293
- Frezza C, Cipolat S, Martins de Brito O, Micaroni M, Beznoussenko GV, Rudka T, Bartoli D, Polishuck RS, Danial NN, De Strooper B, Scorrano L (2006) OPA1 controls apoptotic cristae remodeling independently from mitochondrial fusion. *Cell* **126**: 177–189

Supplementary data

Supplementary data are available at *The EMBO Journal* Online (<http://www.embojournal.org>).

Acknowledgements

This work was supported by grants from the Norwegian Functional Genomics Program, The Research Council of Norway, Novo Nordic Foundation and the European Union (Grant no. 037189, thera-cAMP). We are grateful to Jorun Solheim and Gladys M Tjørhom for technical assistance, to Ola Blingsmo for peptide synthesis, to Dr Sven Enerback for gift of a plasmid with the AP1 promoter, to Dr John D Scott for gift of expression vectors for Ht31, to Dr Ruth Valgardsdottir for gift of Δ MDDX28 plasmid, to Dr Mohammed Amarzguioui for help with OPA1 siRNA design, to Dr Erwan Delbarre for help with colocalization analysis and Drs Line M Grønning Wang and Knut T Dalen for helpful comments and input on various parts of the work.

Author contributions: GP, OW, EJ, LM and AJS did the experiments and analysed the data; KT supervised the project; HU and TK provided essential technologies and analysed the data; and GP, OW and KT wrote the paper. All authors read and commented on the draft versions of the manuscript and approved the final version.

Conflict of interest

The authors declare that they have no conflict of interest.

- Giudicelli H, Combes-Pastre N, Boyer J (1974) Lipolytic activity of adipose tissue. IV. The diacylglycerol lipase activity of human adipose tissue. *Biochim Biophys Acta* **369**: 25–33
- Gold MG, Lygren B, Dokurno P, Hoshi N, McConnachie G, Tasken K, Carlson CR, Scott JD, Barford D (2006) Molecular basis of AKAP specificity for PKA regulatory subunits. *Mol Cell* **24**: 383–395
- Greenberg AS, Egan JJ, Wek SA, Garty NB, Blanchette-Mackie EJ, Londos C (1991) Perilipin, a major hormonally regulated adipocyte-specific phosphoprotein associated with the periphery of lipid storage droplets. *J Biol Chem* **266**: 11341–11346
- Greenberg AS, Egan JJ, Wek SA, Moos Jr MC, Londos C, Kimmel AR (1993) Isolation of cDNAs for perilipins A and B: sequence and expression of lipid droplet-associated proteins of adipocytes. *Proc Natl Acad Sci USA* **90**: 12035–12039
- Haemmerle G, Zimmermann R, Hayn M, Theussl C, Waeg G, Wagner E, Sattler W, Magin TM, Wagner EF, Zechner R (2002) Hormone-sensitive lipase deficiency in mice causes diglyceride accumulation in adipose tissue, muscle, and testis. *J Biol Chem* **277**: 4806–4815
- Hausken ZE, Coghlan VM, Scott JD (1998) Overlay, ligand blotting, and band-shift techniques to study kinase anchoring. *Methods Mol Biol* **88**: 47–64
- Herberg FW, Maleszka A, Eide T, Vossebein L, Tasken K (2000) Analysis of A-kinase anchoring protein (AKAP) interaction with protein kinase A (PKA) regulatory subunits: PKA isoform specificity in AKAP binding. *J Mol Biol* **298**: 329–339
- Ishihara N, Fujita Y, Oka T, Mihara K (2006) Regulation of mitochondrial morphology through proteolytic cleavage of OPA1. *EMBO J* **25**: 2966–2977
- Jarnaess E, Ruppelt A, Stokka AJ, Lygren B, Scott JD, Tasken K (2008) Dual specificity A-kinase anchoring proteins (AKAPs) contain an additional binding region that enhances targeting of protein kinase A type I. *J Biol Chem* **283**: 33708–33718
- Jenkins CM, Mancuso DJ, Yan W, Sims HF, Gibson B, Gross RW (2004) Identification, cloning, expression, and purification of three novel human calcium-independent phospholipase A2 family members possessing triacylglycerol lipase and acylglycerol transacylase activities. *J Biol Chem* **279**: 48968–48975
- Kahn CR, Chen L, Cohen SE (2000) Unraveling the mechanism of action of thiazolidinediones. *J Clin Invest* **106**: 1305–1307
- Kimmel AR, Brasaemle DL, McAndrews-Hill M, Sztalryd C, Londos C (2009) Adoption of PERILIPIN as a unifying nomenclature for the mammalian PAT-family of intracellular, lipid storage droplet proteins. *J Lipid Res* **51**: 468–471
- Kinderman FS, Kim C, von Daake S, Ma Y, Pham BQ, Spraggon G, Xuong NH, Jennings PA, Taylor SS (2006) A dynamic mechanism for AKAP binding to RII isoforms of cAMP-dependent protein kinase. *Mol Cell* **24**: 397–408
- Kita T, Nishida H, Shibata H, Niimi S, Higuti T, Arakaki N (2009) Possible role of mitochondrial remodeling on cellular triacylglycerol accumulation. *J Biochem* **146**: 787–796
- Londos C, Brasaemle DL, Schultz CJ, Segrest JP, Kimmel AR (1999) Perilipins, ADRP, and other proteins that associate with intracellular neutral lipid droplets in animal cells. *Semin Cell Dev Biol* **10**: 51–58
- Michel JJ, Scott JD (2002) AKAP mediated signal transduction. *Annu Rev Pharmacol Toxicol* **42**: 235–257
- Misaka T, Miyashita T, Kubo Y (2002) Primary structure of a dynamin-related mouse mitochondrial GTPase and its distribution in brain, subcellular localization, and effect on mitochondrial morphology. *J Biol Chem* **277**: 15834–15842
- Nomura S, Kawanami H, Ueda H, Kizaki T, Ohno H, Izawa T (2002) Possible mechanisms by which adipocyte lipolysis is enhanced in exercise-trained rats. *Biochem Biophys Res Commun* **295**: 236–242
- Olichon A, Baricault L, Gas N, Guillou E, Valette A, Belenguer P, Lenaers G (2003) Loss of OPA1 perturbs the mitochondrial inner membrane structure and integrity, leading to cytochrome c release and apoptosis. *J Biol Chem* **278**: 7743–7746
- Olichon A, Emorine LJ, Descoins E, Pelloquin L, Brichese L, Gas N, Guillou E, Delettre C, Valette A, Hamel CP, Ducommun B, Lenaers G, Belenguer P (2002) The human dynamin-related protein OPA1 is anchored to the mitochondrial inner membrane facing the inter-membrane space. *FEBS Lett* **523**: 171–176
- Osuga J, Ishibashi S, Oka T, Yagyu H, Tozawa R, Fujimoto A, Shionoiri F, Yahagi N, Kraemer FB, Tsutsumi O, Yamada N (2000) Targeted disruption of hormone-sensitive lipase results in male sterility and adipocyte hypertrophy, but not in obesity. *Proc Natl Acad Sci USA* **97**: 787–792
- Oswald C, Krause-Buchholz U, Rodel G (2009) Knockdown of human COX17 affects assembly and supramolecular organization of cytochrome c oxidase. *J Mol Biol* **389**: 470–479
- Pidoux G, Tasken K (2010) Specificity and spatial dynamics of PKA signaling organized by A kinase anchoring proteins. *J Mol Endocrinol* **44**: 271–284
- Robinson-Steiner AM, Beebe SJ, Rannels SR, Corbin JD (1984) Microheterogeneity of type II cAMP-dependent protein kinase in various mammalian species and tissues. *J Biol Chem* **259**: 10596–10605
- Ruppelt A, Mosenden R, Gronholm M, Aandahl EM, Tobin D, Carlson CR, Abrahamsen H, Herberg FW, Carpen O, Tasken K (2007) Inhibition of T cell activation by cyclic adenosine 5'-monophosphate requires lipid raft targeting of protein kinase A type I by the A-kinase anchoring protein ezrin. *J Immunol* **179**: 5159–5168
- Satoh M, Hamamoto T, Seo N, Kagawa Y, Endo H (2003) Differential sublocalization of the dynamin-related protein OPA1 isoforms in mitochondria. *Biochem Biophys Res Commun* **300**: 482–493
- Sesaki H, Southard SM, Yaffe MP, Jensen RE (2003) Mgm1p, a dynamin-related GTPase, is essential for fusion of the mitochondrial outer membrane. *Mol Biol Cell* **14**: 2342–2356
- Soni KG, Lehner R, Metalnikov P, O'Donnell P, Semache M, Gao W, Ashman K, Pshchetsky AV, Mitchell GA (2004) Carboxylesterase 3 (EC 3.1.1.1) is a major adipocyte lipase. *J Biol Chem* **279**: 40683–40689
- Souza SC, Muliro KV, Liscum L, Lien P, Yamamoto MT, Schaffer JE, Dallal GE, Wang X, Kraemer FB, Obin M, Greenberg AS (2002) Modulation of hormone-sensitive lipase and protein kinase A-mediated lipolysis by perilipin A in an adenoviral reconstituted system. *J Biol Chem* **277**: 8267–8272
- Spinazzi M, Cazzola S, Bortolozzi M, Baracca A, Loro E, Casarin A, Solaini G, Sgarbi G, Casalena G, Cenacchi G, Malena A, Frezza C, Carrara F, Angelini C, Scorrano L, Salviati L, Vergani L (2008) A novel deletion in the GTPase domain of OPA1 causes defects in mitochondrial morphology and distribution, but not in function. *Hum Mol Genet* **17**: 3291–3302
- Stokka AJ, Gesellchen F, Carlson CR, Scott JD, Herberg FW, Tasken K (2006) Characterization of A-kinase-anchoring disruptors using a solution-based assay. *Biochem J* **400**: 493–499
- Subramanian V, Garcia A, Sekowski A, Brasaemle DL (2004) Hydrophobic sequences target and anchor perilipin A to lipid droplets. *J Lipid Res* **45**: 1983–1991
- Tansey JT, Huml AM, Vogt R, Davis KE, Jones JM, Fraser KA, Brasaemle DL, Kimmel AR, Londos C (2003) Functional studies on native and mutated forms of perilipins. A role in protein kinase A-mediated lipolysis of triacylglycerols. *J Biol Chem* **278**: 8401–8406
- Tansey JT, Sztalryd C, Gruija-Gray J, Roush DL, Zee JV, Gavrilova O, Reitman ML, Deng CX, Li C, Kimmel AR, Londos C (2001) Perilipin ablation results in a lean mouse with aberrant adipocyte lipolysis, enhanced leptin production, and resistance to diet-induced obesity. *Proc Natl Acad Sci USA* **98**: 6494–6499
- Tao J, Wang HY, Malbon CC (2003) Protein kinase A regulates AKAP250 (gravin) scaffold binding to the beta2-adrenergic receptor. *EMBO J* **22**: 6419–6429
- Tasken K, Aandahl EM (2004) Localized effects of cAMP mediated by distinct routes of protein kinase A. *Physiol Rev* **84**: 137–167
- Tornqvist H, Belfrage P (1976) Purification and some properties of a monoacylglycerol-hydrolyzing enzyme of rat adipose tissue. *J Biol Chem* **251**: 813–819
- Unger RH (2003) Minireview: weapons of lean body mass destruction: the role of ectopic lipids in the metabolic syndrome. *Endocrinology* **144**: 5159–5165
- Villena JA, Roy S, Sarkadi-Nagy E, Kim KH, Sul HS (2004) Desnutrin, an adipocyte gene encoding a novel patatin domain-containing protein, is induced by fasting and glucocorticoids: ectopic expression of desnutrin increases triglyceride hydrolysis. *J Biol Chem* **279**: 47066–47075
- Wang SP, Laurin N, Himms-Hagen J, Rudnicki MA, Levy E, Robert MF, Pan L, Oligny L, Mitchell GA (2001) The adipose tissue phenotype of hormone-sensitive lipase deficiency in mice. *Obes Res* **9**: 119–128

- Wong W, Scott JD (2004) AKAP signalling complexes: focal points in space and time. *Nat Rev Mol Cell Biol* **5**: 959–970
- Zhang D, Lu C, Whiteman M, Chance B, Armstrong JS (2008) The mitochondrial permeability transition regulates cytochrome c release for apoptosis during endoplasmic reticulum stress by remodeling the cristae junction. *J Biol Chem* **283**: 3476–3486
- Zhang J, Hupfeld CJ, Taylor SS, Olefsky JM, Tsien RY (2005) Insulin disrupts beta-adrenergic signalling to protein kinase A in adipocytes. *Nature* **437**: 569–573
- Zimmermann R, Haemmerle G, Wagner EM, Strauss JG, Kratky D, Zechner R (2003) Decreased fatty acid esterification compensates for the reduced lipolytic activity in hormone-sensitive lipase-deficient white adipose tissue. *J Lipid Res* **44**: 2089–2099
- Zimmermann R, Strauss JG, Haemmerle G, Schoiswohl G, Birner-Gruenberger R, Riederer M, Lass A, Neuberger G, Eisenhaber F, Hermetter A, Zechner R (2004) Fat mobilization in adipose tissue is promoted by adipose triglyceride lipase. *Science* **306**: 1383–1386

A PKA-ezrin-connexin 43 signaling complex controls gap junction communication in cell fusion

Guillaume Pidoux^{1,2,3,5,6}, Pascale Gerbaud^{1,2}, Jim Dompierre⁴, Birgitte Lygren^{5,6,#}, Therese Solstad^{5,6,+}, Danièle Evain-Brion^{1,2,3} & Kjetil Taskén^{5,6,7,*}

¹INSERM, U767, Paris, F-75006 France; ²Université Paris Descartes, Paris F-75006, France; ³PremUp, Paris, F-75006 France; ⁴CNRS, FRC3115, Centre de Recherche de Gif, IMAGIF, Plateforme de Microscopie Photonique, Gif-sur-Yvette, F-91198, France; ⁵Biotechnology Centre of Oslo and ⁶Centre for Molecular Medicine Norway, Nordic EMBL Partnership, University of Oslo, Oslo N-0317, Norway; ⁷Department of Infectious Diseases, Oslo University Hospital, N-0407 Oslo, Norway

Running title: **Ezrin targets PKA to Cx43 gap junctions**
Character count w/o spaces: 39,787 (ex. Materials and Methods and References)
Display items: 1 table, 9 figures
Supplemental data: Figures S1-S5, Videos 1-3 and Supplemental text with legends

*Corresponding author: Professor, Centre Director Kjetil Taskén, M.D., Ph.D.
Centre for Molecular Medicine, Nordic EMBL Partnership
University of Oslo
P.O. Box 1137 Blindern
N-0318 Oslo, Norway
Tel: +47 22840505
Fax: +47 22840506
E-mail: kjetil.tasken@ncmm.uio.no

^{#,+} Present addresses: [#]Roche Diagnostics, Oslo, Norway and ⁺Norwegian Medicines Agency, Oslo, Norway

ABSTRACT

In the differentiation of the human placenta, mononuclear cytotrophoblasts in a human chorionic gonadotropin (hCG)-driven process fuse to form multinucleated syncytia that allow exchange of nutrients and gases between the maternal and fetal circulation. Experiments displacing protein kinase A (PKA) from A kinase anchoring proteins (AKAPs) or depleting specific AKAPs by siRNA-mediated knock down pointed to ezrin as a scaffold required for cAMP and PKA-mediated regulation of the cell fusion process. By a variety of immunoprecipitation and immunolocalization experiments, we showed that ezrin directs PKA to a molecular complex of connexin 43 (Cx43) and zona occludens-1 (ZO-1), previously shown to form gap junctions implicated in cell fusion. Furthermore, by a combination of knock down and reconstitution experiments with ezrin or Cx43 with or without the ability to bind its interaction partner or PKA, we demonstrate that ezrin-mediated coordination of PKA and Cx43 localization is necessary for discrete control of Cx43 phosphorylation and hCG-stimulated gap junction communication leading to trophoblast fusion.

INTRODUCTION

Cell fusion processes are complex biological phenomena essential in fertilization, fetal development, skeletal muscle formation and bone homeostasis (Midgley et al., 1963; Oren-Suissa and Podbilewicz, 2007; Wakelam, 1985; Zamboni Zallone et al., 1984). Moreover, cell fusion has recently been shown to play a role in the metastatic process (Lu and Kang, 2009). Cell fusion and syncytial formation result in the mixing of plasma membrane components and merging of cell content between two or more cells. Although occurring in different biological contexts, cell fusion processes share many of the same steps (Pérot et al., 2011). First, cells commit to differentiation and start to express specific fusogenic proteins. Next, cells recognize their cell-fusion partner via membrane contacts and gap junction communication is initiated leading to synchronization and exchange of fusogenic signals. Subsequently, this triggers the organization of protein complexes necessary to promote the apposition of the outer lipid monolayers of the two cellular membranes before the opening of a fusion pore and progression to full fusion with mixing of cellular contents (Chernomordik and Kozlov, 2005).

Human embryo implantation requires placentation where fetal cytotrophoblasts in early pregnancy invades the maternal endometrium. Throughout pregnancy cytotrophoblasts fuse to form multinucleated syncytia on chorionic villi extending into the maternal placental blood circulation to form an interphase allowing effective exchange of gases and nutrients (Benirschke and Kaufmann, 2000). Furthermore, syncytiotrophoblasts are the source of the pregnancy hormones human chorionic gonadotropin (hCG) and human placental lactogen (hPL) (Eaton and Contractor, 1993; Ogren and Talamantes, 1994). The *in vivo* fusion process in the placenta is reproducible *in vitro* using purified cytotrophoblasts, which aggregate and then fuse to form non-proliferative, multinucleated, endocrinologically active syncytiotrophoblasts (Kliman et al., 1986). In the last two decades, numerous proteins have been reported to be implicated in cell fusion processes such as tight junction, adherens junction and gap junction proteins. In particular, zona occludens-1 (ZO-1), cadherins and connexins have been described to be involved in the apposition and communication stages prior to cell fusion (Charrasse et al., 2007; Coutifaris et al., 1991; Dahl et al., 1995; Frenedo et al., 2003a; Ilvesaro et al., 2000; Mbalaviele et al., 1995; Pidoux et al., 2010). Moreover, syncytin proteins have been shown to play a fundamental role in placentation, fertilization, myoblast and osteoclast fusion and metastasis

(Bjerregaard et al., 2006; Bjerregaard et al., 2011; Blond et al., 2000; Frendo et al., 2003b; Mi et al., 2000; Soe et al., 2011).

The cAMP signaling pathway is known to play a critical role during trophoblast and myoblast cell fusion (Keryer et al., 1998; Mukai and Hashimoto, 2008). In human placentation, hCG as well as other local factors (activin-A, EGF) stimulate trophoblast fusion in an autocrine or paracrine fashion (Alsat et al., 1993; Gerbaud et al., 2011). Human CG induces production of cAMP in trophoblasts (Keryer et al., 1998; Pidoux et al., 2007a; Pidoux et al., 2007b; Shi et al., 1993), and cell fusion proceeds by activation of protein kinase A (PKA) leading to phosphorylation or increased expression of fusogenic proteins such as syncytins (Chen et al., 2008; Knerr et al., 2005), cadherin (Coutifaris et al., 1991) and connexin (Darrow et al., 1996).

Specificity in the activation of PKA in response to distinct extracellular stimuli is controlled by the intracellular compartmentalization and interaction of PKA with A kinase anchoring proteins (AKAPs) (Michel and Scott, 2002; Pidoux and Tasken, 2010; Tasken and Aandahl, 2004; Wong and Scott, 2004). All AKAPs contain an A kinase binding domain (AKB) and a specific targeting domain localizing the PKA-AKAP complex to defined subcellular structures, membranes or organelles (Carr et al., 1992; Gold et al., 2006). Distinct subcellular targeting of type I and type II PKA isozymes provides spatial and temporal regulation of different PKA signaling events by controlling the phosphorylation of specific substrates as delineated by the use of anchoring disruptor peptides that specifically displaces either type I or type II PKA (Carlson et al., 2006; Gold et al., 2006; Ruppelt et al., 2007). In addition, AKAPs form supramolecular signaling complexes by scaffolding other kinases than PKA, protein phosphatases, cAMP phosphodiesterases (PDEs) and other proteins involved in signal transduction (Coghlan et al., 1995; Dodge et al., 2001; Schillace and Scott, 1999; Tasken et al., 2001). Through this essential role in the spatial and temporal integration of effectors and substrates, AKAPs provide a high level of specificity and temporal regulation to the cAMP-PKA-signaling pathway.

Some studies have stipulated the presence of AKAPs in trophoblasts and placenta (Keryer et al., 1998; Weedon-Fekjær and Taskén, 2011). However, no AKAPs have to date been identified to be involved in controlling cell fusion processes in general or trophoblast fusion in particular. Here, we

show that ezrin, first described in the placenta (Bretscher, 1989) and characterized as an AKAP for both type I and type II PKA (Dransfield et al., 1997; Ruppelt et al., 2007), organizes a supramolecular complex with PKA, connexin 43 and ZO-1 which controls the hCG-stimulated gap junction communication that precedes human trophoblast fusion. Ezrin belongs to the ERM (Ezrin-Radixin-Moesin) family of proteins. These proteins are known to connect cytoskeleton filaments to the plasma membrane but also to organize and scaffold protein complexes and signaling effectors. The N-terminal part of the protein contains a FERM domain, which is known to contact transmembrane proteins such as CD44 and ICAMs as well as the adaptor protein EBP50 (Reczek et al., 1997). The central region of the protein is shown to contain an AKB domain binding PKA (Carlson et al., 2006; Ruppelt et al., 2007) and the C-terminal part to interact with F-actin filaments. The interaction with PKA is possible when ezrin is in an “open” conformation promoted by the phosphorylation of the C-terminal threonine residue (T567) (Fievet et al., 2004; Ruppelt et al., 2007).

Communication between adjacent cells can occur via gap junctions, which are composed of connexin (Cx) hexamers in the membrane that align with similar structures on neighboring cells to form gap junction channels that allows for exchange of ions, metabolites and second messengers facilitating coordination of proliferation, differentiation and spatial compartmentalization (Bruzzone et al., 1996; Saez et al., 1993; Willecke et al., 2002). Interestingly, Cx43 was shown to be the one of the key gap junction proteins expressed in fusion competent human cytotrophoblasts (Cronier et al., 2002; Cronier et al., 2003; Dunk et al., 2012; Frendo et al., 2003a). Here, we report a direct interaction between ezrin and Cx43 in trophoblasts and demonstrate that the anchoring of PKA through ezrin is necessary to mediate discrete control of Cx43 phosphorylation and hCG-stimulated gap junction communication leading to trophoblast fusion.

RESULTS

The cAMP-PKA signaling pathway is involved in trophoblast fusion

In order to establish the temporal effect of hCG, cAMP and PKA on cell fusion of primary cytotrophoblasts from the human placenta, cells were cultured for 72 h in the absence or presence of hCG, 8-Br-cAMP or H89 (protein kinase A inhibitor). Mononuclear cytotrophoblasts spontaneously aggregated at 24 h of culture and fused to form multinucleated syncytia at 72 h (syncytiotrophoblast) as evident from microscopy with immunostaining for desmoplakin to visualize cellular membranes (green) and nuclear counterstaining (DAPI, blue) (Fig. 1A, quantified by number of mononuclear cells and fusion index). In contrast, trophoblasts treated with 8-Br-cAMP or hCG presented syncytia already after 24 h of culture indicating that the fusion is accelerated (Fig. 1A) as evident from reduced numbers of mononuclear cells (24% and 15% respectively, $p < 0.001$) compared to control (37.5%) and increased syncytialisation (fusion index up 30%, $p < 0.001$). To assess the effect of PKA cultures were treated with H89, which allowed aggregation of cells but blocked fusion even at 72 h of culture. This may indicate that also the spontaneous fusion is cAMP-driven, which was further corroborated as loading of cytotrophoblasts with a cell-permeable version of the protein kinase inhibitor (PKI), a highly specific inhibitor of PKA, had the same effect (Fig. S1A). Furthermore, H89 and PKI also inhibited hCG-stimulated fusion. The cell fusion process is accompanied by a functional differentiation involving secretion of the pregnancy hormones, hCG and hPL from the syncytialized cells (Fig. 1A). Treatment with 8-Br-cAMP increased the hCG secretion compared to the control ($p < 0.001$) at 24 h and 72 h of culture, confirming accelerated syncytial formation in cAMP-treated cultures. Similarly, the role of exogenously added hCG in stimulating syncytial formation was confirmed by increased levels of hPL secretion at 24 h ($p < 0.025$). Moreover, treatment with H89 decreased the hormonal secretion as expected from its inhibitory effect on syncytial formation. Similar effects were also observed with PKI (Fig. S1).

We next examined the effect of cAMP signaling through Epac on syncytialization of primary cells by using cAMP analogues specific for PKA or Epac. As shown in Fig. S1A and B, the Epac agonist (8-pCPT-2'-O-Me-cAMP) activated syncytialization (1.4-fold increase, $p < 0.001$) and hormonal secretion (2-fold increase, $p < 0.001$). The PKA-selective 6-Bnz-cAMP analogue also

induced cell fusion (1.8-fold, $p < 0.001$) but with little or no effect on hormonal secretion. Together, our data indicate distinct effects of PKA and Epac activation on the differentiation of primary trophoblasts. In the following we have examined in more detail the action of this particular pool of PKA.

Effect of PKA anchoring disruptor peptides on the trophoblast fusion process

To assess the effect of PKA anchoring on hCG-stimulated cell fusion we used the Arg-tagged, cell-permeable versions of the high-affinity anchoring disruptor peptides RI Anchoring Disruptor (RIAD) and SuperAKAP-*IS* to specifically delineate effects mediated by anchored type I or type II PKA, respectively (Carlson et al., 2006; Gold et al., 2006). Optimal peptide concentration (5 μM) and loading conditions (60 min) for effective intracellular delivery ($>95\%$ w/o toxicity) were determined in separate experiments (Fig. S1C and D). Cytotrophoblast cultures pre-incubated with either RIAD or SuperAKAP-*IS* peptides presented significantly less cell fusion and hPL secretion after stimulation with hCG than cultures loaded with scrambled controls (30-40% increase in mononuclear cells, $p < 0.001$; 40-45% reduction in fusion index, $p < 0.001$; 70% reduction in hPL, $p < 0.001$) (Fig. 1B) suggesting specific roles for pools of AKAP-anchored type I and type II PKA in the hCG-stimulated trophoblast fusion. Cytotrophoblast cell cultures treated with a peptide derived from the RI specifier region (RISR) of dual-specific AKAPs that disrupts the interaction with type I PKA (Jarnaess et al., 2008) also showed a reduction in cell fusion and hPL secretion compared to cultures incubated with scrambled control (40% increase in mononuclear cells, 45% reduction in fusion index and reduction in hPL secretion, $p < 0.001$) (Fig. 1B). Similar effects of the anchoring disruptor peptides (RIAD, SuperAKAP-*IS* and RISR) were observed on 8-Br-cAMP-stimulated trophoblast fusion (Fig. S1E).

Identification of trophoblast AKAPs

To identify AKAPs involved in the cell fusion process, we isolated cAMP-signaling complexes from cultured cytotrophoblasts and syncytiotrophoblast either by pull down of cAMP binding proteins using 8-AHA-cAMP-agarose beads or by flag-affinity chromatography after incubation with purified flag-tagged RI and RII and subjected size-fractionated SDS-PAGE bands after tryptic digestion to nanoLC-

LTQ Orbitrap mass spectrometry (MS) analysis. Database searches against UniProt identified D-AKAP2 and ezrin after cAMP-pulldown, but with Mascot scores below 30 (not shown). RI- or RII-pulldown proved to be more sensitive and identified nine AKAPs in cytotrophoblasts including ezrin, five of which were also identified in syncytiotrophoblast extracts (Table 1). A screen by siRNA knock down of the 10 AKAPs identified by cAMP or RI/RII-pulldown allowed us to analyze the involvement of 7 of these, where the knock down was more than 50%, in regulation of cell fusion (Fig. 1C). This analysis showed that ezrin knock down inhibited fusion most potently, but significant effects were also seen for AKAP450 and myomegalin knock down in agreement with the data from the anchoring disruption studies that indicated the involvement of more than one AKAP. Ezrin fits the description of an AKAP candidate with known membrane association that could bind both type I and type II PKA and contained a RISR domain and was also isolated both in the cAMP as well as in RI- and RII-affinity purification experiments. We therefore focused our efforts on examining the role of ezrin in coordinating cAMP regulation of cell fusion. D-AKAP2 (AKAP10) identified by mass spectrometry in the first cAMP-pull down experiments, is also a membrane-associated, dual-specific AKAP with a RISR domain and was included as control.

PKA anchoring to ezrin is required for its effect on trophoblast fusion

Focussing on the possible requirement of ezrin as an AKAP for PKA regulation of trophoblast fusion as suggested from the data in Fig. 1C, cytotrophoblasts were transfected with ezrin or D-AKAP2 siRNA and corresponding scrambled controls and incubated for 48 h (Fig. 2, Supplement Fig. S2A-D). SiRNA-mediated knock down of ezrin or D-AKAP2 reduced protein expression by approximately 90% after normalization to actin levels and compared to cells transfected with scrambled siRNA ($p < 0.001$) (Fig. S2A-B). While knock down of ezrin decreased trophoblast fusion and reduced production of syncytial hormones (hCG and hPL) (Fig. 2, Fig. S2A and C-D), knock down of D-AKAP2 did not (Fig.1D and Fig. S2C-D). Levels of the ERM family members radixin and moesin, homologous to ezrin, were not regulated during the differentiation and fusion process (data not shown), nor were there any compensatory changes following ezrin knock down (Fig. S3A) or in ezrin levels or cell fusion

upon knockdown of radixin or moesin although moesin knock down affected radixin levels (Fig. S3C).

To further assess the role of ezrin as a putative AKAP in trophoblast fusion, we employed a combined strategy of RNA interference and reconstitution experiments with modified forms of ezrin. Cytotrophoblasts were depleted of endogenous ezrin by siRNA transfection. Concomitantly, mammalian expression vectors were introduced in the cytotrophoblasts encoding wild type ezrin or ezrin-T567D (open conformation that binds PKA) fused to green fluorescent protein and made insensitive to functional siRNA (GFP-ezrin[#] and GFP-ezrin*, respectively) with or without substitutions that block PKA binding (K359A, K360A, R381A, L421P; GFP-ezrin*-AKBmut) (Fig. 2) (Jarnaess et al., 2008). Transfection efficiency was determined to be above 45% with all expression vectors (data not shown). Interestingly, cells with endogenous ezrin knocked down and reconstituted with siRNA-insensitive GFP-ezrin[#] or GFP-ezrin* (Fig. 2A) formed syncytia (Fig. 2B, GFP-positive cells (green) and data on mononuclear cells and fusion index). In contrast, cytotrophoblasts reconstituted with GFP-ezrin*-AKBmut displayed aggregated, but not fused cells as evident from microscopy as well as the increased number of remaining mononuclear cells and low fusion index. Similarly, levels of secreted hCG and hPL were restored in cells reconstituted with GFP-ezrin[#] or GFP-ezrin* but not with GFP-ezrin*-AKBmut (Fig. 2C). Together our knock down and reconstitution experiments suggest that ezrin through anchoring of PKA plays a key role in the regulation of trophoblast fusion.

Ezrin co-localizes with PKA, connexin 43 and ZO-1

A complex of the gap junction protein connexin 43 (Cx43) and the tight junction protein ZO-1 is shown to play an important role in trophoblast fusion (Frendo et al., 2003a; Pidoux et al., 2010). For this reason, we investigated the possibility of a physical interaction between PKA, ezrin and the Cx43/ZO-1 complex. Immunoprecipitation of ezrin isolated RI α , RII α , phosphorylated Cx43 and ZO-1 (Fig. 3A). Conversely, immunoprecipitation of Cx43 or ZO-1 pulled down ezrin, phosphorylated ezrin T567 and PKA (Fig. 3B-C). Moreover, immunoprecipitation of RI α and RII α co-precipitated ezrin, phospho-ezrin T567, Cx43 (mainly the phosphorylated P1/P2 forms) and ZO-1 (Fig. 3D and

3E), whereas none of the interaction partners were co-precipitated with control rabbit or mouse IgG in parallel experiments (Fig. S3B). Our results indicate that ezrin forms a supramolecular complex with RI α , RII α , the P1/P2 forms of Cx43 and ZO-1 in trophoblasts (Fig. 3F) and a significant proportion of the immunoprecipitated ezrin appeared to be phosphorylated on T567 (Fig. 3A-E) in line with the notion that it is ezrin in the open conformation interacts with PKA as well as its other partners. In order to validate the hypothesis that ezrin and Cx43 form a macromolecular complex, bands from SDS-PAGE of Cx43 immunoprecipitates were subjected to tryptic digestion and nanoLC-LTQ Orbitrap MS analysis. This approach identified ezrin, ZO-1 and Cx43 in the Cx43 precipitates (Fig. 3G, we did not search for PKA as it co-migrates with and would be diluted by IgG heavy chain).

To examine the co-localization of the complex partners ezrin, PKA, Cx43 and ZO-1 inside the cell, we next incubated permeabilized cells with pairs of specific antibodies followed by proximity ligation assays (PLA, Fig. 4A'-I'). This method is based on the ligation and amplification of DNA tags fixed to secondary antibodies and detected by hybridization with a fluorescently labeled probe (red) which proceeds when two protein targets are in a proximity range of 40 nm or less (Soderberg et al., 2006). Cell membranes were stained with Wheat Germ Agglutinin conjugated to Alexa Fluor 488 (green, Fig. 4A-I), in order to observe cell outlines. PLA experiments demonstrated Cx43 to be in close proximity to ezrin (Fig. 4A'), PKA type I and II (Fig. 4B'-C') and ZO-1 (red, Fig. 4D', previously reported) as evident from the appearance of red dots. Physical proximity was also demonstrated for ezrin *versus* type I and type II PKA and ZO-1 as well as for PKA type I and II *versus* ZO-1 (Fig. 4E'-I'). The intensity of red signal and density of dots indicating proximity ligation was high for ezrin-PKA and Cx43-ZO-1 as well as for ezrin-Cx43, somewhat weaker for Cx43-PKA and ezrin-ZO-1 and weakest for PKA-ZO-1 which may reflect the distance between the interaction partners (Fig. 4J). In contrast, PLA did not result in any staining when either one or the other antibody was omitted from each pair or one antibody substituted with an antibody to the nuclear protein SP1 (Fig. S3E-L'). Nor did pairs of mouse and rabbit IgG primary antibodies produce any signal (Fig. S3D-D'). Furthermore, separate immunostaining of each protein studied revealed localizations that could overlap, although both PKA and ezrin appeared to have a wider distribution than Cx43 and in particular ZO-1, which could indicate that the fraction of the total cellular amount of each binding

partner going into this complex could vary (Fig. S3M-T). In addition, PLA experiments for ezrin *versus* PKA (RI α and RII α) showed a decrease in signal intensity during the fusion process between individual, aggregated and fused trophoblasts consistent with a loss of interaction after the anchored pool of PKA had exerted its effect in regulation of fusion (Fig. S4A). Finally, *in situ* dual-immunofluorescence studies were performed to examine the expression of ezrin in human placental tissue with antibodies against ezrin and cytokeratin 7 (CK7), a specific marker of trophoblasts. This experiment demonstrated that ezrin is not only located at the surface of the villi in the syncytiotrophoblast where it is involved in microvilli formation as previously reported, but also at the apical pole of the mononucleated cytotrophoblasts at the junction to the syncytium, where cell fusion occurs and Cx43 or ZO-1 have earlier been reported to localize (Fig. 4K-P).

Control of gap junction communication by an anchored pool of PKA

Cx43 is the only gap junction protein expressed in human cytotrophoblasts able to fuse and differentiate to syncytiotrophoblasts (Cronier et al., 2002; Cronier et al., 2003; Dunk et al., 2012; Frenzo et al., 2003a). Its phosphorylation by PKA, MAP kinase and protein kinase C is speculated to differentially regulate gap junction assembly, communication and recycling (Solan and Lampe, 2009). Here, we examined the role of anchored PKA by incubation with Arg-tagged, cell-permeable anchoring disruptor peptides RIAD, SuperAKAP-*IS* or a combination in hCG-stimulated trophoblasts and found that this strongly reduced the levels of phosphorylated Cx43 (P1/P2) compared to untreated cells and cells treated with scrambled controls (Fig. 5A, left panel). As positive control, cells were incubated with Arg-tagged PKI, which also reduced Cx43 phosphorylation (Fig. 5A, right panel).

We next analyzed the effect of Arg-tagged, cell-permeable PKA anchoring peptides on gap junctional communication between trophoblasts following hCG stimulation (Fig. 5B and Video 1). Bleaching of isolated trophoblasts after incubation with red fluorescent calcein dye that is transferred via gap junctions allowed for the assessment of gap junction communication by fluorescence recovery after photobleaching (gap-FRAP analysis) (Pidoux et al., 2010). Partial recovery of the fluorescence representing reentry of unbleached fluorescent dye through gap junctions was observed after 500 s (post-bleach) in hCG-treated control cells, but not in cells treated with the gap junction blocker β -GA,

the PKA inhibitor PKI or the PKA anchoring disruptors RIAD or superAKAP-1S (Fig. 5B and Video 1). The observed regulation of gap junction communication by hCG, cAMP, PKI or anchoring disruptor peptides was not due to a relocalization or degradation of Cx43 from the cellular membrane as evident from Cx43 and desmoplakin (DSK) co-localization by PLA (Fig. S4B). Together these data suggest that the activity of an anchored pool of PKA is necessary for discrete control of Cx43 phosphorylation as well as gap junction communication.

Identification of ezrin and Cx43 binding motifs

Based on the co-precipitation and co-localization data, we next studied the possibility of a direct interaction between ezrin and Cx43 (Fig. 6). First we examined interaction *in vitro* by incubating purified His-ezrin T567D with GST-Cx43 or GST. Anti-His immunoprecipitation revealed the presence of both His-ezrin and GST-Cx43 in the precipitate (Fig. 6A, left panel), whereas GST was not precipitated with His-ezrin. The reciprocal anti-GST immunoprecipitation revealed the co-precipitation of His-ezrin with GST-Cx43 (Fig. 6A, right panel), suggesting that ezrin and Cx43 are able to interact directly. To more precisely define the binding regions of ezrin and Cx43, we synthesized libraries of 20-mer overlapping peptides with 3-amino acid shifts of the whole ezrin and Cx43 amino acid sequences on solid phase and overlaid with recombinant GST-Cx43 or GST-ezrin (T567D), respectively, and using GST as control (Fig. S5A). Identified binding regions (amino acids 493 to 527 in ezrin and amino acids 352 to 382 in Cx43) that interacted specifically with its GST-fused binding partner but not with GST alone, were next analyzed in more detail by overlay of overlapping peptide libraries with one residue offset (Fig. 6B) combined with N- and C- terminal truncations and proline substitution scans to reveal the minimal interaction sites (Fig. S5B-D). Together, this identified the minimal binding motifs ⁵¹⁰DDRNEEKR⁵¹⁷ in ezrin and ³⁶⁶RASSR³⁷⁰ in Cx43. Interestingly; the ezrin-binding site in Cx43 overlapped with its putative PKA phosphorylation sites (S364, S365, S368, S369, S372 and S373). A two-dimensional peptide array substitution analysis was also performed for the ezrin-Cx43 contact sites (Fig. S5E) and identified residues D510 and R517 in ezrin and R370 in Cx43 as indispensable for binding. Indeed, peptide substitutions D510I and R517V in ezrin or R370E in Cx43 peptides synthesized on solid phase abolished binding to Cx43 and

ezrin, respectively (Fig. 6C). We next generated a mammalian cell expression vector that directed expression of siRNA-resistant GFP-ezrin* D510I-R517V (Fig. 6D). When cytotrophoblasts with ezrin knock down were reconstituted with GFP-ezrin* D510I-R517V, this did not rescue the effect of ezrin siRNA on cell fusion (Fig. 6E, left), which is in contrast to reconstitution with GFP-ezrin* (see Fig. 2). Similarly, the expression of GFP-ezrin* D510I-R517V did not rescue hormonal secretion (Fig. 6E, right). Together, these data indicate that the ezrin interaction with Cx43 is required for the cell fusion process.

hCG-stimulated gap junction communication requires ezrin-mediated targeting of PKA to Cx43

To assess the ability of exogenously introduced GFP-ezrin to form a complex with endogenous PKA, Cx43 radixin, moesin or actin, immunoprecipitations were performed from cell lysates of cytotrophoblasts co-transfected with ezrin siRNA and siRNA-resistant GFP-ezrin*, GFP-ezrin*-AKBmut or GFP-ezrin*-D510I-R517V (Fig. 7A). Immunoprecipitation with GFP antibody showed the presence of GFP-ezrin, and actin in precipitates from cells expressing either GFP-ezrin*, GFP-ezrin*-AKBmut or GFP-ezrin*-D510I-R517V indicating that all expressed proteins localize normally and interact with actin. PKA RI α and RII α only coprecipitated with GFP-ezrin* and GFP-ezrin*-D510I-R517V but not with GFP-ezrin*-AKBmut which indicates that ezrin with substitutions in PKA-binding sites does not interact with PKA *in situ*. Furthermore, Cx43 was found associated with GFP-ezrin* and GFP-ezrin*-AKBmut but not with GFP-ezrin*-D510I-R517V indicating that mutations in Cx43-binding site abolished the interaction of Cx43 with ezrin *in situ*. Finally, neither radixin nor moesin coprecipitated with any GFP-ezrin variants in cells treated with ezrin siRNA, which indicates that none of the other ERM family proteins were present in the complex.

In order to test the possibility that the control of gap junction communication by anchored PKA is mediated by ezrin, we next performed gap-FRAP analysis of hCG-stimulated trophoblasts with ezrin knock down alone or combined with expression of GFP-ezrin variants (Fig. 7B and Video 2). Cytotrophoblasts transfected with ezrin siRNA, but not scrambled control, lost gap junction communication. However, trophoblasts with ezrin knock down reconstituted with GFP-ezrin[#] (siRNA insensitive, wild type) or GFP-ezrin* (siRNA insensitive and T567D) partially recovered gap junction

communication. In contrast, reconstitution with ezrin variants where the PKA binding site or the Cx43 interaction site was mutated (GFP-ezrin*-AKBmut or GFP-ezrin*-D510I-R517V) did not restore hCG-induced gap junction communication. PLA experiments for Cx43 *versus* DSK did not reveal any differences in signal intensity indicating that the observed reduction of gap junction dye transfer induced by ezrin siRNA was not due to a modification of gap junction assembly or an increase in degradation of Cx43 (Fig. S4C). Moreover, RNA interference and reconstitution experiments with modified forms of ezrin did not alter moesin or radixin protein expression level (Fig. S3A). Lastly, levels of desmoplakin and E-cadherin, known to be involved in cell adhesion were not significantly affected by ezrin knock down or ezrin reconstitution indicating that the aggregation process was not altered (Fig. S4D). In summary, our knock down and reconstitution experiments suggest that ezrin by anchoring PKA and binding to Cx43 provides hCG-regulated spatiotemporal control of Cx43 phosphorylation and gap junction communication, which is intimately linked to cell fusion and syncytial formation (Fig. 7B).

hCG-stimulated gap junction communication requires phosphorylation by an Cx43- and ezrin anchored pool of PKA

In order to extend the testing of our hypothesis that control of gap junction gating by anchored PKA is mediated through the anchoring of ezrin to Cx43, we also performed cell fusion and gap junction communication assays on hCG-stimulated trophoblasts depleted of endogenous Cx43 by siRNA transfection. Concomitantly, mammalian expression vectors were introduced encoding Cx43 fused to green fluorescent protein and made insensitive to functional siRNA (GFP-Cx43[∞]) with or without substitutions that abolish ezrin binding (R370E; GFP-Cx43[∞]-R370E) and/or serine substitutions in all (6SD, 6SA) or some of the six confirmed or putative phosphorylation sites in residues 364, 365, 368, 369, 372 and 373 that possibly could be phosphorylated by anchored PKA (see Fig. 6C and S4F for details of substitutions). As previously observed, cytotrophoblasts transfected with Cx43 siRNA aggregated but did not fuse to form syncytia (Fig. 8A-C). However, cells reconstituted with siRNA-insensitive GFP-Cx43[∞] after knock down of endogenous Cx43 formed syncytia (Fig. 8A-C). In contrast, cytotrophoblasts reconstituted with GFP-Cx43[∞]-R370E that does not bind ezrin aggregated

but did not fuse (Fig. 8A-C). However, cells reconstituted with mammalian expression vectors encoding GFP-Cx43 with the six serine phosphorylation sites substituted with aspartates to mimic phosphorylation (GFP-Cx43[∞]-6SD) fused whereas cells where the six serines were substituted with alanines to block phosphorylation (GFP-Cx43[∞]-6SA) did not. In both cases, the additional introduction of the R370E substitution to block ezrin binding altered the composition of the complex in immunoprecipitations (Fig. 9A), but did not change the phenotype introduced by the expression of GFP-Cx43[∞]-6SD or -6SA indicating that when all the phosphorylation sites were altered the absence or presence of ezrin binding no longer had an effect (Fig. 8B and C).

Since it is not fully elucidated what residues in Cx43 that are phosphorylated and by which kinases (Solan and Lampe, 2009), we chose first to alter all of the putative PKA phosphorylation sites in the region 364 to 373. However, although this region is predicted to be structurally disordered (Solan and Lampe, 2009) and the Cx43-6SD and Cx43-6SA substituted molecules behaved as expected from our hypothesis, we aimed also to reduce the number of substitutions to minimize their effect. For that reason, we also looked specifically at the role of serines 364, 365 and 368 where there are more reports of a regulatory role for PKA. When doing so, we included the R370E substitution to inhibit ezrin binding and avoid targeting of PKA that could phosphorylate remaining serines. Cytotrophoblasts with endogenous Cx43 knock down reconstituted with siRNA-insensitive GFP-Cx43 with serine substitutions mimicking phosphorylated residues in position 364, 365, 368 or the combination without the ability to anchor ezrin (GFP-Cx43[∞]-S364D-R370E, GFP-Cx43[∞]-S365D-R370E, GFP-Cx43[∞]-S368D-R370E or GFP-Cx43[∞]-3SD-R370E) formed syncytia (Fig. 8D). In contrast, cells reconstituted with siRNA-insensitive GFP-Cx43 with either one or all three serines inactive by alanine substitutions (GFP-Cx43[∞]-S364A-R370E, GFP-Cx43[∞]-S365A-R370E, GFP-Cx43[∞]-S368A-R370E or GFP-Cx43[∞]-3SA-R370E) displayed aggregated, but not fused cells as evident from the increased number of mononuclear cells and low fusion index (Fig. 8D). Together these knock down and reconstitution experiments suggest that Cx43 need the anchoring of ezrin and the phosphorylation of PKA to control trophoblast fusion and that one or more phosphorylation events directed at serines in the region 364-373 may activate Cx43 communication and subsequent fusion.

However, to what extent multiple phosphorylations of Cx43 may affect the efficacy of communication is not evident from the present data.

In order to characterize in more detail the effect of manipulating the association between ezrin and Cx43 or the level of Cx43 phosphorylation on control of gap junction communication, gap-FRAP analyses were performed of hCG-stimulated trophoblasts with Cx43 knock down alone or combined with expression of GFP-Cx43 variants that formed complexes with the expected composition (9A-B and Video 3). Cytotrophoblasts transfected with Cx43 siRNA, but not scrambled control, lost gap junction communication, as previously described (Charrasse et al., 2007; Coutifaris et al., 1991; Dahl et al., 1995; Frendo et al., 2003a; Ilvesaro et al., 2000; Mbalaviele et al., 1995; Pidoux et al., 2010). However, trophoblasts with Cx43 knock down reconstituted with GFP-Cx43[∞] (siRNA insensitive), or the phosphomimicking GFP-Cx43[∞]-6SD or GFP-Cx43[∞]-6SD-R370E recovered gap junction communication independently of the ezrin association. In contrast, reconstitution with Cx43 variants where the ezrin binding interaction site was altered to block ezrin binding alone (GFP-Cx43[∞]-6SD-R370E) or in combination with substitutions to mimic unphosphorylated serines in Cx43 (GFP-Cx43[∞]-6SA or GFP-Cx43[∞]-6SA-R370E) did not restore hCG-induced gap junction communication (Fig. 9B-D). PLA experiments for GFP *versus* DSK revealed a strong signal between GFP-Cx43 and desmoplakin indicating that the GFP-tagged Cx43 localized to gap junctions. Moreover, the signal intensity did not reveal any differences between cultures that received different treatment conditions indicating that the observed reduction of gap junction dye transfer induced by Cx43 siRNA or reconstitutions with various GFP-Cx43 variants were not due to a modification of gap junction assembly to the membrane or an increase in degradation of Cx43 (Fig. S4E).

DISCUSSION

Here, we report the identification of ezrin as a component of the Cx43/ZO-1 complex that targets PKA to the complex and thereby facilitates hCG-mediated Cx43 phosphorylation and regulation of gap junction communication leading to trophoblast fusion. While hCG and cAMP are known to induce syncytialization (Keryer et al., 1998; Shi et al., 1993), we established here the kinetics of the hCG and cAMP regulated trophoblast fusion and showed that PKA activation is required. We next displaced compartmentalized PKA by specific anchoring disruptor peptides and demonstrated that the trophoblast fusion activated by the hCG-cAMP-PKA pathway is mediated through anchored pools of both type I and type II PKA. This indicated the involvement of AKAPs specific for both type I and type II PKA or one or more dual-specific AKAPs with a RISR region (Jarnaess et al., 2008) that anchors separate pools of type I and type II PKA in the cell fusion process. A compartmentalized pool of PKA was also required for the endocrine function of the syncytiotrophoblast. In contrast, the use of an Epac agonist indicated that Epac markedly enhanced hormone secretion and to a lesser extent trophoblast fusion which would suggest a different site of interaction. This observation is supported by recent work by Chang et al. where Epac was shown to stimulate the expression of the fusogenic proteins syncytin 1 and 2 and glial cell missing 1 protein (GCM1)-dependent cell fusion (Chang et al., 2011). Together, the available data support the involvement of both PKA and Epac in the control of the cell fusion process, and the possibility of crosstalk between the two signaling pathways in cell fusion and hormone secretion exists.

Several AKAPs have earlier been reported from the human placenta (Weedon-Fekjær and Taskén, 2011). Here we used a chemical proteomics approach with immobilized cAMP or PKA regulatory subunit affinity purification followed by mass spectrometry to characterize the pool of AKAPs available in trophoblasts at the time of cell fusion and identified 10 different AKAPs by the two approaches. However, none of these AKAPs were previously known to be involved in cell fusion. Consequently, the identified AKAPs were tested for their putative role in cell fusion by siRNA knock down, which demonstrated a possible involvement of ezrin, myomegalin, and AKAP450. The identification of both a dual-specific AKAP with a RISR domain (ezrin) and type II-specific AKAPs (AKAP450 and myomegalin) were consistent with the anchoring competitor data. Furthermore, it is

interesting to speculate that myomegalin and AKAP450 that have been described to regulate cytoskeletal organization possibly could be involved in the cell fusion process by mediating control of the necessary cytoskeletal rearrangements. However, since ezrin was the only one of these three AKAPs known to be co-localized with proteins in the plasma membrane we chose to focus on the role of ezrin in cell fusion.

By co-immunoprecipitation and ligand proximity assays we could show that ezrin, and in particular phospho-ezrin T567, is located in a supramolecular complex that includes PKA, the gap junctional protein Cx43 and the tight junctional protein ZO-1. Dynamic studies of the localization of ezrin and PKA relative to one other by ligand proximity assays revealed a decreased association between ezrin and PKA during the process of cell fusion. Interestingly, levels of ezrin/RI colocalization were comparable lower than those of ezrin/RII reduced in syncytia, an observation that could be explained either by the decrease in RI α protein expression post fusion (Keryer et al., 1998; Mukai and Hashimoto, 2008) or by the faster off-rate of RI from ezrin (Ruppelt et al., 2007). We next identified the reciprocal binding motifs in ezrin and Cx43 by peptide array analysis and mutational studies. The Cx43-binding domain in ezrin (amino acids 510-517) is in the proximity of the C-terminal actin-binding region (Saleh et al., 2009). However, association of Cx43 to ezrin did not interfere with the binding of actin to ezrin. The ezrin-binding domain of Cx43 (amino acids 366-370) overlaps with the PKA phosphorylation sites (364S, 365S, 368S, 369S, 372S and 373S) in the C-terminal part of the Cx43 (Solan and Lampe, 2009; TenBroek et al., 2001; Yogo et al., 2006), but introduction of combinations of phosphoserine in these positions in sets of peptides synthesized on solid phase did not appear to affect binding to ezrin (data not shown). In contrast, PKA phosphorylation of phospholamban affects its interaction with AKAP18 δ (Lygren et al., 2007). By silencing and reconstitution experiments, we demonstrated a central role of ezrin in trophoblast fusion and gap junction communication. However, reconstitution with mutant ezrin with impaired ability to bind either PKA or Cx43 did not restore communication. Furthermore, reconstitution experiments with mutant Cx43 that could not bind ezrin produced similar results inferring that association between the two proteins is also critical. In summary, loss of PKA from the ezrin/Cx43/ZO-1 supramolecular complex appears to prevent the exchange of fusogenic signals between cells and consequently the

human cell fusion and syncytial formation. Studies to explore the involvement of this molecular complex in other cell fusion processes would be needed to determine how general the observed regulatory mechanism that involves ezrin is. However, it is interesting to speculate that PKA anchored via ezrin also could control gap junction communication in heart, where Cx43 has been shown to be involved in providing electrical conductance necessary for excitation (Gutstein et al., 2001; Saffitz and Kleber, 2004).

Ezrin is a member of the ERM family protein and is regulated by the phosphorylation of a threonine residue located in the C-terminal part (T567). In the unphosphorylated state, the ezrin N- and C-terminal domains interact to prevent partners binding to ezrin. Upon phosphorylation of T567, ezrin changes its conformation from an inactive state to an open and active form, which allows interaction with cellular partners including PKA (Arpin et al., 2011; Ruppelt et al., 2007). This conformational change also enhances mobility, allowing relocalization in T cells (Ruppelt et al., 2007) and is associated with changes in cellular morphology (Brown et al., 2003; Cullinan et al., 2002). It appeared to be the open form of ezrin (pT567) that was involved in the organization of the macrocomplex composed with Cx43, PKA and ZO-1. For that reason we used both wild type ezrin and an ezrin construct with the T567D substitution in the reconstitution experiments to allow binding of PKA.

In situ, we observed high levels of ezrin at the apical pole of the syncytiotrophoblast in the microvillus structure, confirming previous studies (Berryman et al., 1993). Interestingly, we also observed expression at the apical pole of the cytotrophoblasts where the junction between mononuclear cells and the syncytiotrophoblast are formed. This observation supports the notion of a role for ezrin in coordinating PKA-regulated gap junction communication. ERM proteins, and specially ezrin and moesin, may be functionally redundant in some biological contexts (Takeuchi et al., 1994). However, we found ezrin to be the only ERM family protein member involved in the control of gap junction gating. Indeed, silencing and reconstitution experiments with ezrin did not shown any changes in the levels of radixin and moesin, which were found to be absent from the ezrin/Cx43 macromolecular complex. Moreover radixin and moesin silencing experiments did not affect trophoblast fusion. These observations are supported by other studies demonstrating different

ERM proteins to play specific cellular roles in some contexts without any redundancy (Bonilha et al., 2006; Saotome et al., 2004). Ezrin is a scaffold protein playing an important role in regulation of cell polarity, morphology, division and adhesion. However, we did not observe altered cell morphology upon ezrin knock down. Indeed, as primary trophoblasts are non-proliferative (Kliman et al., 1986) ezrin silencing would not be expected to affect cell polarity or division. While ezrin localized to the apical pole of cytotrophoblasts *in situ*, it was more widely located in cell culture where trophoblasts can potentially fuse with all neighboring cells. Finally, we demonstrated that ezrin silencing and reconstitution experiments did not affect expression of adhesion proteins at the cell membrane in aggregated cells, which argues against loss of trophoblast adhesion in cells with ezrin knock down.

Cx43 is phosphorylated by several kinases including PKA (Jordan et al., 1999; Shah et al., 2002) and activation of PKA by an intracellular increase in cAMP is shown to increase gap junctional communication (Burghardt et al., 1995; Nnamani et al., 1994; Saez et al., 1986). Furthermore, this increase in junctional conductance appears to be elicited by PKA phosphorylation of Cx43 on S364, which enhances gap junction assembly (Davies et al., 2000; Makaula et al., 2005; Paulson et al., 2000; TenBroek et al., 2001). Here, we observed an effect of anchored PKA on gap junction conductance linked to Cx43 phosphorylation whereas PKA did not appear to regulate gap junction assembly or stability as the Cx43 levels remained constant. By silencing and reconstitution experiments with various Cx43 mutants, we demonstrated that the loss of ezrin anchoring to wild type Cx43 impaired gating and cell fusion. In contrast, reconstitution with mutants of Cx43 with one or more phosphoserine-mimicking substitutions in the PKA phosphorylation sites made the interaction with ezrin and PKA redundant and restored gap junction communication and cell fusion indicating that the role of ezrin is to serve as an AKAP and target PKA to Cx43. However, our studies did not allow us to determine the exact roles of single or multiple phosphorylated residues in the region 364 to 373 of Cx43.

Our results allow us to propose a model to explain the control and regulation of communication through gap junctions in human trophoblasts promoting the cell fusion process (Fig. 9E). In the basal state, ezrin is in its open conformation (pT567) with PKA anchored and bound to Cx43. A Cx43 hexamer forms a gap junctional channel between aggregated cells. The tight junction

protein ZO-1 is associated with the C-terminal part of Cx43. Upon a local increase in the pool of cAMP following hCG stimulation, PKA bound to ezrin is activated and phosphorylates Cx43. The phosphorylation of Cx43 by PKA at one or more sites promotes the opening of the gap junction and allows the passage of yet unknown fusogenic signals. Subsequently, this promotes cell fusion by inducing expression of specific fusogenic genes and proteins. In summary, using a physiological model of primary culture of human trophoblasts, we report for the first time that ezrin organizes a supramolecular signal complex at the cellular membrane of trophoblasts and is directly linked to the gap junctional protein Cx43. We provide direct evidence that ezrin promotes gap junctional communication by facilitating discrete control of Cx43 phosphorylation by PKA thereby controlling hCG-regulated cell fusion.

MATERIALS AND METHODS

Cell culture

Villous cytotrophoblasts were isolated from term placentas as previously described (Pidoux et al., 2007b). Briefly, purified cells were diluted to final density of 1×10^6 per ml and plated in 60 mm plastic dishes. Differentiated syncytiotrophoblasts were obtained after 3 days of culture in DMEM containing high glucose, 10% fetal calf serum and incubated at 37°C in 5% CO₂. Cytokeratin 7 immunohistochemistry was performed to confirm the trophoblast origin of attached cells and routinely revealed 95-98% of the cells to be positively stained. After 12 h of culture cytotrophoblasts were treated with 1 μM hCG (Sigma-Aldrich), 100 μM 8-Br-cAMP (Sigma-Aldrich) or 3 μM H89 dihydrochloride hydrate (Sigma-Aldrich), 30 μM 2'-MeO-(8-CPT)-cAMP (Biolog), 100 μM 6-Bnz-cAMP (Biolog) loaded with peptides or transfected with siRNA alone or in combination with expression vectors as described below. The culture medium was replaced every day.

Immunolocalization studies

Immunocytofluorescence staining was performed at 24, 48 and 72 h of culture. Cells were washed in PBS, fixed, and permeabilized in methanol at -20°C for 8 min and blocked for 1 h in 1% fatty acid-free BSA (FFA BSA). Primary monoclonal antibody (2.5 μg each) to desmoplakin (DSK, Abcam), Cx43 (Sigma-Aldrich), ezrin (Sigma-Aldrich), RIα (BD Biosciences), RIIα (BD Biosciences), ZO-1 (Invitrogen) and SP1 (Santa Cruz), were prepared in PBS with 1% FFA BSA and incubated 1 h at room temperature. Cells were next incubated with fluorochrome-conjugated secondary antibody (Alexa Fluor 488 or 555 (1:500, Invitrogen)) in PBS with 1% FFA BSA for 1 h at room temperature. After washing, samples were mounted in medium with DAPI for nuclear staining, examined and photographed on a BX60 epifluorescence microscope (Olympus) equipped with a 40x objective (oil, Olympus 1.00), a ultrahigh-vacuum mercury lamp and a Hamamatsu camera (C4742-95). Pictures were analyzed by VisionStage Orca software (v 1.6). All controls performed by omitting the primary antibody or using a nonspecific IgG of the same isotype were negative. Immunohistochemistry was performed on human placenta biopsies. Tissue samples were first fixed in 4% paraformaldehyde (PFA) for 4 h followed with 1% PFA for 16 h and then embedded in 4% agarose. Blocks were cut to

120 μm thick sections using vibratome (Technical Products International). Sections were permeabilized for 30 min with 0.5% triton X-100 and blocked for 2 h in 10% fatty acid-free BSA, 0.01% triton X100. Primary antibodies anti-ezrin (1 $\mu\text{g}/\text{ml}$; Sigma-Aldrich) and anti-CK7 (0.9 $\mu\text{g}/\text{ml}$; Dako) were prepared in PBS with 1% BSA and incubated overnight at 4°C. Sections were next incubated with the appropriate fluorochrome-conjugated secondary antibodies (Alexa Fluor 488 and Alexa Fluor 555 (1:500; Invitrogen)). After washing, samples were mounted in medium with TO-PRO-3 for nuclear staining, examined and photographed on a Leica TCS SP2 confocal microscope. Controls without primary antibody or with non-specific IgG of the same isotype were all negative.

Trophoblast fusion assay

Syncytium formation was followed by the distribution of desmoplakin and nuclei in cells after fixation and immunostaining as described above. The staining of desmoplakin present at the intercellular boundaries in aggregated cells progressively disappears with syncytium formation. From a random point near the middle of the coverslips, nuclei contained in 100 desmoplakin-delimited syncytia were counted. Three coverslips were examined for each experimental condition. Results are expressed as fusion index, $(N - S)/T$, where N is the number of nuclei per syncytium, S is the number of syncytia, and T is the total number of nuclei counted. Results are expressed as percentage of the control fusion index.

Hormone assays

hCG and hPL concentrations were determined in culture medium after 24, 48 and 72 h of culture by using an enzyme-linked fluorescence assay (Vidas System, BioMerieux) with a detection limit of 2 mU/ml for hCG and an ELISA kit (DiaSource) with a detection limit of 0.043 mg/l for hPL. All reported values are means \pm SEM of triplicate determinations.

Protein sample preparation and immunoblot analysis

Total cell lysates were prepared in lysis buffer (Invitrogen, 50 mM Tris pH 7.4, 250 mM NaCl, 50 mM NaF, 5 mM EDTA, 1% Nonidet P40, 0.02% NaN_3 , 1 mM sodium orthovanadate supplemented

with protease inhibitor cocktail (Merck) and phosphatase inhibitor cocktail (Merck)). Cell fractionated proteins were prepared by using the Qproteome cell compartment kit (Qiagen) as described by the manufacturer. Protein samples were resolved by SDS-PAGE and blotted onto nitrocellulose membranes. The resulting filters were blocked in 5% non-fat dry milk in Tris-buffered saline pH 7.4 (TBS) with 0.1% Tween 20 (TBS-T) for 45 min at room temperature and incubated overnight at 4°C with antibodies to PKA RI α (0.25 μ g/ml, BD Biosciences), PKA RII α (0.25 μ g/ml, BD Biosciences), ezrin (0.5 μ g/ml, Invitrogen), phospho-ezrin T567 (1:1000, Cell signaling), actin (0.8 μ g/ml, Sigma-Aldrich), ZO-1 (0.5 μ g/ml, Invitrogen), Cx43 (0.25 μ g/ml, Sigma-Aldrich), unphosphorylated Cx43 (0.5 μ g/ml, Invitrogen), GST-horse-radish peroxidase conjugate (1:5000, GE Healthcare), His (0.7 μ g/ml, Sigma-Aldrich), D-AKAP2 (1 μ g/ml, Sigma-Aldrich), moesin (1 μ g/ml, Abcam), radixin (1 μ g/ml, Sigma-Aldrich), desmoplakin (0.5 μ g/ml, AbCam), or E-cadherin (0.25 μ g/ml, BD). After washing in TBS-T and incubation with appropriate HRP-conjugated secondary antibody, blots were developed by using Supersignal West Pico substrate (Thermo Scientific).

Peptide synthesis and loading

Peptides used in trophoblast fusion assay (RIAD: LEQYANQLADQIIEKATE-R11, scrambled RIAD: IEKELAQQYQNADAITLE-R11, SuperAKAP-*IS*: R11-QIEYVAKQIVDYAIHQ, scrambled SuperAKAP-*IS*: R11-VVHEIQDAAYYQKQIAI, RISR: R9-ESKRRQEEAEQRK, scrambled RISR: R9-ESKRRPEEAEQPK, PKI: R9-TYADFIASGRTGRRNAI and scrambled PKI: R11-ANITSGYFDTIAAGR) were synthesized on an Intavis MultiPep robot (Intavis Bioanalytical Instruments AG), uncoupled and verified by high performance liquid chromatography (HPLC). The concentrations of the peptides were determined by amino acid analysis using an amino acid analyzer from Thermo Scientific Dionex. RIAD, SuperAKAP-*IS* peptides and their respective control were used in cell cultures at 5 μ M, whereas PKI, RISR peptides and their respective controls were used at 10 μ M. The cell viability after peptide loading (5 μ M for RIAD or SuperAKAP-*IS*) was determined using trypan blue cytotoxicity assay (Sigma-Aldrich) according to the manufacturer's protocol (Fig. S1C). The efficiency of peptide loading of trophoblasts was assessed with FITC-RIAD and SuperAKAP-*IS*-FITC at 5 μ M each after 1 h and the degree of peptide loading was then determined

by the number of positive green cells normalized by the number of total cell (Fig. S1D).

Protein expression and purification

Bovine RI α (RI α and RI α -flag tagged) and human RII α (RII α and RII α -flag tagged) protein were expressed in *Escherichia coli* BL21 and *Escherichia coli* Rosetta, respectively, using 0.1 – 1.0 mM isopropyl-beta-D-thiogalactopyranoside (IPTG) induction at RT (4 h) and purified on Rp-8-AHA-cAMP agarose beads [8-(6-aminohexyl)aminoadenosine-3',5'-cyclic monophosphorothioate, Rp-isomer, immobilized on agarose] (Biolog) and eluted with cAMP. To remove any bound or unbound cAMP, the purified recombinant proteins were dialysed extensively against a buffer containing 20 mM MOPS, pH 7.0 and 150 mM NaCl. Protein concentrations were determined using the Bradford protein assay and SDS-PAGE (10% gels) using BSA as a standard. His-ezrin, GST-ezrin were expressed and purified as previously described (Ruppelt et al., 2007) whereas GST-Cx43 was described in (Gnidehou et al., 2011).

Pull-down assays

The cAMP-coupled-agarose beads (8-AHA-cAMP agarose) were purchased from Biolog. Prior to pull down, 50 μ l dry volume of immobilized cAMP beads (~ 300 nmol of cAMP) were washed with 1 ml of PBS buffer. For control, beads blocked by ethanolamine were used in a parallel identical pulldown procedure. Prior to the pull-down assays, cell lysates were incubated with 10 mM ADP/GDP for 15 min at 4°C to reduce nonspecific binding, mainly contributed by ADP- and GDP-binding protein (Raijmakers et al., 2008; Scholten et al., 2006). cAMP-agarose beads were added to the lysate (5 mg proteins) in a volume ratio of 1:100 beads to lysate. The lysate-bead suspension was next incubated for 16 h at 4°C by rotary shaking in presence of 10 mM MgCl₂ and 1 mM ATP to increase the binding of cAMP to the PKA regulatory subunit. RI and RII-flag affinity chromatographies were performed by adding 100 μ g of purified RI or RII-flag proteins to cell lysate (500 μ g proteins) in a volume ratio of 1:1 beads to lysate. The lysate-bead suspension was next incubated overnight at 4°C on a rocker platform. 30 μ l of flag-agarose beads (Sigma-Aldrich) were added for 2 h at 4°C. The lysate-bead of

cAMP or R-flag subunit suspensions were next washed five times in lysis buffer and subjected to in-gel trypsin digestion.

In-gel trypsin digestion

Proteins were separated by SDS-PAGE as described above and stained using SimplyBlue SafeStain (Invitrogen). Each stained lane was cut into 14 individual bands and subjected to in-gel digestion with 0.1 µg trypsin (Promega) in 20 µl 25 mM ammonium bicarbonate, pH 7.8 at 37°C for 16 h. For each band the tryptic peptides were purified with µ-C18 ZipTips (Millipore), and dried using a Speed Vac concentrator (Savant).

NanoLC-LTQ Orbitrap mass spectrometry

Dried peptides were dissolved in 10 µl 1% formic acid in water and 5 µl were injected onto an LC/MS system consisting of a Dionex Ultimate 3000 nano-LC system (Sunnyvale CA, USA) connected to a linear quadrupole ion trap – Orbitrap (LTQ Orbitrap) mass spectrometer (ThermoElectron, Bremen, Germany) equipped with a nanoelectrospray ion source. For liquid chromatography separation we used an Acclaim PepMap 100 column (C18, 3 µm, 100 Å) (Dionex, Sunnyvale CA, USA) capillary of 12 cm bed length. The flow rate used was 300 nL/min for the nano column, and the solvent gradient used was 7% B to 50% B in 40 minutes. Solvent A was 0.1% formic acid, whereas aqueous 90% acetonitrile in 0.1% formic acid was used as solvent B.

The mass spectrometer was operated in the data-dependent mode to automatically switch between Orbitrap-MS and LTQ-MS/MS acquisition. Survey full scan MS spectra (from m/z 300 to 2,000) were acquired in the Orbitrap with resolution $R = 60,000$ at m/z 400 (after accumulation to a target of 1,000,000 charges in the LTQ). The method used allowed sequential isolation of the most intense ions, up to six, depending on signal intensity, for fragmentation on the linear ion trap using collisionally induced dissociation at a target value of 100,000 charges. Other instrument parameters were used as previously described (Solstad et al., 2010).

Data analysis

Raw data were processed using DTA supercharge software to generate mgf files. The resulting mgf files were searched against the Uniprot database (<http://uniprot.org>) using an in-house version of Mascot 2.2.1 (<http://matrixsciences.com>) as the search engine. Trypsin was selected as the proteolytic enzyme and a tolerance of 5 ppm for the precursor ion and 0.5 Da for the MS/MS fragments was applied. Moreover, methionine oxidation, acetylation at protein N-terminus, deamidation of asparagines and glutamines and propionamide formation of cysteines were allowed as variable modifications. Proteins were considered to be identified by Mascot if probability < 0.05 was achieved and Mascot score was > 30.

SiRNA, mammalian expression vectors and transfection

The 21-nucleotide siRNA duplex targeting human ezrin mRNA (Ez799, 5'-cccuuggacugaaauuuuaug-3'; 5'-uaaaauaucaguccaaggga-3') and a triple G/C-mutated control (Ez799M3, 5'-cgcuucgagugaaauuuuaug-3'; 5'-uaaaauaucacucgaagcgca-3') were described previously (Ruppelt et al., 2007), an siRNA duplex targeting human D-AKAP2 mRNA (D-AKAP2.258, 5'-gaccucagaugugaaguccauuaaa-3'; 5'-uuuaauggacuucacaucugagguc-3') and a scrambled (scrambled D-AKAP2.258, 5'-gacgacguaaguugaaccuucuaaa-3'; 5'-uuuagaagguucaacuacgucguc-3') were synthesized in-house. Specific siRNA targeting identified AKAPs (OPA1, D-AKAP1, AKAP-KL, AKAP95, AKAP450, gravin, AKAP-Lbc and myomegalin) or ERM proteins (radixin and moesin) were purchased from Santa Cruz Biotechnology Inc. and correspond to a pool of three target-specific siRNAs. SiRNA transfection was performed using Lipofectamine 2000 CD reagent (Invitrogen) according to the manufacturer's protocol. Briefly, 100 pmoles siRNA or scrambled siRNA were mixed with the lipofectamine reagent, diluted in Opti-MEM medium (Invitrogen) and incubated with the cells for 48 h at 37°C. Subsequently, cells were incubated in media and used for analyses at 72 h of culture when target protein levels were below 50% of control. The transfection efficiency for siRNA into trophoblasts was above 80% as analyzed by adding fluorescein-labeled dsRNA oligomer to parallel cell cultures. Knock down efficiency were followed by semi-quantitative RT-PCR with specific primers purchased from Santa Cruz Biotechnology Inc. for siRNA targeting AKAPs

according to the manufacturer's protocol, whereas knock down efficiency for siRNA targeting ERM proteins or D-AKAP2 were performed by immunoblot.

Ezrin clones resistant to siRNA Ez799 were generated by introducing three nucleotide switches, C798G, T781G and G787C to avoid recognition by siRNA Ez799 in coexpression experiments. Mutagenesis was performed by using one set of primers P1(+), 5'-gcttgagttgatgcgctgggactcaatattatgagaaagatga-3'; P1(-), 5'-tcattcttctcataaattaggagtcaccagcgcatcaactccaagc-3' and the QuickChange XL kit (Stratagene) according to the manufacturer's protocol. Sequences (wild type ezrin, siRNA insensitive ezrin, labeled by # and siRNA insensitive ezrin T567D, labeled *) were cloned into pENTR/D-TOPO vector using the gateway cloning technology (Invitrogen) and thereafter transferred into pDEST-EGFP to yield an GFP-ezrin fusion protein (GFP-tag in N-terminus). Ezrin*-AKBmut substituted to abolish PKA binding was generated from siRNA insensitive ezrin* in the pENTR vector as previously described (Jarnaess et al., 2008). Ezrin*-D510I-R517V substituted to abolish Cx43 association was generated from siRNA insensitive ezrin* in the pENTR vector by introducing two amino acids switches (D510I, R517V). Mutagenesis was performed as described above by using two sets of primers P2(+), 5'-gagggcatccggattgaccgcaatga-3'; P2(-), 5'-tcattgcggatcaatccggatgcctc-3'; P3(+), 5'-atgaggagaaggtcatcactgaggcag-3'; P3(-), 5'-ctgcctcagtgatgacctctcctca-3'. Ezrin*-AKBmut and ezrin*-D510I-R517V were cloned into pENTR/D-TOPO and then transferred into pDEST-EGFP. Cx43 clones resistant to siRNA Cx43 were generated by introducing three nucleotide switches, T1294C, T1297G and A1300G to avoid recognition by siRNA Cx43 in coexpression experiments. Mutagenesis was performed as described above by using one set of primers P4(+), 5'-ctaaaaaactagccgcggggatgaattacagccact-3'; P4(-), 5'-agtggtgtaattcatgccccgaggtagtttttag-3'. Sequences (wild type Cx43, siRNA resistant Cx43, labeled by °) were cloned into pENTR/D-TOPO vector and transferred into pDEST-EGFP to yield a GFP-Cx43 fusion protein (GFP-tag in N-terminus). GFP-Cx43° R370E substituted to abolish ezrin association was generated from siRNA insensitive Cx43° in the pENTR vector by introducing one amino acid switch (R370E) by using one set of primers P5(+), 5'-gcagagccagcagtggaagccagcagcagacct-3'; P5(-), 5'-aggctctgctgctggcttactgctggctctgc-3'. GFP-Cx43° S364A R370E, GFP-Cx43° S365A R370E, GFP-

Cx43[∞] S368A R370E and GFP-Cx43[∞] S364D R370E, GFP-Cx43[∞] S365D R370E, GFP-Cx43[∞] S368D R370E were generated from Cx43[∞] R370E entry vector by using one set of primers for each respectively P6(+), 5'-gaccagcgacctgcaagcagagcc-3'; P6(-), 5'-ggctctgcttcaggtcgctggtc-3'; P7(+), 5'-cagcgaccttcagccagagccagc-3'; P7(-), 5'-gctggctctggctgaaggtcgctg-3'; P8(+), 5'-caagcagagccgccagtgaagccagc-3'; P8(-), 5'- gctggcttcactggcgctctgcttg-3' and P9(+), 5'-gaccagcgacctgacagcagagccagt-3'; P9(-), 5'- actggctctgctgtcaggtcgctggtc-3'; P10(+), 5'-cagcgaccttcagacagagccagc-3'; P10(-), 5'- gctggctctgtctgaaggtcgctg-3'; P11(+), 5'-caagcagagccgacagtgaagccagc-3'; P11(-), 5'- gctggcttcactgtcgctctgcttg-3'. GFP-Cx43[∞] R370E and GFP-Cx43[∞] S364A R370E, GFP-Cx43[∞] S365A R370E, GFP-Cx43[∞] S368A R370E or GFP-Cx43[∞] S364D R370E, GFP-Cx43[∞] S365D R370E, GFP-Cx43[∞] S368D R370E were cloned into pENTR/D-TOPO and then transferred into pDEST-EGFP. Cx43[∞] 3SA R370E and Cx43[∞] 3SD R370E were generated from Cx43[∞] entry clone by using successively primers P5, P6, P8, P7 and P5, P9, P11, P10 respectively. Sequences corresponding to Cx43[∞] presenting serine substitutions (S364, S365, S368, S369, S372 and S373) in alanine (A) or aspartic acid (D) were purchased from GeneArt (Invitrogen) in an EcoRI and BglII restriction enzyme sites. For 6SA; 5'-gaattctaaaaaactagccgcggggcatgaattacagccactagccattgtggaccagcgacctgcagccagagccgccgctcgtgccgccagacctcggcctgatgacctggagatct-3' and for 6SD; 5'-gattctaaaaaactagccgcggggcatgaattacagccactagccattgtggaccagcgacctgacgacagagccgacgacctgcccagcagacacctcggcctgatgacctggagatct-3'. Cx43[∞] 6SA and 6SD were cloned into Cx43[∞] pENTR and then transferred into pDEST-EGFP. Cx43[∞] 6SA R370E or 6SD R370E were generated as described above. All constructs were verified by sequencing. The resulting mammalian transfection vectors were introduced into trophoblasts at 24 h by using Lipofectamine 2000 CD reagent (Invitrogen) according to the manufacturer's protocol. Briefly 2 µg of plasmids were mixed with the transfection reagent, diluted in Opti-MEM medium (Invitrogen) and incubated or co-incubated with ezrin siRNA or Cx43 siRNA with the cells for 48 h at 37°C.

Immunoprecipitation

The following antibodies were cross-linked to Dynabead protein G (Invitrogen): monoclonal anti-PKA RI α (4 μ g, BD Biosciences), monoclonal anti-PKA RII α (4 μ g, BD Biosciences), polyclonal anti-ezrin (4 μ g, Sigma-Aldrich), polyclonal anti-Cx43 (4 μ g, Sigma-Aldrich), monoclonal anti-ZO-1 (4 μ g, Invitrogen), monoclonal anti-GFP-tag (5 μ g, Clontech) and nonspecific rabbit or mouse IgG (2 μ g Jackson ImmunoResearch). Antibodies were covalently coupled to beads using BS³ (5 mM, Thermo Scientific) as cross-linker according to the manufacturer instruction (Invitrogen) for 30 min at room temperature. Total cell lysates (200 μ g of protein) prepared as above, were added to the antibody-cross-linked beads immunocomplex and incubated overnight at 4°C on a rocker platform. 25 μ g of purified His-ezrin and GST-Cx43 or GST were mixed in binding buffer (50 mM Tris-HCl pH 7.4, 10 mM Hepes, 50 μ M EDTA and 0.1% BSA) at room temperature for 30 min on a rocker platform. Co-immunoprecipitation of His and GST were performed with Dynabead protein G as described above with a monoclonal anti-His (4 μ g, Sigma-Aldrich) and a polyclonal anti-GST (2 μ g, Sigma-Aldrich). Immunocomplexes were washed three times in lysis buffer. Protein elution was performed with LDS by heating the beads for 10 min at 70°C and subjected to SDS-PAGE and immunoblotted with the indicated antibodies or subjected to in-gel trypsin digestion.

DuolinkTM Proximity Ligation Assay

Interaction between ezrin, Cx43, PKA RI α , PKA RII α , ZO-1, DSK, GFP and SP1 in trophoblasts were analysed using the DuolinkTM proximity ligation assay according to manufacturer's instructions. Trophoblasts were fixed as described above and blocked using Duolink blocking solution 30 min at 37°C. Combinations of antibodies (2.5 μ g each) were incubated with the cells 1 h at 37°C. The incubation with the PLA probes, hybridization, ligation, amplification steps were performed following Duolink kit instructions. In order to visualize cellular boundaries, cells were next stained with 5 μ g/ml of Wheat Germ Agglutinin conjugated to Alexa Fluor 488 (Invitrogen) for 10 min at room temperature. After washing, cells were mounted in medium with DAPI for nuclear staining, examined and photographed on a BX60 epifluorescence microscope (Olympus). Positive controls were obtained using proteins already known to interact together with a combination of an anti-Cx43 and an anti-ZO-

1. Negative controls were obtained using a combination of mouse and rabbit IgG or a combination of anti-SP1 and an anti-Cx43 or anti-ezrin. Moreover, a series of technical negative controls were performed by leaving one primary antibody out. The quantification of the proteins proximity was performed by using Image J and by normalizing the fluorescence spots generated with the number of nuclei.

Gap-Fluorecence Recovery After Photobleaching (gap-FRAP) experiments

Gap junction communication was quantitatively followed in live cells by gap-FRAP experiments as previously described (Frendo et al., 2003a; Wade et al., 1986). Cells were plated on eight-well chamber slides (Ibidi) at density of 100,000 cells per well and treated with 8-beta-glycyrrhetic acid (β -GA) loaded with cell-permeable anchoring disruptor peptides or PKI peptide or transfected ezrin siRNA alone or concomitantly with mammalian expression vectors encoding GFP-ezrin[#], GFP-ezrin^{*}, GFP-ezrin^{*}-AKBmut or GFP-ezrin^{*}-D510I-R517V or transfected Cx43 siRNA alone or with mammalian expression vectors encoding GFP-Cx43[∞], GFP-Cx43[∞] R370E or either with combinations of substituions in the Cx43 PKA phosphorylation sites as described above and listed in Fig S4F. Cells were next loaded with calcein red-orange AM (Invitrogen) for 30 min at 37°C and subsequently washed to remove excess extracellular calcein to avoid further loading during measurements. Confocal experiments were performed by using an inverted spinning disk microscope (Nipkow spinning disk microscope associated with a Yokogawa CSU-X1 spinning disk) with a dual band excitation 491/561 nm laser source with a 37°C temperature-controlled CO₂ chamber (Okolab). Transfected cells with GFP-tagged expression vectors were visualized with 491 nm laser source. FRAP was conducted using a laser (561 nm) output power adjusted to 10 mW for a prebleaching period of 5 s, then to 100 mW for 1 s to achieve sufficient photobleaching for FRAP observations, without causing visible cell damage. The intensity of the fluorescence signal was next measured at 607 nm with the laser output power being adjusted to 10 mW in a 60x objective (oil, TIRF/ON 1.49) fluorescence recovery was recorded for 500 s with frames shot every 60 s and images were acquired with a camera (EM-CCD eVolve, pixel: (16 μ m)²). In each experiment, one labeled, isolated cell was left unbleached as a refence for the loss of fluorescence due to repeated scanning and dye leakage. The microscope was controlled by

Metamorph software (v 7.7.0). The exponential fluorescence recovery for bleached cells was analyzed by the equation: $(F_i - F_t) / (F_i - F_0) = e^{-t/\tau}$, where F_i , F_t and F_0 are fluorescence intensities before bleaching, at time t and $t = 0$, respectively, and τ is a time constant (s). The transfer constant $\kappa = 1/\tau$ was calculated and corrected by dividing by the number of cells connected to target cell.

Peptide array synthesis and detection

Peptide arrays were synthesized on nitrocellulose membranes using a MultiPep automated peptide synthesizer (INTAVIS Bioanalytical Instruments AG) as described (Kramer and Schneider-Mergener, 1998). Peptide interactions with GST or GST fusion proteins were determined by overlaying the cellulose membranes with 1 $\mu\text{g}/\text{ml}$ of proteins. Bound proteins were detected with horse-radish peroxidase-conjugated anti-GST antibody (GE Healthcare) and visualized by using Supersignal West Pico substrate (Thermo Scientific).

Statistics

The StatView F-4.5 software package (Abacus Concepts, Inc., Berkeley, CA) was used for statistical analysis. Statistical differences between groups were evaluated using Student's unpaired t-test or ANOVA, as appropriate. Post hoc analysis (Tukey) was used for individual comparisons and to generate P values that are stated in the figure legends. The sample size and significance level is shown in the figure legends for each graph. All data are presented as means \pm SEM. A value of $p < 0.05$ was considered statistically significant.

Online supplemental material

Fig. S1 shows the effect of PKA, Epac and anchoring disruptor peptides on trophoblast fusion. Fig. S2 shows AKAPs expressed and the effect of ezrin and D-AKAP2 silencing on trophoblast fusion. Fig. S3 shows effect of ezrin silencing on ERM family proteins, effect of silencing other ERM proteins on trophoblast fusion, co-immunoprecipitation and proximity ligation assay controls. Fig. S4 shows the effect of anchoring disruptor peptides, ezrin silencing and Cx43 silencing combined with GFP-Cx43 transfection variants on Cx43 expression and localization, desmoplakin and E-cadherin protein

expression upon ezrin silencing, PLA with ezrin and PKA (RI α and RII α) during trophoblast fusion and a summary of GFP-Cx43 variants. Fig. S5 shows the identification and characterization of minimal residues binding motifs in ezrin and Cx43. Video 1 corresponds to Fig 5B and shows the effect of gap junction inhibitor (beta-GA), Arg-tagged protein kinase inhibitor (PKI) or Arg-tagged anchoring disruptors RIAD or SuperAKAP-1S and their scrambled controls on gap junction communication in live cells examined by calcein transfer as fluorescence recovery after photobleaching (gap-FRAP). Video 2 corresponds to Fig. 7B and shows trophoblasts transfected with scrambled ezrin siRNA or ezrin siRNA with or without co-transfection with GFP-ezrin[#], GFP-ezrin*, GFP-ezrin*-AKBmut plasmid or GFP-ezrin*-D510I-R517V on gap junction communication in live cells examined by calcein transfer as gap-FRAP. Video 3 corresponds to Fig. 9B and shows trophoblasts transfected with scrambled siRNA or Cx43 siRNA with or without co-transfection with GFP-Cx43[∞], GFP-Cx43[∞] R370E or either with substitutions in putative Cx43 PKA phosphorylation sites on gap junction communication in live cells examined by calcein transfer as gap-FRAP.

ACKNOWLEDGEMENTS

This work was supported by the Research Council of Norway, a fellowship from the foundation PremUP and the French-Norwegian bilateral research programme Yggdrasil. We are grateful to Jorun Solheim and Fatima Ferreira for technical assistance, to Ola Blingsmo for peptide synthesis, to Dr. Jean Guibourdenche for hormone assays to Dr. Dominique Segretain and Dr. Bernd Thiede for helpful comments and input on various parts of the work and to members of the Taskén and Evain-Brion laboratories for critical reading of the manuscript. This work has benefitted from the facilities and expertise of the Imagif Cell Biology Unit of the Gif campus (www.imagif.cnrs.fr), which is supported by the Conseil Général de l'Essone.

Author contribution: KT, DEB and GP designed the research; GP, PG, JD, BL and TS did the experiments and analyzed data together with DEB and KT; GP and KT wrote the paper. All authors read and commented on draft versions of the manuscript and approved the final version.

CONFLICT OF INTEREST

The authors declare that they have no conflict of interest. The University of Oslo Technology Transfer Office, Inven2 AS, has in cooperation with INSERM and PremUP filed a patent application on the possibility to regulate the opening and closing of connexin 43 gap junctions in different contexts by targeting the ezrin and PKA interaction connexin 43.

LIST OF ABBREVIATIONS

Abbreviations used in this paper: 6-Bnz-cAMP, N6-benzoyladenine 3',5'-cyclic monophosphate; 8-Br-cAMP, 8-bromoadenosine 3',5'-cyclic monophosphate; ADAM, a disintegrin and metalloproteinase domain; AKAP, A kinase anchoring protein; AKB, A kinase binding domain; β -GA, 18 beta-glycyrrhetic acid; CK7, cytokeratin 7; Cx43, connexin 43; DSK, desmoplakin; EBP50, ezrin-radixin-moesin-binding phosphoprotein 50; Epac, exchange protein activated by cAMP; ERM, ezrin-radixin-moesin; gap-FRAP, gap junction communication by fluorescence recovery after photobleaching; GCM1, glial cell missing 1 protein; hCG, human chorionic gonadotropin; hPL, human placental lactogen; ICAM, intercellular adhesion molecule; PDE, phosphodiesterase; PKA, protein kinase A; PKI, PKA inhibitor; RIAD, RI anchoring disruptor; RISR, RI specifier region; ZO-1, zona occludens-1.

REFERENCES

- Alsat, E., J. Haziza, and D. Evain-Brion. 1993. Increase in epidermal growth factor receptor and its messenger ribonucleic acid levels with differentiation of human trophoblast cells in culture. *J Cell Physiol.* 154:122-128.
- Arpin, M., D. Chirivino, A. Naba, and I. Zwaenepoel. 2011. Emerging role for ERM proteins in cell adhesion and migration. *Cell Adh Migr.* 5:199-206.
- Benirschke, K., and P. Kaufmann. 2000. Pathology of the human placenta. Springer-Verlag, New-York. 22-70 pp.
- Berryman, M., Z. Franck, and A. Bretscher. 1993. Ezrin is concentrated in the apical microvilli of a wide variety of epithelial cells whereas moesin is found primarily in endothelial cells. *J Cell Sci.* 105 (Pt 4):1025-1043.
- Bjerregaard, B., S. Holck, I.J. Christensen, and L.I. Larsson. 2006. Syncytin is involved in breast cancer-endothelial cell fusions. *Cell Mol Life Sci.* 63:1906-1911.
- Bjerregaard, B., J.F. Talts, and L.I. Larsson. 2011. The endogenous envelope protein syncytin is involved in myoblast fusion. In *Cell Fusions: regulation and control*. Vol. 1. L.I. Larsson, editor. Springer. 267-275.
- Blond, J.-L., D. Lavillette, V. Cheynet, O. Bouton, G. Oriol, S. Chapel-Fernandes, B. Mandrand, F. Mallet, and F.L. Cosset. 2000. An envelope glycoprotein of the human endogenous retrovirus HERV-W is expressed in the human placenta and fuses cells expressing the type D mammalian retrovirus receptor. *J Virol.* 74:3321-3329.
- Bonilha, V.L., M.E. Rayborn, I. Saotome, A.I. McClatchey, and J.G. Hollyfield. 2006. Microvilli defects in retinas of ezrin knockout mice. *Exp Eye Res.* 82:720-729.
- Bretscher, A. 1989. Rapid phosphorylation and reorganization of ezrin and spectrin accompany morphological changes induced in A-431 cells by epidermal growth factor. *J Cell Biol.* 108:921-930.
- Brown, M.J., R. Nijhara, J.A. Hallam, M. Gignac, K.M. Yamada, S.L. Erlandsen, J. Delon, M. Kruhlak, and S. Shaw. 2003. Chemokine stimulation of human peripheral blood T lymphocytes induces rapid dephosphorylation of ERM proteins, which facilitates loss of microvilli and polarization. *Blood.* 102:3890-3899.
- Bruzzone, R., T. White, and D. Paul. 1996. Connections with connexins: the molecular basis of direct intercellular signaling. *Eur J Biochem.* 15:1-27.
- Burghardt, R.C., R. Barhoumi, T.C. Sewall, and J.A. Bowen. 1995. Cyclic AMP induces rapid increases in gap junction permeability and changes in the cellular distribution of connexin43. *J Membr Biol.* 148:243-253.
- Carlson, C.R., B. Lygren, T. Berge, N. Hoshi, W. Wong, K. Tasken, and J.D. Scott. 2006. Delineation of type I protein kinase A-selective signaling events using an RI anchoring disruptor. *J Biol Chem.* 281:21535-21545.
- Carr, D.W., Z.E. Hausken, I.D. Fraser, R.E. Stofko-Hahn, and J.D. Scott. 1992. Association of the type II cAMP-dependent protein kinase with a human thyroid RII-anchoring protein. Cloning and characterization of the RII-binding domain. *J Biol Chem.* 267:13376-13382.

- Chang, C.W., G.D. Chang, and H. Chen. 2011. A novel cyclic AMP/Epac1/CaMKI signaling cascade promotes GCM1 desumoylation and placental cell fusion. *Mol Cell Biol.* 31:3820-3831.
- Charrasse, S., F. Comunale, M. Fortier, E. Portales-Casamar, A. Debant, and C. Gauthier-Rouviere. 2007. M-cadherin activates Rac1 GTPase through the Rho-GEF trio during myoblast fusion. *Mol Biol Cell.* 18:1734-1743.
- Chen, C.P., L.F. Chen, S.R. Yang, C.Y. Chen, C.C. Ko, G.D. Chang, and H. Chen. 2008. Functional characterization of the human placental fusogenic membrane protein syncytin 2. *Biol Reprod.* 79:815-823.
- Chernomordik, L.V., and M.M. Kozlov. 2005. Membrane hemifusion: crossing a chasm in two leaps. *Cell.* 123:375-382.
- Coghlan, V.M., B.A. Perrino, M. Howard, L.K. Langeberg, J.B. Hicks, W.M. Gallatin, and J.D. Scott. 1995. Association of protein kinase A and protein phosphatase 2B with a common anchoring protein. *Science.* 267:108-111.
- Coutifarís, C., L. Kao, H. Sehdev, U. Chin, G. Babalola, O. Blaschuk, and J. Strauss 3d. 1991. E-cadherin expression during the differentiation of human trophoblasts. *Development.* 113:767-777.
- Cronier, L., N. Defamie, L. Dupays, M. Théveniau-Ruissy, F. Goffin, F. Pointis, and A. Malassiné. 2002. Connexin expression and gap junctional intercellular communication in human first trimester trophoblast. *Mol Hum Reprod.* 8:1005-1013.
- Cronier, L., J.L. Frendo, N. Defamie, G. Pidoux, G. Bertin, J. Guibourdenche, G. Pointis, and A. Malassiné. 2003. Requirement of gap junctional intercellular communication for human villous trophoblast differentiation. *Biol Reprod.* 69:1472-1480.
- Cullinan, P., A.I. Sperling, and J.K. Burkhardt. 2002. The distal pole complex: a novel membrane domain distal to the immunological synapse. *Immunol Rev.* 189:111-122.
- Dahl, E., E. Winterhager, O. Traub, and K. Willecke. 1995. Expression of gap junction genes, connexin40 and connexin43, during fetal mouse development. *Anat Embryol (Berl).* 191:267-278.
- Darrow, B.J., V.G. Fast, A.G. Kleber, E.C. Beyer, and J.E. Saffitz. 1996. Functional and structural assessment of intercellular communication. Increased conduction velocity and enhanced connexin expression in dibutyryl cAMP-treated cultured cardiac myocytes. *Circ Res.* 79:174-183.
- Davies, S.P., H. Reddy, M. Caivano, and P. Cohen. 2000. Specificity and mechanism of action of some commonly used protein kinase inhibitors. *Biochem J.* 351:95-105.
- Dodge, K.L., S. Khouangsathiene, M.S. Kapiloff, R. Mouton, E.V. Hill, M.D. Houslay, L.K. Langeberg, and J.D. Scott. 2001. mAKAP assembles a protein kinase A/PDE4 phosphodiesterase cAMP signaling module. *Embo J.* 20:1921-1930.
- Dransfield, D.T., A.J. Bradford, J. Smith, M. Martin, C. Roy, P.H. Mangeat, and J.R. Goldenring. 1997. Ezrin is a cyclic AMP-dependent protein kinase anchoring protein. *EMBO J.* 16:35-43.
- Dunk, C.E., A. Gellhaus, S. Drewlo, D. Baczyk, A.J. Potgens, E. Winterhager, J.C. Kingdom, and S.J. Lye. 2012. The Molecular Role of Connexin 43 in Human Trophoblast Cell Fusion. *Biology of reproduction.*

- Eaton, B., and S. Contractor. 1993. In vitro assessment of trophoblast receptors and placental transport mechanisms. *In The human placenta*. C.W. Redman, I.L. Sargent, and P.M. Starkey, editors. Blackwell Scientific Publication, London. 471-503.
- Fievet, B.T., A. Gautreau, C. Roy, L. Del Maestro, P. Mangeat, D. Louvard, and M. Arpin. 2004. Phosphoinositide binding and phosphorylation act sequentially in the activation mechanism of ezrin. *J Cell Biol.* 164:653-659.
- Frendo, J.-L., L. Cronier, G. Bertin, J. Guibourdenche, M. Vidaud, D. Evain-Brion, and A. Malassine. 2003a. Involvement of connexin 43 in human trophoblast cell fusion and differentiation. *J Cell Sci.* 116:3413-3421.
- Frendo, J.-L., D. Olivier, V. Cheynet, J.-L. Blond, M. Vidaud, M. Rabreau, D. Evain-Brion, and F. Mallet. 2003b. Direct involvement of HERV-W Env glycoprotein in human trophoblast cell fusion and differentiation. *Mol Cell Biol.* 23:3566-3574.
- Gerbaud, P., G. Pidoux, J. Guibourdenche, N. Pathirage, J.M. Costa, J. Badet, J.L. Frendo, P. Murthi, and D. Evain-Brion. 2011. Mesenchymal activin-a overcomes defective human trisomy 21 trophoblast fusion. *Endocrinology.* 152:5017-5028.
- Gnidehou, S., P. Gerbaud, G. Ducarme, F. Ferreira, J. Badet, A. Malassine, D. Evain-Brion, and J.L. Frendo. 2011. Expression in Escherichia coli and purification of human recombinant connexin-43, a four-pass transmembrane protein. *Protein Expr Purif.* 78:174-180.
- Gold, M.G., B. Lygren, P. Dokurno, N. Hoshi, G. McConnachie, K. Tasken, C.R. Carlson, J.D. Scott, and D. Barford. 2006. Molecular basis of AKAP specificity for PKA regulatory subunits. *Mol Cell.* 24:383-395.
- Gutstein, D.E., G.E. Morley, and G.I. Fishman. 2001. Conditional gene targeting of connexin43: exploring the consequences of gap junction remodeling in the heart. *Cell Commun Adhes.* 8:345-348.
- Ilvesaro, J., K. Vaananen, and J. Tuukkanen. 2000. Bone-resorbing osteoclasts contain gap-junctional connexin-43. *J Bone Miner Res.* 15:919-926.
- Jarnaess, E., A. Ruppelt, A.J. Stokka, B. Lygren, J.D. Scott, and K. Tasken. 2008. Dual specificity A-kinase anchoring proteins (AKAPs) contain an additional binding region that enhances targeting of protein kinase A type I. *J Biol Chem.* 283:33708-33718.
- Jordan, K., J.L. Solan, M. Dominguez, M. Sia, A. Hand, P.D. Lampe, and D.W. Laird. 1999. Trafficking, assembly, and function of a connexin43-green fluorescent protein chimera in live mammalian cells. *Mol Biol Cell.* 10:2033-2050.
- Keryer, G., E. Alsat, K. Tasken, and D. Evain-Brion. 1998. Cyclic AMP-dependent protein kinases and human trophoblast cell differentiation in vitro. *J Cell Sci.* 111:995-1004.
- Kliman, H., J. Nestler, E. Sermasi, J. Sanger, and J. Strauss III. 1986. Purification, characterization, and *in vitro* differentiation of cytotrophoblasts from human term placentae. *Endocrinology.* 118:1567-1582.
- Knerr, I., S.W. Schubert, C. Wich, K. Amann, T. Aigner, T. Vogler, R. Jung, J. Dotsch, W. Rascher, and S. Hashemolhosseini. 2005. Stimulation of GCMa and syncytin via cAMP mediated PKA signaling in human trophoblastic cells under normoxic and hypoxic conditions. *FEBS Lett.* 579:3991-3998.

- Kramer, A., and J. Schneider-Mergener. 1998. Synthesis and screening of peptide libraries on continuous cellulose membrane supports. *Methods Mol Biol.* 87:25-39.
- Lu, X., and Y. Kang. 2009. Cell fusion as a hidden force in tumor progression. *Cancer Res.* 69:8536-8539.
- Lygren, B., C.R. Carlson, K. Santamaria, V. Lissandron, T. McSorley, J. Litzenberg, D. Lorenz, B. Wiesner, W. Rosenthal, M. Zaccolo, K. Tasken, and E. Klussmann. 2007. AKAP complex regulates Ca²⁺ re-uptake into heart sarcoplasmic reticulum. *EMBO Rep.* 8:1061-1067.
- Makaula, S., A. Lochner, S. Genade, M.N. Sack, M.M. Awan, and L.H. Opie. 2005. H-89, a non-specific inhibitor of protein kinase A, promotes post-ischemic cardiac contractile recovery and reduces infarct size. *J Cardiovasc Pharmacol.* 45:341-347.
- Mbalaviele, G., H. Chen, B.F. Boyce, G.R. Mundy, and T. Yoneda. 1995. The role of cadherin in the generation of multinucleated osteoclasts from mononuclear precursors in murine marrow. *J Clin Invest.* 95:2757-2765.
- Mi, S., X. Lee, X.-P. Li, G.M. Veldman, H. Finnerty, L. Racie, E. LaVallie, X.-Y. tang, P. Edouard, S. Howes, J.C. Keith, and J.M. McCoy. 2000. Syncytin is a captive retroviral envelope protein involved in human placental morphogenesis. *Nature.* 403:785-789.
- Michel, J.J., and J.D. Scott. 2002. AKAP mediated signal transduction. *Annu Rev Pharmacol Toxicol.* 42:235-257.
- Midgley, A., G. Pierce, G. Denau, and J. Gosling. 1963. Morphogenesis of syncytiotrophoblast in vivo: an autoradiographic demonstration. *Science.* 141:350-351.
- Mukai, A., and N. Hashimoto. 2008. Localized cyclic AMP-dependent protein kinase activity is required for myogenic cell fusion. *Exp Cell Res.* 314:387-397.
- Nnamani, C., A. Godwin, C.A. Ducsay, L.D. Longo, and W.H. Fletcher. 1994. Regulation of cell-cell communication mediated by connexin 43 in rabbit myometrial cells. *Biol Reprod.* 50:377-389.
- Ogren, L., and F. Talamantes. 1994. The placenta as an endocrine organ: polypeptides. In *Physiology of reproduction*. E. Knobil and J. Neill, editors. Raven Press, New-York. 875-945.
- Oren-Suissa, M., and B. Podbilewicz. 2007. Cell fusion during development. *Trends Cell Biol.* 17:537-546.
- Paulson, A.F., P.D. Lampe, R.A. Meyer, E. TenBroek, M.M. Atkinson, T.F. Walseth, and R.G. Johnson. 2000. Cyclic AMP and LDL trigger a rapid enhancement in gap junction assembly through a stimulation of connexin trafficking. *J Cell Sci.* 113 (Pt 17):3037-3049.
- Pérot, P., C. Montgiraud, D. Lavillette, and F. Mallet. 2011. A comparative portrait of retroviral fusogens and syncytins. In *Cell fusions: regulation and control*. Vol. 1. L.I. Larsson, editor. Springer. 63-115.
- Pidoux, G., P. Gerbaud, S. Gnidehou, M. Grynberg, G. Geneau, J. Guibourdenche, D. Carette, L. Cronier, D. Evain-Brion, A. Malassine, and J.L. Frendo. 2010. ZO-1 is involved in trophoblastic cells differentiation in human placenta. *Am J Physiol Cell Physiol.* 298:C1517-1526.
- Pidoux, G., P. Gerbaud, O. Marpeau, J. Guibourdenche, F. Ferreira, J. Badet, D. Evain-Brion, and J.L. Frendo. 2007a. Human Placental Development Is Impaired by Abnormal Human Chorionic Gonadotropin Signaling in Trisomy 21 Pregnancies. *Endocrinology.* 148:5403-5413.

- Pidoux, G., P. Gerbaud, V. Tsatsaris, O. Marpeau, F. Ferreira, G. Meduri, J. Guibourdenche, J. Badet, D. Evain-Brion, and J.-L. Frendo. 2007b. Biochemical characterization and modulation of LH/CG-receptor during human trophoblast differentiation. *J Cell Physiol.* 212:26-35.
- Pidoux, G., and K. Tasken. 2010. Specificity and spatial dynamics of PKA signaling organized by A kinase anchoring proteins. *J Mol Endocrinol.* 44:271-284.
- Raijmakers, R., C.R. Berkers, A. de Jong, H. Ovaa, A.J. Heck, and S. Mohammed. 2008. Automated online sequential isotope labeling for protein quantitation applied to proteasome tissue-specific diversity. *Mol Cell Proteomics.* 7:1755-1762.
- Reczek, D., M. Berryman, and A. Bretscher. 1997. Identification of EBP50: A PDZ-containing phosphoprotein that associates with members of the ezrin-radixin-moesin family. *J Cell Biol.* 139:169-179.
- Ruppelt, A., R. Mosenden, M. Gronholm, E.M. Aandahl, D. Tobin, C.R. Carlson, H. Abrahamsen, F.W. Herberg, O. Carpen, and K. Tasken. 2007. Inhibition of T cell activation by cyclic adenosine 5'-monophosphate requires lipid raft targeting of protein kinase A type I by the A-kinase anchoring protein ezrin. *J Immunol.* 179:5159-5168.
- Saez, J., V. Berthoud, A. Moreno, and D. Spray. 1993. Gap junctions. Multiplicity of controls in differentiated and undifferentiated cells and possible functional implications. *Adv Second Messenger Phosphoprotein Res.* 27:163-198.
- Saez, J.C., D.C. Spray, A.C. Nairn, E. Hertzberg, P. Greengard, and M.V. Bennett. 1986. cAMP increases junctional conductance and stimulates phosphorylation of the 27-kDa principal gap junction polypeptide. *Proc Natl Acad Sci U S A.* 83:2473-2477.
- Saffitz, J.E., and A.G. Kleber. 2004. Effects of mechanical forces and mediators of hypertrophy on remodeling of gap junctions in the heart. *Circ Res.* 94:585-591.
- Saleh, H.S., U. Merkel, K.J. Geissler, T. Sperka, A. Sechi, C. Breithaupt, and H. Morrison. 2009. Properties of an ezrin mutant defective in F-actin binding. *J Mol Biol.* 385:1015-1031.
- Saotome, I., M. Curto, and A.I. McClatchey. 2004. Ezrin is essential for epithelial organization and villus morphogenesis in the developing intestine. *Dev Cell.* 6:855-864.
- Schillace, R.V., and J.D. Scott. 1999. Association of the type 1 protein phosphatase PP1 with the A-kinase anchoring protein AKAP220. *Curr Biol.* 9:321-324.
- Scholten, A., M.K. Poh, T.A. van Veen, B. van Breukelen, M.A. Vos, and A.J. Heck. 2006. Analysis of the cGMP/cAMP interactome using a chemical proteomics approach in mammalian heart tissue validates sphingosine kinase type 1-interacting protein as a genuine and highly abundant AKAP. *J Proteome Res.* 5:1435-1447.
- Shah, M.M., A.M. Martinez, and W.H. Fletcher. 2002. The connexin43 gap junction protein is phosphorylated by protein kinase A and protein kinase C: in vivo and in vitro studies. *Mol Cell Biochem.* 238:57-68.
- Shi, Q., Z. Lei, C. Rao, and J. Lin. 1993. Novel role of human chorionic gonadotropin in differentiation of human cytotrophoblasts. *endocrinology.* 132:1387-1395.
- Soderberg, O., M. Gullberg, M. Jarvius, K. Ridderstrale, K.J. Leuchowius, J. Jarvius, K. Wester, P. Hydbring, F. Bahram, L.G. Larsson, and U. Landegren. 2006. Direct observation of individual endogenous protein complexes in situ by proximity ligation. *Nat Methods.* 3:995-1000.

- Soe, K., T.L. Andersen, A.S. Hobolt-Pedersen, B. Bjerregaard, L.I. Larsson, and J.M. Delaisse. 2011. Involvement of human endogenous retroviral syncytin-1 in human osteoclast fusion. *Bone*. 48:837-846.
- Solan, J.L., and P.D. Lampe. 2009. Connexin43 phosphorylation: structural changes and biological effects. *Biochem J*. 419:261-272.
- Solstad, T., E. Bjorgo, C.J. Koehler, M. Strozynski, K.M. Torgersen, K. Tasken, and B. Thiede. 2010. Quantitative proteome analysis of detergent-resistant membranes identifies the differential regulation of protein kinase C isoforms in apoptotic T cells. *Proteomics*. 10:2758-2768.
- Takeuchi, K., N. Sato, H. Kasahara, N. Funayama, A. Nagafuchi, S. Yonemura, and S. Tsukita. 1994. Perturbation of cell adhesion and microvilli formation by antisense oligonucleotides to ERM family members. *J Cell Biol*. 125:1371-1384.
- Tasken, K., and E.M. Aandahl. 2004. Localized effects of cAMP mediated by distinct routes of protein kinase A. *Physiol Rev*. 84:137-167.
- Tasken, K.A., P. Collas, W.A. Kemmner, O. Witczak, M. Conti, and K. Tasken. 2001. Phosphodiesterase 4D and protein kinase a type II constitute a signaling unit in the centrosomal area. *J Biol Chem*. 276:21999-22002.
- TenBroek, E.M., P.D. Lampe, J.L. Solan, J.K. Reinhout, and R.G. Johnson. 2001. Ser364 of connexin43 and the upregulation of gap junction assembly by cAMP. *J Cell Biol*. 155:1307-1318.
- Wade, M., J. Trosko, and M. Schindler. 1986. A fluorescence photobleaching assay of gap junction-mediated communication between human cells. *Science*. 232:525-528.
- Wakelam, M. 1985. The fusion of myoblasts. *Biochem J*. 15:1-12.
- Weedon-Fekjær, M.S., and K. Taskén. 2011. Spatiotemporal dynamics of hCG/cAMP signaling and regulation of placental function. *Placenta*:1-5.
- Willecke, K., J. Eiberger, J. Degen, D. Eckardt, A. Romualdi, M. Guldenagel, U. Deutsch, and G. Sohl. 2002. Structural and functional diversity of connexin genes in the mouse and human genome. *Biol Chem*. 383:725-737.
- Wong, W., and J.D. Scott. 2004. AKAP signalling complexes: focal points in space and time. *Nat Rev Mol Cell Biol*. 5:959-970.
- Yogo, K., T. Ogawa, M. Akiyama, N. Ishida-Kitagawa, H. Sasada, E. Sato, and T. Takeya. 2006. PKA implicated in the phosphorylation of Cx43 induced by stimulation with FSH in rat granulosa cells. *J Reprod Dev*. 52:321-328.
- Zambonin Zallone, A., A. Teti, and M. Primavera. 1984. Monocytes from circulating blood fuse in vitro with purified osteoclasts in primary culture. *J Cell Sci*. 66:335-342.

FIGURE LEGENDS

Figure 1: An anchored cAMP/PKA signaling pathway controls human trophoblast fusion. (A)

Effect of 8-Br-cAMP, hCG and H89 on trophoblast fusion at 24 and 72 h of culture. Cells were immunostained for desmoplakin (green) and nuclei counterstained with DAPI (upper left panel). Effect of 8-Br-cAMP, hCG and H89 on cell fusion represented as remaining mononuclear cells (upper right panel) and fusion index histograms (lower left panel). Levels of hCG and hPL secreted into the culture medium of the same cultures as above (lower middle and right panels). Results are expressed as the mean \pm SEM of $n = 3$ independent experiments (* $p < 0.05$, ** $p < 0.01$, *** $p < 0.001$). Scale bar: 15 μm . (B) Trophoblasts were stimulated with hCG and treated with the RI-anchoring disruptor peptide (RIAD), the RII specific anchoring disruptor peptide (SuperAKAP-*IS*) or the RI specifier region anchoring peptide (RISR). The corresponding scrambled controls (Sc) were included in all experiments. The effect of anchoring disruptor peptides on cell fusion was assessed as remaining mononuclear cells and fusion indices (left and middle panels). Levels of hPL secreted into the medium of the same cultures at 24 h were also measured (right panel). Results are expressed as the mean \pm SEM of $n = 3$ independent experiments (* $p < 0.05$, ** $p < 0.01$, *** $p < 0.001$). (C) Trophoblasts were transfected with siRNA to AKAPs identified by MS or scrambled controls. Levels of knock down were assessed by densitometric scanning of AKAP mRNAs in knock down and control samples after RT-PCR and gel electrophoresis and normalized to actin levels in the same gels (left panel). Effect of AKAP-specific siRNAs on cell fusion was assessed as fusion indices (right panel). Results are expressed as mean \pm SEM of $n = 3$ independent experiments (ns for non-significant, * $p < 0.05$, ** $p < 0.01$, *** $p < 0.001$).

Figure 2: The A kinase binding domain in ezrin is required for regulation of cell fusion. (A)

Trophoblasts were transfected with ezrin siRNA or scrambled control alone or together with mammalian expression vectors directing expression of siRNA-resistant GFP-ezrin wild type (GFP-ezrin[#]), GFP-ezrin T567D (GFP-ezrin*), or GFP-ezrin with a mutated A-kinase binding domain (GFP-ezrin*-AKBmut), cultured for another 72 h and subjected to immunoblot analysis with indicated antibodies. Note: higher molecular weight of GFP-ezrin than ezrin is due to the GFP-tag. (B) Cells

with ezrin knock down and/or reconstitution (GFP: green) were immunostained for desmoplakin (red) and nuclei were counterstained with DAPI. Histograms represent percentage of mononuclear cells and fusion indices at 72 h of culture. Scale bar: 30 μ m. (C) Level of hCG and hPL secreted into the medium at 72 h of culture by cells treated with scrambled ezrin siRNA or ezrin siRNA with or without co-transfection with GFP-ezrin[#], GFP-ezrin* or GFP-ezrin*-AKBmut. Results are expressed as the mean \pm SEM of n = 3 independent experiments (*** p < 0.001, ** p < 0.01, ns – not significantly different from ezrin siRNA alone).

Figure 3: Ezrin organizes a supramolecular complex with PKA, Cx43 and ZO-1. (A-G) Lysates from trophoblasts were subjected to immunoprecipitation with ezrin (A), Cx43 (B), ZO-1 (C), RI α (D, G), and RII α (E). (A-E) Immunoprecipitates and corresponding lysates were analyzed by immunoblotting for the presence of the indicated proteins. Dotted lines indicate lanes combined from a single gel and exposure. See Supplement Figure S3B and C for controls with isotype-matched control antibodies. (F) Schematic illustration of the supramolecular complex including ezrin, PKA, Cx43 and ZO-1. (G) Precipitates from cytotrophoblasts subjected to immunoprecipitation with Cx43 antibody were identified by nanoLC-LTQ Orbitrap mass spectrometry analysis of tryptic digests of bands excised from SDS-PAGE. Acc. No, accession number; MW, molecular weight.

Figure 4: Ezrin colocalizes with PKA and the Cx43/ZO-1 complex. To further examine colocalization, trophoblasts were subjected to ligation proximity assay (A'-I'). Cells were stained with pairs of antibodies as depicted in the figure: Cx43-ezrin (A'), Cx43-RI α (B'), Cx43-RII α (C'), Cx43-ZO-1 (D'), ezrin-RI α (E'), ezrin-RII α (F'), ezrin-ZO-1 (G'), ZO-1-RI α (H') and ZO-1-RII α (I') and the physical proximity of the molecules stained with each pair of antibodies was then assessed using Duolink technology. Red spots show molecular proximity (< 40 nm). Cell membranes were next immunostained with Wheat Germ Agglutinin coupled to Alexa 488 conjugate (green; A to I) and nuclei counterstained with DAPI. Scale bar: 15 μ m. See Fig. S3 for negative controls. (J) Quantification of the PLA staining was performed by use of ImageJ. The intensities of the

fluorescence spots generated were normalized by the number of nuclei. (K-P) Immunohistofluorescence of ezrin (green) and cytokeratin 7 (CK7, red) in human placenta biopsies, nuclei were counterstained with TOPRO-3 (K-M) or with isotype-matched IgG (N-P). Scale bar: 10 μm .

Figure 5: Anchored PKA controls gap junction communication. (A) Trophoblasts treated with Arg-tagged anchoring disruptor peptides RIAD, SuperAKAP-1S, both peptides or scrambled controls (left panel) or with Arg-tagged PKI or its scrambled control (right panel) were examined by immunoblot for unphosphorylated (P0) and phosphorylated (P1/P2) Cx43 and actin. Representative of three experiments. Dotted lines indicate lanes combined from a single gel and exposure. (B) Gap junction communication in live trophoblasts (*) examined by calcein transfer as fluorescence recovery after photobleaching (gap-FRAP). Calcein fluorescence intensity (F), in arbitrary units (a.u.), is mapped to pseudocolors as indicated by the color-scale bar (bright yellow represents basal dye fluorescence) before (pre-bleach, $t=0$ min), just after (bleach, $t=120$ s) and 500 s after photobleaching (post-bleach) in hCG-treated cells (control) and hCG-treated cells incubated with the gap junction inhibitor (β -GA), Arg-tagged protein kinase inhibitor (PKI) or Arg-Tagged anchoring disruptors RIAD or SuperAKAP-1S and their scrambled controls. Left panel shows a representative cell for each treatment. Scale bar: 10 μm . Right top panel: Time courses of fluorescence recovery in experiments shown in left panel, F_t/F_i (bleached area/unbleached area) versus time. Right bottom panel: Diffusion rate constants (κ) for calcein transfer in $n = 6$ independent gap-FRAP experiments (mean \pm SEM; *** $p < 0.001$).

Figure 6: Delineation of the Ezrin and Cx43 interaction domains. (A) His-tagged ezrin was incubated with GST-tagged Cx43 or GST alone and subjected to immunoprecipitation with anti-His (left panel) or anti-GST antibodies (right panel). Precipitates and input mixtures were analyzed for the presence of ezrin-His, GST-Cx43 and GST by immunoblots. (B) Human ezrin and Cx43 were synthesized as 20-mer peptides on solid phase with 1-amino acid offset and probed with GST-Cx43,

GST-ezrin, respectively or GST alone. Red underscore: ezrin and Cx43 interacting regions. (C) Filters with peptides encompassing the minimal binding motifs of ezrin and Cx43 with or without substitutions (blue underscore) were overlaid with purified GST-Cx43 or GST-ezrin. (D, E) Trophoblasts transfected with ezrin specific-siRNA or scrambled control and co-transfected with siRNA insensitive GFP-ezrin D510I-R517V (GFP-ezrin* D510I-R517V) and cultured for 72 h. (D) Immunoblot with indicated antibodies. Note: higher molecular weight of GFP-ezrin than endogenous ezrin due to the GFP-tag. (E) Cells immunostained for desmoplakin (red) and nuclei (DAPI) (top panels). Histograms represent remaining mononuclear cells and fusion index (left panels) and level of hCG and hPL (right panels) secreted to the medium. Scale bar: 30 μ m. Results are expressed as the mean \pm SEM of n = 3 independent experiments (ns for non significant, *** p < 0.001).

Figure 7: Ezrin bound to Cx43 is necessary for PKA control of gap junction communication. (A) Lysates from trophoblasts transfected with ezrin siRNA and GFP-ezrin*, GFP-ezrin*-AKBmut or GFP-ezrin*-D510I-R517V plasmids were subjected to immunoprecipitation with GFP antibody. Lysate and precipitate were analyzed for the presence of ezrin, RI α , RII α , Cx43, radixin, moesin and actin. Dotted lines indicate lanes combined from single gel and exposure. (B) Trophoblasts were transfected with scrambled ezrin siRNA or ezrin siRNA with or without co-transfection with GFP-ezrin[#], GFP-ezrin*, GFP-ezrin*-AKBmut plasmid or GFP-ezrin*-D510I-R517V, stimulated with hCG and subjected to gap-FRAP analysis. Left: calcein fluorescence intensity (*F*) transfer in individual trophoblasts (asterisk) mapped to pseudocolors as indicated by the color-scale bar (in arbitrary units (a.u.)) before (pre-bleach, t=0 min), just after (bleach, t=120 s) and 500 s after photobleaching (post-bleach). Scale bar: 10 μ m. Right: calcein percent fluorescence ratio *F*_t/*F*_i (bleached area/unbleached area) *versus*. time (top). Calcein diffusion rate constants (κ) (bottom; mean \pm SEM of n = 6 independent experiments; *** p < 0.001).

Figure 8: Cell fusion is controlled by PKA-mediated phosphorylation of Cx43 through ezrin anchoring. (A) Trophoblasts were transfected with Cx43 siRNA or scrambled control alone or

together with mammalian expression vectors directing expression of siRNA-resistant GFP-Cx43 (GFP-Cx43[∞]), GFP-Cx43 R370E (GFP-Cx43[∞]-R370E), or GFP-Cx43 with substitutions in the Cx43-PKA phosphosite (GFP-Cx43[∞]-6SD, GFP-Cx43[∞]-6SD-R370E, GFP-Cx43[∞]-6SA, GFP-Cx43[∞]-6SA-R370E), cultured for another 72 h and subjected to immunoblot analysis with indicated antibodies. Note: higher molecular weight of GFP-Cx43 than ezrin is due to the GFP-tag. (B) Cells with Cx43 knock down and/or reconstitution as in A were immunostained for desmoplakin (red) and nuclei were counterstained with DAPI. Scale bar: 30 μ m. (C) Histograms represent percentage of mononuclear cells and fusion indices at 72 h of culture as in A and B. (D) The GFP-Cx43[∞]-R370E fusion protein with out ability to bind ezrin and with individual phospho- or dephospho-mimicking S to D and S to A substitutions in residues 364, 365, 368 or all 3 (3SD and 3SA) was expressed in trophoblasts with Cx43 knock down and cell fusion assessed as in C. Histograms in panels C and D show mean \pm SEM of n = 3 independent experiments; *** p < 0.001).

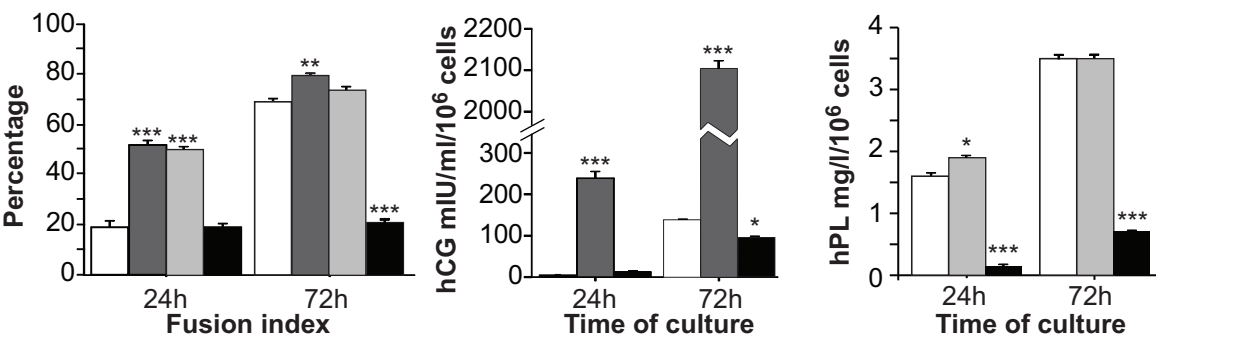
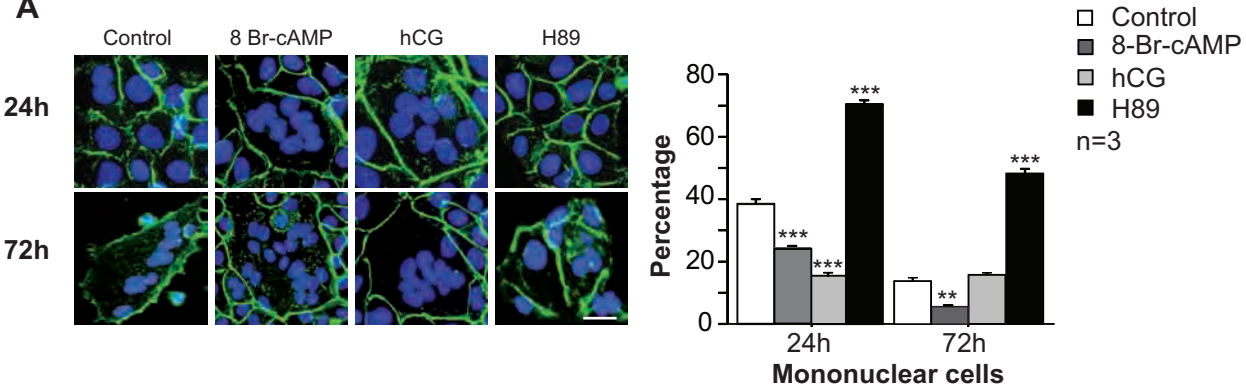
Figure 9: Gap junction communication in trophoblasts is controlled by PKA anchored through Cx43.

(A-D) Trophoblasts were transfected with scrambled Cx43 siRNA or Cx43 siRNA with or without co-transfection with Cx43 variants as in Fig. 8 as indicated, stimulated with hCG and subjected to GFP-immunoprecipitation (A) and gap-FRAP analysis (B). (C) Calcein fluorescence intensity (*F*) transfer in individual trophoblasts (asterisk) mapped to pseudocolors as indicated by the color-scale bar (in arbitrary units (a.u.)) before (pre-bleach, t=0 min), just after (bleach, t=120 s) and 500 s after photobleaching (post-bleach). Scale bar: 10 μ m. (D) Calcein percent fluorescence ratio *F_t/F_i* (bleached area/unbleached area) *versus* time (top). Calcein diffusion rate constants (κ) (bottom; mean \pm SEM of n = 3 independent experiments; *** p < 0.001). (E) Schematic depiction of trophoblast gap junction with Cx43 and ZO-1 with a compartmentalized pool of PKA anchored by ezrin bound to Cx43 (left). Upon hCG stimulation, increased cAMP activates PKA leading to a spatiotemporally controlled phosphorylation of Cx43 that increases the communication through the gap junction.

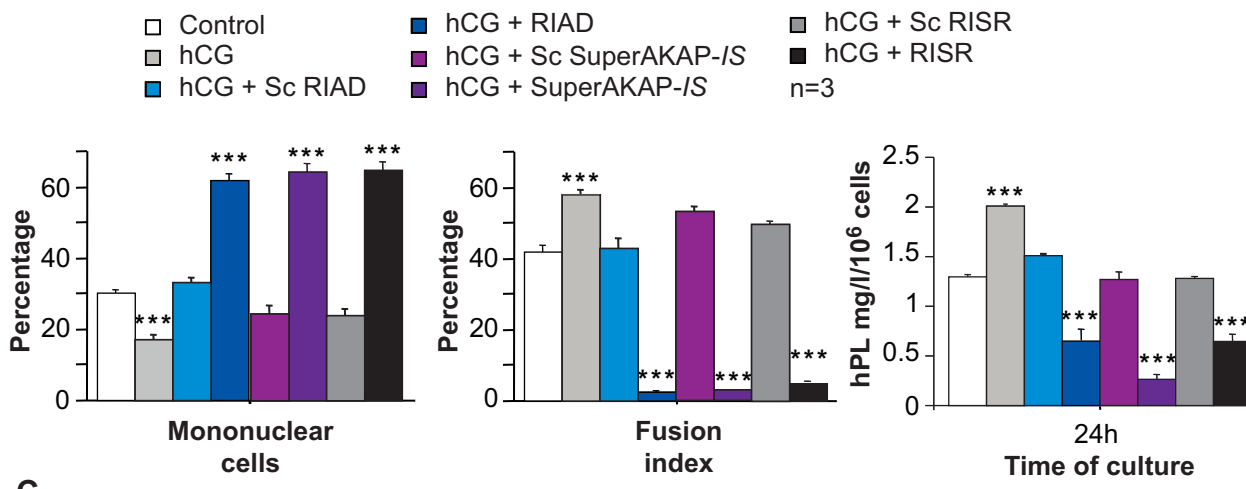
TABLES

Table 1: AKAPs associated with PKAs in trophoblasts. Proteins from cytotrophoblasts and syncytiotrophoblast were subjected to affinity chromatography with flag-tagged PKA RI and RII and identified by nanoLC-LTQ Orbitrap mass spectrometry analysis of tryptic digests of bands excised from SDS-PAGE. Acc. No, Accession number; Mw, molecular weight.

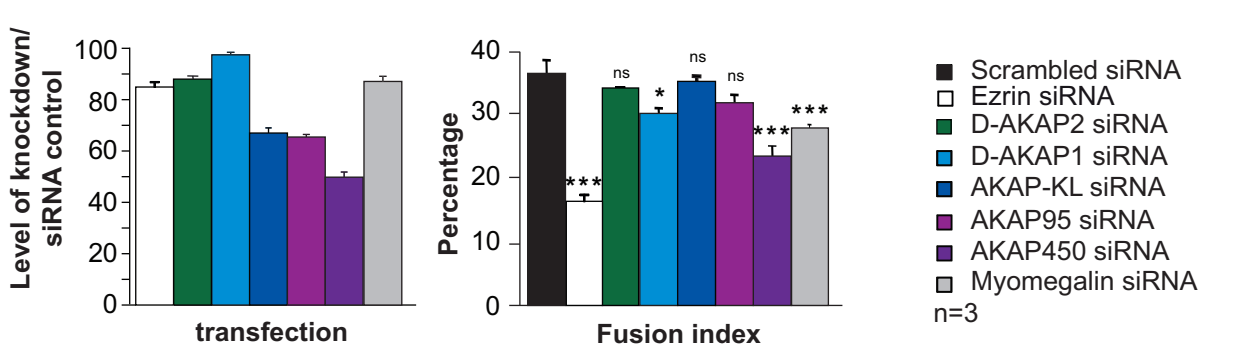
A



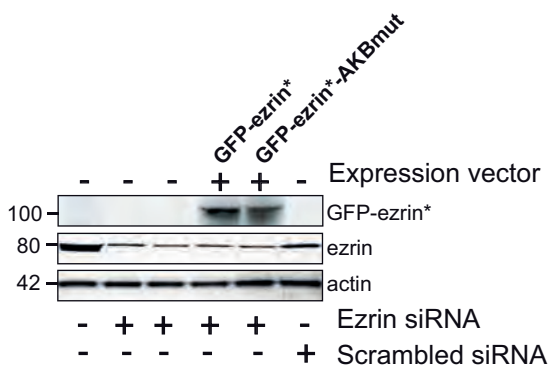
B



C

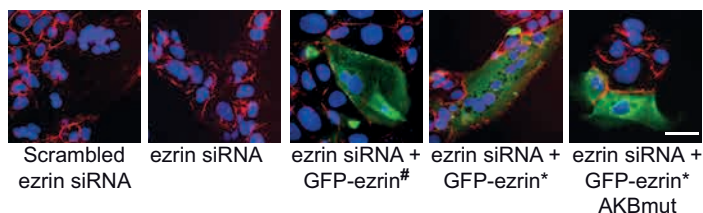


A

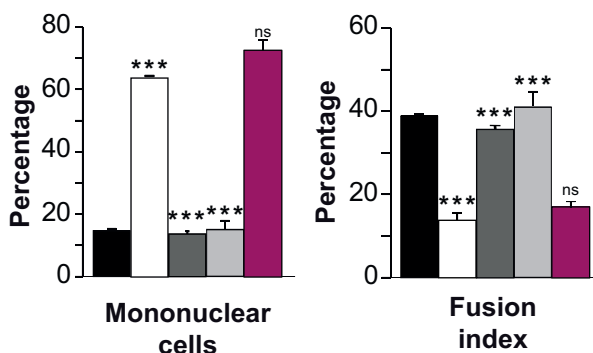


siRNA resistant ezrin wild type; * siRNA resistant ezrin T567D

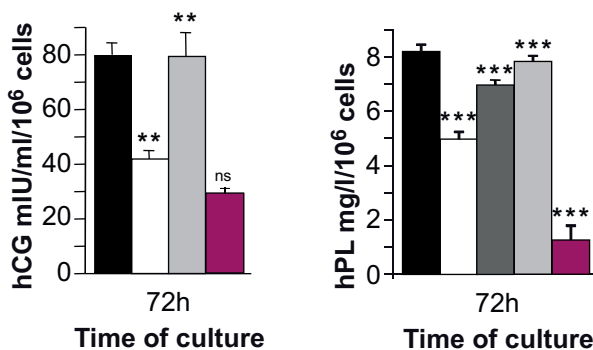
B

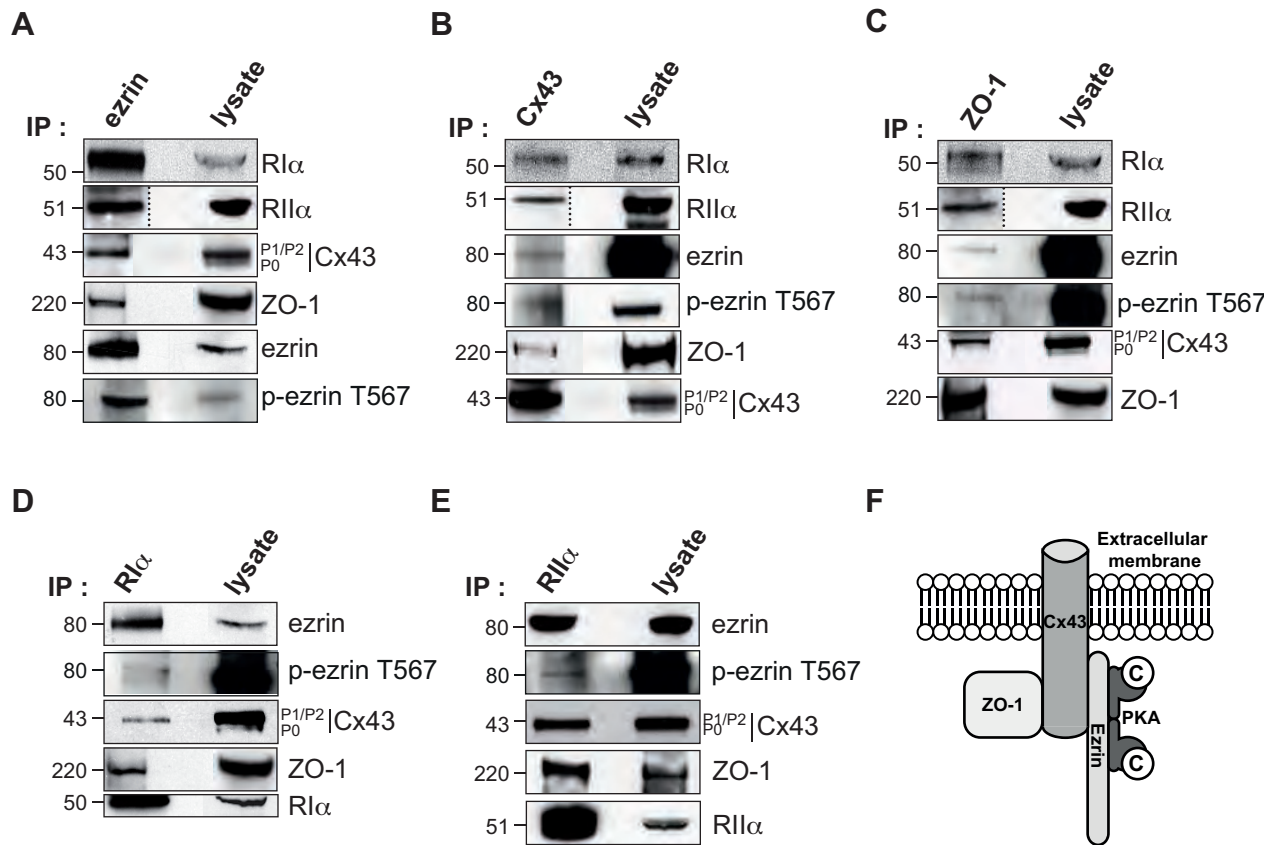


- Scrambled ezrin siRNA
 - Ezrin siRNA
 - Ezrin siRNA + GFP-ezrin#
 - Ezrin siRNA + GFP-ezrin*
 - Ezrin siRNA + GFP-ezrin* AKBmut
- n=3



C

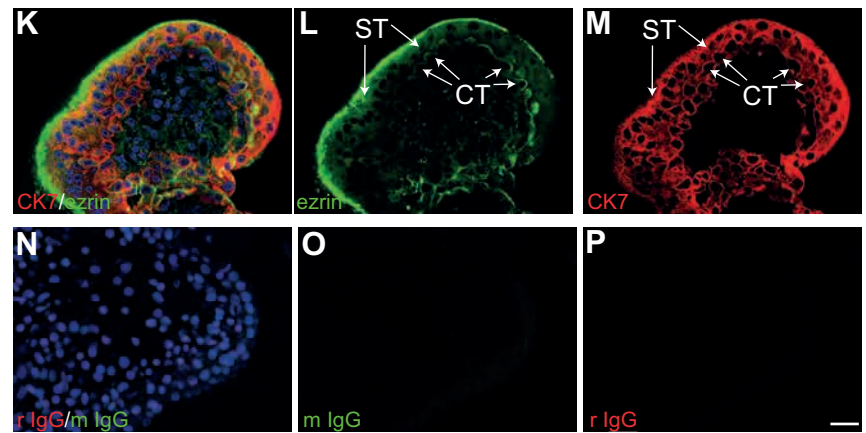
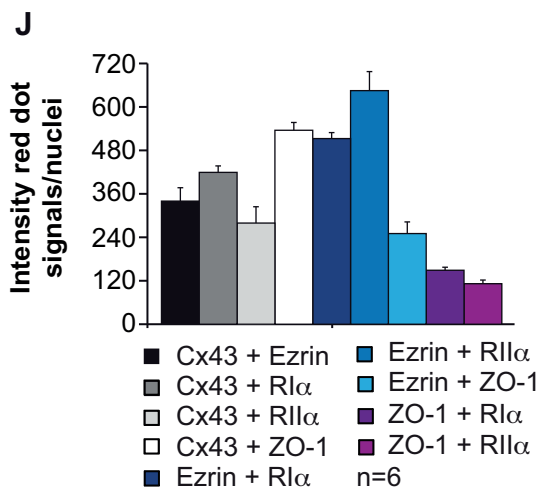
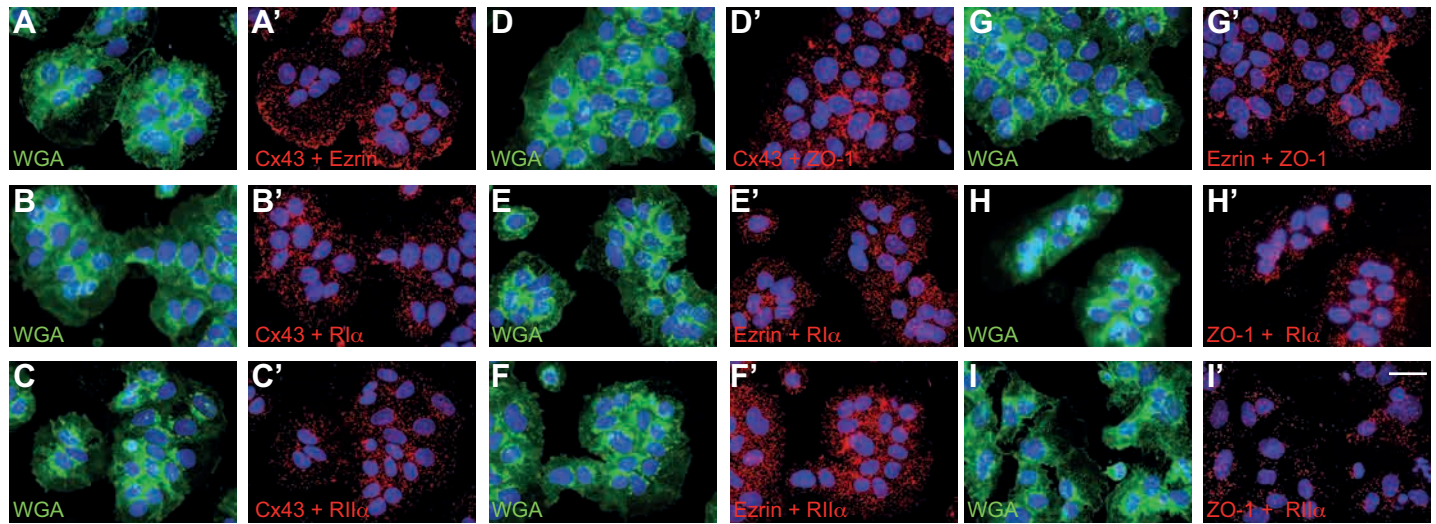


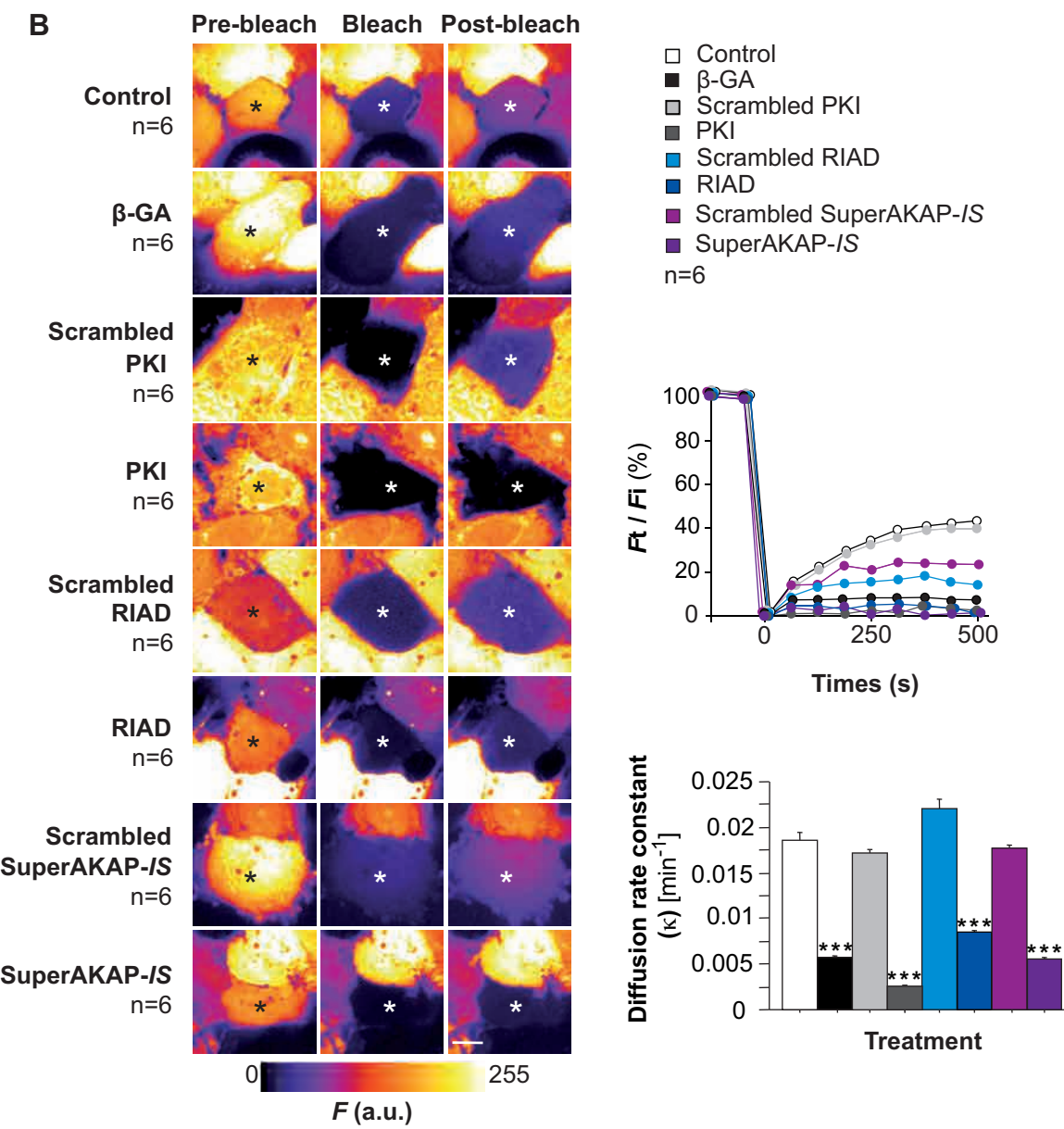
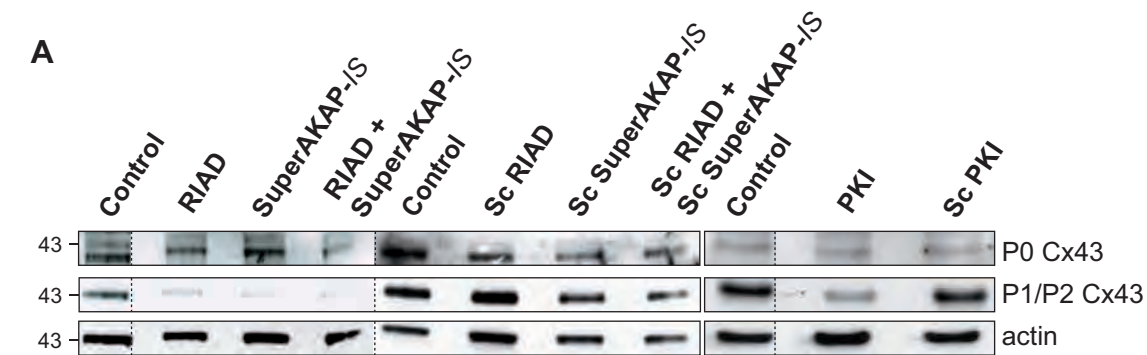


G

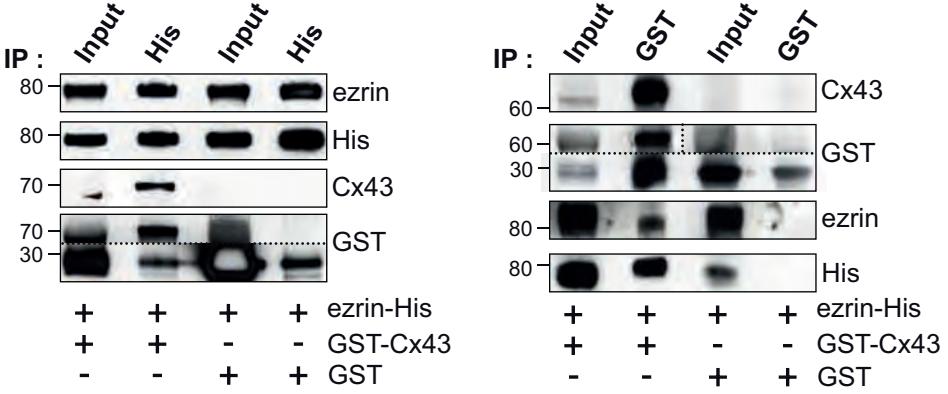
Protein name	Common name	UniProt. Acc. No.	No. of peptides	Mascot score	MW (Da)
Cx43 Immunoprecipitation					
EZRI	Ezrin	P15311	3	142	69413
TJP1	Tight junction protein ZO-1	Q07157	1	53	195459
GJA1	Gap junction alpha-1 protein	P17302	4	122	43008

Pidoux et al, Figure 4

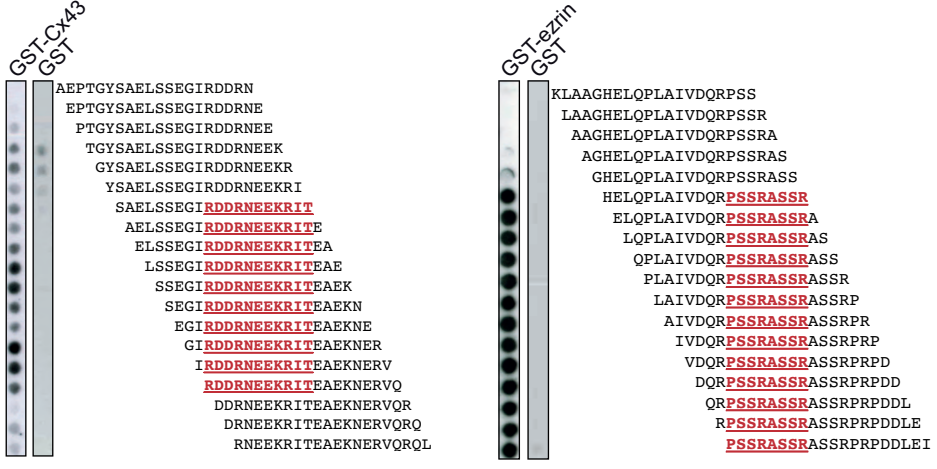




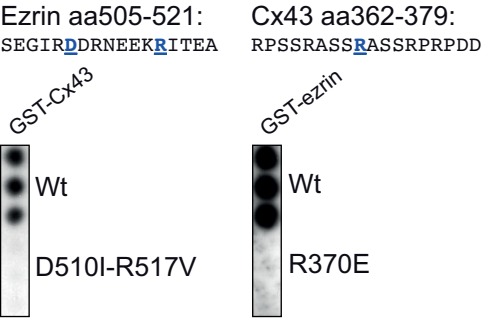
A



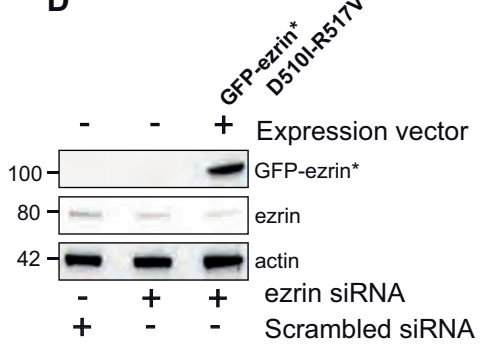
B



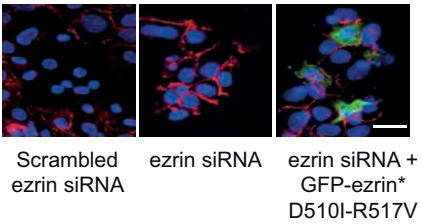
C



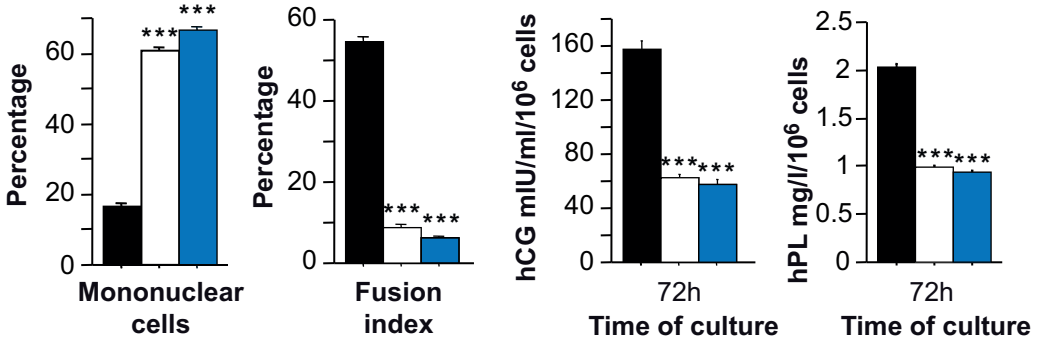
D



E

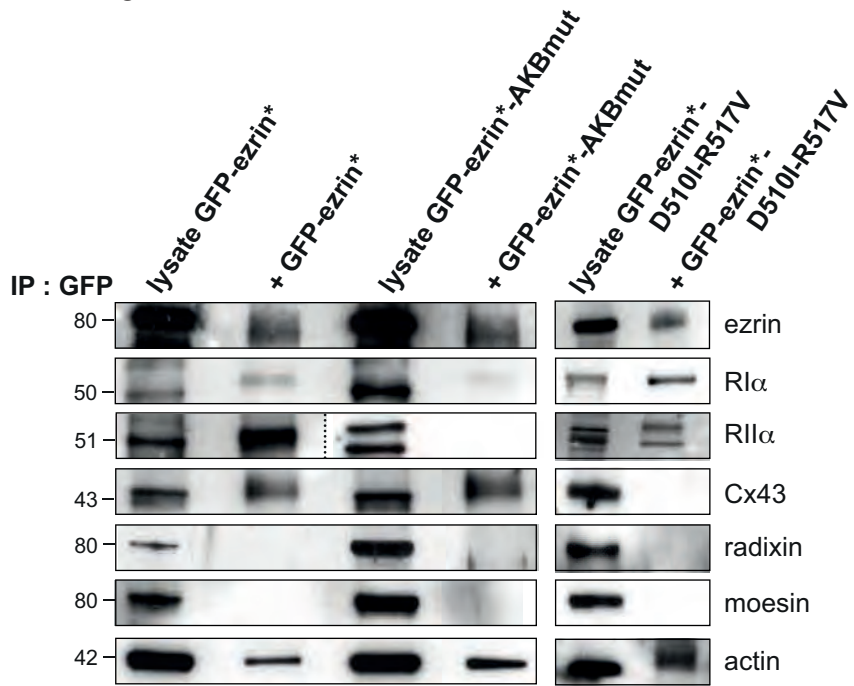


■ Scrambled ezrin siRNA
 □ ezrin siRNA
 ■ ezrin siRNA + GFP-ezrin* D510I-R517V
 n=3



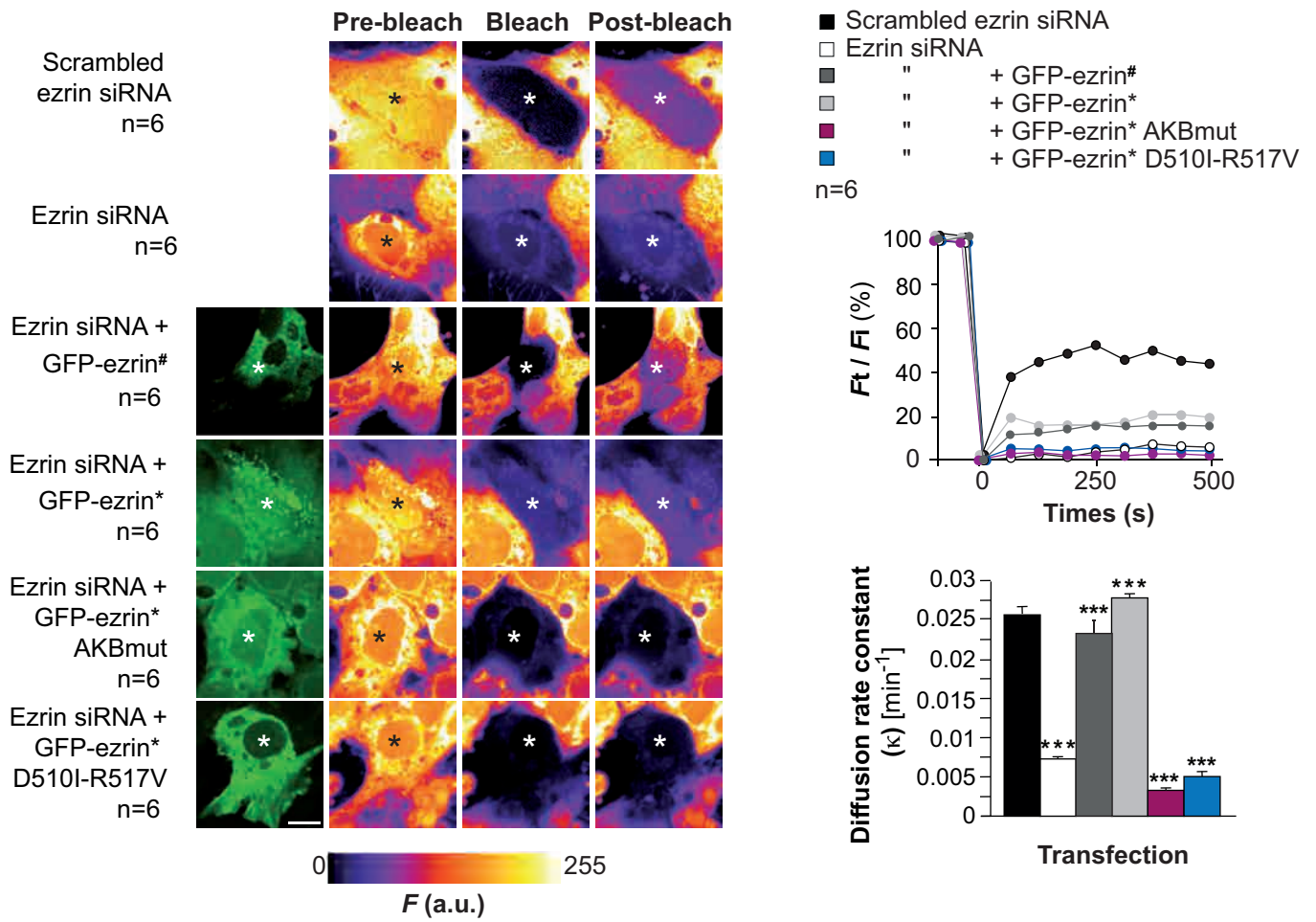
* siRNA resistant ezrin T567D

A

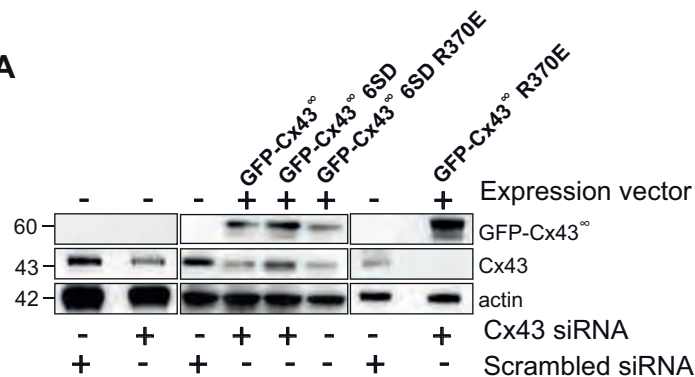


siRNA resistant ezrin wild type; * siRNA resistant ezrin T567D

B

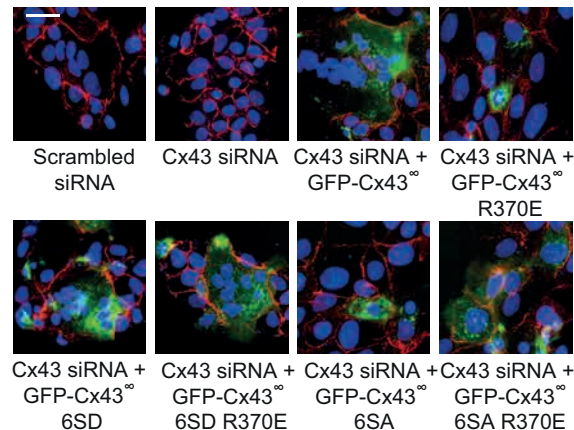


A

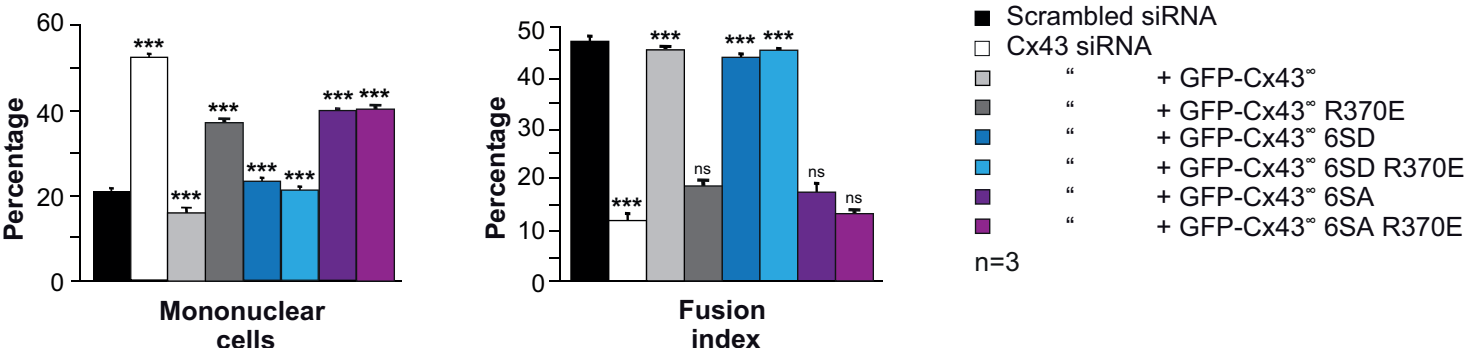


° siRNA resistant Cx43 wild type

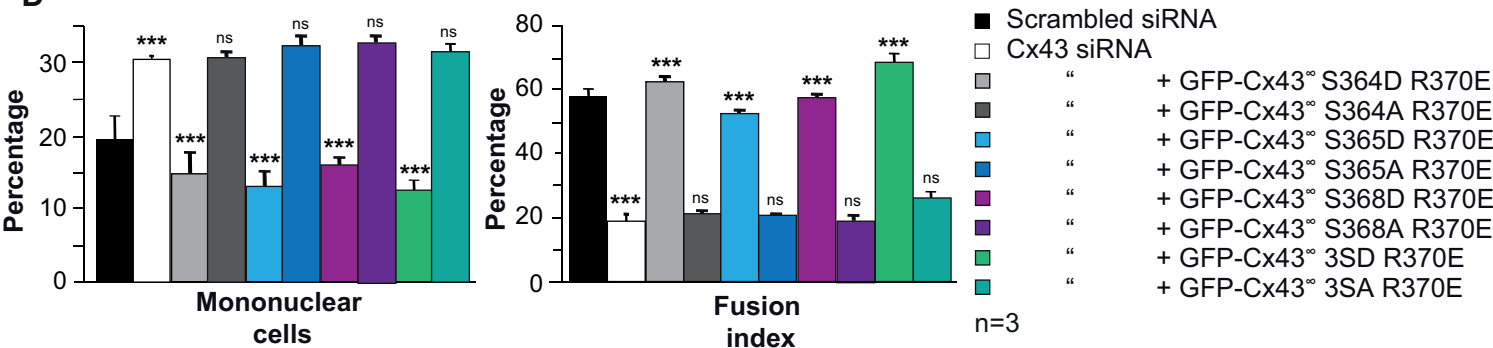
B



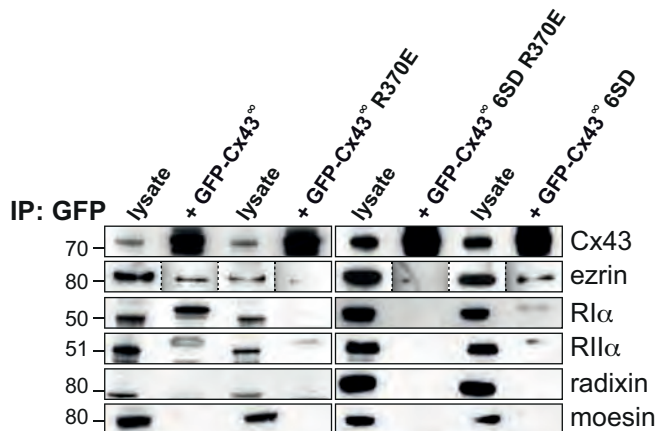
C



D

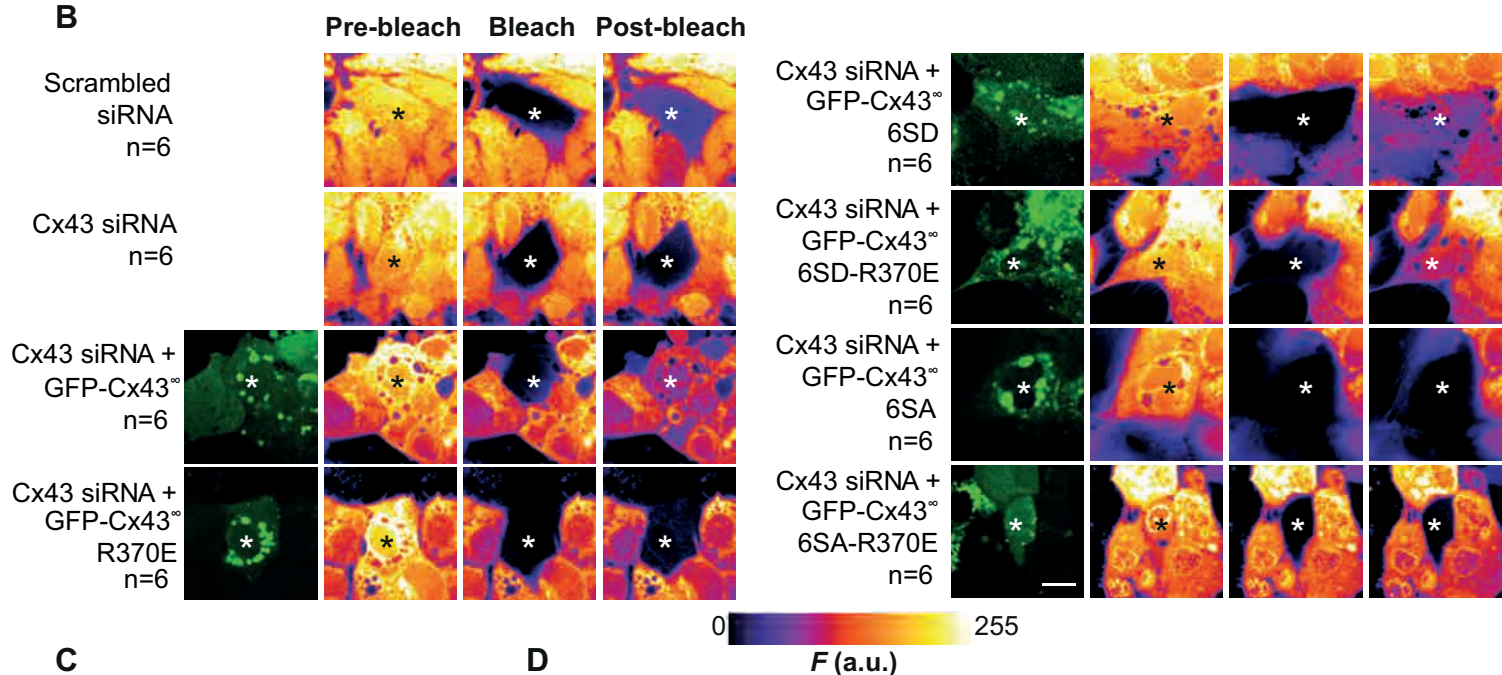


A

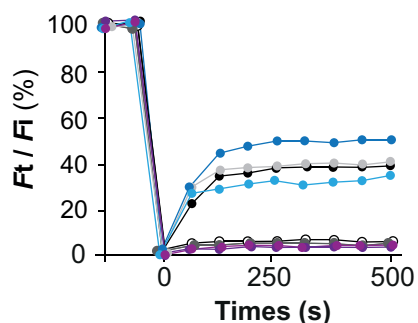


^{si} siRNA resistant Cx43 wild type

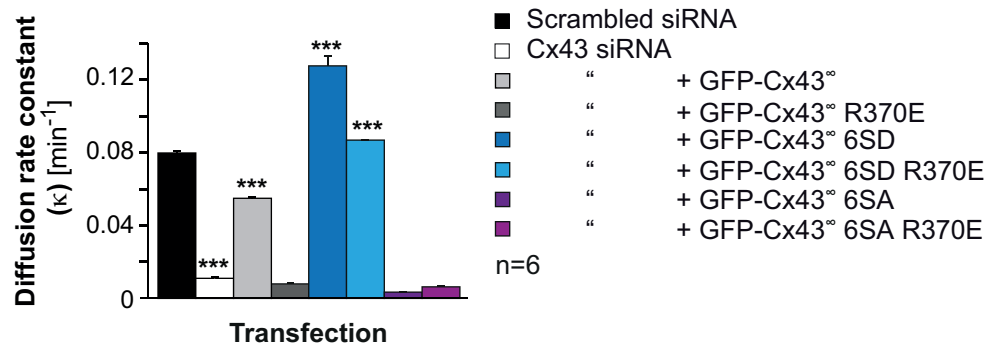
B



C



D



E

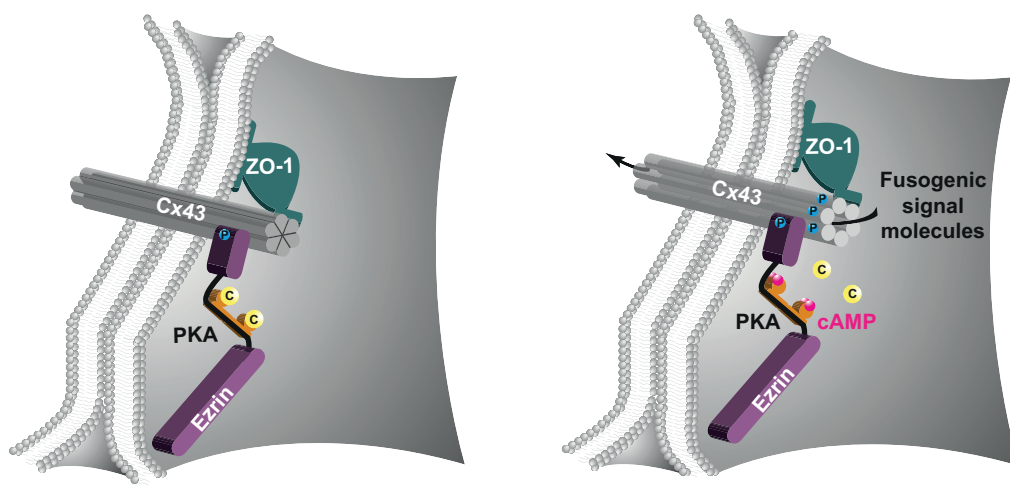


Table 1

Cytotrophoblast	Protein name	Common name	UniProt. Acc. No.	No. of peptides	Mascot score	MW (Da)	
RI affinity chromatography							
	EZRI	Ezrin	Ezrin	P15311	4	112	69413
	OPA1	Dynamin-like 120 kDa protein	OPA1	O60313	1	31	111561
RII affinity chromatography							
	AKAP1	A kinase anchor protein 1	D-AKAP1	Q92667	3	58	97342
	AKAP2	A kinase anchor protein 2	AKAP-KL	Q9Y2D5	15	790	96101
	AKAP8	A kinase anchor protein 8	AKAP95	O43823	3	184	76108
	AKAP9	A kinase anchor protein 9	AKAP450	Q99996	52	750	453667
	AKAP12	A kinase anchor protein 12	Gravin	Q02952	2	39	191483
	AKP13	A kinase anchor protein 13	AKAP-Lbc	Q12802	32	1258	307550
	EZRI	Ezrin	Ezrin	P15311	3	114	69413
	MYOME	Myomegalin	Myomegalin	Q5VU43	9	231	265080
Syncytiotrophoblast							
Syncytiotrophoblast	Protein name	Common name	UniProt. Acc. No.	No. of peptides	Mascot score	MW (Da)	
RI affinity chromatography							
	EZRI	Ezrin	Ezrin	P15311	1	43	69413
RII affinity chromatography							
	AKAP2	A kinase anchor protein 2	AKAP-KL	Q9Y2D5	12	478	96101
	AKAP8	A kinase anchor protein 8	AKAP95	O43823	1	24	76108
	AKAP9	A kinase anchor protein 9	AKAP450	Q99996	8	251	453667
	AKP13	A kinase anchor protein 13	AKAP-Lbc	Q12802	8	270	307550
	EZRI	Ezrin	Ezrin	P15311	1	39	69413

SUPPLEMENTAL MATERIAL TO:

A PKA-ezrin-connexin 43 signaling complex controls gap junction communication in cell fusion

by Guillaume Pidoux, Pascale Gerbaud, Jim Dompierre, Birgitte Lygren, Therese Solstad,
Danièle Evain-Brion and Kjetil Taskén

Supplemental Figure Legends

Supplemental Figure S1: Effect of PKA, Epac and anchoring disruptor peptides on trophoblast fusion. (A) Effect of H89 in the presence of hCG, PKI in the absence and presence of 8-Br-cAMP or hCG, the Epac specific agonist 8-pCPT-2'-O-Me-cAMP, and the PKA specific agonist 6-Bnz-cAMP on cell fusion at 72 h of culture assessed as mononuclear cell numbers and fusion index. (B) Levels of hCG and hPL secreted into the culture medium at 72 h of culture by untreated cells (control) and cells treated as in A. Results are expressed as the mean \pm SEM of n = 3 independent experiments (* p < 0.05, ** p < 0.01, *** p < 0.001). (C) Histogram representing viability (%) of untreated cells (control) and cells incubated with RIAD or SuperAKAP-*IS*. (D) Trophoblasts were incubated with FITC-RIAD or SuperAKAP-*IS*-FITC. Cells were fixed and nuclei were stained with DAPI (left panel). Histogram represents the percentage of cells positive for FITC-RIAD or SuperAKAP-*IS*-FITC. Scale bar: 75 μ m. (E) Trophoblasts were stimulated with 8-Br-cAMP alone or in combination with loading of the RI-anchoring disruptor peptide (RIAD), the scrambled RIAD peptide, the RII specific anchoring disruptor (SuperAKAP-*IS*), the scrambled SuperAKAP-*IS*, the RI specifier region anchoring peptide (RISR) or the scrambled RISR. Effect of anchoring disruptor peptides and scrambled peptides on the cell fusion are represented as mononuclear cell numbers and fusion indices. Levels of hCG secreted into the culture medium at 24 h of culture by cells treated with the different anchoring disruptor peptides were also examined (right histograms). Results are expressed as the mean \pm SEM of n = 3 independent experiments (** p < 0.01, *** p < 0.001).

Supplemental Figure S2: Effect of ezrin and D-AKAP2 silencing on trophoblast fusion. (A-B) Immunoblot analysis of ezrin (A), D-AKAP2 (B) and actin (A, B) levels in trophoblasts transfected with specific siRNAs or scrambled controls at 72 h of culture. Levels of ezrin (A) or D-AKAP2 (B) were assessed by densitometric scanning of immunoblots and normalized to actin levels in the same blots. Cells were immunostained for desmoplakin (green) and nuclei were counterstained with DAPI after siRNA transfection. Scale bar: 15 μ m. (C) Effect of ezrin-specific siRNA, D-AKAP2-specific siRNA and scrambled siRNA controls on cell fusion assessed as remaining mononuclear cells and fusion indices. (D) Levels of hCG and hPL secreted into the culture medium at 72 h of culture by cells treated with ezrin siRNA, D-AKAP2 siRNA and scrambled control siRNAs. Results are expressed as mean \pm SEM of n = 3 independent experiments (ns for non-significant, *** p < 0.001).

Supplemental Figure S3: ERM proteins, co-immunoprecipitation and proximity ligation assay controls. (A) Western blot analysis of moesin, radixin and actin levels in trophoblasts transfected with ezrin specific-siRNA or scrambled control and co-transfected with siRNA insensitive GFP-ezrin (GFP-ezrin*) or AKB-mutated, siRNA insensitive GFP-ezrin (GFP-ezrin*-AKBmut) after 72 h of culture. (B) As control for experiments in Figure 3, lysates from trophoblasts were subjected to immunoprecipitation with IgG from rabbit (left) and mouse (right) and analyzed by immunoblotting with RI α , RII α , ezrin, Cx43 and ZO-1 antibodies. (C) Left panel: Immunoblot analysis of radixin, moesin, ezrin and actin levels in trophoblasts transfected with radixin- and moesin-specific siRNAs or scrambled control at 72 h of culture. Middle panels: Levels of ERM proteins were assessed by densitometric scanning of immunoblots and normalized to actin levels in the same blots. Right panels: histograms represent the effect of radixin- and moesin-specific siRNAs and scrambled siRNA on cell fusion assessed as remaining mononuclear cells and fusion indices. Results are expressed as mean \pm SEM of n = 3 independent experiments (*** p < 0.001). (D-L') As controls for experiments in Figure 4A-J, trophoblasts were subjected to proximity ligation *in vitro* assay using Duolink technology (D'-L'). Trophoblast membranes were immunostained with Wheat Germ Agglutinin 488 conjugate (green;

D-L) and cells were stained with pairs of antibodies or individual antibody alone as depicted in the figure: mIgG-rIgG (D'), Cx43 (E'), ezrin (F'), RI α (G'), RII α (H'), ZO-1 (I'), SP1 (J'), Cx43-SP1 (K') and ezrin-SP1 (L') and nuclei were counterstained with DAPI (D-K'). (M-T) Cells were separately immunostained for mIgG, rIgG, Cx43, ezrin, RI α , RII α , ZO-1, SP1 (green) and nuclei were counterstained with DAPI. Scale bars: 30 μ m.

Supplemental Figure S4: Effect of anchoring disruptor peptides, ezrin silencing and Cx43 variants on cell adhesion, Cx43 expression and localization. (A) PLA experiments were performed on trophoblasts during the fusion process with pairs of antibodies to ezrin and RI α or RII α (left panels). Scale bar: 15 μ m. Histograms show the intensity of the red dot signals normalized by the number of nuclei (right panels; mean \pm SEM of n = 3 independent experiments. (B, C, E) Trophoblast were treated with 8-Br-cAMP or hCG alone or together with anchor disrupting peptides or their scrambled controls (B), with ezrin siRNA or its scrambled control (C) or with GFP-Cx43 variants (E). Cells were next stained with a pair of antibodies to Cx43 or GFP and desmoplakin (DSK) and subjected to proximity ligation *in vitro* assay (PLA). The interaction of molecules stained with the pairs of antibodies was then assessed using Duolink technology. Red dots show molecular proximity (< 40 nm). Nuclei were counterstained with DAPI. Histograms represent the intensity of the red dot signals normalized by the number of nuclei. Scale bars: 15 μ m. Results are expressed as the mean \pm SEM of n = 6 (B, C) or n=3 (E) independent experiments (***) p < 0.001). (D) Immunoblot analysis of desmoplakin, E-cadherin and actin levels in trophoblasts transfected with ezrin specific-siRNA or scrambled control and co-transfected with siRNA insensitive GFP-ezrin (GFP-ezrin*), siRNA insensitive GFP-ezrin AKB mutated (GFP-ezrin*-AKBmut) or siRNA insensitive GFP-ezrin* with mutation in the ezrin binding domain (GFP-ezrin*-D510I-R517V) after 72 h of culture. (F) Table describing the GFP-Cx43 variants, their amino acids sequences and the location of mutations (red: phosphorylation site substitutions; blue, underlined: ezrin interaction site substitution).

Supplemental Figure S5: Identification and characterization of minimal residues binding motifs in ezrin and Cx43. (A) The full length human ezrin (upper panels) and Cx43 (lower panels)

sequences were synthesized as overlapping 20-mer peptides with 3-amino acid shifts on cellulose membranes and incubated with recombinant Cx43-GST or ezrin-GST, respectively or GST alone as control. Binding was detected by immunoblotting using HRP-conjugated anti-GST antibodies. Numbered boxes correspond to putative binding sequences between ezrin and Cx43. (B) N-, C- and N&C terminal truncations of the ezrin amino acid 501 to 528 sequence (shown to interact with Cx43) coupled to on cellulose membrane and incubated with recombinant Cx43-GST. Binding was detected by immunoblotting using HRP-conjugated anti-GST antibodies. (C) N-, C- and N&C terminal truncations of the Cx43 amino acid 351 to 382 sequence (shown to interact with ezrin) coupled to cellulose membranes and incubated with recombinant ezrin-GST. Binding was detected by immunoblotting using HRP-conjugated anti-GST antibody. (D) The Cx43 and ezrin-interacting sequences were subjected to proline scan by sequential substitution with proline in order to identify amino acids essential for the binding of ezrin (left panel) and Cx43 (right panel) respectively. (E) Two dimensional peptide arrays were synthesized for the ezrin and Cx43 binding sequences by substituting the residues with all natural amino acids as indicated. The first two rows correspond to the wild type ezrin (left panel) and Cx43 (right panel). Filters were probed using recombinant Cx43-GST and ezrin-GST, respectively. Interactions were detected using HRP-conjugated anti-GST antibody. Red boxes correspond to the essential residues for binding of Cx43 and ezrin, respectively and are identified by the absence of positive spots.

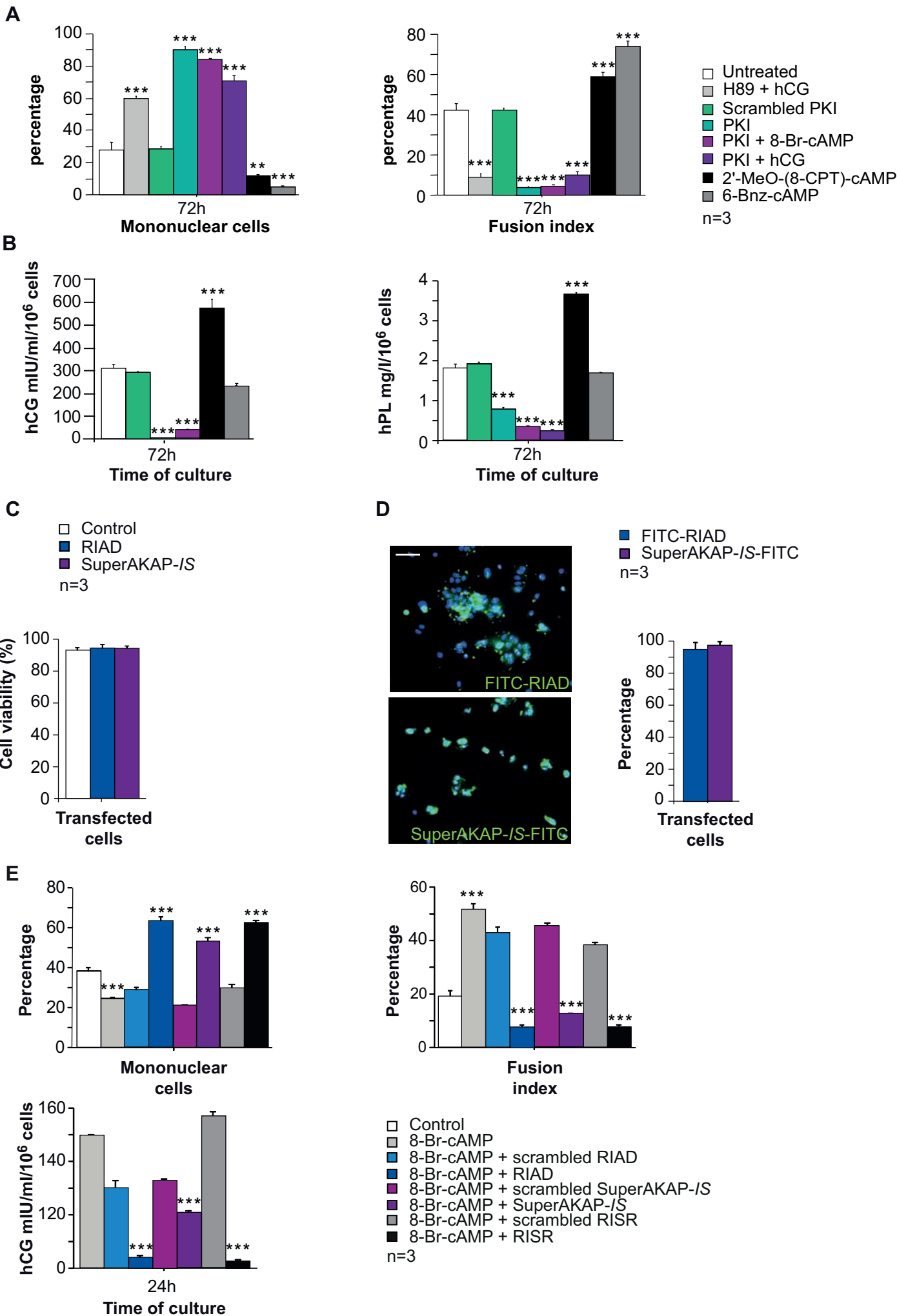
Video 1: Effect of PKI and anchoring disruptor peptides on gap junction communication in live cells examined by calcein transfer as fluorescence recovery after photobleaching (gap-FRAP).

Video corresponding to still pictures of the same gap-FRAP experiment as shown in Fig. 5B. Time courses of calcein red-orange AM transfer as fluorescence recovery after photobleaching appears in sequence in the same order as the rows in Fig. 5B and as indicated as the start of each recording in hCG-treated cells (control), hCG-treated cells incubated with the gap junction inhibitor (β -GA), Arg-tagged protein kinase inhibitor (PKI) and Arg-Tagged anchoring disruptors RIAD or SuperAKAP-1S and their scrambled controls. Confocal images were collected using a microscope fitted with a

spinning disk (Yokogawa CSU-X1). Time in minutes and seconds is indicated in the top right corner. Scale: 0.5 cm = 10 μ m.

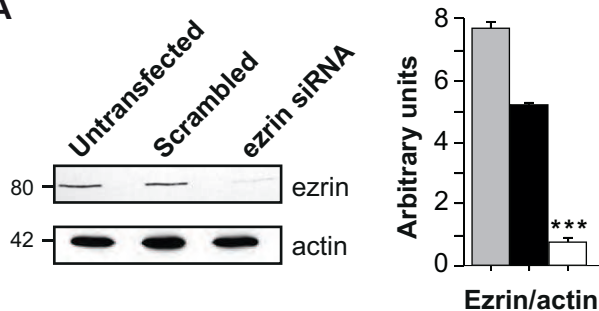
Video 2: Effect of ezrin siRNA with or without co-transfection with GFP-ezrin*, GFP-ezrin*-AKBmut plasmid or GFP-ezrin*-D510I-R517V on gap junction communication in live cells examined by calcein transfer as gap-FRAP. Video corresponds to still pictures from the same experiments as shown in Fig. 7B. Video shows sequentially time courses of calcein red-orange AM transfer as fluorescence recovery after photobleaching in hCG-treated cells transfected with scrambled ezrin siRNA or ezrin siRNA with or without co-transfection with GFP-ezrin*, GFP-ezrin*-AKBmut plasmid or GFP-ezrin*-D510I-R517V. Confocal images were collected using a microscope (Nipkow spinning disk) fitted with a spinning disk (Yokogawa CSU-X1). Time in minutes and seconds is indicated in the top right corner. Scale: 0.5 cm = 10 μ m.

Video 3: Effect of Cx43 siRNA with or without co-transfection with GFP-Cx43[∞], GFP-Cx43[∞] R370E, GFP-Cx43[∞] 6SD, GFP-Cx43[∞] 6SD R370E, GFP-Cx43[∞] 6SA or GFP-Cx43[∞] 6SA R370E on gap junction communication in live cells examined by calcein transfer as gap-FRAP. Video corresponds to still pictures from the same experiments as shown in Fig. 9B. Video sequentially shows time courses of calcein red-orange AM transfer as fluorescence recovery after photobleaching in hCG-treated cells transfected with scrambled Cx43 siRNA or Cx43 siRNA with or without co-transfection with GFP-Cx43[∞], GFP-Cx43[∞] R370E, GFP-Cx43[∞] 6SD, GFP-Cx43[∞] 6SD R370E, GFP-Cx43[∞] 6SA or GFP-Cx43[∞] 6SA R370E plasmids. Confocal images were collected using a microscope (Nipkow spinning disk) fitted with a spinning disk (Yokogawa CSU-X1). Time in minutes and seconds is indicated in the top right corner. Scale: 0.5 cm = 10 μ m.

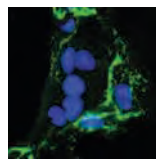
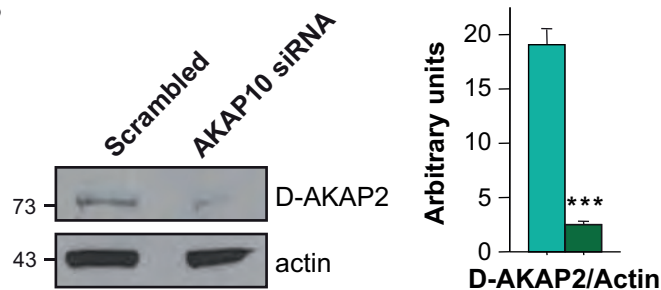


Untransfected
 Scrambled ezrin siRNA
 ezrin siRNA
 Scrambled AKAP10 siRNA
 D-AKAP2 siRNA
 n=3

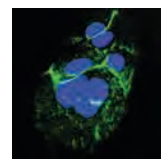
A



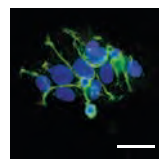
B



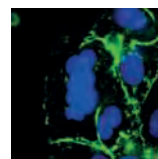
Untransfected



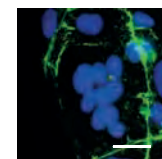
Scrambled ezrin siRNA



ezrin siRNA

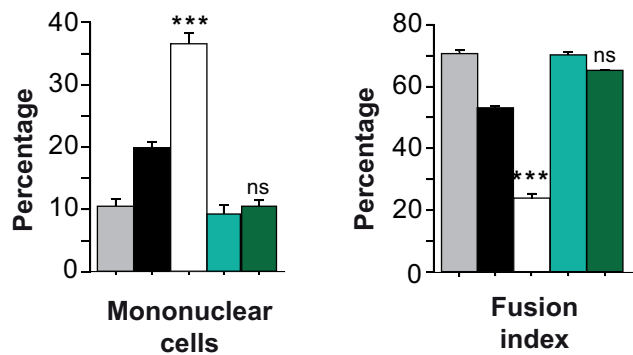


Scrambled D-AKAP2 siRNA

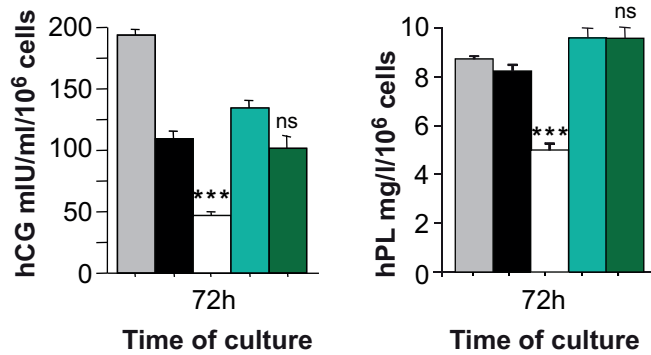


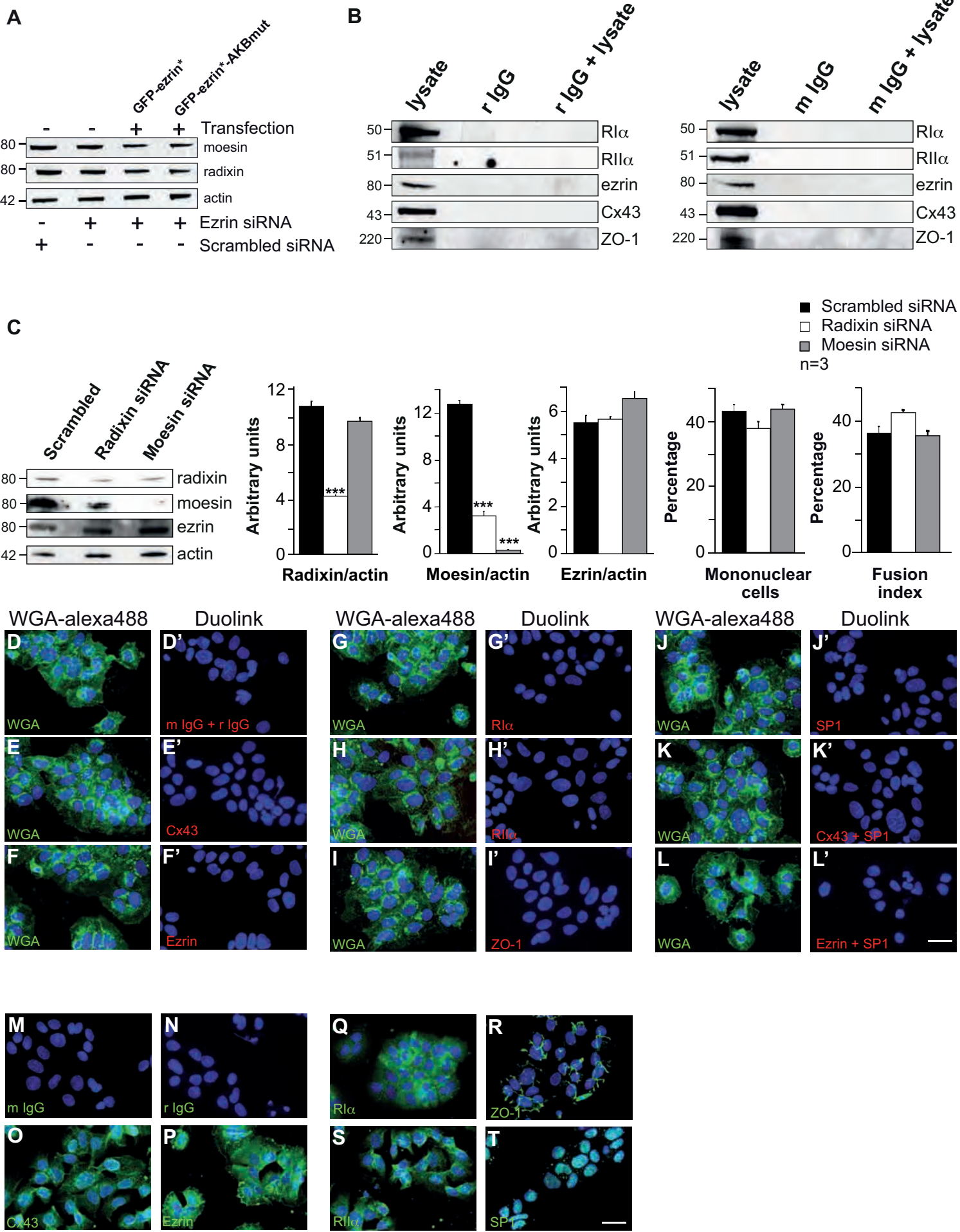
D-AKAP2 siRNA

C

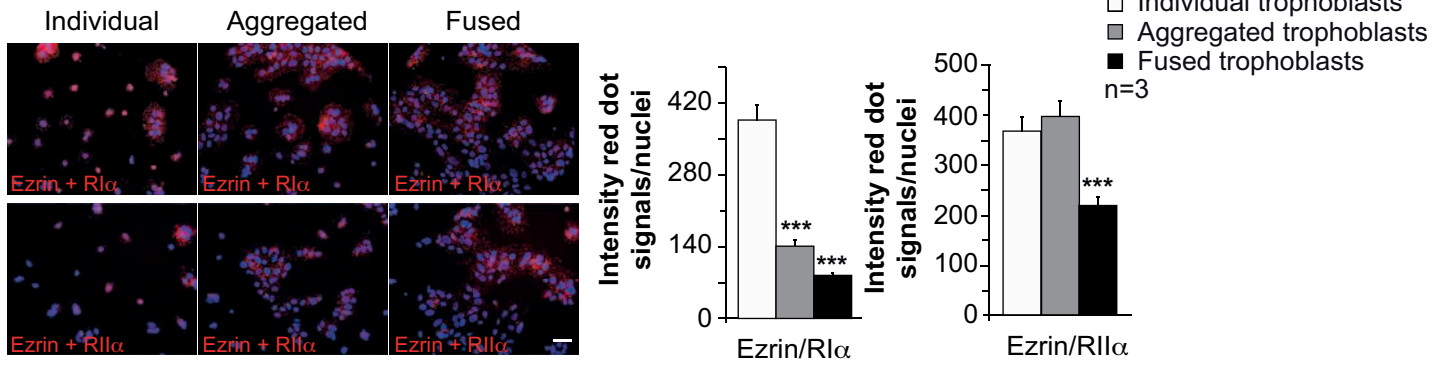


D

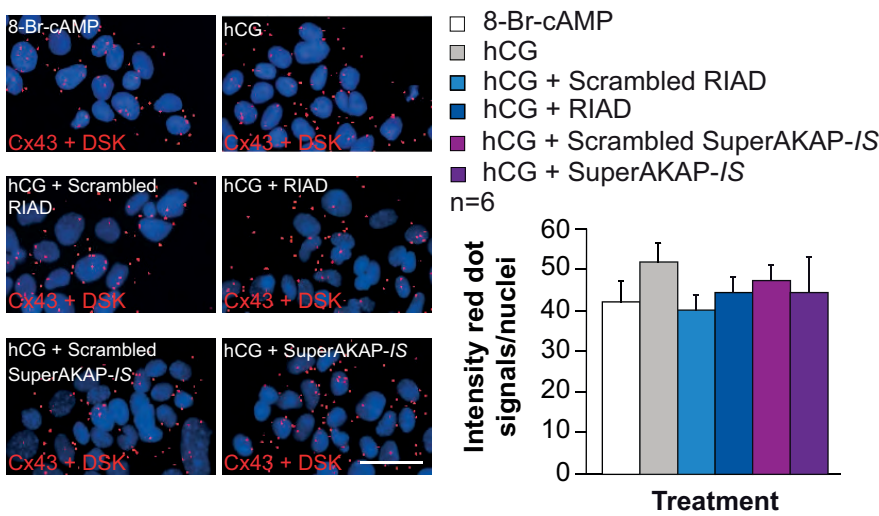




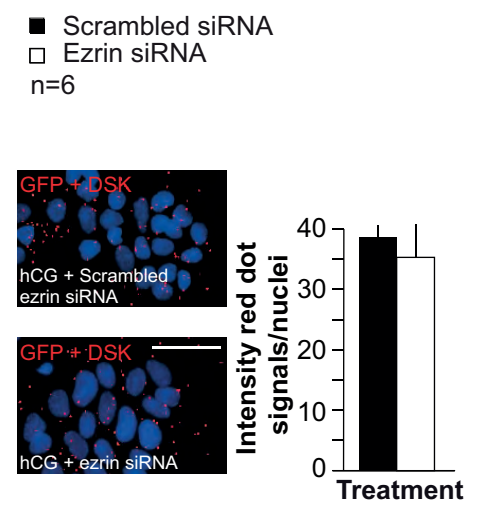
A



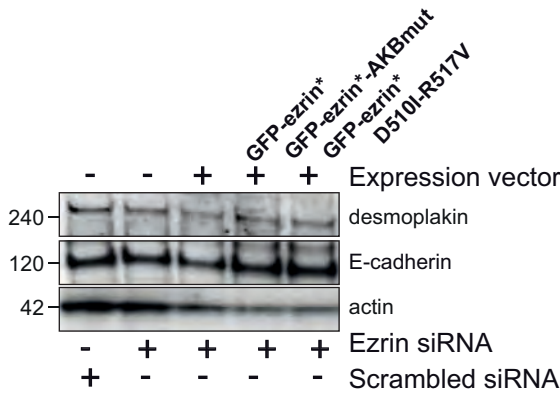
B



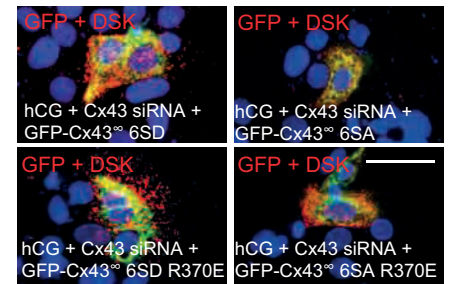
C



D



E

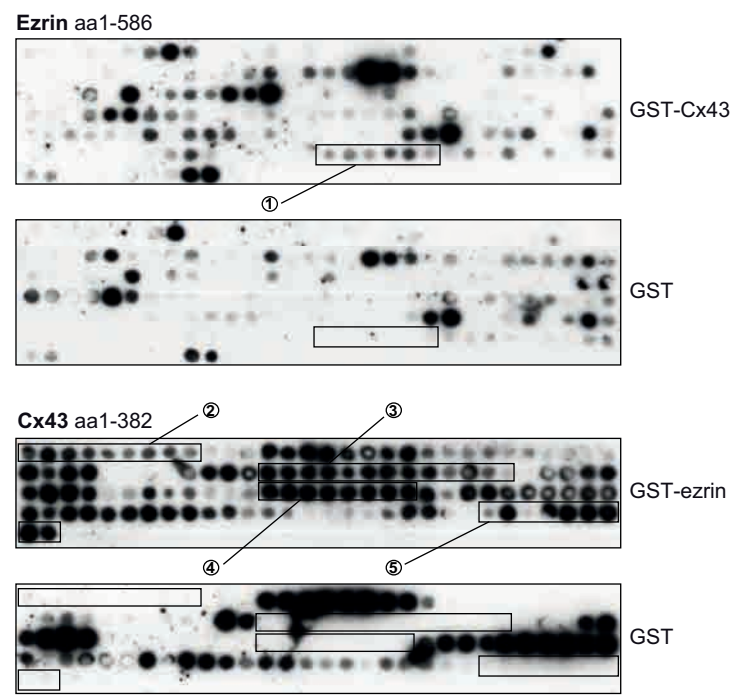


F

Name	Sequence	Mutations
GFP-Cx43 [∞]	362-RPSSRASSRASSRPRPDD-379	
GFP-Cx43 [∞] R370E	362-RPSSRASSRASSRPRPDD-379	R370E
GFP-Cx43 [∞] 6SD	362-RPDDRADDRAADDPRPDD-379	S364D S365D S368D S369D S372D S373D
GFP-Cx43 [∞] 6SD R370E	362-RPDDRADDRAADDPRPDD-379	S364D S365D S368D S369D S372D S373D R370E
GFP-Cx43 [∞] 6SA	362-RPAAAAAARPRPDD-379	S364A S365A S368A S369A S372A S373A
GFP-Cx43 [∞] 6SA R370E	362-RPAAAAAARPRPDD-379	S364A S365A S368A S369A S372A S373A R370E
GFP-Cx43 [∞] 3SD R370E	362-RPDDRADSEASSRPRPDD-379	S364D S365D S368D R370E
GFP-Cx43 [∞] 3SA R370E	362-RPAAARASEASSRPRPDD-379	S364A S365A S368A R370E
GFP-Cx43 [∞] S364D R370E	362-RPDSRASSRASSRPRPDD-379	S364D R370E
GFP-Cx43 [∞] S364A R370E	362-RPASRASSRASSRPRPDD-379	S364A R370E
GFP-Cx43 [∞] S365D R370E	362-RPSDRASSRASSRPRPDD-379	S365D R370E
GFP-Cx43 [∞] S365A R370E	362-RPSARASSRASSRPRPDD-379	S365A R370E
GFP-Cx43 [∞] S368D R370E	362-RPSSRADSEASSRPRPDD-379	S368D R370E
GFP-Cx43 [∞] S368A R370E	362-RPSSRAASEASSRPRPDD-379	S368A R370E

* siRNA resistant ezrin T567D; ∞ siRNA resistant Cx43 wild type

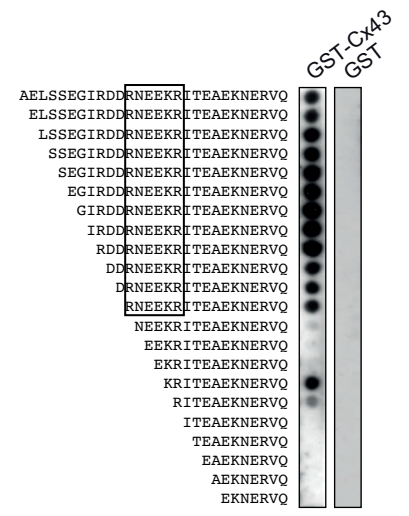
A



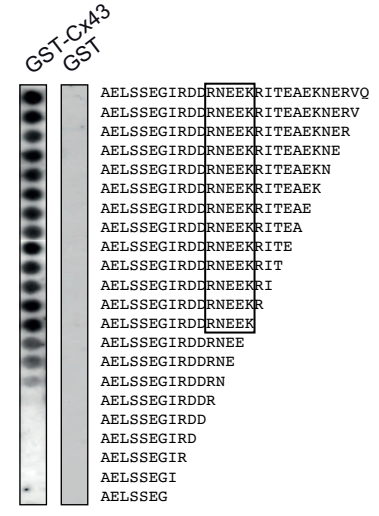
- 1: ⁴⁹³GAEPTGYS AELSSEGI RDDRNEEKRI TEAEKNERV⁵²⁷
- 2: ¹MGDWSALGKLLDKVQAYSTAGGKVLVSVLFI RILLGTAVESA⁴⁴
- 3: ¹²⁷LKQIEIKKFKYIEEHGKVKMRGGLRTYIISILFKSIFEVAFLLIQWYIYGFSL¹⁸²
- 4: ²¹⁷SLVSLALNIIELFYVFKGKDRVKGSDPYHATSGALSPA²⁵⁷
- 5: ³⁵²ELQPLAIVDQRPSSRASSRASSRPRPDDLEI³⁸²

B

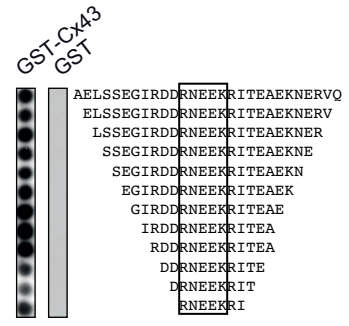
Ezrin aa501-528
N-terminal truncations:



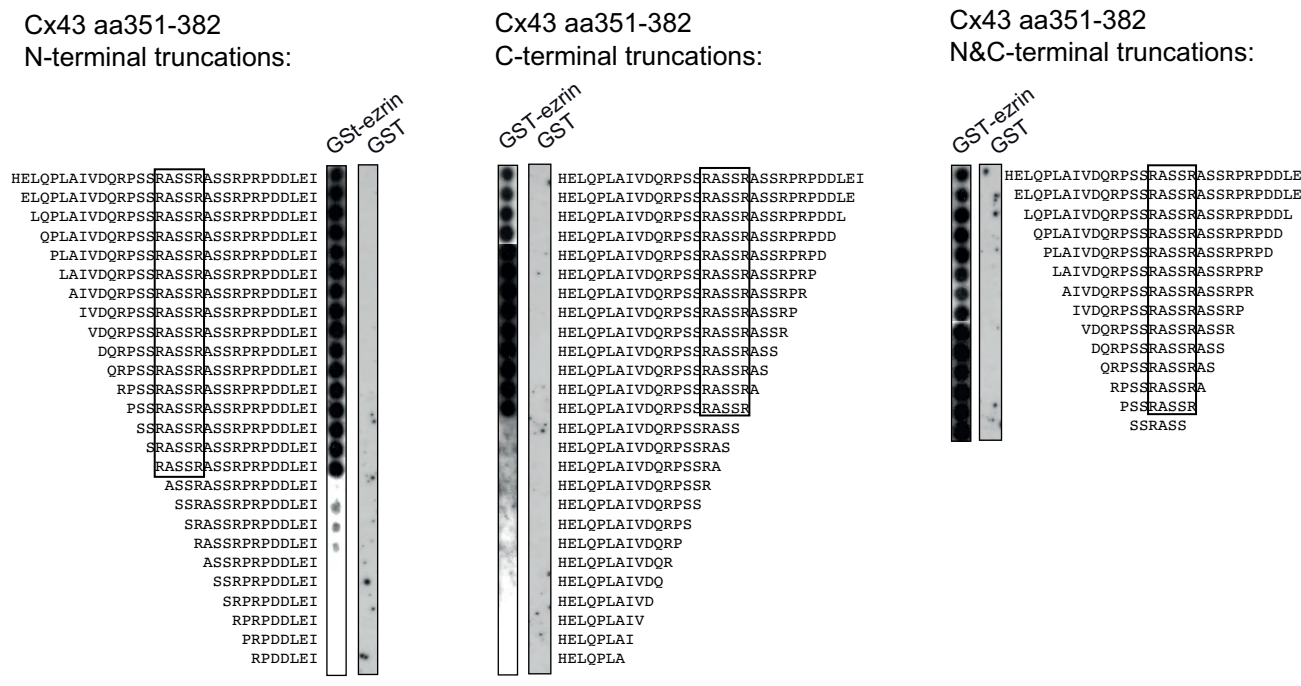
Ezrin aa501-528
C-terminal truncations:



Ezrin aa501-528
N&C-terminal truncations:

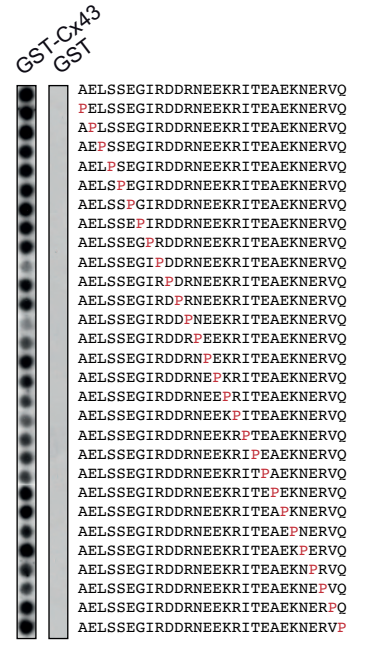


C

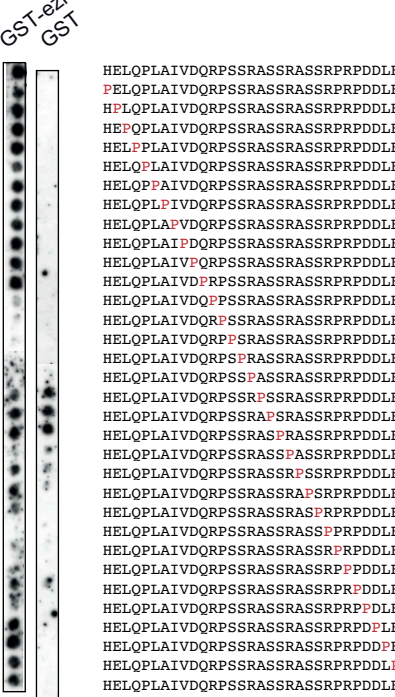


D

Ezrin aa501-528
Proline scan:



Cx43 aa351-382
Proline scan:



E

